



Homo- and co-polymerization of disubstituted ketenes

Bo Jiang

► To cite this version:

Bo Jiang. Homo- and co-polymerization of disubstituted ketenes. Polymers. Normandie Université, 2019. English. NNT : 2019NORMIR02 . tel-02299103

HAL Id: tel-02299103

<https://theses.hal.science/tel-02299103>

Submitted on 27 Sep 2019

HAL is a multi-disciplinary open access archive for the deposit and dissemination of scientific research documents, whether they are published or not. The documents may come from teaching and research institutions in France or abroad, or from public or private research centers.

L'archive ouverte pluridisciplinaire **HAL**, est destinée au dépôt et à la diffusion de documents scientifiques de niveau recherche, publiés ou non, émanant des établissements d'enseignement et de recherche français ou étrangers, des laboratoires publics ou privés.



Normandie Université

THESE

Pour obtenir le diplôme de doctorat

Chimie

Préparée au sein de L'Institut National des Sciences Appliquées Rouen Normandie

HOMO- and CO-POLYMERIZATION OF DISUBSTITUTED KETENES

Présentée et soutenue par
Bo JIANG

Thèse soutenue publiquement le 29 mars 2019
devant le jury composé de

Mr Jean-Francois PILARD	Professeur des Universités, Université du Maine, IMMM	Rapporteur
Mme Sophie GUILLAUME	Directeur de Recherche, Université de Rennes 1, ISCR	Rapporteur
Mr Daniel GRANDE	Directeur de Recherche, Université Paris-Est Créteil, ICMPE	Examineur
Mr Nicolas DESILLES	Maître de Conférences, INSA Rouen Normandie, PBS	Directeur de Thèse
Mr Fabrice BUREL	Professeur des Universités, INSA Rouen Normandie, PBS	Co-directeur de Thèse

Thèse dirigée par Nicolas DESILLES et Fabrice BUREL, Laboratoire Polymères Biopolymères Surfaces



Polymères
Biopolymères
Surfaces
UMR 6270



Acknowledgments

First and foremost, I would express my sincere acknowledgment to China Scholarship Council (CSC) for its financial support of my study in France.

I would like to express my heartfelt gratitude to Mr. Jean-Francois PILARD, professor of Maine University, and Mme. Sophie GUILLAUME, CNRS research director of Renne 1 University, for spending time of reviewing this work and acting as the reporters.

I am also greatly indebted to Mr. Daniel GRANDE, CNRS research director of Paris-Est Créteil University, who honored me of serving as President of the Jury and evaluating my research.

Also, I would like to express my gratitude to all those who helped me during the writing of this thesis. My deepest gratitude goes to my supervisor Mr. Nicolas DESILLES, assistant professor of INSA-Rouen Normandie, for his constant encouragement and guidance in the academic studies, as well as his considerate help to my life in France. He has walked me through all the stages of the writing of this thesis. Without his consistent and illuminating instruction, this thesis could not have reached its present form.

I also owe my sincere gratitude to my co-director Mr. Fabrice BUREL, professor of INSA-Rouen Normandie, who spent much time reading through each draft and provided me with inspiring advices, especially offered me expert guidance and patient instruction to the French introduction part.

I am also deeply indebted to all the other tutors and teachers in the Laboratory Polymers, Biopolymers, Surfaces (PBS, UMR CNRS 6270) for their direct and indirect help to me: Nasreddine KÉBIR, Philippe LEBAUDY, Laurence LECAMP, Gaëlle MORANDI, Daniela VULUGA-LEGROS.

I also owe a special debt of gratitude to the engineers, Catherine LEGRAND and Jérémy DESHAIS, and the assistante secretary of the lab, Giovanna DELAMARE, for their

help to the chemical orders, drug deliveries, experimental handling and instrument analysis. Especially, I appreciate that Catherine instructed and helped me a lot with my French learning.

Great thanks should also go to my colleagues in the lab, Yuhui ZHAO, Ludovic GEELHAND DE MERXEM, Arlette EL ASMAR, Ghislain RABODON, Pierre BOISAUBERT, Cyrielle IBANEZ, Alice GONTIER, Yuzhen LOU, Juan OSEGUEDA, other post-docs, trainees and students, I appreciate working together with you all.

Special thanks should go to my families, my father, mother and twin brother, for their continuous support and encouragement in my life.

Last my thanks would go to my beloved girlfriend Xuelian, also one of my colleagues, for everything she did to help me and everything between us.

To my life in France

my forever memory

Publications

Period of Ph.D:

High molecular weight polyester obtained by polymerization of dimethylketene using the metallocene initiators: a step toward Ziegler-Natta supporting application in non-olefin systems. (manuscript in preparation)

Cationic copolymerization of dimethylketene (DMK) with diethylketene (DEK) and diphenylketene (DPK): synthesis, characterization and reactivity ratio estimation. (manuscript in preparation)

Period of M.Sc:

Bo Jiang, Daye Sun, Ye Zhu, et al. Effects of biphenyl groups on the dry sliding behavior of poly (ether-ether-ketone-ketone) copolymers against stainless steel [J]. Materials & Design, 2018, 158: 39-45

Yongpeng Wang, Mengzhu Liu, Yang Sun, Yingshuang Shang, **Bo Jiang**, et al. Aluminum borate whiskers grafted with boric acid containing poly(ether ether ketone) as a reinforcing agent for the preparation of poly(ether ether ketone) composites [J]. RSC Advance, 2015, 5(122): 100856-100864

Wenlong Jiang, Haibo Zhang, **Bo Jiang**, et al. Poly (ether ether ketone)/wrapped graphite nano-sheets with poly (ether sulfone) composites: preparation, mechanical properties and tribological behavior [J]. Journal of Applied Polymer Science, 2015, 132(14)

Na Li, **Bo Jiang**, Daye Sun, et al. Investigations on the tribological properties of poly (arylene ether ketone) copolymer with 3-(trifluoromethyl) phenyl pendants and biphenyl units [J]. High Performance Polymers, 2014, 26(3): 247-254

Contents

Acknowledgments	I
Publications	III
Contents	V
List of Abbreviations	IX
List of Figures.....	XI
List of Tables	XVII
Résumé de la Thèse en Français	I
Introduction Générale	II
Organisation de la Thèse.....	V
Conclusion Générale.....	XXII
General Introduction	1
1. State of the Art	5
1.1 Ketene Synthesis	6
1.1.1 <i>The Staudinger Method</i>	8
1.1.2 <i>Thermal Generation Method</i>	10
1.1.3 <i>Photochemical Generation Method</i>	16
1.1.4 <i>Wolff Rearrangement Method</i>	18
1.1.5 <i>Conclusion on Ketene Synthesis</i>	22
1.2 Generalities on Ketene Polymerization	22
1.3 Anionic Polymerization of Ketenes	24
1.3.1 <i>Anionic Initiators</i>	26

1.3.2	<i>Anionic Homopolymerization of Ketenes</i>	27
1.3.3	<i>Copolymerization of Ketenes</i>	35
1.4	Cationic Polymerization of Ketenes	40
1.4.1	<i>Cationic Initiators</i>	40
1.4.2	<i>Cationic Homopolymerization of Ketenes</i>	42
1.4.3	<i>Cationic Copolymerization of Ketenes</i>	45
1.5	Commercial Aliphatic Polyketones	45
1.5.1	<i>Aliphatic Polyketones Involving 1,4-Dicarbonyl Units</i>	46
1.5.2	<i>Functionalized Polymers by Postpolymeric Modification</i>	46
1.6	Conclusion	48
1.7	References.....	49
2.	Cationic Polymerization of Different Aliphatic and Aromatic Ketenes	58
2.1	Monomer Synthesis	59
2.1.1	<i>Methylethylketene (MEK)</i>	59
2.1.2	<i>Diethylketene (DEK)</i>	60
2.1.3	<i>Ethylphenylketene (EPK)</i>	61
2.1.4	<i>Diphenylketene (DPK)</i>	61
2.2	Cationic Homopolymerization of Ketenes.....	62
2.2.1	<i>MEK</i>	63
2.2.2	<i>DEK</i>	64
2.2.3	<i>EPK</i>	65
2.2.4	<i>DPK</i>	66
2.3	Cationic copolymerization with Dimethylketene (DMK)	72

2.3.1	<i>DMK Synthesis</i>	72
2.3.2	<i>Copolymerization of DEK / DMK</i>	74
2.3.3	<i>Copolymerization of DPK / DMK</i>	81
2.3.4	<i>Monomer reactivity ratios</i>	85
2.4	Conclusion	91
2.5	References.....	92
3.	Modification of Dimethylketene-based Polyketone	94
3.1	Superiority and Limitation of PDMK	95
3.2	Generalities on Modification Pathways	96
3.2.1	<i>Conversion to Polypyrazole from Polyketones</i>	96
3.2.2	<i>One-step Beckmann Rearrangement</i>	97
3.2.3	<i>Dithioketal Functionalized Reaction</i>	99
3.3	Experimental Modification on PDMK.....	100
3.3.1	<i>Experimental Procedure</i>	100
3.3.2	<i>Experimental Results and Discussion</i>	102
3.4	Conclusion	105
3.5	References.....	107
4.	Novel Initiators Approach to Cationic Polymerization of Ketene Monomers ...	108
4.1	Generalities on Novel Initiators	109
4.1.1	<i>Montmorillonitic Clay</i>	109
4.1.2	<i>Photoinitiators</i>	114
4.1.3	<i>Metallocene</i>	122
4.2	Polymerization with Montmorillonite Clays	124

4.2.1	<i>Preparation of Clay Initiators</i>	124
4.2.2	<i>Polymerization</i>	125
4.3	Polymerization with Photoinitiators	126
4.4	Polymerization with Metallocene	129
4.4.1	<i>Polymerization Procedure and Results</i>	129
4.4.2	<i>Polyester from EPK</i>	131
4.4.3	<i>Polyester from DMK</i>	134
4.5	Conclusion	146
4.6	References.....	148
General Conclusions		154
Annexes		157

List of Abbreviations

AMA: alumina / methanesulfonic acid
AN: acrylonitrile
Cp: cyclopentadienyl
CQ: camphorquinone
DEK: diethylketene
DMF: dimethylformamide
DMK: dimethylketene
DMSO: dimethyl sulfoxide
DPK: diphenylketene
DSC: differential scanning calorimetry
 \bar{M}_w : dispersity of molecular weight
EDT: 1,2-ethanedithiol
EK: ethylketene
EPCO: ethylene / propylene / CO terpolymer
EPK: ethylphenylketene
EVOH: copolymer of ethylene and vinyl alcohol
FT-IR: fourier transform infrared
GC-MS: gas chromatography mass spectrometry
 ΔH_m : melting enthalpy
HFIP: hexafluoro-2-propanol
H-Maghnite: proton-exchanged montmorillonite clay
HOMO: highest occupied molecular orbital
IBA: isobutyric acid
IBAN: isobutyric anhydride
IR: infrared
LED: light-emitting diode
LUMO: lowest unoccupied molecular orbital
MA: methyl acrylate
MALS: multi-angle light scattering
MAN: methacrylonitrile
MAO: methylaluminoxane

MEK: methylethylketene
MMA: methyl methacrylate
NMR: nuclear magnetic resonance
NVP: *N*-vinyl-2-pyrrolidone
PA: polyacetal
PDMK: dimethylketene-based polyketone
PDT: 1,3-propanedithiol
PE: polyester
PEEK: poly(ethyl ethyl ketone)
PEtG: poly(ethylglyoxylate)
PK: polyketone
PMMA: poly(methyl methacrylate)
PVDC: poly(vinylidene chloride)
SEC: size exclusion chromatography
s-PU: substituted polyurethanes
 $T_d^{5\%}$: degradation temperature (5% weight loss)
 T_d^{Max} : degradation temperature (maximum of derivative curve)
TFA: trifluoroacetic acid
 T_g : glass transition temperature
TGA: thermogravimetric analysis
THF: tetrahydrofuran
 T_m : melting point
UV: ultraviolet
VAc: vinyl acetate

List of Figures

Figure 1-1. Ketene cumulene structure [1]	6
Figure 1-2. Isoelectronic structures of ketenes [2]	6
Figure 1-3. The $[2+2]$ cycloaddition of ketenes [10].....	7
Figure 1-4. Reactions between ketenes and H ₂ O or O ₂ [11].....	7
Figure 1-5. Dehalogenation of 2-chloro(diphenyl)acetyl chloride using zinc [13]	8
Figure 1-6. Debromination of 2-bromoisobutyryl bromide using zinc [15]	9
Figure 1-7. Debrominate the 2-bromobutyryl bromide using zinc [16]	9
Figure 1-8. Dehydrohalogenation of diphenylacetyl chloride with triethylamine [14]	9
Figure 1-9. Dehydrochlorination of (trimethylsilyl)acetyl chloride with triethylamine [17]	10
Figure 1-10. Reaction between isobutyryl chloride and triethylamine [18, 19]	10
Figure 1-11. Pyrolysis of acetone [20]	11
Figure 1-12. Pyrolysis of acetic acid [23].....	11
Figure 1-13. Gold ketenylidene formed by acetic acid [24]	12
Figure 1-14. Pyrolysis of malonic anhydrides [25, 26]	12
Figure 1-15. Pyrolysis of acetic anhydride	13
Figure 1-16. Triethylsilylketene, dimethylketene and ethylketene preparation by pyrolysis of anhydrides	13
Figure 1-17. Pyrolysis of phenyl acetate [32].....	13
Figure 1-18. Pyrolysis of isopropenyl esters in the case of n-hexadecylketene [33].....	14
Figure 1-19. Pyrolysis of alkyl acetaoacetates with different R groups [34, 35].....	14
Figure 1-20. Pyrolysis of ketene dimers	15
Figure 1-21. Pyrolysis of Meldrum's acids	15
Figure 1-22. Synthesis of Meldrum's acid-containing polymer and its thermolytic crosslinking [41] ...	16
Figure 1-23. Photolysis of dimethylketene dimer [42, 43].	16
Figure 1-24. Photolysis of the cyclobutanedione [44]	17
Figure 1-25. Photochemical ring opening of cyclohexadienones	17

Figure 1-26. Photochemical ring opening of furfuryl alcohol [49].....	18
Figure 1-27. Photolysis of 2,3,5,6-tetra(trimethylsilyl)-1,4-benzoquinone [50]	18
Figure 1-28. Possible steps in Wolff rearrangement [53].....	19
Figure 1-29. Thermal Wolff rearrangement of diazoacetophenone [54]	19
Figure 1-30. Phenyl substituted ketenes from thermal Wolff rearrangement [58-60].....	20
Figure 1-31. Silylketenes by Wolff rearrangement [66, 67].....	20
Figure 1-32. One-pot procedure from aryl diazo ketone to aryl(trialkylsilyl)ketene [68].	21
Figure 1-33. Photolysis of diazoacetone and azibenzil [70]	21
Figure 1-34. Photolysis of diazo Meldrum's acid [71]	22
Figure 1-35. Dimer and trimer structures of dimethylketene	23
Figure 1-36. Polymerization of dimethylketene	23
Figure 1-37. Dioxygen permeability of PDMK, EPCO (like Ketonex or Poketone, see 1.5.1), EVOH and PET [88]	24
Figure 1-38. Possible pathways by the rearrangement of chain growth [93]	25
Figure 1-39. Tetrahydrofuran based sodium-naphthalene (Na-C ₁₀ H ₈) initiator [95].....	26
Figure 1-40. Propagation step of chain growth for organolithium initiator.....	27
Figure 1-41. General anionic copolymerization of ketene and other compounds	35
Figure 1-42. General pathways to ester, ketone and acetal units by cationic polymerization	40
Figure 1-43. Reaction between protic acid and dimethylketene [121]	41
Figure 1-44. Reaction between Lewis acid SnCl ₄ and dimethylketene [30]	42
Figure 1-45. Two examples for Friedel-Craft style initiators [123]	42
Figure 1-46. Keto-enol equilibrium (Keto-enol was estimated about 30 : 70%).....	43
Figure 1-47. Synthesis of ethylene-propylene-carbon monoxide copolymer (EPCO) [126].....	46
Figure 1-48. Chemical modification of ethylene-carbon monoxide copolymer	47
Figure 1-49. Ketone reduction of PDMK using LiAlH ₄	48
Figure 2-1. Synthesis route of MEK.....	59
Figure 2-2. Synthesis and pyrolysis of diethyl malonic anhydride.....	60
Figure 2-3. Synthesis of EPK by dehydrochlorination reaction	61
Figure 2-4. Synthesis of DPK by dehydrochlorination reaction.....	61

Figure 2-5. IR spectra of DPK tested at different storage times	62
Figure 2-6. Desired cationic polymerization of the four ketenes.....	63
Figure 2-7. Preparation of a special Brønsted acid initiator by $n(\text{acid}) : n(\text{B}(\text{C}_6\text{F}_5)_3) = 1 : 2$	65
Figure 2-8. Products from DEK after polymerization procedure and precipitation in ethanol.....	65
Figure 2-9. Product from EPK after polymerization procedure and precipitation in ethanol.....	66
Figure 2-10. An undesired ester from DPK after polymerization procedure and precipitation in ethanol	67
Figure 2-11. FT-IR monitoring of Run 39~42 (DPK-based polyesters).....	68
Figure 2-12. ^1H NMR spectrum (300 Mhz, 20°C, CD_2Cl_2) of Run 39 (DPK-based polyester)	68
Figure 2-13. ^{13}C NMR spectrum (75 Mhz, 20°C, CD_2Cl_2) of Run 39 (DPK-based polyester).....	69
Figure 2-14. TGA spectra of Run 39~42 (DPK-based polyesters).....	70
Figure 2-15. DSC analysis of Run 39 (DPK-based polyester $M_n = 1\,510\text{ g}\cdot\text{mol}^{-1}$).....	70
Figure 2-16. Glass transition temperature versus molecular weight for the obtained DPK-based polyesters	71
Figure 2-17. Synthesis of DMK by pyrolysis of isobutyric anhydride.....	73
Figure 2-18. Apparatus of synthesis, purification and collection for DMK and reactor for copolymerization	74
Figure 2-19. ^1H NMR spectrum (300 Mhz, 20°C, $\text{CD}_2\text{Cl}_2 + \text{HFIP}$) of Run 98 ($[\text{DMK}] : [\text{DEK}] = 26 : 1$)	76
Figure 2-20. ^{13}C NMR spectrum (75Mhz, 20°C, $\text{CD}_2\text{Cl}_2 + \text{HFIP}$) of Run 98 ($[\text{DMK}] : [\text{DEK}] = 26 : 1$)	77
Figure 2-21. TGA spectra of DMK / DEK copolymers	78
Figure 2-22. Thermal degradation of DMK / DEK copolymers at the 'junction points'	79
Figure 2-23. Comparison of DSC spectra of Run 58, Run 75 and Run 98.....	80
Figure 2-24. ^1H NMR spectrum (300 Mhz, 20°C, $\text{CD}_2\text{Cl}_2 + \text{HFIP}$) of Run 95 ($[\text{DMK}] : [\text{DPK}] = 6 : 1$)	82
Figure 2-25. ^{13}C NMR spectrum (75 Mhz, 20°C, $\text{CD}_2\text{Cl}_2 + \text{HFIP}$) of Run 95 ($[\text{DMK}] : [\text{DPK}] = 6 : 1$).....	83
Figure 2-26. TGA spectra of DMK / DPK copolymers.....	83
Figure 2-27. Comparison of DSC spectra of Run 58 and Run 95	85
Figure 2-28. Kelen-Tudos method applied to DEK / DMK and DPK / DMK copolymers.....	89

Figure 2-29. 3D predicted space filling structures of DMK, DEK and DPK	90
Figure 2-30. Phenyl as electron withdrawing group decreases the electronegativity of C ₁ and O	90
Figure 2-31. Formation of the intercalated copolymer	91
Figure 3-1. From cyclic polyketones to heterocyclophanes containing isopyrazole or pyrrole units [2]	96
Figure 3-2. Conversion of 1,3- and 1,4-diketone in the aliphatic flexible polyketone chain into isopyrazole or furan subunits [3]	97
Figure 3-3. General transformation from a ketone to an amide via Beckmann rearrangement	98
Figure 3-4. General Beckmann rearrangement reaction [7]	98
Figure 3-5. Conversion of cyclohexanone oxime into ϵ -caprolactam using AMA [7]	98
Figure 3-6. Dithioketalization and deprotection of PEEK with EDT ($r = 0$) and PDT ($r = 1$), respectively	100
Figure 3-7. ¹ H spectrum (300 Mhz, 20°C, CD ₂ Cl ₂) of Run 99 in CD ₂ Cl ₂ (dithioketal functionalized reaction)	103
Figure 3-8. ¹³ C spectrum (75 Mhz, 20°C, CD ₂ Cl ₂) of Run 99 in CD ₂ Cl ₂ (dithioketal functionalized reaction)	104
Figure 3-9. TGA spectra of Run 99 (dithioketal functionalized reaction) and original PDMK	105
Figure 4-1. Montmorillonite samples	110
Figure 4-2. Structure of montmorillonite [9]	111
Figure 4-3. Synthesis of PEtG [20]	113
Figure 4-4. Polymerization of N-vinyl-2-pyrrolidone [7]	113
Figure 4-5. Mechanism of polymerization of N-vinyl-2-pyrrolidone using H-Maghnite [7]	114
Figure 4-6. General photolysis of diaryliodonium salts [40]	116
Figure 4-7. Structure of IRGACURE 250 [42]	116
Figure 4-8. UV absorbance spectra of IRGACURE 250 in methanol	117
Figure 4-9. UV absorbance spectra of ferrocene in 1-methyl-3-nonylimidazolium bis[(trifluoromethane)sulfonyl]amide [47]	118
Figure 4-10. Photochemical dissociation of ferrocene carbon tetrachloride complex [48]	118
Figure 4-11. Structure of 1,1'-bis(dimethylsilyl)ferrocene	119
Figure 4-12. Proposed photosensitization mechanism of three-component initiator which accounts for the regeneration of CQ during irradiation with visible light [68]	121

Figure 4-13. UV absorbance spectrum of camphorquinone (CQ) in ethanol ($9.6 \times 10^{-3} \text{ mol} \cdot \text{L}^{-1}$)	121
Figure 4-14. Sandwich structure of the metallocene	122
Figure 4-15. Several metallocene initiators [72]	123
Figure 4-16. Formation of alkyl metallocene (Cp = cyclopentadienyl ligand; M = Ti, Zr, Hf; R = alkyl; R' = alkyl or halide; A = Activator)	123
Figure 4-17. Insertion (Ziegler-Natta) polymerization of ethylene	124
Figure 4-18. UV Emission spectral distribution of Hamamatsu lamp	127
Figure 4-19. UV absorbance spectrum of DMK in ethyl acetate ($8.3 \times 10^{-4} \text{ mol} \cdot \text{L}^{-1}$)	129
Figure 4-20. IR spectrum of Run 31 (EPK-based polyester)	131
Figure 4-21. ^1H NMR (300 Mhz, 20°C , CD_2Cl_2) spectrum of Run 31 (EPK-based polyester)	132
Figure 4-22. ^{13}C NMR spectrum (75 Mhz, 20°C , CD_2Cl_2) of Run 31 (EPK-based polyester)	132
Figure 4-23. TGA analysis of Run 31 (EPK-based polyester)	133
Figure 4-24. IR spectrum of Run 88 (DMK-based polyester)	134
Figure 4-25. ^1H NMR spectrum (300 Mhz, 20°C , CD_2Cl_2) of Run 88 (DMK-based polyester)	135
Figure 4-26. ^{13}C NMR spectrum (75 Mhz, 20°C , CD_2Cl_2) of Run 88 (DMK-based polyester)	135
Figure 4-27. Activate reaction of metallocenes	137
Figure 4-28. Insertion polymerization mechanism of DMK	138
Figure 4-29. Insertion polymerization of DMK	138
Figure 4-30. Association of 'Obsessive-Compulsive Snake' with ketene insertion mechanism	139
Figure 4-31. TGA spectra of DMK-based polyesters	140
Figure 4-32. DSC spectra of DMK-based polyesters (heat at $10^\circ\text{C} / \text{min}$ after a cooling at $0.5^\circ\text{C} / \text{min}$)	141
Figure 4-33. SEC comparison of DMK-based polyesters before and after degradation	143
Figure 4-34. DSC comparison of DMK-based polyesters before and after degradation	144
Figure 4-35. TGA comparison of DMK-based polyesters before and after degradation	145
Figure 4-36. Possible reasons for the degradation	146

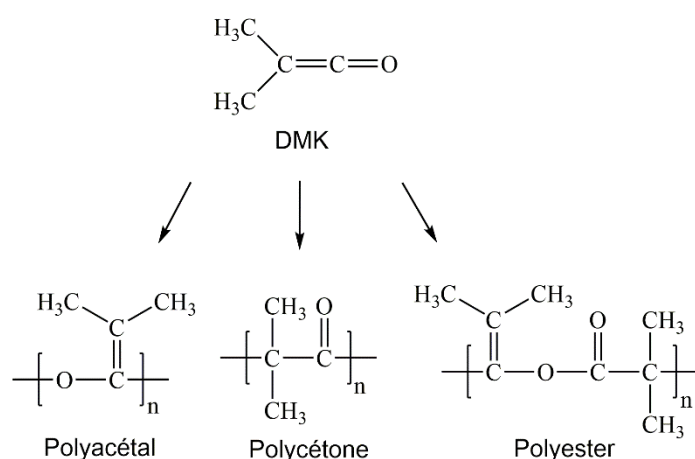
List of Tables

Table 1-1. Anionic homopolymerization summary of ketene monomers	28
Table 1-2. Anionic copolymerization summary of ketene monomers.....	35
Table 1-3. Cationic homopolymerization summary of ketene monomers.....	43
Table 1-4. Cationic copolymerization summary of ketene monomers	45
Table 2-1. Summary of cationic polymerization conditions of methylethylketene	63
Table 2-2. Summary of cationic polymerization conditions of diethylketene	64
Table 2-3. Summary of cationic polymerization conditions of ethylphenylketene	65
Table 2-4. Summary of cationic polymerization conditions of diphenylketene	66
Table 2-5. Properties of Run 39~42 (DPK-based polyesters) ^a	69
Table 2-6. Results of DMK and DEK copolymerization.....	75
Table 2-7. Summary of thermal properties of DMK / DEK copolymers	78
Table 2-8. Results of DMK and DPK copolymerization.....	81
Table 2-9. Summary of thermal properties of DMK / DPK copolymers.....	84
Table 2-10. Listing of the various methods used to estimate the reactivity ratios.....	86
Table 2-11. Data for the copolymerization of DMK and DEK including Kelen-Tudos parameters	88
Table 2-12. Data for the copolymerization of DMK and DPK including Kelen-Tudos parameters	88
Table 3-1. Postpolymerization modification and results	102
Table 4-1. Polymerization summary of ketenes using clay initiators.....	126
Table 4-2. Photoinitiator systems involved	127
Table 4-3. Photopolymerization of ketenes	128
Table 4-4. Summary of ketene polymerization using metallocene initiators.....	130
Table 4-5. Polymerization conditions of dimethylketene and results using metallocene initiators.....	136
Table 4-6. Thermal properties of DMK-based polyesters	140
Table 4-7. Summary of property changes of DMK-based polyesters after 6 month-storage	142

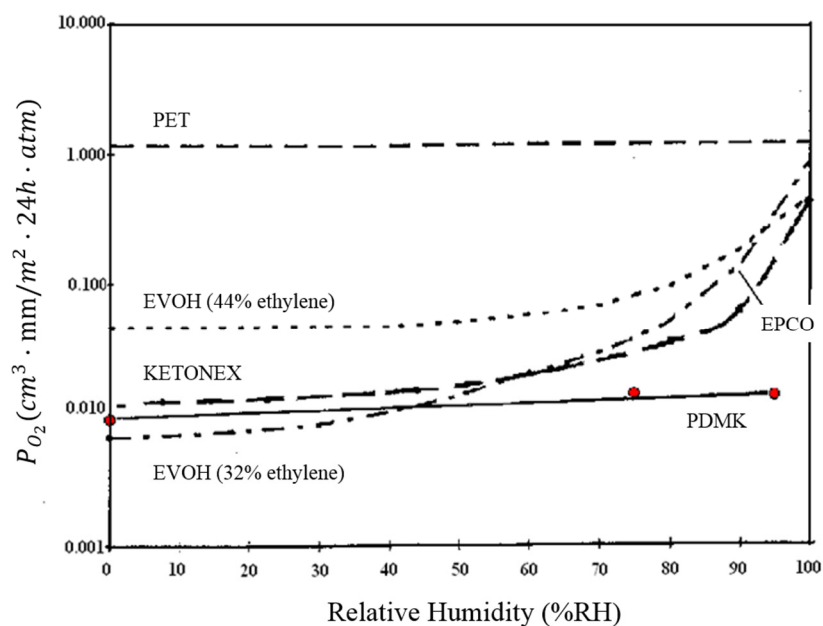
Résumé de la Thèse en Français

Introduction Générale

La polymérisation des cétoalcènes est un sujet peu étudié, mais qui mérite une grande attention en raison du fort potentiel des polymères qui en découlent. L'étude de la polymérisation du plus connu d'entre eux, le diméthylcétène (DMK), a montré que, suivant les conditions opératoires, trois structures pouvaient être obtenues [1-2] :

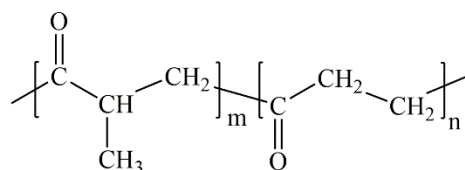


La structure polyacétal ne conduit pas à un polymère d'intérêt, les propriétés thermiques de ce dernier étant faibles. Les structures polyesters du DMK, obtenues par homopolymérisation ou par copolymérisation (avec l'acétaldéhyde, l'acétone ou la méthyléthylcétone) sont obtenues par voies anioniques. Les polymères présentent généralement des masses molaires moyennes inférieures à 30 000 g.mol⁻¹ et des propriétés thermiques tributaires de la présence ou non de groupements acétal dans la chaîne [3-4]. La polycétone du diméthylcétène (PDMK), obtenue par voie cationique, a permis de confirmer les excellentes propriétés physicochimiques de ces polycétones aliphatiques, notamment les propriétés barrières à l'oxygène. Celles obtenues avec le PDMK sont exceptionnelles et restent inégalées aujourd'hui à fort taux d'humidité [4-5].



Ces structures présentent en effet, des groupements carbonyles polaires répartis de manière régulière favorisant les interactions inter- et intra-moléculaires, entraînant de forts taux de cristallinité (jusqu'à 50%) et conférant ainsi d'excellentes propriétés physicochimiques (excellente résistance aux produits chimiques, résistance à l'usure exceptionnelle, et propriétés barrière optimales).

Obtenus par catalyse au palladium, les copolymères et terpolymères oléfines / monoxyde de carbone parfaitement alternés sont considérés comme les membres principaux de la famille des polycétones aliphatiques. Cela a été rendu possible par l'utilisation de catalyseurs au Pd (II) en présence de ligands bidantés et d'anions faiblement coordonnés (dérivés d'un acide de Brønsted) à 80°C sous 55 bar [6]. Initialement commercialisés par Shell (Carilon®) ou British Petroleum (Ketonex™), puis abandonnés, ces polymères sont de nouveaux sur le marché grâce à Hyosung depuis quelques années, et plus particulièrement les terpolymères à base d'éthylène, propylène et CO :



Notons, en effet, que le copolymère éthylène / CO, bien que présentant de bonnes propriétés, n'est pas le copolymère de choix car il possède un fort taux de cristallinité (30-40%) et une température de fusion très élevée proche de sa dégradation ($T_f = 257^\circ\text{C}$, $T_{deg} = 300^\circ\text{C}$). L'insertion d'un troisième co-monomère permet de moduler les propriétés, et l'incorporation de 6% de propylène dans la structure conduit aux versions commerciales avec $T_f = 222^\circ\text{C}$ et un taux de cristallinité inférieur à 30% facilitant ainsi leur mise en œuvre [7].

Ce constat peut aussi être fait avec le PDMK ($T_f = 250^\circ\text{C}$, $T_{deg} = 300^\circ\text{C}$). Lors de travaux précédents au laboratoire, nous avons ainsi tenté de synthétiser de nouvelles architectures PDMK, à partir d'un amorceur ramifié ou par copolymérisation avec l'éthylcétène afin d'abaisser la T_f sans altérer les autres propriétés. Cependant, la réactivité de l'éthylcétène s'est avérée très différente de celle du DMK ce qui nous a limité dans la gamme de composition des copolycétones obtenues, la polycétone de l'éthylcétène possédant quant à elle de moins bonnes propriétés thermiques ($T_{deg} = 220^\circ\text{C}$) [8].

L'objectif de ce travail est ainsi de poursuivre nos efforts de synthèse dans le but d'obtenir des polycétones aliphatiques à partir de céto-cétènes, et possédant de bonnes propriétés physicochimiques et des propriétés thermiques en adéquation avec une mise en œuvre aisée.

Pour ce faire nous avons synthétisé différents céto-cétènes et leurs précurseurs, tels que le diméthylcétène, le méthyléthylcétène, le diéthylcétène, l'éthylphénylcétène et le diphénylcétène. Leurs homopolymérisations et copolymérisations ont été étudiées et les polymères obtenus caractérisés. Différents catalyseurs ont été utilisés, notamment avec le DMK, et la photopolymérisation cationique tentée. Enfin, à l'image des polycétones aliphatiques de type éthylène / propylène / CO, plusieurs tentatives de modification chimique ont été envisagées afin de moduler les propriétés du PDMK.

Organisation de la Thèse

Cette thèse s'articule en quatre chapitres. Après cette introduction générale, le Chapitre 1 présente un bref aperçu de la synthèse des cétones et l'état de l'art des polymères à base de cétones ainsi que les techniques de modification des polycétones.

Le Chapitre 2 étudie la polymérisation cationique des différents cétones aliphatiques et aromatiques sélectionnés. La synthèse des monomères est détaillée et l'homopolymérisation du méthyléthylcétène (MEK), du diéthylcétène (DEK), de l'éthylphénylcétène (EPK) et du diphénylcétène (DPK) est réalisée à l'aide de catalyseurs cationiques classiques. Nous avons ensuite étudié le comportement en copolymérisation du DEK aliphatique et du DPK aromatique avec le diméthylcétène (DMK) dans des conditions de polymérisation cationique spécifiques.

Le Chapitre 3 présente nos essais de modification sur le PDMK, selon trois voies de réaction possibles, notamment la conversion du polypyrazole en polycétone, le réarrangement de Beckmann et la réaction de fonctionnalisation avec un dithioacétal.

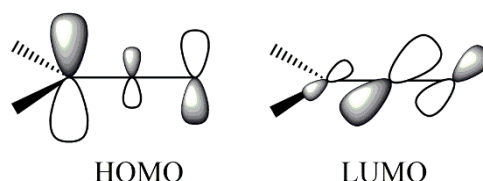
Le Chapitre 4 décrit trois types d'amorceurs cationiques différents (solide, photosensible et métallocène) et leurs performances catalytiques sur nos monomères cétones (DMK, MEK, DEK, EPK et DPK).

Premier Chapitre: Etat de L'art de la Synthèse des Cétones et de Leur Polymérisation

Synthèses des cétones

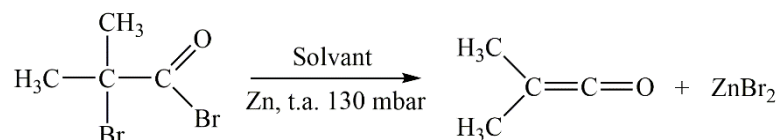
Le cétène est un type de dérivés particuliers d'acides carboxyliques, contenant deux doubles liaisons consécutives ($R_1R_2C=C=O$). En fonction des groupes fonctionnels R_1 et R_2 présents, les cétones peuvent être classés en aldocétones (monosubstitués, $R_1 = H$) et en céto-cétones (disubstitués).

La réactivité des cétones est étroitement liée à leur structure électronique [9]. Une orbitale moléculaire occupée de plus haute énergie (HOMO) perpendiculaire au plan, et une autre orbitale moléculaire vacante de plus basse énergie (LUMO) dans le plan, permettent une large gamme de réactions d'additions nucléophile et électrophile :



Plusieurs méthodes de préparation et d'isolation des cétones existent à commencer par celles de Staudinger par déshalogénéation de dérivés d'acides α -halogénocarboxyliques ou par déshydrohalogénéation d'halogénures d'acyle.

Pour rappel, la synthèse du diméthylcétène par déhalogénéation du bromure de 2-bromoisobutyryle est réalisée en présence de zinc suivant l'équation ci-dessous :

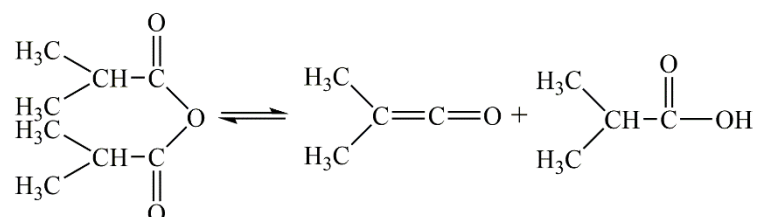


Cette méthode est très efficace notamment pour les cétones contenant des groupements volumineux ou aryles, mais conduit à des solutions de cétones.

Les méthodes de génération thermique des cétones, notamment par pyrolyse, sont multiples. Ainsi la pyrolyse de précurseurs de type cétone, acide, ester, de dimères de cétones, ou d'anhydrides permet d'obtenir les cétones désirés. Largement développée au laboratoire pour le diméthylcétène puis pour l'éthylcétène, la synthèse des cétones par pyrolyse des anhydrides correspondants permet d'obtenir ces monomères en grande quantité avec une

bonne pureté (> 95%). Il est ensuite possible de les polymériser avec le solvant sélectionné, avantage majeur par rapport à la méthode de Staudinger.

A titre d'exemple la pyrolyse de l'anhydride isobutyrique pour la production du diméthylcétène s'effectue à 625°C sous 40 mbar. On obtient une conversion de 80% de l'anhydride et une pureté supérieure à 95% pour le DMK après purification.



Des méthodes photochimiques ont aussi été développées. Ainsi certains cétones ont été obtenus par photolyse de leurs dimères, ou par ouverture d'hétérocycles sous rayonnement UV. Enfin, les cétones peuvent être obtenus à partir de diazo cétones par réarrangement de Wolff. Notons cependant que les rendements restent faibles pour ces deux dernières voies.

Polymérisation des cétones.

Dans cette deuxième partie bibliographique, nous rappelons les méthodes de polymérisation des cétones. Les travaux de Natta et Pregaglia [10-11] ont montré que les deux doubles liaisons du diméthylcétène peuvent être ouvertes sélectivement par voies anionique ou cationique. Néanmoins, quelle que soit la voie envisagée, elle est généralement effectuée à basse température pour éviter les réactions secondaires telles que la dimérisation des cétones.

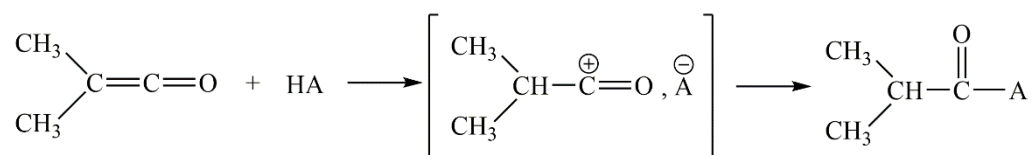
La polymérisation anionique des cétones utilise des amorceurs nucléophiles. Ces amorceurs anioniques peuvent être des bases (bases de Lewis ou alcoolates), des organolithiens, et des complexes aromatiques de métaux alcalins.

De nombreux solvants ont été testés, polaires ou non, pour des températures de polymérisation comprises entre -78°C et la température ambiante. Le DMK est le cétène le plus étudié et conduit quasi systématiquement à des mélanges polyacétal / polyester quels que soient les systèmes, pour des rendements de polymérisation de 1 à 100%. Notons l'exception du mélange toluène/acétone à -78°C en présence de $n\text{-BuLi}$ qui conduit à une structure polyester issue de la copolymérisation alternée de l'acétone avec le DMK. Pour les cétènes homologues supérieurs, la structure polyester est systématiquement mentionnée. L'ensemble des conditions est résumé Tableau 1-1 dans le chapitre suivant.

Les copolymérisations anioniques (cétène / aldéhyde ou cétone) conduisent uniquement à des polyesters alors que les copolymérisations (cétène / isocyanate) conduisent à des polyuréthanes substitués en présence de Na-naphtalène. La bibliographie est résumée Tableau 1-2.

Les amorceurs cationiques sont généralement des accepteurs d'électrons. Outre la capacité du cation de l'amorceur à activer le monomère, la réactivité des centres actifs est étroitement déterminée par la nature de l'anion associé, issu du système d'amorçage.

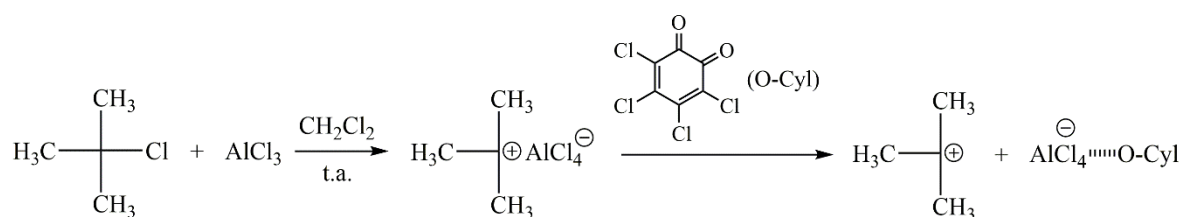
Les quelques essais réalisés avec les acides de Brønsted se sont révélés inefficaces dans la polymérisation cationique du DMK [4], certainement car ils aboutissent à un composé inactif :



Les acides de Lewis peuvent être utilisés seuls ou en présence d'un coamorceur, qui est généralement un acide de Brønsted faible (H_2O , CCl_3COOH , CH_3COOH ...). Dans le cas du diméthylcétène, seuls les acides de Lewis forts sont efficaces. A basse température (-30 à -78°C), AlBr_3 et AlCl_3 , employés dans des solvants apolaires comme le toluène ou le n -heptane, ou encore dans des mélanges de solvants (nitrobenzène / CCl_4 ou toluène) forment quasi systématiquement des polymères de structure cétone avec des rendements

compris entre 6 et 33%. L'éthylcétène [4] conduit à une structure parfaitement polycétone dans ces mêmes conditions.

Les systèmes de type Friedel-Craft sont la combinaison d'un acide de Lewis et d'un co-amorceur capable de générer des carbocations. Un système comprenant le trichlorure d'aluminum, le chlorure de tertiobutyle, et un agent complexant, l'*o*-chloranyl (3,4,5,6-tétrachloro-1,2-benzoquinone) a été développé et breveté par la société Arkema [12]. Utilisé dans le dichlorométhane à -30°C , il a permis d'obtenir la polycétone avec un rendement de 43%.



En revanche, ce système, utilisé avec l'éthylcétène mais sans agent complexant, n'a donné qu'un rendement faible de 10% [8].

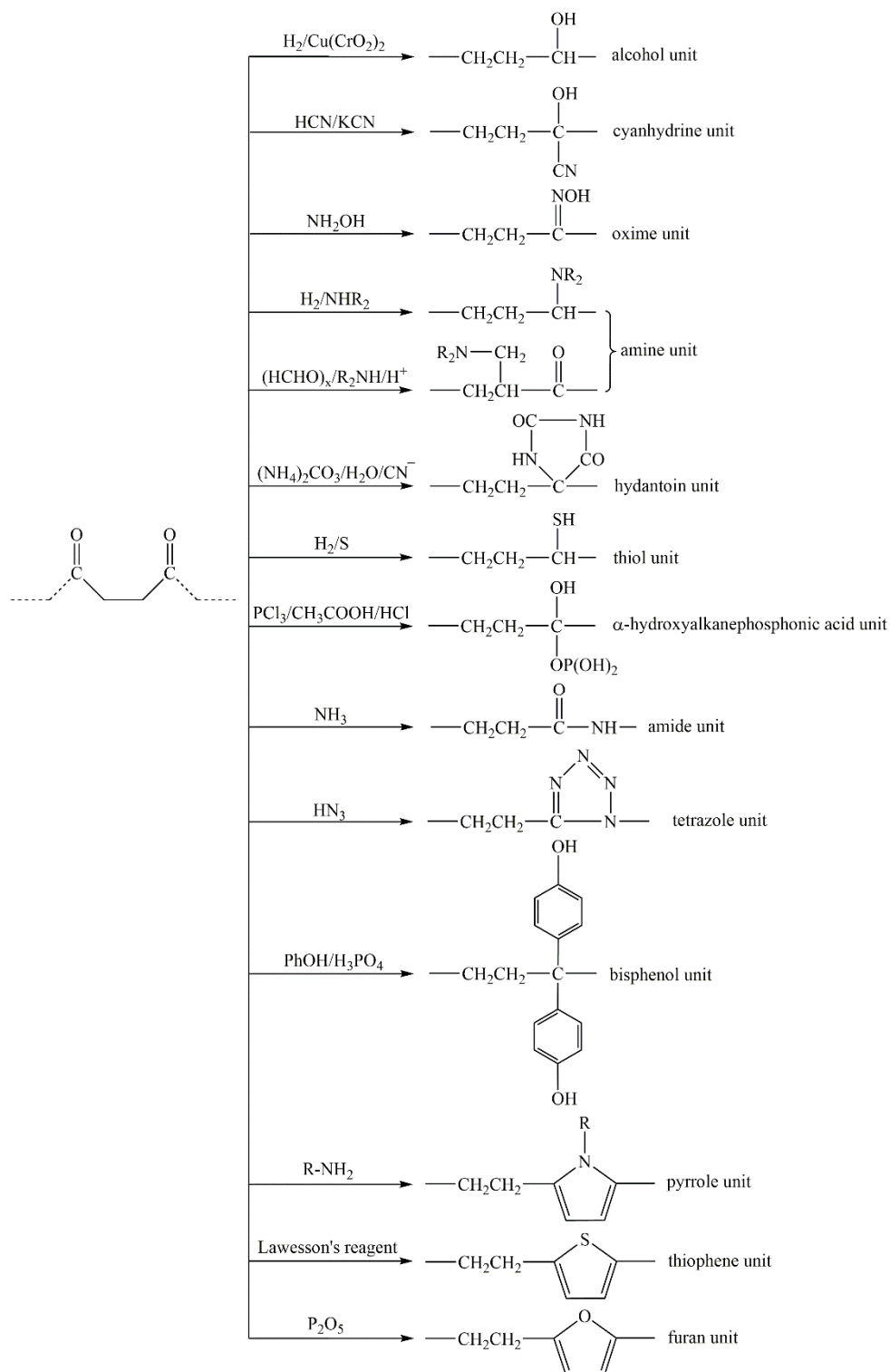
Aucun homologue supérieur n'a été polymérisé par voie cationique. L'ensemble des résultats est résumé tableau 1-3.

Modification chimique de polycétones aliphatiques

Concernant la polycétone PDMK, seule la réduction par LiAlH_4 en suspension dans le THF conduit à un polymère. Le polyol obtenu avec un rendement de 90% est amorphe et soluble dans l'acide acétique et l'alcool éthylique, mais il reste peu caractérisé [13].

Les autres modifications concernent les polycétones aliphatiques de type éthylène / propylène / CO. En effet, leur structure fait apparaître des unités 1,4-dicarbonyle plus enclines à la modification. Une grande variété de polymères contenant des groupes fonctionnels comme les pyrroles [14], les furanes [15], les thiophènes [15], les bisphénols

[16], les alcools [6], les amines [17], les thiols [18], les oximes [19], les amides [20], les cyanhydrines [21], etc... ont ainsi été obtenus :



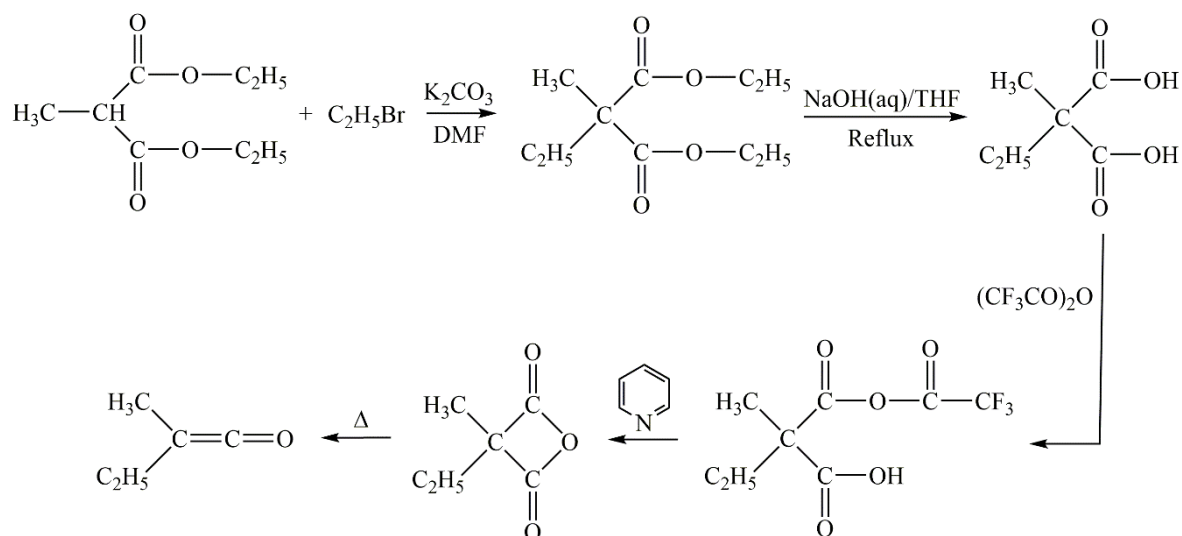
Deuxième Chapitre: Polymérisation Cationique de Différents Cétènes Aliphatiques et Aromatiques

Dans ce chapitre nous avons étudié les comportements en polymérisation et en copolymérisation cationiques de différents céto-cétènes substitués par des groupes alkyles et/ou aromatiques.

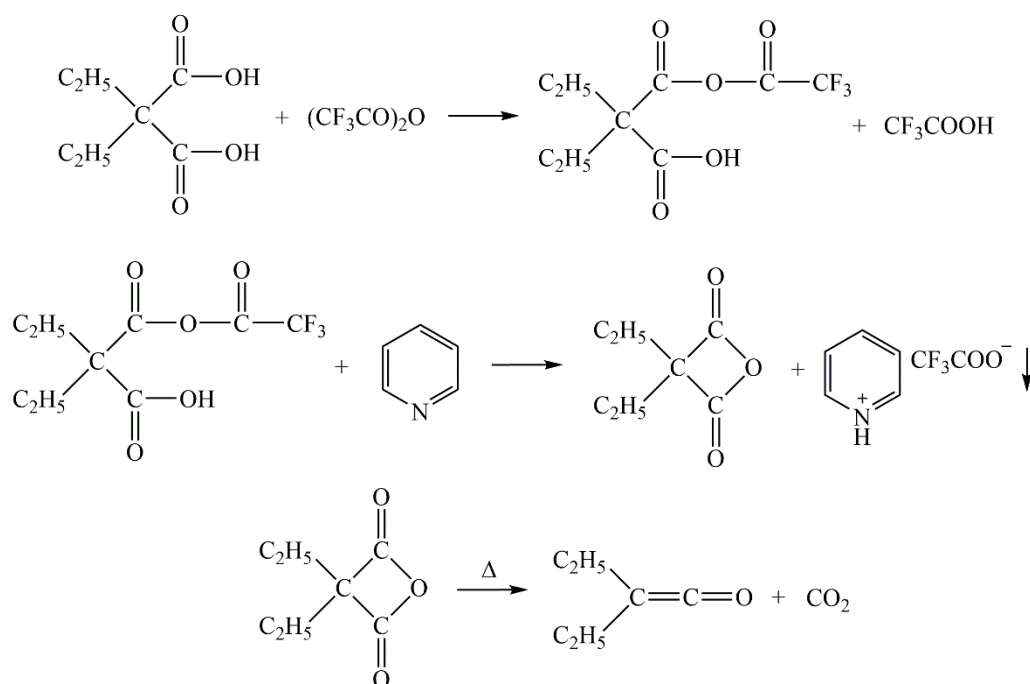
Synthèse des monomères

Les méthyléthylcétène (MEK), diéthylcétène (DEK), éthylphénylcétène (EPK) et diphenylcétène (DPK) ont été choisis en tant qu'homologues supérieurs du diméthylcétène.

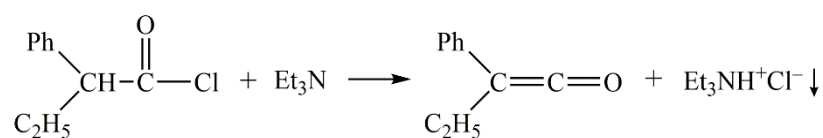
Le MEK a été formé par décomposition de l'anhydride méthyléthyl malonique à haute température sous pression réduite. En partant du diéthyl-2-méthylmalonate commercial, la procédure est la suivante (rendement global 22%) :



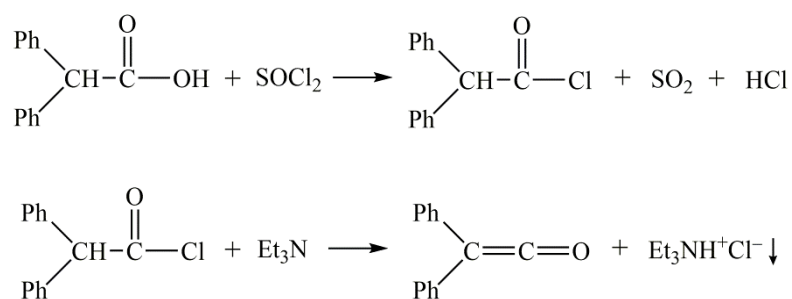
De manière similaire le DEK a été préparé par décomposition de l'anhydride diéthylmalonique à haute température sous pression réduite. À partir de l'acide diéthylmalonique commercial, la procédure de synthèse est la suivante (rendement global 25%) :



L'EPK a été préparé en utilisant une réaction de déshydrochloration à partir du chlorure de 2-phénylbutanoyle (rendement global 22%) :



Après la préparation du chlorure d'acyle précurseur, le DPK a également été obtenu par un procédé de déshydrochloration (rendement global 18%) :



Les monomères fraîchement synthétisés ont été manipulés avec précaution et conservés au réfrigérateur (à 4°C) sous une atmosphère sans oxygène, puis utilisés soit immédiatement soit au plus tard le lendemain (laps de temps < 15 h).

Homopolymérisation cationique

Un schéma général des conditions de polymérisation cationique, optimisé par les travaux précédents, a été adopté : température de réaction inférieure à 25°C, utilisation d'un solvant anhydre, $[\text{Monomère}]_0 = 3 \text{ mol} \cdot \text{L}^{-1}$, $[\text{Monomère}]_0 / [\text{Amorceur}]_0 = 100 / 1$.

Les quatre cétènes MEK, DEK, EPK et DPK ont été testés dans les essais d'homopolymérisation cationique utilisant des catalyseurs classiques à base d'acide de Brønsted ($\text{CF}_3\text{SO}_3\text{H}$, HClO_4 , acide stéarique), d'acide de Lewis (AlBr_3) ou de systèmes Friedel-Craft (AlCl_3 et FeCl_3 avec des ligands) pour des températures comprises entre -78°C et 25°C dans divers solvants (CH_2Cl_2 , toluène, DMF, NMP, ...).

Plus de 30 essais ont été réalisés et, quelles que soient les conditions, aucun polymère n'a été obtenu pour le MEK, le DEK et l'EPK. Le dérivé du monomère neutralisé par l'éthanol en fin de réaction est systématiquement retrouvé.

Seule la polymérisation dans le toluène ou CH_2Cl_2 amorcée par $\text{CF}_3\text{SO}_3\text{H}$ dans le cas du DPK a donné des polyesters de très faible masse molaire avec de bons rendements.

Essai	Monomère	Amorceur	Solvant	Température (°C)	Remarques
38	DPK	AlBr_3	CH_2Cl_2	-78	Pas de réaction
53		AlCl_3	CH_2Cl_2	-78	Pas de réaction
36		AlCl_3 , $(\text{CH}_3)_3\text{CCl}$	NMP	-20	Pas de réaction
37			Toluène	-78	Pas de réaction
34			CH_2Cl_2	-78	Pas de réaction
55				-20	Pas de réaction
35				0	Pas de réaction

39			-78	Rendement 83%, oligoester
40		CH₂Cl₂	-20	Rendement 48%, oligoester
41	CF₃SO₃H		0	Rendement 44%, oligoester
42		Toluène	0	Rendement 90%, oligoester
43		DMF	0	Pas de réaction
46			-78	Pas de réaction
47	HClO ₄	CH ₂ Cl ₂	0	Pas de réaction
68	Acide Stéarique, B(C ₆ F ₅) ₃	CH ₂ Cl ₂	-78	Pas de réaction

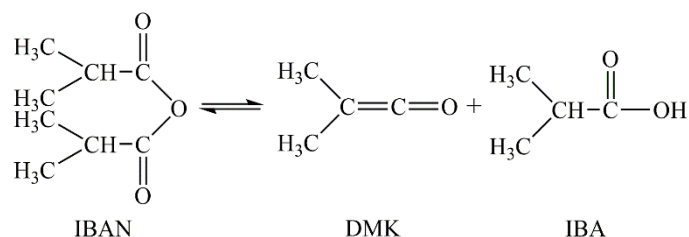
Les propriétés des polyesters obtenus sont compilées ci-après. Les oligomères (masses molaires en équivalent PMMA) présentent une T_g supérieure à l'ambiante, très sensible à \overline{M}_n , ainsi qu'une tenue thermique supérieure à 200°C.

Essai	\overline{M}_w (g.mol ⁻¹)	\overline{M}_n (g.mol ⁻¹)	D_M	T_g (°C) (2 ^{ème} chauffage)	$T_d^{5\%}$ (°C)	T_d^{Max} (°C)
39	1 940	1 516	1.28	88	284	372
40	1 396	1 066	1.31	59	225	326
41	1 042	785	1.33	58	227	291
42	1 080	796	1.36	46	203	277

Copolymérisation cationique avec le diméthylcétène

Étant donné que les quatre cétènes ci-dessus ont présenté une très faible réactivité dans des conditions d'homopolymérisation cationique, par analogie avec les alcènes, (dont seuls l'éthylène et le propylène homopolymérisent) il est devenu intéressant d'étudier leur copolymérisation avec le DMK.

Le diméthylcétène (DMK) a été synthétisé par pyrolyse de l'anhydride isobutyrique (IBAN) (rendement total 27%) :



Le DEK aliphatique et le DPK aromatique ont été respectivement choisis comme deuxième monomère, compte tenu du prix et de l'accessibilité des matières premières. Les conditions de polymérisation cationique choisies sont les suivantes : température de réaction à -20°C , CH_2Cl_2 anhydre comme solvant, mélange AlCl_3 / $(\text{CH}_3)_3\text{CCl}$ comme amorceur cationique, $[\text{Monomère}]_0 = 3 \text{ mol} \cdot \text{L}^{-1}$, et $[\text{Monomère}]_0 / [\text{Amorceur}]_0 = 100 / 1$.

Les résultats de la copolymérisation ont été répertoriés dans les deux tableaux ci-dessous:

Essai	Structure	Monomères : DMK : DEK (rapport molaire)	Polymères : n : m (rapport molaire)	Rendement (%)	$T_f(^{\circ}\text{C})$ (1 ^{er} chauffage) $T_f(^{\circ}\text{C})$ (2 ^{er} chauffage)	$\Delta H_f(\text{J} \cdot \text{g}^{-1})$ (2 ^{ème} chauffage)	$T_d^{5\%}$ ($^{\circ}\text{C}$)	T_d^{Max} ($^{\circ}\text{C}$)
58		DMK	DMK homopolymère	24	231 175 / 233	72,6	285	338
107		35 : 1	386 : 1	17	194 / 241 234	59,0	216	331
75		11 : 1	108 : 1	17	187 / 224 168 / 220	45,7	222	327
106		8 : 1	90 : 1	12	180 / 237 211 / 222 / 234	24,2	221	331
98		2 : 1	26 : 1	3	203 155 / 164	15,8	259	331
54		DEK	-	-	- -	-	-	-

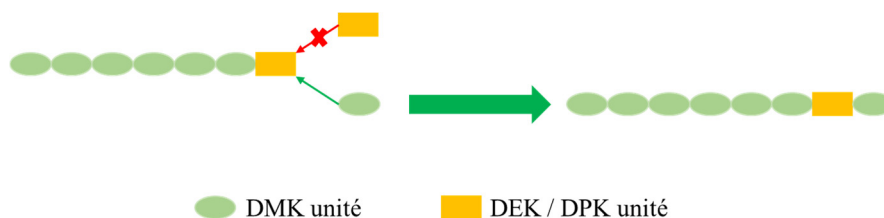
Essai	Structure	Monomères : DMK : DPK (rapport molaire)	Polymères : n : m (rapport molaire)	Rendement (%)	$T_f(^{\circ}\text{C})$ (1 ^{er} chauffage) $T_f(^{\circ}\text{C})$ (2 ^{er} chauffage)	$\Delta H_f(\text{J} \cdot \text{g}^{-1})$ (2 ^{ème} chauffage)	$T_d^{5\%}$ ($^{\circ}\text{C}$)	T_d^{Max} ($^{\circ}\text{C}$)
58		DMK	DMK homopolymère	24	231 175 / 233	72,6	285	338
69		36 : 1	436 : 1	28	191 / 235 164 / 231	46,4	290	340
93		13 : 1	196 : 1	20	188 / 247 239 / 252	45,7	248	334
103		6 : 1	84 : 1	16	188 / 238 224 / 231	24,2	229	333
95		1 : 1	6 : 1	3	196 185	15,8	212	341
55		DPK	-	-	- -	-	-	-

Dans ces conditions, un polymère de structure cétone est systématiquement obtenu. Le rendement de copolymérisation varie de 3% à 24% et est affecté proportionnellement à la quantité de DEK ou DPK introduite initialement. La composition du polymère obtenu, estimée par RMN ^1H , montre qu'une très faible quantité de DEK ou DPK est incorporée. Enfin, les propriétés thermiques sont aussi affectées par la composition finale du copolymère : la température de fusion, l'enthalpie de fusion et la tenue thermique diminuent. Pour les copolymères DPK / DMK, la fusion rime souvent avec dégradation. Il en est sensiblement de même pour les copolymères DEK / DMK sauf pour l'essai 98 qui conduit à une polycétone ($T_f = 164^\circ\text{C}$, $T_d^{5\%} = 259^\circ\text{C}$) possédant encore une fenêtre de mise oeuvre significative.

Nous avons par ailleurs estimé les rapports de réactivité r_1 et r_2 pour les copolymères DEK / DMK et DPK / DMK par la méthode de Kelen-Tudos :

- pour les systèmes DMK et DEK : $r_1 = 11,55$, $r_2 = 0,05$;
- pour les systèmes DMK et DPK : $r_1 = 15,58$, $r_2 = 0,83$.

En conséquence, nous considérons que des séquences DEK ou DPK ne peuvent exister. Il est donc raisonnable de considérer ces copolycétones comme des structures contenant un ou plusieurs motifs DEK ou DPK répartis au milieu de longues séquences de motifs DMK :



Troisième Chapitre: Modification de la Polycétone Issue du Diméthylcétène

Dans ce petit chapitre, trois réactions différentes de modification post-polymérisation (conversion du polypyrazole en polycétone, réarrangement de Beckmann one-pot, et réaction de fonctionnalisation avec un dithiocétal) sont présentées puis testées sur le PDMK. Ces trois voies de modification ne parviennent pas, sans exception, à fonctionnaliser le PDMK. Ces échecs ont néanmoins le mérite de prouver que la structure de type 1,3-dicétone du PDMK reste très spéciale par rapport aux autres polycétones, et lui assure une excellente stabilité chimique. Dans les conditions de la littérature, l'action du 1,2-éthanedithiol ne conduit pas aux fonctions dithioacétal, mais à des coupures de chaîne : en fin de réaction, une fraction s'avère soluble dans le CH_2Cl_2 ; après analyse, il s'agirait d'oligomères du PDMK de $\overline{M}_n = 2\,500 \text{ g.mol}^{-1}$.

Quatrième Chapitre: Autres Amorceurs Pour la Polymérisation Cationique des Cétènes

Jusqu'à présent, les quelques études sur la polymérisation cationique des cétènes étaient limitées à l'utilisation d'amorceurs classiques, principalement des acides de Lewis. Ce chapitre décrit trois autres types d'amorceurs cationiques et leurs performances sur nos monomères cétènes.

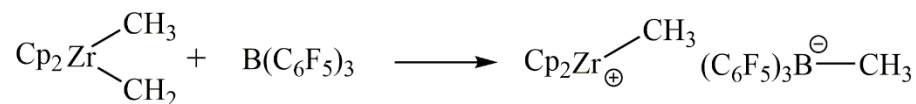
En comparaison des amorceurs «classiques» pour les polymérisations cationiques, les recherches sur de nouveaux types d'amorceurs se concentrent davantage sur la mise au point de composés écologiques, non toxiques, faciles à manipuler, permettant une polymérisation contrôlée et très efficace. Pour suivre ces tendances, nous avons testé successivement les catalyseurs solides, photosensibles et métallocènes sur les monomères DMK, DEK et DPK.

Résultats généraux

Les argiles comme la montmorillonite sont des composés acides pouvant jouer le rôle d'acides de Lewis ou de Brønsted : l'H-Maghnite se comporte comme un acide de Brønsted et polymérise cationiquement l'éthylglyoxylate, et l'Al-Montmorillonite se comporte comme un acide de Lewis si elle est parfaitement anhydre. Nous avons vu précédemment que les acides de Brønsted classiques ne semblent pas être de bons candidats pour la polymérisation du DMK, probablement à cause d'une addition rapide du contre-ion sur l'espèce créée, empêchant ainsi toute propagation. L'hypothèse faite dans ces essais était que la formation d'espèces stables soit difficile, voire n'ait pas lieu, avec un amorceur solide telles que les montmorillonites. Elles ont donc été mises en jeu avec le DMK, le DEK et le DPK, sans succès cependant.

Par voie photochimique, nous avons travaillé avec deux systèmes absorbant à plus de 400 nm (l'absorption maximum du DMK étant à 375 nm) en utilisant deux sources lumineuses différentes (lampe à vapeur de Mercure et LED à 460 nm). Un premier système à trois composés a fait ses preuves dans la polymérisation cationique des oxiranes. Il est composé d'un sel de diaryliodonium jouant le rôle de photoamorceur, de la camphorquinone jouant le rôle de photosensibilisateur et d'une troisième molécule donneuse de proton. Le second système utilise des ferrocènes tel que le 1,1'-bis(diméthylsilyl)ferrocène. Il a en effet été montré que ce type de molécules jouait le rôle d'amorceur cationique dans le cadre de la polymérisation du pyrrole et d'oxiranes. Quel que soit le système et les sources utilisées, les tentatives sont restées vaines. Aucun polymère n'est obtenu en fin de réaction. Notons qu'il reste beaucoup de monomère en fin de réaction, la neutralisation à l'éthanol restant toujours très exothermique. En effet, la polymérisation est réalisée à 3 mol.L⁻¹ (il a été montré dans les travaux précédents qu'elle n'a pas lieu en milieu plus dilué), et à cette concentration la solution de cétène absorbe certainement la totalité des longueurs d'ondes des sources employées.

Les catalyseurs métallocènes issus de la réaction du bis(cyclopentadiényl) diméthylzirconium (Cp_2ZrMe_2) avec des tris(penta-fluorophényl)boranes ($\text{B}(\text{C}_6\text{F}_5)_3$) sont le dernier système utilisé :



C'est un type de métallocène simple ayant l'énorme avantage d'être commercial.

Si aucun polymère n'a été obtenu avec les MEK, DEK et DPK nous avons en revanche réussi à polymériser les monomères EPK et DMK. Dans le cas de l'EPK, le rendement ne dépasse pas 3%, et un oligoester thermiquement peu stable est obtenu ($\overline{M}_n = 3\,500 \text{ g.mol}^{-1}$, $T_d^{5\%} = 168^\circ\text{C}$). En revanche, pour le DMK, le système métallocène s'est révélé très efficace dans un mécanisme de polymérisation par insertion, conduisant à un polyester aliphatique semicristallin de masse molaire importante, décrit ci-après.

Polyester de DMK utilisant des catalyseurs à base de métallocène

Toutes les expériences ont été conduites avec $[\text{Monomère}]_0 = 3 \text{ mol.L}^{-1}$ et $[\text{Monomère}]_0 / [\text{Amorceur}]_0 = 1\,000 / 1$ dans des conditions sans oxygène et anhydres. Le catalyseur a été ajouté sous forme de solution, préparée juste avant utilisation, de bis(cyclopentadiényl)diméthyl zirconium (Cp_2ZrMe_2) et de tris(pentafluorophényl)borane ($\text{B}(\text{C}_6\text{F}_5)_3$) dans le solvant correspondant ($[\text{Cp}_2\text{ZrMe}_2]_0 = [\text{B}(\text{C}_6\text{F}_5)_3]_0 = 0,125 \text{ mol.L}^{-1}$) après que le système réactionnel se soit stabilisé à la température visée. Le milieu réactif a été maintenu sous agitation pendant 5 h à cette température (négative) puis laissé à atteindre la température ambiante. Le temps de polymérisation a toujours duré toute une nuit.

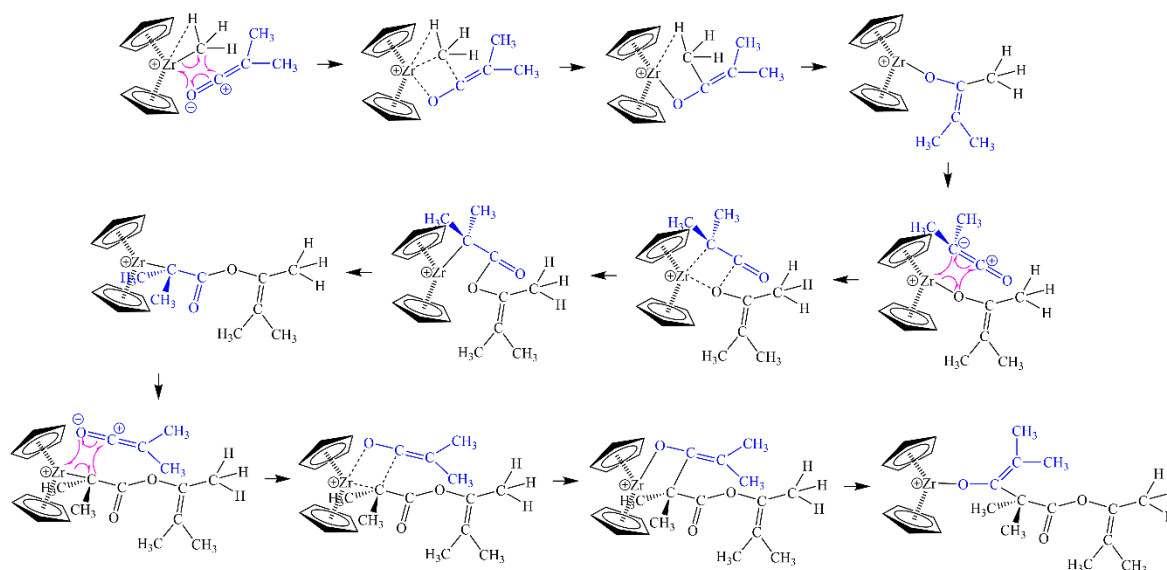
Les différentes conditions expérimentales et les résultats sont présentés dans le tableau suivant:

Essai	Solvant	Température de reaction (°C)	\overline{M}_w (g·mol ⁻¹)	\overline{M}_n (g·mol ⁻¹)	D_M	Rendement (%)	T_g (°C)	T_f (°C)	ΔH_f (J·g ⁻¹)	$T_d^{5\%}$ (°C)	T_d^{Max} (°C)
							(2 ^{ème} chauffage)				
59	CH ₂ Cl ₂	-20	33 800	16 000	2,11	24	35	-	-	254	383
60	CH ₂ Cl ₂	-78	128 900	76 600	1,68	58	51	-	-	328	390
86	Toluene	-78	236 500	120 100	1,97	31	76	198	21.2	322	392
88	Diethyl ether	-78	359 700	306 000	1,19	68	69	200	22.2	332	391

Une diminution de la température de polymérisation réduit les cinétiques des réactions de transfert au profit de la propagation de la polymérisation cationique et favorise l'obtention de fortes masses molaires. La polarité du milieu (CH₂Cl₂ > diéthyéther > toluène) aurait aussi pu jouer un rôle, un solvant polaire pouvant faciliter des réactions de transfert.

D'après le tableau, à -78°C, nous obtenons des masses molaires jusque là jamais atteintes pour une structure polyester du DMK. Les conditions optimum dans le diéthyéther conduisent à un polymère possédant d'excellentes propriétés ($\overline{M}_n \sim 300\,000$ g·mol⁻¹, $T_g \sim 70^\circ\text{C}$, $T_f \sim 200^\circ\text{C}$, $T_d^{5\%} \sim 330^\circ\text{C}$), avec un rendement satisfaisant de 68%.

La structure polyester obtenue à partir du catalyseur à base métallocène, nécessite l'ouverture alternative de la double liaison vinylique et du carbonyle. Les céto-cétènes pouvant avoir une charge négative délocalisée sur le carbone substitué ou sur l'oxygène le zirconium à deux choix. Ainsi, lorsqu'un cétène approche du centre actif déficient en électrons, le Zr⁺, lié à un méthyl, pourrait réagir d'abord avec l'oxygène. Puis un réarrangement s'opère faisant apparaître une liaison Zr-O différente de la précédente et ne réagissant qu'avec les carbones, cette insertion alternante conduisant au polyester :



Notons par ailleurs, qu'après plusieurs mois de stockage (six mois) à l'air à température ambiante, ces polyesters à base de DMK se seraient légèrement dégradés au regard de l'analyse de leurs masses molaires modifiant quelque peu leur propriétés.

Essai	SEC			MALS	T_g (°C)	T_f (°C) (2 ^{ème} chauffage)	ΔH_f (J·g ⁻¹)	$T_d^{5\%}$ (°C)	T_d^{Max} (°C)
	\overline{M}_w	\overline{M}_n	D_M	\overline{M}_w					
	(g·mol ⁻¹)	(g·mol ⁻¹)		(g·mol ⁻¹)					
59 (t_0)	33 800	16 000	2,11	-	35	-	-	254	383
59 ($t_0 + 180j$)	7 000	2 200	3,16	4 500	25	-	-	143	385
60 (t_0)	128 900	76 600	1,68	-	51	-	-	328	390
60 ($t_0 + 180j$)	6 100	2 500	2,47	31 000	25	-	-	143	389
86 (t_0)	236 500	120 100	1,97	-	76	198	21.2	322	392
86 ($t_0 + 180j$)	33 200	12 500	2,66	44 000	44	187	2.5	264	390
88 (t_0)	359 700	306 000	1,19	-	69°C	200	22.2	332	391
88 ($t_0 + 180j$)	135 800	43 800	3,10	210 100	66°C	199	6.0	326	389

Deux possibilités pourraient être retenues. La première, peu probable étant données les conditions atmosphériques de stockage, serait une hydrolyse de quelques fonctions esters ; la seconde serait la présence de quelques unités acétal dans la structure polyester qui occasionneraient les coupures de chaîne. Prenant en compte les masses molaires avant et

après dégradation, ce taux de motifs acétal a été estimé à de très faibles valeurs (par exemple 0,4% dans le toluène et 0,1% dans le diéthyléther), expliquant leur non détection par RMN.

Conclusion Générale

L'objectif de ce travail était d'élargir la famille des structures des polycétone aliphatiques issues de céto-cétènes. Plusieurs verrous étaient à franchir, à commencer par la synthèse de ces céto-cétènes, voire de leur précurseur dans certains cas, et en quantités suffisantes.

Leurs homopolymérisations et copolymérisations ont ensuite été étudiées et les polymères obtenus caractérisés. Avec les acides de Lewis, force est de constater que seul le DMK a conduit à une structure polycétone par polymérisation cationique. Les homologues supérieurs, ayant probablement un encombrement stérique trop important, n'ayant presque rien donné seul. Par copolymérisation, une ou deux structures (DMK-DEK et DMK-DPK) sont à retenir même si celles-ci possèdent de moins bonnes tenues thermiques par rapport au PDMK et qu'elles sont obtenues avec des rendements faibles. Les rapports de réactivités estimés attesteraient de structures PDMK contenant quelques motifs isolés du co-monomère dans la chaîne : DMK-DEK ($r_1 = 11,55$, $r_2 = 0,05$) et DMK / DPK ($r_1 = 20,39$, $r_2 = 2,24$).

La modification chimique du PDMK s'est également révélée très délicate, révélant la très bonne stabilité chimique de la structure 1,3-dicétone.

Enfin, différents catalyseurs ont été utilisés afin de tester des catalyses hétérogènes, sous rayonnement ou à partir de catalyseurs métallocène. Avec les montmorillonites, rien de probant n'a été obtenu. Sous UV, le procédé utilisé ne conduit pas au polymère non plus. Seule la voie métallocène s'avère être une bonne surprise, à la fois par la structure obtenue (polyester) et par les masses molaires très élevées jamais atteintes jusqu'ici ($\overline{M}_n \sim 300\,000$ g·mol⁻¹, $T_g \sim 70^\circ\text{C}$, $T_f \sim 200^\circ\text{C}$, $T_d^{5\%} \sim 330^\circ\text{C}$), ainsi qu'un rendement satisfaisant (68%).

Les perspectives envisagées à la suite de ce travail sont principalement orientées vers la voie métallocène. En effet, le potentiel des polyesters de très fortes masses obtenus reste à explorer. Ce premier essai avec un amorceur commercial en appelle d'autres. L'influence du milieu réactionnel, du contre ion plus ou moins électrophile et de la structure du catalyseur lui-même sont à étudier. Enfin, une étude complète de la dégradation serait très intéressante à mener afin d'accroître les connaissances sur ces polymères peu étudiés jusqu'à présent.

[1] H. Egret, J.-P. Couvercelle, J. Belleney, C. Bunel, Cationic polymerization of dimethyl ketene, *European Polymer Journal*, 38 (2002) 1953-1961.

[2] H. Staudinger, Ketene: L. Mitteilung. Über additions- und polymerisations-reaktionen des dimethylketens. 1. Über neue verbindungen des dimethylketens mit kohlendioxyd, *Helvetica Chimica Acta*, 8 (1925) 306-332.

[3] M. Brestaz, Synthèse et caractérisation de polyesters à partir du diméthylcétène et de composés carbonylés, INSA de Rouen, 2009.

[4] H. Egret, Synthèse et caractérisation des polymères du diméthylcétène. Application à la perméabilité aux gaz, Rouen, 1998.

[5] A. Bienvenu, Modification et perfectionnement du procédé de synthèse et de polymérisation du diméthylcétène. Caractérisation et propriétés des polydiméthylcétènes et de leurs mélanges, INSA de Rouen, 2004.

[6] E. Drent, Polymeric polyalcohols, U.S. Patent 5,071,926[P]. 1991-12-10.

[7] J. E. Flood, D. H. Weinkauff and M. Londa, in *Proceedings of the 53rd Society of Plastics Engineers Annual Technical Conference (ANTEC)*, Boston, May 1995, p. 2326.

[8] H. Wang, Synthèse et caractérisation de nouvelles polycétones aliphatiques à partir des cétènes, Rouen, INSA, 2013.

[9] A.D. Allen, T.T. Tidwell, Ring opening of cyclobutene-1,2-dione and 3-trimethylsilyl-cyclobutene-1,2-dione. Dimerization/decarbonylation of a bisketene to a ketenylbutenolide, *Canadian Journal of Chemistry*, 77 (1999) 802-805.

[10] G. Natta, G. Mazzanti, G.F. Pregaglia, M. Binaghi, Crystalline polymers of dialkyl ketenes, *Die Makromolekulare Chemie*, 44 (1961) 537-549.

[11] G.F. Pregaglia, M. Binaghi, M. Cambini, Polydimethylketene with carbon-oxygen backbone structure, *Die Makromolekulare Chemie*, 67 (1963) 10-30.

[12] Linemann, R.; Le, G., Synthesis method for polydimethylketene by Friedel-Craft cationic polymerization of dimethylketene, FR. Pat. 2,846,660[P]. 2004.

[13] G. Natta, G. Mazzanti, G. Pregaglia, M. Binaghi, M. Peraldo, Crystalline polymers of dimethylketene, *Journal of the American Chemical Society*, 82 (1960) 4742-4743.

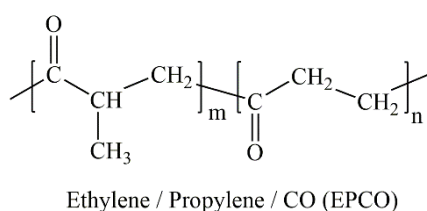
[14] T.E. Kiovsky, R.C. Kromer, Polymeric pyrrollic derivative, U.S. Patent 3,979, 374[P]. 1976-9-7.

-
- [15] Z. Jiang, S. Sangneria, A. Sen, Polymers incorporating backbone thiophene, furan, and alcohol functionalities formed through chemical modifications of alternating olefin-carbon monoxide copolymers, *Journal of Polymer Science Part A: Polymer Chemistry*, 32 (1994) 841-847.
- [16] C.W. Fitko, R. Abraham, Thermosetting polybisphenols, U.S. Patent 3,317,472 [P]. 1967-5-2.
- [17] D. Coffman, H. Hoehn, J. Maynard, Reductive amination of ethylene/carbon monoxide polyketones. A new class of polyamines, *Journal of the American Chemical Society*, 76 (1954) 6394-6399.
- [18] S.L. Scott, Polymeric polythiols, U.S. Patent 2,495,293[P]. 1950-1-24.
- [19] S.-Y. Lu, R.M. Paton, M.J. Green, A.R. Lucy, Synthesis and characterization of polyketoximes derived from alkene-carbon monoxide copolymers, *European polymer journal*, 32 (1996) 1285-1288.
- [20] R. Michel, W. Murphey, Intramolecular rearrangements of polyketones, *Journal of Polymer Science*, 55 (1961) 741-751.
- [21] K. Nozaki, N. Kosaka, V.M. Graubner, T. Hiyama, Methylenation of an optically active γ -polyketone: Synthesis of a new class of hydrocarbon polymers with main-chain chirality, *Macromolecules*, 34 (2001) 6167-6168.

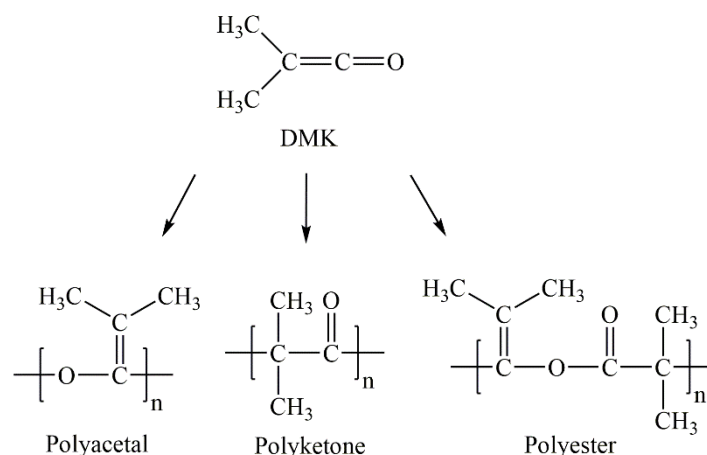
General Introduction

With only a few still active laboratories all around the world focusing on, ketene polymerization is a less mainstreamed topic, but it needs more research concerns and further investigations because of its potentially industrial output. Indeed, ketenes can represent an original way to obtain polyketones.

Polyketone is a unique engineering plastics, the backbone of which is only composed of carbons. Its flexible chains together with the molecular symmetry enhances crystallization which results in many differentiated properties such as excellent chemical and impact resistance, exceptional wear resistance and barrier properties. Perfectly alternating olefin(s) / carbon monoxide copolymers and terpolymers are considered to be the main members of this polymer family, as exemplified in the following figure with the ethylene / propylene / CO terpolymer:



Another synthetic route makes it possible to obtain aliphatic polyketones by polymerization of ketenes. Indeed, the Macromolecular Materials team of the PBS Laboratory has been studying, for several years, these particular monomers. Thus, a ketoketene, dimethylketene, has already been the subject of four theses defended in 1998, 2004, 2009 and 2013. These works have studied its synthesis and ionic polymerization, and furthermore have highlighted the possibility that, according to the experimental conditions used, three types of polymers can be obtained: a polyacetal, a polyester and a polyketone, represented on the next figure.



Structures obtained by the polymerization of DMK

As a polymer material for potential industrial applications, having an excellent gas barrier property even at high humidity degree, dimethylketene-based polyketone (PDMK), mainly obtained with cationic initiators, presented a major limitation: its high melting point, close to its degradation temperature, leads to a narrow processing window.

Another monomer, ethylketene, was also successfully polymerized and co-polymerized with DMK into a polyketone thanks to the team expertise. Unfortunately, the properties were not satisfactory.

To tackle these problems, three different directions were considered:

- different di-substituted aliphatic and aromatic ketenes were tried to be homo- or co-polymerized, into polyketones, with the well-studied dimethylketene under classic cationic conditions, aiming to improve polymer properties by changing the molecular chain structure from a synthetic point of view;

- PDMK was functionalized by ketone group conversion reactions to change its properties by changing the molecular chain structure from a post-synthetic point of view;

- the revolutionized cationic polymerization of aliphatic and phenyl ketenes including DMK was tried with some new types of initiators and polymerization systems, in order to

improve catalytic efficiency and selectivity, and to broaden the knowledge on these special monomers.

This thesis is organized in four chapters. After this general introduction, Chapter 1 gives the state of the art of ketene cationic polymerization. The overview, current stage and development trend of ketene synthetic chemistry, ketene polymerization and polyketone modification techniques are presented.

Chapter 2 investigates the cationic polymerization of different aliphatic and aromatic ketenes. Monomer synthesis are detailed and homopolymerization of methylethylketene (MEK), diethylketene (DEK), ethylphenylketene (EPK) and diphenylketene (DPK) are carried out using classical cationic initiators. We also study the copolymerization behaviors of typical aliphatic DEK and aromatic DPK with dimethylketene (DMK).

Chapter 3 presents our post-polymerization modification trials upon our well-investigated and reliable PDMK, in three possible reaction pathways including conversion of polypyrazole from polyketone, one-pot Beckmann rearrangement and dithioketal functionalized reaction using different reagents.

Finally, Chapter 4 describes three different types of updated cationic initiators (solid, photo and metallocene) and their catalytic performance on our ketene monomers (DMK, MEK, DEK, EPK and DPK).

1. State of the Art

This chapter presents a brief overview of ketene chemistry and the state of the art of ketene-based polymer science and polyketone modification techniques.

1.1 Ketene Synthesis

Ketene is a type of particular derivative from carboxylic acids, which contains two consecutive double bonds ($R_1R_2C=C=O$). The unique adjacent double-double bond structure has enabled significantly high reactivity to ketenes, which derives from their unique cumulene structure, with the highest occupied molecular orbital (HOMO) perpendicular to the ketene plane and the lowest unoccupied molecular orbital (LUMO) in the ketene plane (Figure 1-1).

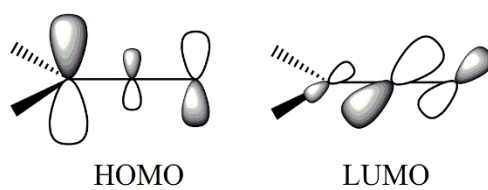


Figure 1-1. Ketene cumulene structure [1]

The partial negatively charged end-carbon (C_2) and oxygen atoms attract electrophiles in most ketene reactions, while the partial positive charge on the central carbon atom (C_1) enables the attack from nucleophiles (Figure 1-2).

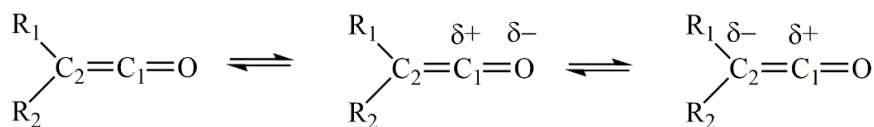


Figure 1-2. Isoelectronic structures of ketenes [2]

In view of a class of highly reactive difunctional species, ketenes have shown potential utility and fascinating value in organic synthesis of nucleophile, electrophile and cycloaddition reactions [3-6], and have played a role of critical intermediates for considerable organic procedures [7-9], among which $[2+2]$ cycloaddition was considered as a feature of ketene chemistry (Figure 1-3).

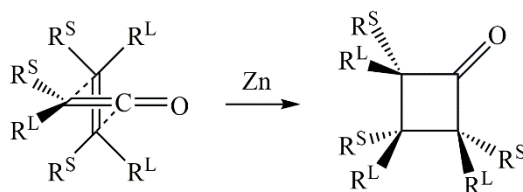


Figure 1-3. The $[2+2]$ cycloaddition of ketenes [10]

However, acting as a double-edged sword, the high reactivity makes ketenes intrinsically unstable when isolated and exposed to the air or high temperature conditions (Figure 1-4). One can notice that the polyperoxides obtained with dioxygen are considered explosives.

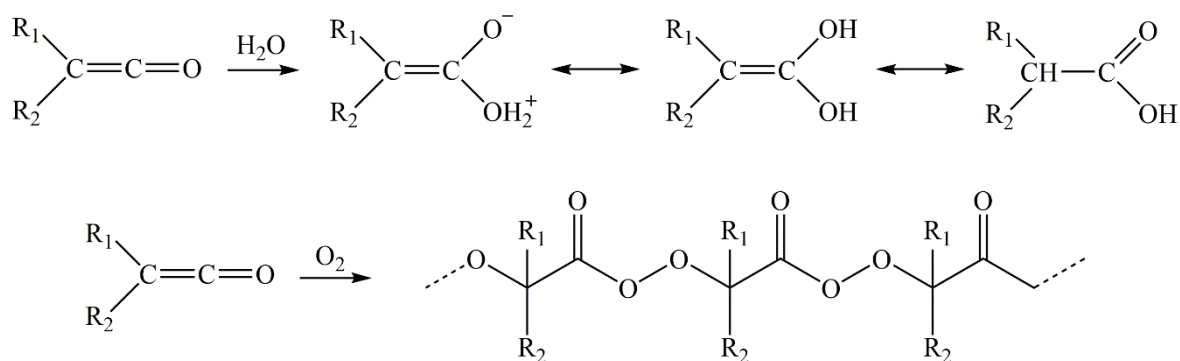


Figure 1-4. Reactions between ketenes and H_2O or O_2 [11]

Depending on the contained functional groups R_1 and R_2 , ketenes are generally classified by aldoketenes and ketoketenes [12]. The existence of ketenes has been established

more than 100 years, since the first diphenylketene ($\text{Ph}_2\text{C}=\text{C}=\text{O}$) as a relative stable ketoketene was synthesized and isolated by Staudinger in 1905 [13], who founded the modern polymer science and was awarded the Nobel Prize in 1958. After that, other aldoketenes or ketoketenes with various substances were successfully synthesized according to the updated methods.

1.1.1 The Staudinger Method

Preparation and isolation of ketenes by dehalogenation of α -halo carboxylic acid derivatives or dehydrohalogenation of acyl halides was developed and confirmed by Staudinger relatively in 1905 and 1911 [14].

1.1.1.1 Dehalogenation of α -halo carboxylic acid derivatives

The first diphenylketene derived from dechlorination of 2-chloro(diphenyl)acetyl chloride using zinc or triphenylphosphine as a catalyst (Figure 1-5), which was regarded as the typical Staudinger Method.

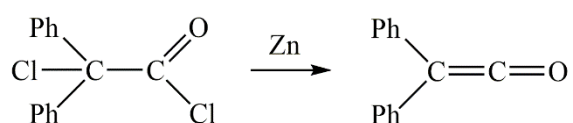


Figure 1-5. Dehalogenation of 2-chloro(diphenyl)acetyl chloride using zinc [13]

Dimethylketene was successfully prepared by Norton and Smith in a Staudinger method, via debromination of 2-bromoisobutyryl bromide with zinc in ethyl acetate and distillation as a solution under reduced pressure (Figure 1-6). The dimethylketene was finally obtained with a satisfying yield from 46 to 54%, in the solution of ethyl acetate with an overall 10% concentration.

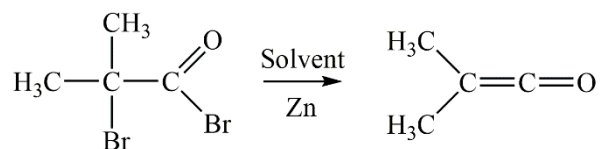


Figure 1-6. Debromination of 2-bromoisobutyryl bromide using zinc [15]

C.C. McCarney et al [16] also succeeded to extend the Staudinger method to aldoketene synthesis. They used Zn as the catalyst and THF as the solvent to debrominate the 2-bromobutyryl bromide (Figure 1-7). Ethylketene / THF solution mixture was then distilled under 100 mmHg pressure in 60~65% yield.

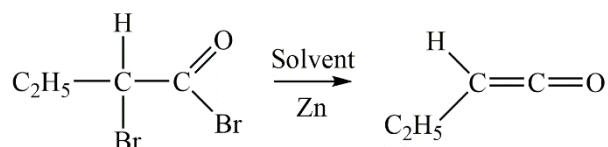


Figure 1-7. Debrominate the 2-bromobutyryl bromide using zinc [16]

1.1.1.2 Dehydrohalogenation of acyl halides

Dehydrohalogenation of diphenylacetyl chloride was another feasible route to produce diphenylketene (Figure 1-8). This method has usually been effective for the isolation of ketenes only when two bulky or aryl substituents existed.

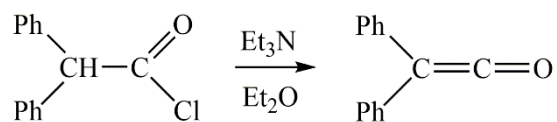


Figure 1-8. Dehydrohalogenation of diphenylacetyl chloride with triethylamine [14]

Dehydrochlorination was also successful in the preparation of the very stable trimethylsilylketene (Figure 1-9).

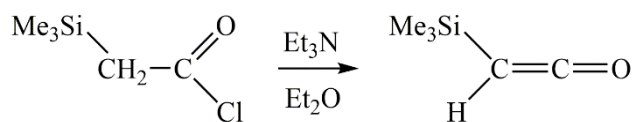


Figure 1-9. Dehydrochlorination of (trimethylsilyl)acetyl chloride with triethylamine [17]

It is important to note, however, that the isolation of more reactive ketenes by dehydrohalogenation may be difficult to approach. Indeed, it is evidenced that the dehydrohalogenation step is reversible (Figure 1-10).

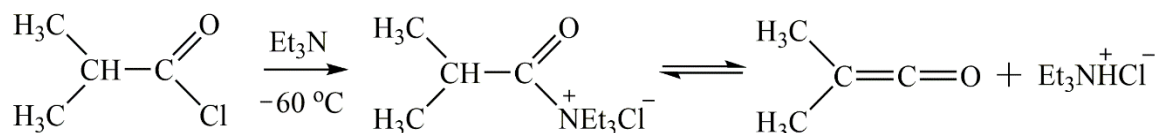


Figure 1-10. Reaction between isobutyryl chloride and triethylamine [18, 19]

The Staudinger method still remains as one of the most effective way to produce solutions of isolated ketenes even in this new era of chemical synthesis.

1.1.2 Thermal Generation Method

Coming after the Staudinger method, pyrolysis of ketones, acids, malonic anhydrides, acetic anhydrides, esters, ketene dimers and other substances were sequentially proved to be the efficient way to produce neat ketenes in satisfying yields.

1.1.2.1 Pyrolysis of Ketones

Ketene itself was conveniently prepared by the pyrolysis of acetone with burners in a glass tube [20] or with a metal filament (Hurd lamp) [21]. The optimized conditions were

given in the literature: temperature at 695~705°C, flow rate of acetone at 5 mL·min⁻¹, resulting yields ranged from 35% to 45% (Figure 1-11).

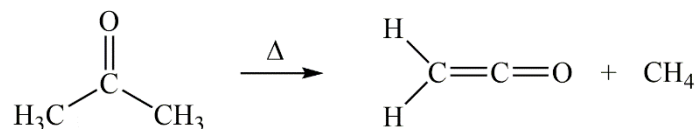


Figure 1-11. Pyrolysis of acetone [20]

1.1.2.2 Pyrolysis of Acids

Ketene was also directly prepared on the industrial scale by pyrolysis of acetic acid [22]. The kinetic investigation demonstrated that the decomposition of acetic acid proceeded homogeneously and molecularly via two competing first-order reaction channels at nearly equal rates over the temperature range of 1300~1950 K in a single-pulse shock tube, to form methane and carbon dioxide on the one hand, and ketene and water on the other (Figure 1-12).

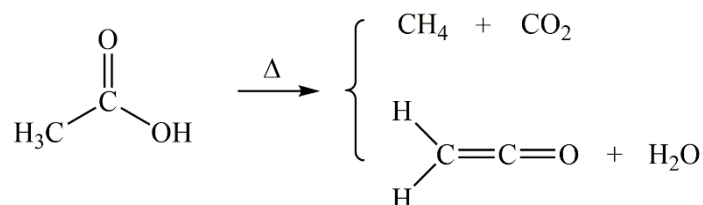


Figure 1-12. Pyrolysis of acetic acid [23]

A special gold ketenylidene was reported by Green et al, which formed around 400K from acetic acid chemisorbed on a nano-Au / TiO₂ catalyst by oxidation with O₂ (Figure 1-13). This ketenylidene material was identified by the observed characteristic IR stretching frequency at 2040 cm⁻¹, and was found to possess ketene characteristics in some typical reactions. This acetate-to-ketenylidene formation path is regarded as a crucial step for biomass conversion into more valuable industrial chemicals.

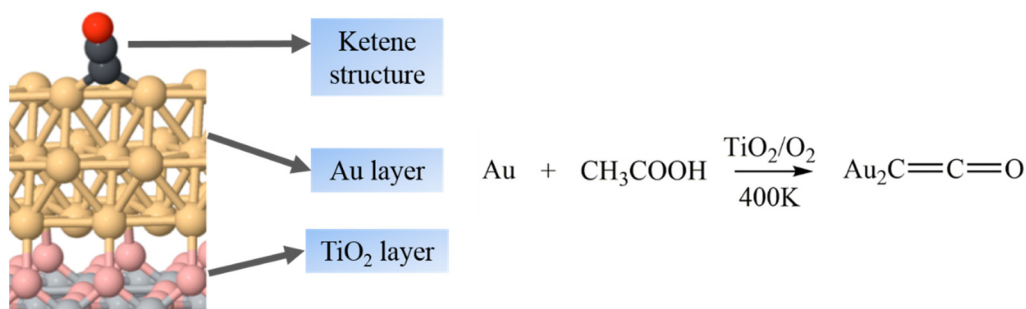


Figure 1-13. Gold ketenylidene formed by acetic acid [24]

1.1.2.3 Pyrolysis of Malonic Anhydrides

An alternative preparation route of ketenes is thermal decomposition of malonic anhydrides, which is capable of leading neat ketenes with good yields. Ketene, methylketene, dimethylketene and other ketenes with methyl or ethyl substituents are formed by this methodology (Figure 1-14).

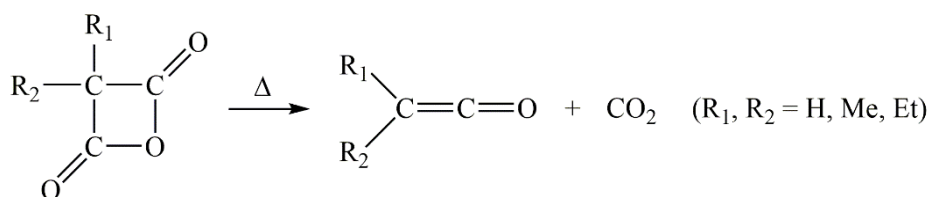


Figure 1-14. Pyrolysis of malonic anhydrides [25, 26]

1.1.2.4 Pyrolysis of Acetic Anhydrides

Acetic anhydride can also be pyrolyzed to ketene and acetic acid at atmospheric pressure in a hot tube maintained at a temperature of 500~510°C (Figure 1-15). It was confirmed that other decomposition products (e.g. carbon dioxide, methane) would be mixed in the desired products at a temperature of 600°C, or above. To prevent recombination, rapid separation of the reaction products is essential. A final conversion value from 17 to 31% with corresponding efficiencies of 80~96% can be obtained due to different residence time [27, 28].

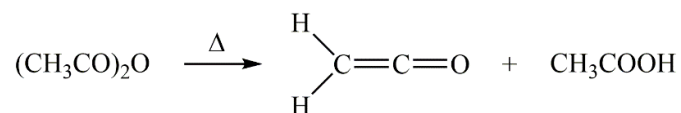


Figure 1-15. Pyrolysis of acetic anhydride

Generation of triethylsilylketene [17], dimethylketene [29, 30] and ethylketene [31] were additionally reported by pyrolysis of the corresponding anhydrides (Figure 1-16).

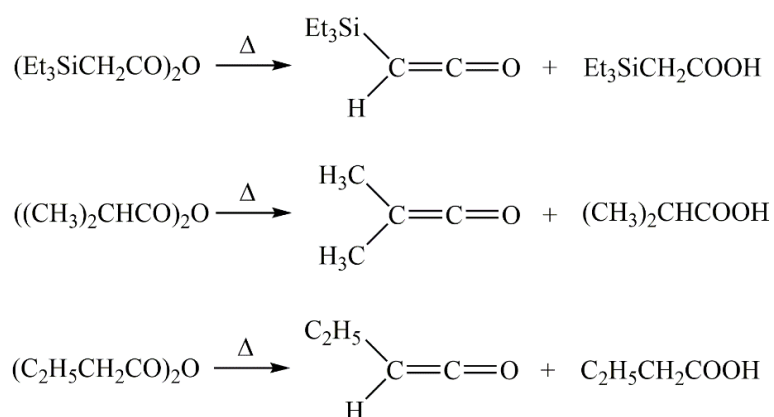


Figure 1-16. Triethylsilylketene, dimethylketene and ethylketene preparation by pyrolysis of anhydrides

1.1.2.5 Pyrolysis of Esters

Heated at 625°C, phenyl acetate pyrolysis occurred into ketene and phenol at a yield of 84% (Figure 1-17).

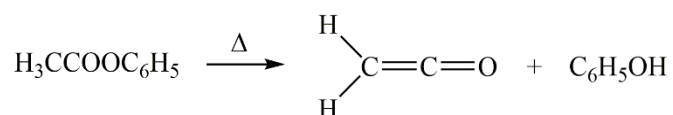


Figure 1-17. Pyrolysis of phenyl acetate [32]

Pyrolysis of isopropenyl esters at 170°C was also used to generate ketenes with long hydrocarbon chains through a mechanism involving transition of the ester enol, whereas

only the dimer can be finally obtained in the case of n-hexadecylketene due to its high reactivity (Figure 1-18).

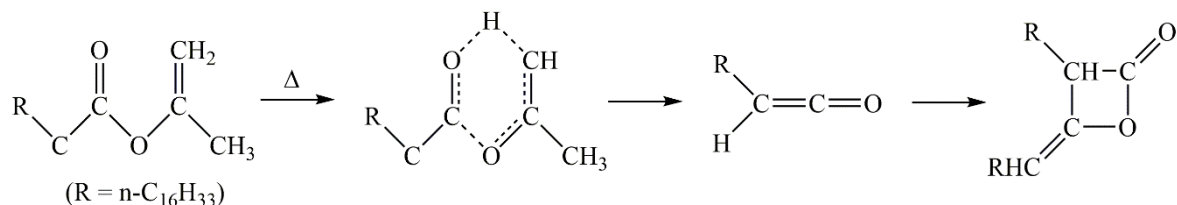


Figure 1-18. Pyrolysis of isopropenyl esters in the case of n-hexadecylketene [33]

Pyrolysis of alkyl acetoacetates led to an acylketene and the alcohol, and evidently proceeded through a pericyclic mechanism involving transition of the ester enol. Accelerations in reactivity of the ester thermolysis varied with the different R groups, among which the isopropenyl and tert-butyl esters proved to be significant owing to the more dissociative ROH from a steric effect (Figure 1-19).

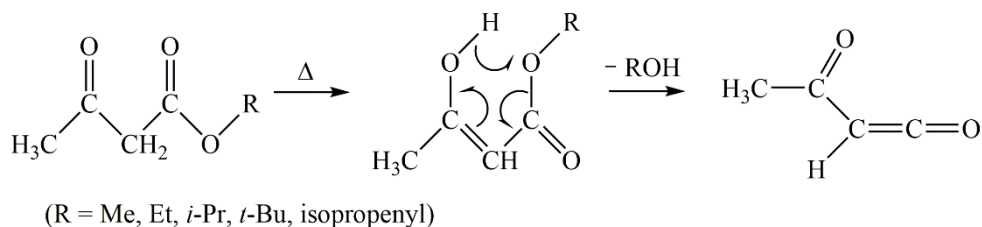


Figure 1-19. Pyrolysis of alkyl acetoacetates with different R groups [34, 35]

1.1.2.6 Pyrolysis of Ketene Dimers

Pyrolysis of ketene dimers provides a simple synthesis route to ketenes. Ketene itself [36] and dimethylketene [37] were successfully obtained by thermolysis of diketene as the colorless solid and tetramethyl-1,3-cyclobutanedione as the yellow oil (Figure 1-20).

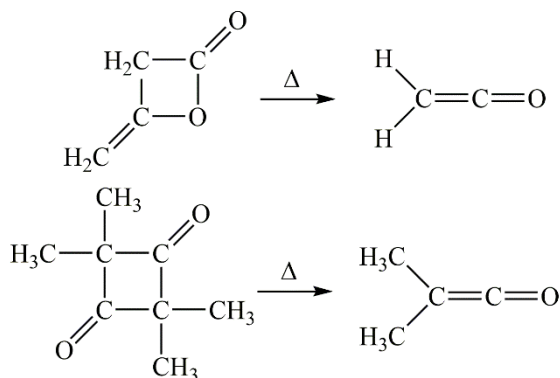


Figure 1-20. Pyrolysis of ketene dimers

1.1.2.7 Pyrolysis of Meldrum's Acid

A special synthetic route to ketenes involves thermal treatment of Meldrum's acids. In the reports, this generating reaction was performed under flash vacuum pyrolysis conditions (500°C, 0.01 torr) to give the dialkyl ketene after loss of acetone and carbon dioxide [38, 39]. Moreover, recent studies showed that heating the dibenzyl Meldrum's acid at 200°C or above can also result in highly efficient formation of the corresponding ketene [40]. These pyrolysis reactions are illustrated by Figure 1-21.

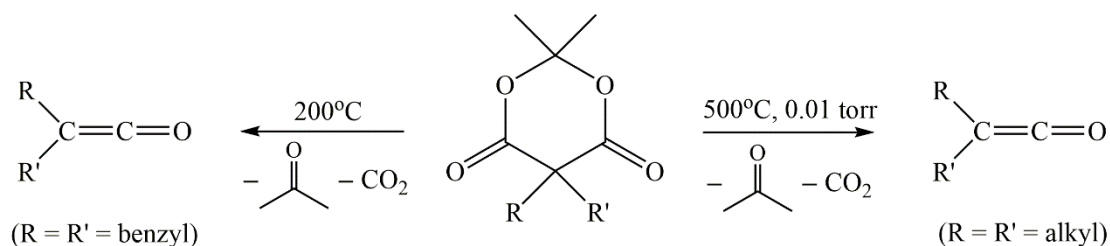


Figure 1-21. Pyrolysis of Meldrum's acids

In a pathbreaking strategy, Leibfarth et al. [41] applied Meldrum's acid-containing monomers in radical polymerizations and thermally treated the derivative to successfully provide crosslinked polymers via ketene dimerization reactions (Figure 1-22).

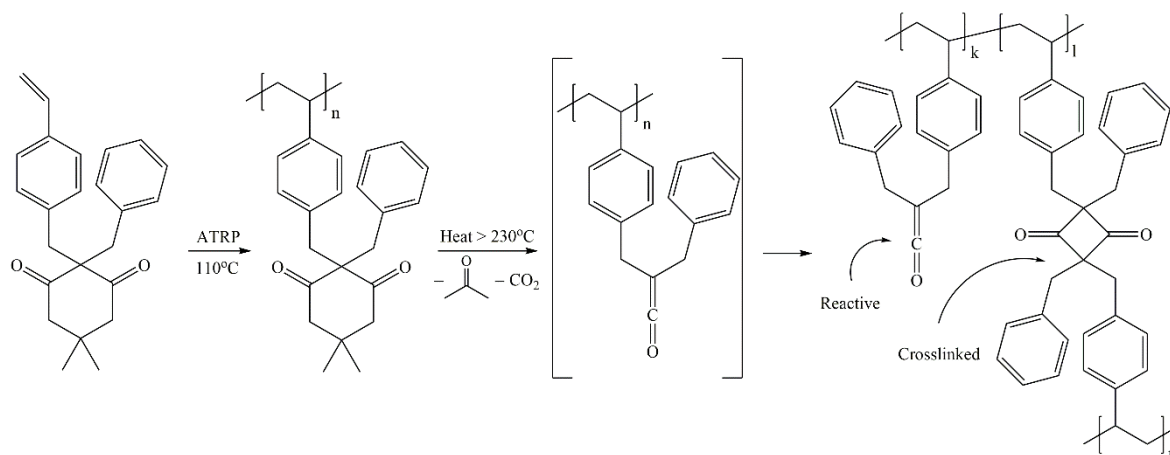


Figure 1-22. Synthesis of Meldrum's acid-containing polymer and its thermolytic crosslinking [41]

1.1.3 Photochemical Generation Method

1.1.3.1 Photolysis of Ketene Dimers

Although the conversions are quite limited, photolysis of ketene dimers is supposed to be a possible method to produce ketenes in solution. Photolysis of some dimers of dialkylketenes (e.g. dimethylketene) in benzene gave the ketenes in yields of 20~30% and better yields of 70~80% for the corresponding tetraalkylethylene (Figure 1-23).

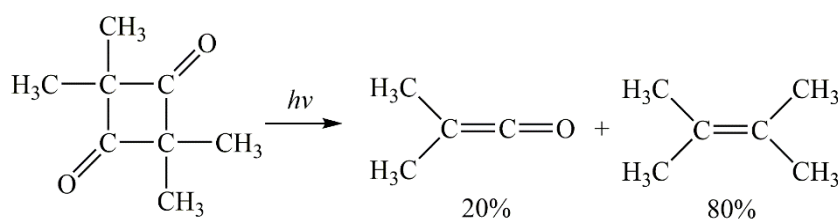


Figure 1-23. Photolysis of dimethylketene dimer [42, 43].

Photolysis of the cyclobutanedione in CH₂Cl₂ can generate pentamethyleneketene in a yield of about 20%, which provided a better ketene formation efficiency comparing with other smaller or larger rings involving dimers (Figure 1-24).

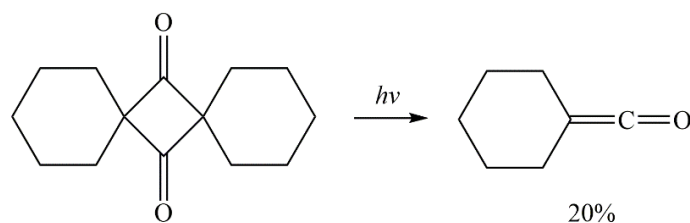


Figure 1-24. Photolysis of the cyclobutanedione [44]

1.1.3.2 Photochemical Ring Opening

Barton and Quinkert first reported the photochemical ring-opening reaction of cyclohexadienones in 1960 [45] and proposed a facile synthesis route of complex structure molecules from commercial chemicals, even under the incandescent light [46-48]. Ketenes were generated by the long wavelength light driving ring opening reaction of cyclohexadienones and evidenced by the spectroscopy to form *Z* and *E* conformation interconversion structures at the same time (Figure 1-25).

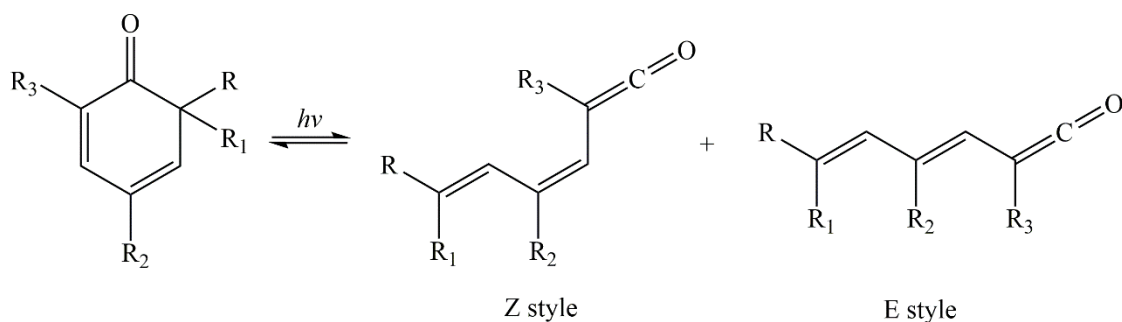


Figure 1-25. Photochemical ring opening of cyclohexadienones

An alternative unique ring-opening reaction of photolysis of furfuryl alcohol at 229 nm in an argon matrix at 14 K was observed by Araujo-Andrade and colleagues, which gave several species including vinylketene identified by the IR absorption at 2138 cm^{-1} (Figure 1-26).

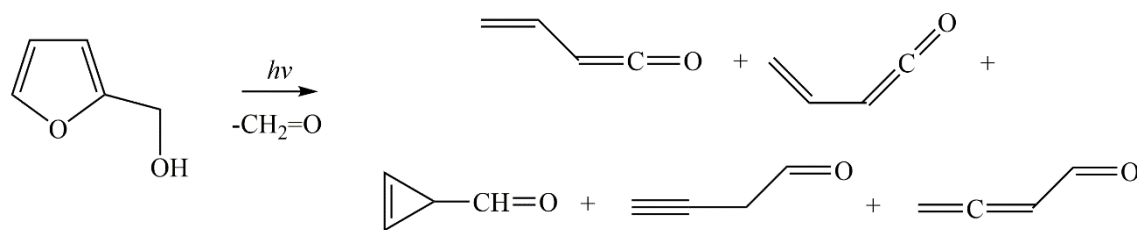


Figure 1-26. Photochemical ring opening of furfuryl alcohol [49]

1.1.3.3 Other Photochemical Generation Method

A special cyclic ketene was obtained by Tsutsui et al with use of photolysis of 2,3,5,6-tetra(trimethylsilyl)-1,4-benzoquinone. The yielding pale yellow crystals at a 21% conversation efficiency were given proof of ketenes by IR absorption at 2089 cm^{-1} (Figure 1-27).

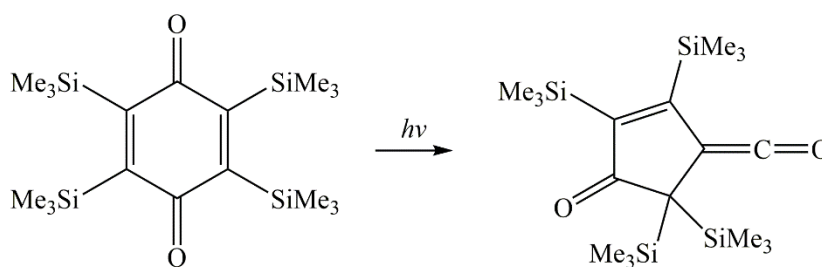


Figure 1-27. Photolysis of 2,3,5,6-tetra(trimethylsilyl)-1,4-benzoquinone [50]

1.1.4 Wolff Rearrangement Method

The Wolff rearrangement reaction undergoes to form ketenes by the rearrangement of diazo ketones, which can be motivated by thermokinetic, metal-catalysts, or photokinetic. This reaction was first reported by Wolff in 1902 [51], before the mechanistic issues were figured out in 1912 [52]. The general mechanism of the Wolff rearrangement of *syn*-diazo ketones and *anti*-diazo ketones was reasonably positioned thanks to observations of some possible reactive intermediates (Figure 1-28). As the reaction proceeds by loss of N_2 , Wolff rearrangement presents significant preparative value for isolable and stable ketenes.

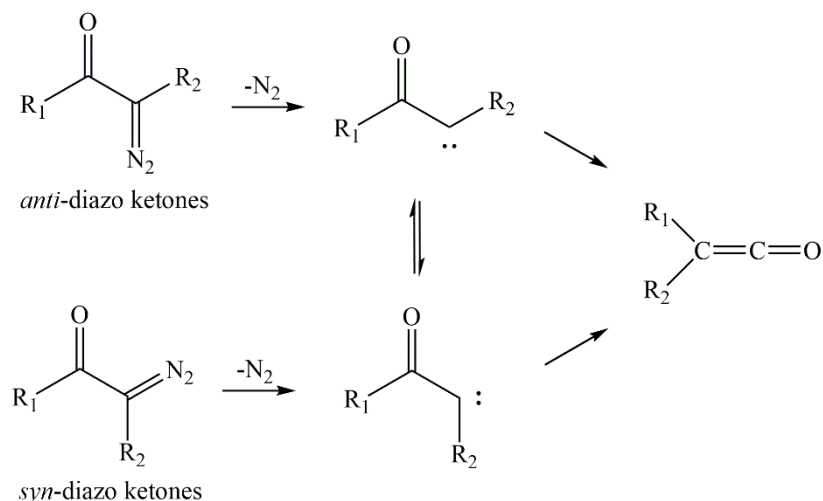


Figure 1-28. Possible steps in Wolff rearrangement [53]

1.1.4.1 Thermal Wolff Rearrangement

Preparation and isolation of ketenes from diazo ketones with use of the thermal Wolff rearrangement reactions sometimes cannot undergo very well, as a result of the occurring reactions between the ketenes and residual diazo ketone [54-57]. An example was given that phenylketene, deriving from the thermal decomposition of diazoacetophenone, would further undergo the undesired reaction with the unreacted residues (Figure 1-29).

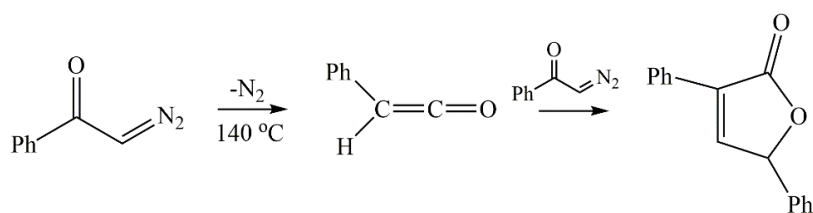


Figure 1-29. Thermal Wolff rearrangement of diazoacetophenone [54]

Some kinetic studies of Wolff rearrangement showed that phenyl groups were more favorable than acyl groups for diazo ketones to decompose. As a consequence of this, diphenylketene and other ketenes involving different phenyl groups were made preparatively by thermal Wolff rearrangement (Figure 1-30).

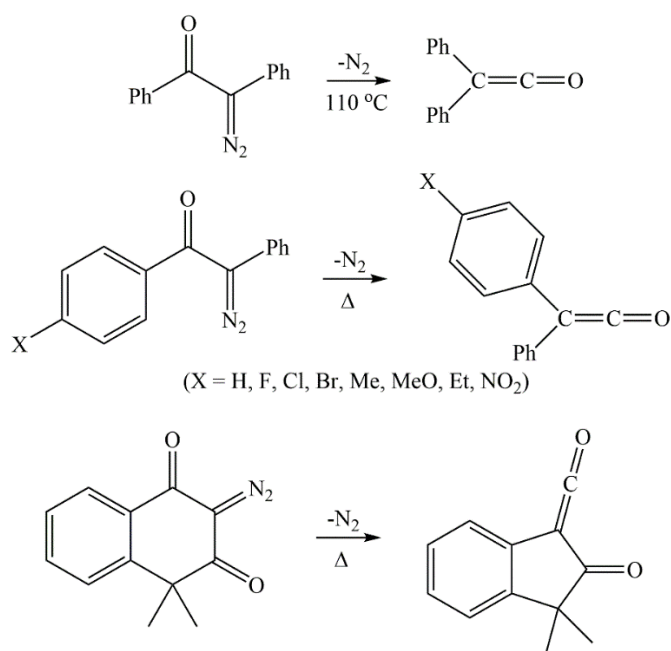


Figure 1-30. Phenyl substituted ketenes from thermal Wolff rearrangement [58-60]

1.1.4.2 Catalyzed Wolff Rearrangement

Metal catalysts were found to be efficient drivers of Wolff rearrangement reactions, which included but not limited to, silver, copper, platinum, palladium, rhodium metals and salts [61-65]. The Rh (II) octanoate catalyst was capable to activate the Wolff rearrangement of Et₃Si-substituted diazo ketones to give silylketenes in yields of 12~80% (Figure 1-31).

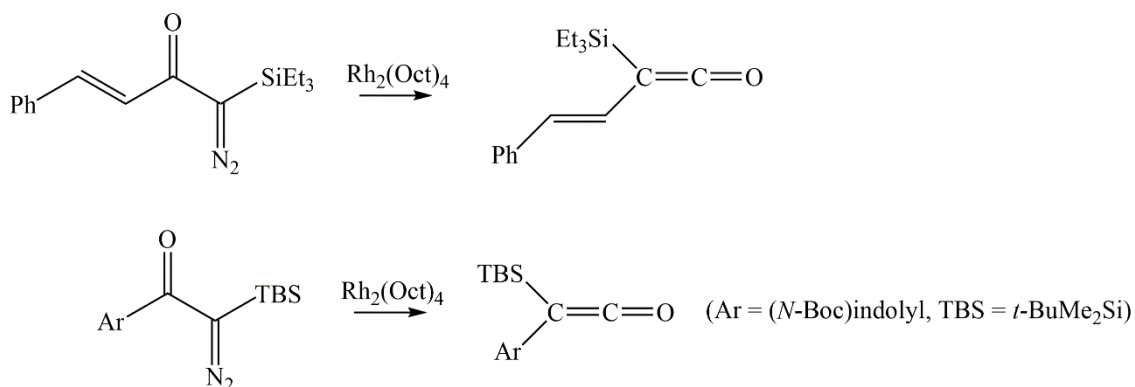


Figure 1-31. Silylketenes by Wolff rearrangement [66, 67]

Except for metal catalysts, triflic acid proved to be useful to Wolff rearrangement. Bucher et al proposed a special route to make aryl diazo ketone conversion into the silylated diazo ketone using a silyl triflate, and then Wolff rearranged the product into the stable aryl(trialkylsilyl)ketene by triflic acid catalyst in a one-pot procedure (Figure 1-32). The conversion efficiency reached 60% [68].

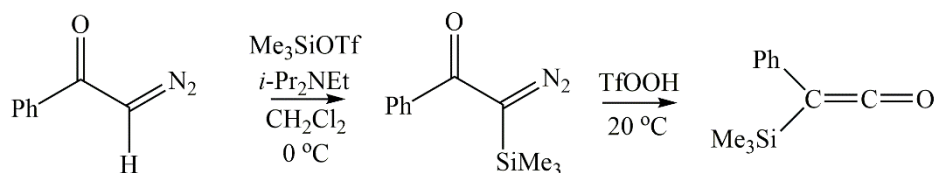


Figure 1-32. One-pot procedure from aryl diazo ketone to aryl(trialkylsilyl)ketene [68].

1.1.4.3 Photochemical Wolff Rearrangement

The photochemical variation of the Wolff rearrangement was discovered by Horner in 1952 [69], and is superior to other methods for the operational convenience and output efficiency advantage. The photolysis at 270 nm of diazoacetone produced methylketene which was detected by IR absorption at at 2100 cm^{-1} . The photolysis of azibenzil with UV-visible detection shows generation of diphenylketene in a concerted process of *syn*- and *anti*-formation in acetonitrile (Figure 1-33). However, limitation occurred to the photochemical method when the desired ketene product itself suffered decomposition under the irradiation conditions.

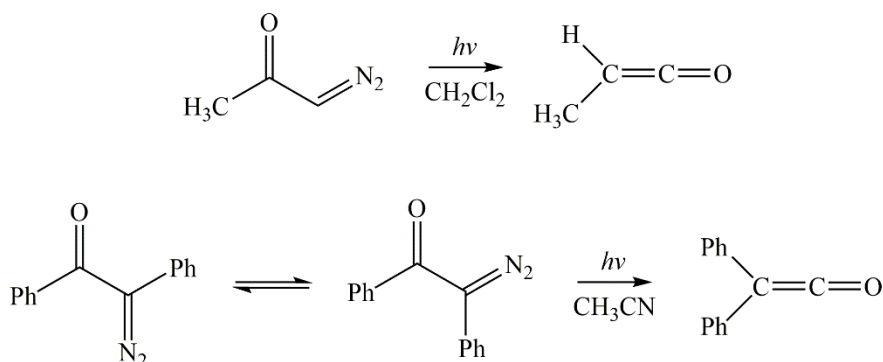


Figure 1-33. Photolysis of diazoacetone and azibenzil [70]

A unique example for Wolff rearrangement was the photolysis of diazo Meldrum's acid. With the UV absorption maximum at 248 nm, the diazo Meldrum's acid underwent mainly Wolff rearrangement to the formation of ketene. However, the photolysis at 355 nm gave almost exclusively the diazirine generation (Figure 1-34).

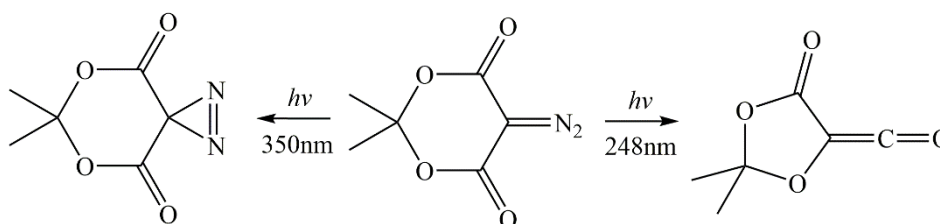


Figure 1-34. Photolysis of diazo Meldrum's acid [71]

1.1.5 Conclusion on Ketene Synthesis

Among all these reported ketene synthetic pathways, the Staudinger method is very efficient for ketenes involving bulky or aryl substituents, provided that recovering ketenes in a given solvent is not a problem. In addition, the advantage of the thermal generation method is that ketenes can be efficiently obtained in a pure state from various families of starting chemicals, although the high energy cost is always necessary. However, the photochemical generation method does not make sense because of its poor yield and possible side reactions.

Taking all the above factors into consideration, we choose the Staudinger and thermal generation method for our synthesis in the present work.

1.2 Generalities on Ketene Polymerization

The investigation of ketene-based polymerization started to undergo systematically in the sixties [72, 73], although the polymers were already observed by many researchers before [74-76]. A significant limitation is that only simple ketenes and disubstituted ketenes can be obtained and isolated in high yields, and further purified approaching 99% purity by

distillation or recrystallization to meet the requirement of monomers. Moreover, in the absence of other possibilities, simple neat ketenes can easily dimerize [77, 78], trimerize [79] and/or oligomerize (dimethylketene example see Figure 1-35). To avoid this, for any polymerization occurring to ketenes, the rate of the reaction must be faster than, or at least competitive with, the rates of ketene decomposition pathways [80]. Therefore, most ketene polymerizations chose to proceed at low temperature and under inert gas flowing atmosphere regarding the sensitivity to water and oxygen.

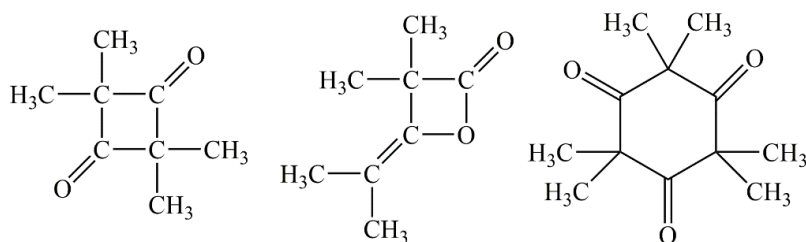


Figure 1-35. Dimer and trimer structures of dimethylketene

Taking the above issues into account, reported polymerizations were most carried out with the ketene itself and dimethylketene in either an anionic or a cationic mechanism, whereby three different structures (polyketone, polyester and polyacetal, see Figure 1-36 in the case of DMK) were obtained by optimized solvent and initiator systems [81, 82].

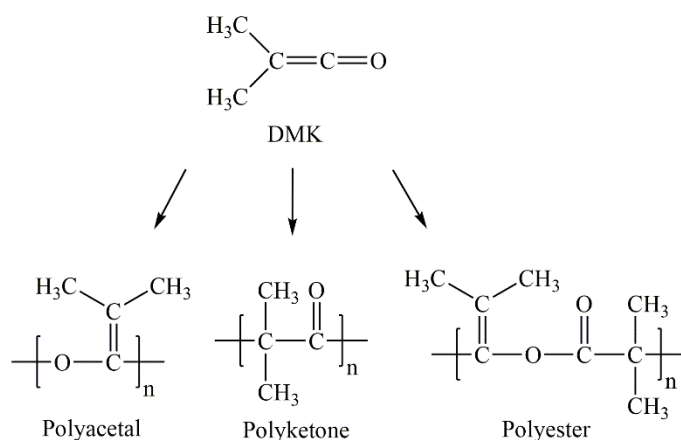


Figure 1-36. Polymerization of dimethylketene

The polyesters presented potential values in the area of biodegradable and hydrolyzable materials (e.g. films, sheets, bottles etc) [83, 84]. The polyketones attracted more focuses owing to their impressive thermal stability, chemical resistance, mechanical behavior and gas barrier properties [85]. It has been reported that unlike other commonly used gas barrier materials, the dimethylketene-based polyketone (PDMK) performs impressively low dioxygen permeability (P_{O_2}) even in the condition of high relative humidity (Figure 1-37). For polyacetals, which have rarely been fully independent products, they still need further investigation [86, 87].

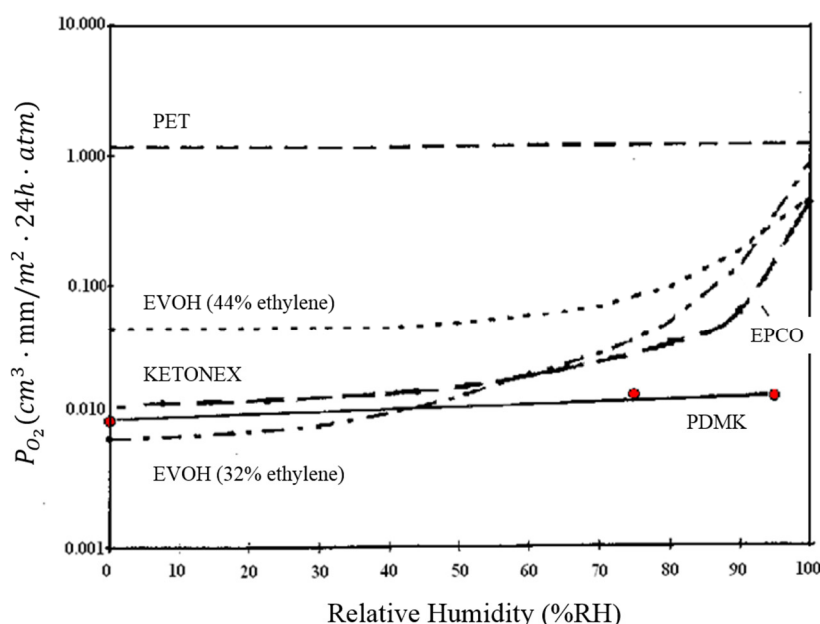


Figure 1-37. Dioxygen permeability of PDMK, EPCO (like Ketonex or Poketone, see 1.5.1), EVOH and PET [88]

1.3 Anionic Polymerization of Ketenes

By now, depending on the reported articles, it can be concluded that polyester structure is preferred by ketene anionic polymerization upon specific temperatures and solvents, although the products frequently remain mixed with the other two structures [78, 89, 90]. It

has been discovered that the polyester structural units will dominate by lowering the degree of polarity of the reaction medium, as a matter that alkylation of ambident anion on the more electronegative (oxygen) atom is favored in dipolar aprotic solvents [91], which leads to the acetal units. However the result seemed more dependent on the initiator type when experiments without solvents have been conducted upon diethylketene using lanthanoid alkoxide [92].

The three pathways to the three different structures for anionic polymerization have been widely accepted by the rearrangement of chain growth (Figure 1-38).

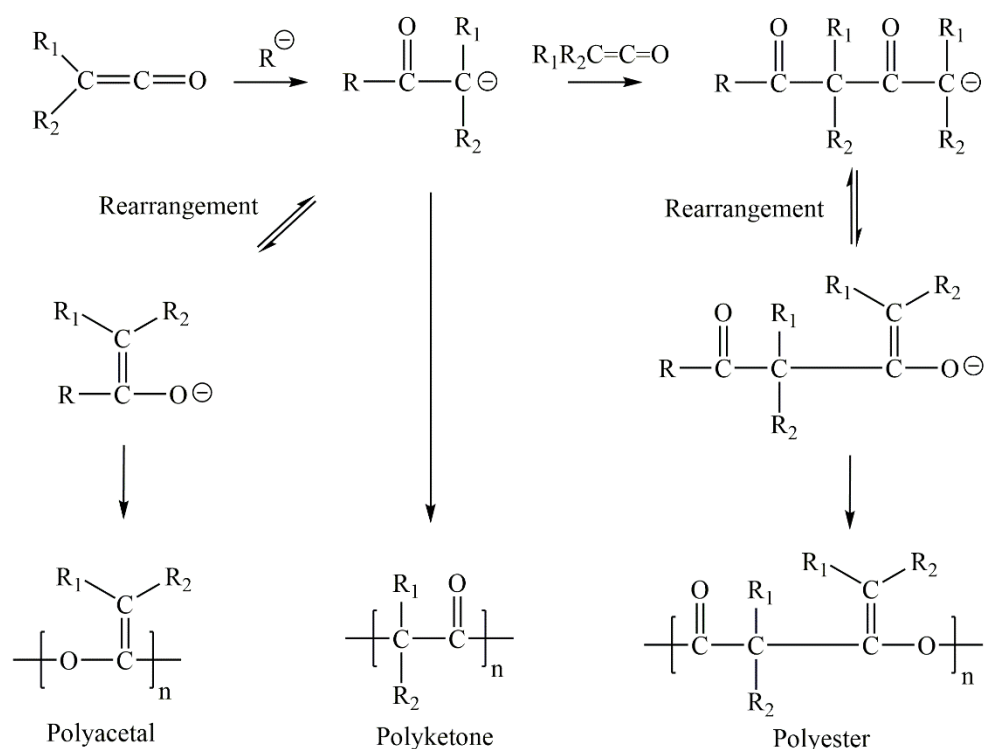


Figure 1-38. Possible pathways by the rearrangement of chain growth [93]

However, it is quite difficult to understand the existence of polyesters compared to polyketones and polyacetals, even if this proposed mechanism can, in some way, explain the formation of different ketene-based polymer backbones. In fact, these pathways have still not been clearly demonstrated [92].

1.3.1 Anionic Initiators

In general, traditional anionic initiators (or electron donors), which are either electron transfer agents or strong anions, can be divided into four groups.

1.3.1.1 Aromatic Complexes of Alkali Metals

These complexes are often used as a combination of alkali metals with organic aromatic compounds having a high electron density, sodium with the naphthalene ($\text{Na-C}_{10}\text{H}_8$) as a typical example (Figure 1-39). The mixture then allows to function as an electronic transfer basement, whereby the key of the initiation step can be explained by a rapid “electron transfer” from the naphthalene to the monomer. These species prove to be radical-anions which possess an extra electron in the lowest unoccupied π orbital and that the solvent plays an especially important role in assisting the transfer of electron through interorbital exchanges with the electrons available from the oxygen of the tetrahydrofuran solvent [94].

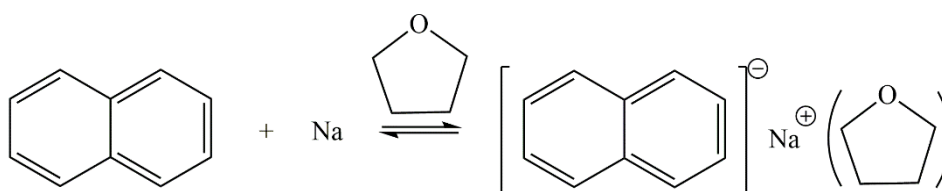


Figure 1-39. Tetrahydrofuran based sodium-naphthalene ($\text{Na-C}_{10}\text{H}_8$) initiator [95]

1.3.1.2 Lewis Bases

The Lewis bases generally used as initiators are amines, pyridine, tertiary phosphines (triethylamine, triphenylphosphine, tributylamine ...) or else lithium alkoxides (LiOBu , LiOMe) [96]. These initiators perform more effective upon highly active monomers in an apolar solvent (toluene or n-heptane).

1.3.1.3 Organolithium Initiators

These initiators differ from the alkali metals in operating by a direct anionic (nucleophilic) attack rather than by an electron transfer mechanism [97]. This also leads to a mono-functional chain-growth reaction, which results in a better control of dispersity than the dianionic propagation involved in initiation by electron transfer. The most commonly used initiators of this type are $\text{C}_4\text{H}_9\text{Li}$, $\text{C}_2\text{H}_5\text{Li}$, $\text{C}_3\text{H}_7\text{Li}$, $(\text{CH}_3)_3\text{SiCH}_2\text{Li}$, $\text{C}_6\text{H}_5\text{CH}_2\text{Li}$ etc [98-100]. The mechanism can be more easily understood by the relation in Figure 1-40.

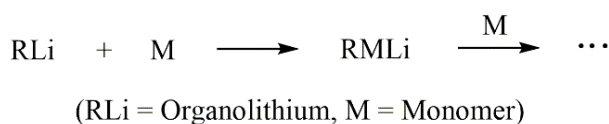


Figure 1-40. Propagation step of chain growth for organolithium initiator

1.3.1.4 Lanthanoid Alkoxide Initiators

Another novel type of initiator for anionic polymerization is lanthanoid alkoxide ($\text{Ln}(\text{OR})_3$), which is widely utilized for efficient organic reactions [101, 102]. Since lanthanoid metals possess some interesting features, such as low electronegativity, large ionic radii, and 4f orbitals, these lanthanoid alkoxides were expected to be very active and efficient for polymerizations [103-105].

1.3.2 Anionic Homopolymerization of Ketenes

Applied to ketenes, these anionic initiators gave the results which are summarized in Table 1-1.

Table 1-1. Anionic homopolymerization summary of ketene monomers

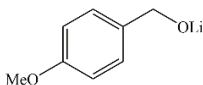
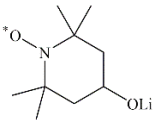
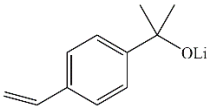
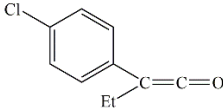
Monomer	Initiating system	Structure	Yield	Remarks	Ref.
$\text{Me}_2\text{C}=\text{C}=\text{O}$	KCN	PE + PA	14%	in DMF at -45°C	[90]
	NaCN	PE + PA	14~22%	in DMF at -45°C depends on [initiator]	[90]
	Naphthalene K (K-C ₁₀ H ₈)	PE + PA	18%	in toluene at -78°C	[90]
		PE + PA	13%	in DMF at -78°C	
	Naphthalene Na (Na-C ₁₀ H ₈)	PE + PA	20~45%	in toluene at -78°C	[90]
		PE + PA	1~40%	in DMF at -60 or -78°C	
		PE + PA	43%	in THF at -78°C	
		PE + PA	45%	in CS ₂ at -78°C	
		PE + PA	40%	in CH ₃ CN at -78°C	
		PE	23%	in DMSO at RT	
		reaction hardly proceeds		in pyridine, acetone or PhNO ₂	
	K ₂ (Ph ₂ CO)	PE	12%	in toluene at -78°C	[90]
		PE + PA	14%	in DMF at -78°C	
	Na(Ph ₂ CO)	PE + PA	19%	in DMF at -78°C	[90]
		reaction hardly proceeds		in toluene at -78°C	
	Na ₂ (Ph ₂ CO)	PE + PA	14%	in DMF at -78°C	[90]

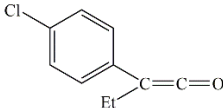
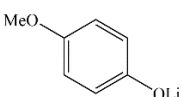
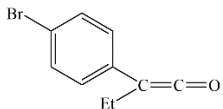
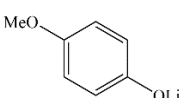
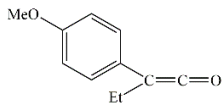
Monomer	Initiating system	Structure	Yield	Remarks	Ref.
$\text{Me}_2\text{C}=\text{C}=\text{O}$	$\text{Na}_2(\text{Ph}_2\text{CO})$	PE + PA	28%	in toluene at -78°C	
	$n\text{-BuLi}$	PE + PA	< 30%	in toluene at -78°C	
		PE + PA	25~45%	in DMF at -78°C	
		PE + PA	24%	in THF at -78°C	[90]
		PE + PA	28%	in CS_2 at -78°C	
		PE + PA + PK	14%	in DMSO at -78°C	
		reaction hardly proceeds		in pyridine, CH_3CN or PhNO_2	
	sec-BuLi	PE + PA + PK	< 20%	in toluene or DMF at -78°C	[90]
	tert-BuLi	PE + PA + PK	< 20%	in toluene or DMF at -78°C	[90]
	Naphthalene Li (Li- C_{10}H_8)	PE + PA	35~45%	in toluene or DMF at -78°C	[90, 106]
	$\text{Li}(\text{Ph}_2\text{CO})$	PE + PA	30~35%	in toluene or DMF at -78°C	[90]
	$\text{Li}_2(\text{Ph}_2\text{CO})$	PE + PA	30~50%	in toluene or DMF at -78°C	[90]
	PhLi	PE + PA	< 20%	in toluene or DMF at -78°C	[90]
	EtLi	PE + PA	< 10%	in toluene or DMF at -78°C	[90]
	$n\text{-BuLi}$	PE + PA	50~90%	in toluene or diethyl ether at -78°C	[106]
	$n\text{-BuOLi}$	PE + PA	86%	in toluene at -78°C	[106]
	$\text{C}_2\text{H}_5\text{ONa}$	PE + PA	100%	in toluene at -78°C	[106]

Monomer	Initiating system	Structure	Yield	Remarks	Ref.
$\text{Me}_2\text{C}=\text{C}=\text{O}$	<i>n</i> -BuMgBr	PE + PA + PK	< 5%	in toluene or THF at −78°C, in DMF at −45°C	[90]
	<i>n</i> -BuMgCl	PE + PA + PK	21%	in toluene at −78°C	[90]
	<i>sec</i> -BuMgBr	PE + PA + PK	< 5%	in toluene at −78°C	[90]
	<i>tert</i> -BuMgCl	PE + PA + PK	4%	in toluene at −78°C	[90]
	<i>tert</i> -BuMgBr	reaction hardly proceeds		in toluene at −78°C	[90]
	PhMgBr	PE + PA + PK	< 10%	in toluene or DMF at −78°C	[90]
		PE	20%	in THF at −78°C	
	PhMgI	PE + PA	10~20%	in toluene, DMF or THF at −78°C	[90]
	Cyclohexyl-MgCl	PE + PA + PK	< 5%	in toluene, DMF or THF at −78°C	[90]
	Allyl-MgCl	PE + PA	< 5%	in toluene at −78°C	[90]
	NEt ₃	PE + PA	< 10%	in toluene at −78°C	[90] [107]
		PE + PA	1~85%	in cyclohexanone, acetone, diethyl ketone, acetonitrile or diethyl ether at −40°C	
		PE + PA + PK	< 5%	in DMF at −78°C	
	NBu ₃	PE + PA + PK	< 5%	in toluene at −78°C	[90]

Monomer	Initiating system	Structure	Yield	Remarks	Ref.
Et ₂ C=C=O	La(O ⁱ Pr) ₃	PE	20~80%	in toluene at 6~80°C $\overline{M}_n = 10\ 000\sim60\ 000$ $\overline{D}_M = 1.5\sim2.1$	[92] ^b
	Sm(O ⁱ Pr) ₃	PE	13%	in toluene at RT $\overline{M}_n = 27\ 000$ $\overline{D}_M = 1.7$	[92] ^b
	Yb(O ⁱ Pr) ₃	reaction hardly proceeds		solvent and temperature unknown	[92] ^b
EtMeC=C=O	La(O ⁱ Pr) ₃	PE	50%	$\overline{M}_n = 10\ 900$ in bulk $\overline{D}_M = 2.1$	[92] ^b
EtHC=C=O	Naphthalene Na (Na-C ₁₀ H ₈)	PE	3~70%	in THF at -78~-40°C $\overline{M}_n < 10\ 000$ $\overline{D}_M = 1.4\sim1.5$	[86] ^a
	<i>n</i> -BuLi	PE	20~90%	in THF at -78~-40°C $\overline{M}_n = 10\ 000\sim25\ 000$ $\overline{D}_M = 1.3\sim1.9$	[86] ^a
	<i>tert</i> -BuOLi	PE	91%	in THF at -78°C $\overline{M}_n = 18\ 400$ $\overline{D}_M = 2.0$	[86] ^a
	<i>sec</i> -BuLi	PE	20~80%	in THF at -78~-40°C $\overline{M}_n = 10\ 000\sim22\ 000$ $\overline{D}_M = 1.3\sim1.9$	[86] ^a
	Lithium diisopropylamide (LDA)/BuLi	PE	76%	in THF at -78°C $\overline{M}_n = 24\ 000$ $\overline{D}_M = 1.5$	[86] ^a
	1,1'-Diphenyl-3-methylpentyllithium (DPMPLi)	PE	78%	in THF at -78°C $\overline{M}_n = 14\ 700$ $\overline{D}_M = 1.9$	[86] ^a

Monomer	Initiating system	Structure	Yield	Remarks	Ref.
$\text{Ph}_2\text{C}=\text{C}=\text{O}$	$\text{La}(\text{O}^i\text{Pr})_3$	reaction hardly proceeds		solvent and temperature unknown	[92] ^b
$\text{Si}^i\text{Pr}_3\text{HC}=\text{C}=\text{O}$	<i>tert</i> -BuOK	PE + PA + PK	> 85%	in THF, DMF, diethyl ether or dioxane at -78°C $\overline{M}_n = 1\,100\sim 12\,000$ $\overline{D}_M = 1.1\sim 2.3$	[82] ^a
$\text{MePhC}=\text{C}=\text{O}$	PhMgBr	PE	86%	in toluene at -78°C	[108]
	<i>tert</i> -BuONa	PE	82%	in toluene at -78°C	[108]
	AlEt_3	reaction hardly proceeds		solvent and temperature unknown	[108]
	ZnEt_2	PE	75%	in toluene at -78 or -20°C	[108]
	<i>n</i> -BuLi	PE	> 80%	in toluene, diethyl ether and DMF at -78°C	[108]
$\text{EtPhC}=\text{C}=\text{O}$	<i>n</i> -BuLi	PE	> 90%	living polymerization in THF at $-78\sim 0^\circ\text{C}$ $\overline{M}_n = 5\,000\sim 22\,000$ $\overline{D}_M = 1.1\sim 1.3$	[109] ^c [110] ^a
		PE	99%	living polymerization in DMF at -20°C $\overline{M}_n = 44\,000$ $\overline{D}_M = 2.0$	
	<i>n</i> -BuLi	PE	64%	living polymerization in toluene at -20°C $\overline{M}_n = 188\,600$ $\overline{D}_M = 2.2$	[110] ^a
		PE	94%	living polymerization in THF at -20°C $\overline{M}_n = 11\,700$ $\overline{D}_M = 1.1$	

Monomer	Initiating system	Structure	Yield	Remarks	Ref.
EtPhC=C=O	<i>sec</i> -BuLi	PE	80%	living polymerization in THF at -20°C $\overline{M}_n = 28\,000$ $\overline{D}_M = 1.1$	[110] ^a
	<i>tert</i> -BuLi	PE	35%	living polymerization in THF at -20°C $\overline{M}_n = 54\,800$ $\overline{D}_M = 2.8$	[110] ^a
	Naphthalene Na (Na-C ₁₀ H ₈)	PE	> 95%	living polymerization in THF at -20 or -78°C $\overline{M}_n = 15\,000\sim 27\,000$ $\overline{D}_M = 1.2\sim 1.3$	[110] ^a
		PE	> 90%	living polymerization in THF at -20°C $\overline{M}_n = 2\,000\sim 13\,000$ $\overline{D}_M = 1.1\sim 1.2$	[110] ^a
		PE	92%	living polymerization in THF at -20°C $\overline{M}_n = 3\,800$ $\overline{D}_M = 1.1$	[110] ^a
		PE	77%	living polymerization in THF at -20°C $\overline{M}_n = 3\,000$, $\overline{D}_M = 1.2$	[110] ^a
	<i>n</i> -BuLi	PE	> 95%	living polymerization in THF at -20°C $\overline{M}_n = 5\,000\sim 16\,000$ $\overline{D}_M = 1.1\sim 1.3$	[111] ^a

Monomer	Initiating system	Structure	Yield	Remarks	Ref.
		PE	> 85%	living polymerization in THF at -20°C $\overline{M}_n = 5\,000\sim 10\,000$ $D_M = 1.1\sim 1.3$	[111] ^a
		PE	> 90%	living polymerization in THF at -20°C $\overline{M}_n = 7\,000\sim 70\,000$ $D_M = 1.1\sim 1.2$	[111] ^a
	<i>n</i> -BuLi	PE	> 95%	living polymerization in THF at -20°C $\overline{M}_n = 4\,000\sim 17\,000$ $D_M = 1.1\sim 1.2$	[112] ^a
	<i>tert</i> -BuOLi	PE	91%	living polymerization in THF at -20°C $\overline{M}_n = 4\,300$, $D_M = 1.1$	[112] ^a

PA: polyacetal; PE: polyester; PK: polyketone

 \overline{M}_n : expressed in $\text{g}\cdot\text{mol}^{-1}$ a: calibration of \overline{M}_n and \overline{M}_w by SEC with polystyrene standardsb: calibration of \overline{M}_n and \overline{M}_w by SEC with poly(hexyl isocyanate) standardsc: calibration of \overline{M}_n and \overline{M}_w by SEC with unidentified standards

In conclusion, general trends of these anionic homopolymerizations are very difficult to establish, since lots of monomers, solvents, initiators and temperatures were tested. Indeed, using very different solvents like DMF ($\epsilon = 38$) and toluene ($\epsilon = 2.4$) can give polymers in good yields. Furthermore for initiators, we can notice that Naphthalene Na and lithium compounds (like *n*-BuLi and *tert*-BuOLi) perform very efficient in yielding polymers, as well as the polymerization using lanthanoid alkoxide initiators, which undergoes a living mechanism to give polyesters with satisfying molecular weights.

It is important to note that all the obtained products of these anionic ketene polymerizations remain mainly polyester structures, however often mixed with other structures.

1.3.3 Copolymerization of Ketenes

The reported anionic copolymerization can be generally divided into two different types: copolymerization of ketene and aldehyde / ketone compound, and copolymerization of ketene and isocyanate (Figure 1-41).

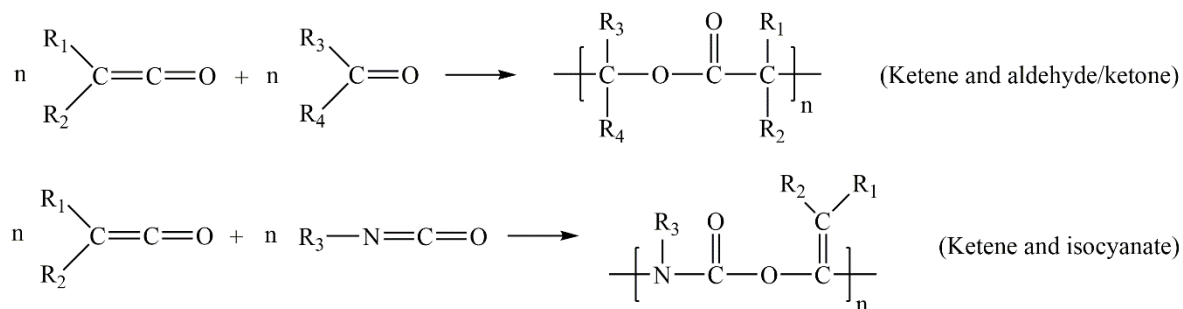
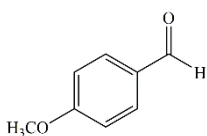
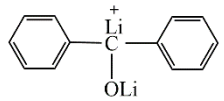
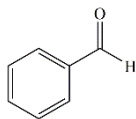
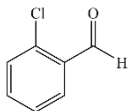
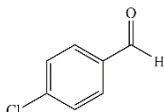
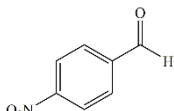
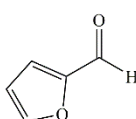


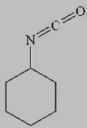
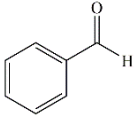
Figure 1-41. General anionic copolymerization of ketene and other compounds

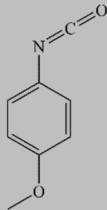
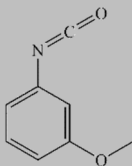
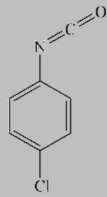
The detailed anionic copolymerizations of ketenes are summarized in Table 1-2.

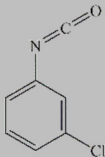
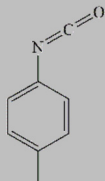
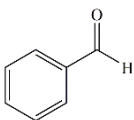
Table 1-2. Anionic copolymerization summary of ketene monomers
(grey lines refer to copolymerization with isocyanates)

Monomers	Initiating system	Structure	Yield	Remarks	Ref.
$\text{Me}_2\text{C}=\text{C}=\text{O}$ Acetone	<i>n</i> -BuLi	PE	72~82%	in toluene or CH_2Cl_2 at -60°C $\overline{M}_n = 4\,500\sim 8\,400$ $D_M = 1.9\sim 2.2$ $T_m = 139\sim 171^\circ\text{C}$	[113] [114] ^b
$\text{Me}_2\text{C}=\text{C}=\text{O}$ <i>p</i> -anisaldehyde 	Benzophenone-dilithium 	PE	1~72%	in THF at -78°C $\overline{M}_n = 5\,200\sim 14\,000$	[115] ^c
	<i>n</i> -BuLi	PE	29%	in toluene at -78°C	[96]

Monomers	Initiating system	Structure	Yield	Remarks	Ref.
$\text{Me}_2\text{C}=\text{C}=\text{O}$ Benzaldehyde 	<i>n</i> -BuLi	PE	65~75%	in toluene at -12 or -50°C	[96]
	<i>n</i> -BuOLi	PE	77%	in toluene at -40°C	
	Naphthalene Na (Na-C ₁₀ H ₈)	PE	86%	in toluene at -30°C	
	C ₂ H ₅ ONa	PE	100%	in toluene at -78°C	
$\text{Me}_2\text{C}=\text{C}=\text{O}$ <i>o</i> -chlorobenzaldehyde 	<i>n</i> -BuLi	PE	40%	in toluene at -50°C	[96]
$\text{Me}_2\text{C}=\text{C}=\text{O}$ <i>p</i> -chlorobenzaldehyde 	<i>n</i> -BuLi	PE	100%	in toluene at -35°C	[96]
$\text{Me}_2\text{C}=\text{C}=\text{O}$ <i>p</i> -nitrobenzaldehyde 	<i>n</i> -BuLi	PE	29%	in toluene at -30°C	[96]
$\text{Me}_2\text{C}=\text{C}=\text{O}$ Furfural 	<i>n</i> -BuLi	PE	12%	in toluene at -78°C	[96]
$\text{Me}_2\text{C}=\text{C}=\text{O}$ Acetaldehyde (CH ₃ CHO)	<i>n</i> -BuLi	PE	9%	in toluene at -60°C $\overline{M}_n = 2\,000$ $\overline{D}_M = 2.0$	[116] ^b
$\text{Ph}_2\text{C}=\text{C}=\text{O}$ Phenylisocyanate (PhNCO)	Naphthalene Na (Na-C ₁₀ H ₈)	<i>s</i> -PU	unknown	in DMF at -45°C	[117]

Monomers	Initiating system	Structure	Yield	Remarks	Ref.
$\text{Ph}_2\text{C}=\text{C}=\text{O}$ Ethylisocyanate (EtNCO)	Naphthalene Na (Na-C ₁₀ H ₈)	<i>s</i> -PU	6%	in THF at -78°C	[117]
$\text{Ph}_2\text{C}=\text{C}=\text{O}$ <i>n</i> -butylisocyanate (<i>n</i> -BuNCO)	Naphthalene Na (Na-C ₁₀ H ₈)	s -PU reaction hardly proceeds	5%	in DMF at -45°C in THF -78°C	[117]
$\text{Ph}_2\text{C}=\text{C}=\text{O}$ Cyclohexyl isocyanate 	Naphthalene Na (Na-C ₁₀ H ₈)	reaction hardly proceeds		in DMF -45°C	[117]
$\text{MePhC}=\text{C}=\text{O}$ Phenylisocyanate (PhNCO)	Naphthalene Na (Na-C ₁₀ H ₈)	<i>s</i> -PU	unknown	in DMF at -45°C	[117]
$\text{MePhC}=\text{C}=\text{O}$ Ethylisocyanate (EtNCO)	Naphthalene Na (Na-C ₁₀ H ₈)	<i>s</i> -PU	72%	in THF at -78°C	[117]
$\text{MePhC}=\text{C}=\text{O}$ <i>n</i> -butylisocyanate (<i>n</i> -BuNCO)	Naphthalene Na (Na-C ₁₀ H ₈)	reaction hardly proceeds		in THF	[117]
$\text{MePhC}=\text{C}=\text{O}$ Benzaldehyde 	<i>n</i> -BuLi/ZnEt ₂	PE	67%	in toluene at -78°C	[108]
	PhMgBr	PE	71%	in toluene at -78°C	
	Naphthalene Li (Li-C ₁₀ H ₈)	PE	71%	in toluene at -78°C	
	<i>n</i> -BuLi	PE	80%	in toluene at -78°C	
	<i>t</i> -BuONa	PE	62%	in toluene at -78°C	
	ZnEt ₂	PE	18%	in toluene at -78°C	

Monomers	Initiating system	Structure	Yield	Remarks	Ref.
EtPhC=C=O (<i>n</i> -butylisocyanate) <i>n</i> -BuNCO	Naphthalene Na (Na-C ₁₀ H ₈)	reaction hardly proceeds		in THF	[117]
EtPhC=C=O (<i>n</i> -hexyl isocyanate) CH ₃ (CH ₂) ₄ CH ₂ NCO	Naphthalene Na (Na-C ₁₀ H ₈)	reaction hardly proceeds		in THF	[117]
EtPhC=C=O Phenylisocyanate (PhNCO)	Naphthalene Na (Na-C ₁₀ H ₈)	<i>s</i> -PU	4~51%	in DMF at -45°C <i>T_m</i> = 170~220°C	[117]
EtPhC=C=O 1-isocyanato-4- methoxybenzene 	Naphthalene Na (Na-C ₁₀ H ₈)	<i>s</i> -PU	1~65%	in DMF at -45°C <i>T_m</i> = 174~209°C \overline{M}_n = 2 000~4 000	[117] ^a
		<i>s</i> -PU	60~85%	in THF at -78°C <i>T_m</i> = 154~214°C \overline{M}_n = 2 800~9 500	
EtPhC=C=O 1-isocyanato-3- methoxybenzene 	Naphthalene Na (Na-C ₁₀ H ₈)	<i>s</i> -PU	7~46%	in DMF at -45°C <i>T_m</i> = 167~192°C \overline{M}_n = 3 000~4 000	[117] ^a
		<i>s</i> -PU	1~28%	in THF at -78°C <i>T_m</i> = 167~183°C \overline{M}_n = 5 400~5 900	
EtPhC=C=O 1-chloro-4- isocyanatobenzene 	Naphthalene Na (Na-C ₁₀ H ₈)	<i>s</i> -PU	45%	in DMF at -45°C <i>T_m</i> = 152~167°C \overline{M}_n = 1 740	[117] ^a

Monomers	Initiating system	Structure	Yield	Remarks	Ref.
EtPhC=C=O 1-chloro-3-isocyanatobenzene 	Naphthalene Na (Na-C ₁₀ H ₈)	<i>s</i> -PU	18%	in DMF at -45°C $T_m = 148\sim 156^\circ\text{C}$ $\overline{M}_n = 2\,400$	[117] ^a
EtPhC=C=O 1-isocyanato-4-methylbenzene 	Naphthalene Na (Na-C ₁₀ H ₈)	<i>s</i> -PU	25~67%	in THF at -78°C $T_m = 173\sim 197^\circ\text{C}$ $\overline{M}_n = 6\,300\sim 10\,500$	[117] ^a
EtPhC=C=O Benzaldehyde 	ZnEt ₂ with ligands	PE	92%	in THF at -40°C $\overline{M}_n = 9\,800$ $\overline{D}_M = 1.6$	
		PE	92%	in toluene at -40°C $\overline{M}_n = 26\,000$ $\overline{D}_M = 1.9$	[118] ^b
		PE	90~92%	in CH ₂ Cl ₂ at -78~0°C $\overline{M}_n = 4\,700\sim 22\,700$ $\overline{D}_M = 1.4\sim 2.3$	

PE: polyester; *s*-PU: substituted polyurethanes \overline{M}_n : expressed in g·mol⁻¹a: by vapor-pressure osmometry in CH₂Cl₂b: calibration of \overline{M}_n and \overline{M}_w by SEC with polystyrene standards

c: by vapor-pressure osmometry in benzene at 37°C

In conclusion, most of the polyester-targeted anionic copolymerizations were conducted in toluene with *n*-BuLi initiators, at the same time the substituted-polyurethane-targeted reactions were catalysed by Naphthalene Na in THF or DMF to give better yields.

1.4 Cationic Polymerization of Ketenes

Comparing with the anionic polymerization of ketenes, the cationic ones have been much less reported, among which our team has devoted considerable work in order to obtain aliphatic polyketones [30, 31, 81, 119].

In theory, cationic method can also separately lead to ester, ketone and acetal units from ketenes by a selective opening of the double bonds using a suitable choice of both initiator system and solvent (Figure 1-42).

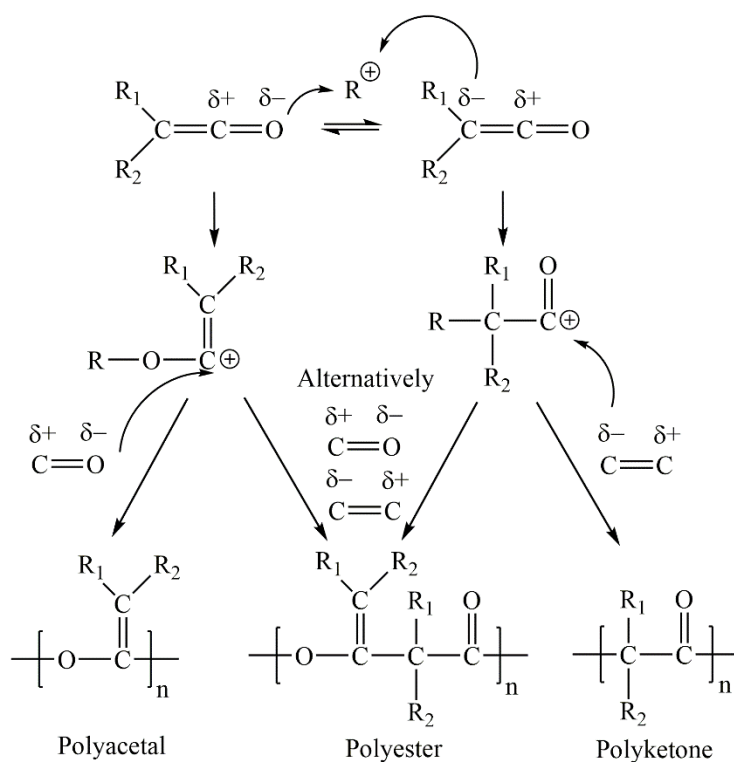


Figure 1-42. General pathways to ester, ketone and acetal units by cationic polymerization

1.4.1 Cationic Initiators

Cationic initiators are generally electron acceptors. Except for the nature of the cationic initiators themselves, the reactivity of the active centers is slightly determined by the

associated anionic ligands. Commonly used cationic initiators can be distinguished by three main categories as the followings.

1.4.1.1 Brønsted Acids

Brønsted acids are usually strong mineral acids such as sulfuric acid H_2SO_4 , perchloric acid HClO_4 , triflic acid $\text{CF}_3\text{SO}_3\text{H}$, or trifluoroacetic acid CF_3COOH . Sometimes weak protonic acids such as acetic acid CH_3COOH or hydrochloric acid HCl (weak in non-aqueous solvents) can also polymerize very reactive monomers such as vinylcarbazole [120].

However, some experiments carried out in the cationic polymerization of dimethylketene showed that they usually result in an inactive compound (Figure 1-43) [121].

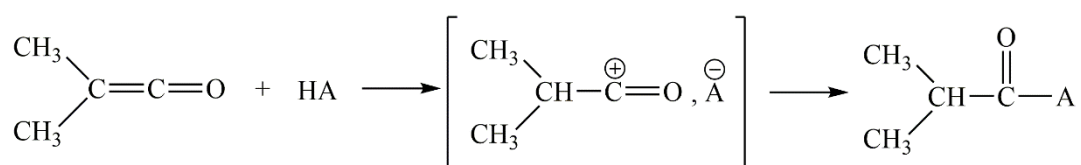
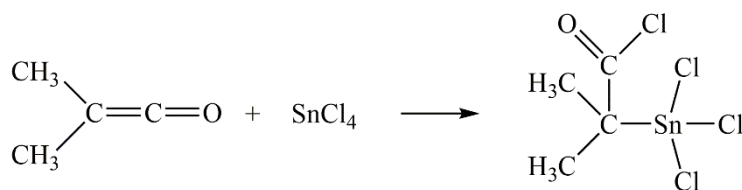


Figure 1-43. Reaction between protic acid and dimethylketene [121]

1.4.1.2 Lewis Acids

Lewis Acids present as the most important type of cationic initiators. These initiators including BF_3 , AlBr_3 , AlCl_3 , TiCl_3 , SnCl_4 , ... can be used alone or in the presence of a coinitiator, which is generally a weak Brønsted acid (H_2O , CCl_3COOH , CH_3COOH ...) as a proton donor.

However, in the case of dimethylketene, TiCl_4 , SnCl_4 , and BF_3OMe_2 have shown to be ineffective due to the formation of a stable complex between dimethylketene and the Lewis acid, which prevents further propagation steps (Figure 1-44).

Figure 1-44. Reaction between Lewis acid SnCl_4 and dimethylketene [30]

1.4.1.3 Friedel-Craft Style Systems

As a combination of a Lewis acid (AlCl_3 , FeCl_3 , ZnCl_2 , TiCl_4 , BF_3 , SbCl_5) and a co-initiator capable of generating carbocations, Friedel-Craft style initiator has been used successfully in many cationic polymerizations. As an example, a highly reactive Friedel Craft type system derives from ethanoyl chloride and Lewis acid AlCl_3 at high temperature (150°C), which can be also obtained by reaction of methyl chloride and AlCl_3 in the presence of CO (Figure 1-45). A more reactive ternary system initiator was developed and patented by Arkema in 2004 [122], which is composed of a Lewis acid initiator, a co-initiator and a complexing agent.

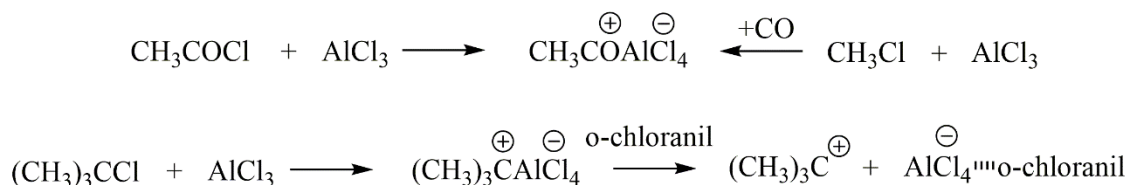


Figure 1-45. Two examples for Friedel-Craft style initiators [123]

1.4.2 Cationic Homopolymerization of Ketenes

Applied to ketenes, these initiators gave the results which are summarized in Table 1-3.

Table 1-3. Cationic homopolymerization summary of ketene monomers

Monomer	Initiating system	Structure	Yield	Remarks	Ref.
$\text{H}_2\text{C}=\text{C}=\text{O}$	BF_3	keto-enol (see Figure 1-46)	unknown	solvent and temperature unknown	[124]
Figure 1-46. Keto-enol equilibrium (Keto-enol was estimated about 30 : 70%)					
$\text{Me}_2\text{C}=\text{C}=\text{O}$	BF_3OEt_2	reaction hardly proceeds		solvent and temperature unknown	[30]
	TiCl_4	reaction hardly proceeds		solvent and temperature unknown	[30]
	SnCl_4	reaction hardly proceeds		solvent and temperature unknown	[30]
	HClO_4	reaction hardly proceeds		solvent and temperature unknown	[30]
	$\text{CF}_3\text{SO}_3\text{H}$	reaction hardly proceeds		solvent and temperature unknown	[30]
	AlEt_3	PE + PK	unknown	in toluene at -60°C	[30, 125]
	BeEt_2	unknown mixed structures	unknown	solvent and temperature unknown	[30]
				in nitrobenzene / CCl_4 at -30°C	
	AlBr_3	PK	1~65%	$\overline{M}_n = 20\,000\sim 40\,000$ $\overline{D}_M = 5\sim 25$ similar results in toluene, CCl_4 , cyclohexane, diethyl	[30] ^a

Monomer	Initiating system	Structure	Yield	Remarks	Ref.
Me ₂ C=C=O				ether, CH ₂ Cl ₂ , acetonitrile, nitrobenzene or nitrobenzene/toluene, nitrobenzene/CCl ₄ , nitrobenzene/CH ₂ Cl ₂ , nitrobenzene/acetonitrile, nitrobenzene/diethyl ether, nitrobenzene/cyclohexane, toluene/CH ₂ Cl ₂ , at −5~−30°C	
	AlBr ₃ / <i>n</i> -Bu ₄ N ⁺ Br [−]	PK	6~31%	in CH ₂ Cl ₂ at −30°C $\overline{M}_n = 20\,000\sim50\,500$ $\overline{D}_M = 2.6\sim9.4$	[81] ^a
	AlCl ₃	PK	unknown	in polar solvents, temperature unknown	[72]
EtHC=C=O	AlBr ₃	PK	25~60%	in CH ₂ Cl ₂ , heptane, toluene or ethyl acetate at −78°C $\overline{M}_n = 14\,000\sim28\,000$ $\overline{D}_M = 4.2\sim8.4$ $T_{deg} = 205\sim215^\circ\text{C}$ $T_g = 64\sim75^\circ\text{C}$ crystallinity = 28~40%	[31] ^b [81] ^a
MePhC=C=O	BF ₃ OEt ₂	reaction hardly proceeds		solvent and temperature unknown	[108]
	SnCl ₄	reaction hardly proceeds		solvent and temperature unknown	

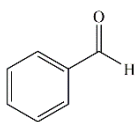
PE: polyester; PK: polyketone

 \overline{M}_n : expressed in g·mol⁻¹a: calibration of \overline{M}_n and \overline{M}_w by SEC with polystyrene standardsb: calibration of \overline{M}_n and \overline{M}_w by SEC with poly(methylmethacrylate) standards

1.4.3 Cationic Copolymerization of Ketenes

The detailed cationic copolymerizations of ketenes were summarized in Table 1-4. The only successful example was given in the previous work from our team.

Table 1-4. Cationic copolymerization summary of ketene monomers

Monomer	Initiating system	Structure	Yield	Remarks	Ref.
$\text{MePhC}=\text{C}=\text{O}$ Benzaldehyde 	AlEt_3	reaction hardly proceeds		solvent and temperature unknown	[108]
$\text{Me}_2\text{C}=\text{C}=\text{O}$ $\text{EtHC}=\text{C}=\text{O}$	AlBr_3	PK	26~39%	in toluene at -78°C	[81]

PK: polyketone

In conclusion, it is believed that polyketone is favored with cationic initiators like AlBr_3 and AlCl_3 in polar solvents. However, according to the presently reported work, very limited, only ketenes with small substituents have been successfully cationically polymerized.

1.5 Commercial Aliphatic Polyketones

Except the direct polymerization from ketenes, aliphatic polyketones are commercially prepared by the perfectly alternating polymerization of olefins and carbon monoxide.

1.5.1 Aliphatic Polyketones Involving 1,4-Dicarbonyl Units

Historically implemented, but later abandoned, by BP Chemical and Shell, and more recently developed again by Hyosung Polyketone, aliphatic polyketones involving 1,4-dicarbonyl units are derived from ethylene and carbon monoxide, or from ethylene, propylene and carbon monoxide (Figure 1-47). Their flexible chains together with the molecular symmetry enhances crystallization which results in many differentiated properties such as excellent chemical and impact resistance, exceptional wear resistance and barrier properties.

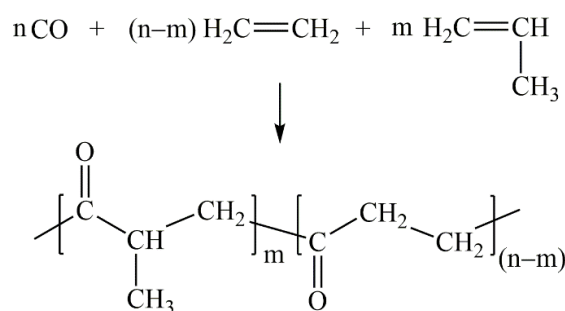


Figure 1-47. Synthesis of ethylene-propylene-carbon monoxide copolymer (EPCO) [126]

1.5.2 Functionalized Polymers by Postpolymeric Modification

Considering the chemical modification potential of the carbonyl group, aliphatic polyketones should be excellent pre-polymers for other types of functionalized polymers. Dozens of functionalized derivatives incorporating a wide variety of functional groups from the 1,4-dicarbonyl polyketones have already been prepared [126-141].

Apart from the reactive carbonyl itself, the structure feature of 1,4-dicarbonyl units additionally contributes to the high reactivity of this copolymer. Transition reactions from carbonyl group to alcohol [127-129], oxime [130], cyanhydrine [131], amine [132], hydantoin [133], thiol [134], nitrile [135], amide [136], tetrazole [136], bisphenol [137],

pyrrole [130, 138, 139], furan [140, 141], thiophene [142], etc... have been reported (Figure 1-48).

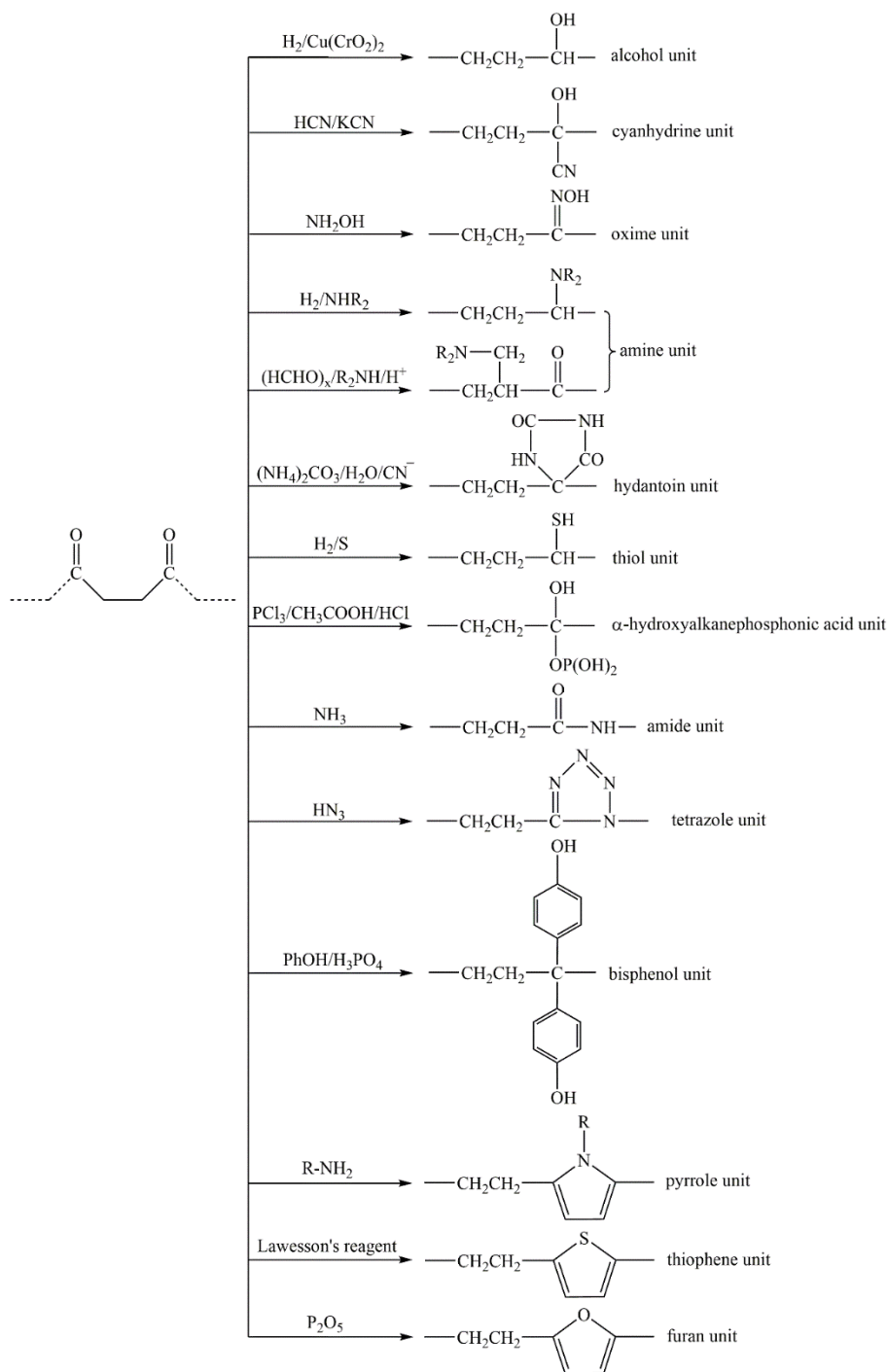


Figure 1-48. Chemical modification of ethylene-carbon monoxide copolymer

However, almost all these modifications require the unique 1,4-dicarbonyl units. To our knowledge, the modification of ketene-based-polymers containing 1,3-dicarbonyl units (PDMK) have rarely been experienced. The only successful attempt was a ketone group reduction reaction of PDMK using LiAlH_4 reported by G. Natta et al in 1960 [125], which gave a polyalcohol (Figure 1-49). The experimental conditions and polyalcohol properties were not clearly described in the literature.

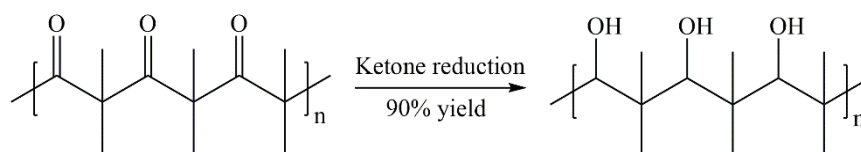


Figure 1-49. Ketone reduction of PDMK using LiAlH_4

1.6 Conclusion

Ketene chemistry still receives steady attention due to its excellent reactivity on the basis of the unique consecutive double bond structure. Ketene polymerization will continue to arise interest, as one single monomer possibly results in three totally different types of polymers, upon optimized conditions. However, cationic chain growth reactions of ketenes, which can lead a preferring useful polyketone structure, are poorly documented in literature, but need of going further. Besides, discovery of more efficient and structure-selective initiators for the synthesis of ketene-based polymers is a valuable challenge.

We listed almost all the ketene polymerizations in the tables, clearly and simply line by line. However, the great efforts behind each lines can hardly be expressed in terms of the difficulty of ketene chemistry, which requires researchers of rich organic synthesis experience, the wealth of polymerization knowledge, fully skilled experimental handlings and the most important, no fear of failure.

1.7 References

- [1] A.D. Allen, T.T. Tidwell, Ring opening of cyclobutene-1,2-dione and 3-trimethylsilylcyclobutene-1,2-dione. Dimerization/decarbonylation of a bisketene to a ketenylbutenolide, *Canadian Journal of Chemistry*, 77 (1999) 802-805.
- [2] P. Zarras, O. Vogl, Ketenes and bisketenes as polymer intermediates, *Progress in Polymer Science*, 16 (1991) 173-201.
- [3] M. Li, Y. Wei, J. Liu, H. Chen, L. Lu, W. Xiao, Sequential visible-light photoactivation and palladium catalysis enabling enantioselective [4+2] cycloadditions, *Journal of the American Chemical Society*, 139 (2017) 14707-14713.
- [4] P.A. Wender, C. Ebner, B.D. Fennell, F. Inagaki, B. Schröder, Ynol ethers as ketene equivalents in rhodium-catalyzed intermolecular [5 + 2] cycloaddition reactions, *Organic Letters*, 19 (2017) 5810-5813.
- [5] P. Rulli  re, J. Grisel, C. Poittevin, P. Cividino, S. Carret, J.-F. Poisson, Thermal [2 + 2]-cycloaddition of ketenes with chiral enol ethers: Route to densely substituted cyclobutanones, *Organic Letters*, 18 (2016) 2824-2827.
- [6] C.M. Rasik, Y.J. Hong, D.J. Tantillo, M.K. Brown, Origins of diastereoselectivity in lewis acid promoted ketene-alkene [2 + 2] cycloadditions, *Organic Letters*, 16 (2014) 5168-5171.
- [7] D.B. Rasmussen, J.M. Christensen, B. Temel, F. Studt, P.G. Moses, J. Rossmeisl, A. Riisager, A.D. Jensen, Ketene as a reaction intermediate in the carbonylation of dimethyl ether to methyl acetate over mordenite, *Angewandte Chemie International Edition*, 54 (2015) 7261-7264.
- [8] K.X. Rodriguez, N. Kaltwasser, T.A. Toni, B.L. Ashfeld, Rearrangement of an intermediate cyclopropyl ketene in a rhii-catalyzed formal [4 + 1]-cycloaddition employing vinyl ketenes as 1,4-dipoles and donor-acceptor metallocarbenes, *Organic Letters*, 19 (2017) 2482-2485.
- [9] F. Jiao, X. Pan, K. Gong, Y. Chen, G. Li, X. Bao, Shape-selective zeolites promote ethylene formation from syngas via a ketene intermediate, *Angewandte Chemie International Edition*, 57 (2018) 4692-4696.
- [10] R.B. Woodward, R. Hoffmann, The conservation of orbital symmetry, *Angewandte Chemie International Edition in English*, 8 (1969) 781-853.
- [11] V. Lavallo, Y. Canac, B. Donnadi  u, W.W. Schoeller, G. Bertrand, Co fixation to stable acyclic and cyclic alkyl amino carbenes: Stable amino ketenes with a small HOMO-LUMO gap, *Angewandte Chemie*, 118 (2006) 3568-3571.
- [12] A.A. Ibrahim, D. Nalla, M. Van Raaphorst, N.J. Kerrigan, Catalytic asymmetric heterodimerization of ketenes, *Journal of the American Chemical Society*, 134 (2012) 2942-2945.
- [13] H. Staudinger, Ketene, eine neue K  rperklasse, *Berichte der deutschen chemischen Gesellschaft*, 38 (1905) 1735-1739.
- [14] H. Staudinger,   ber ketene. Xix.   ber bildung und darstellung des diphenylketens, *Berichte der deutschen chemischen Gesellschaft*, 44 (1911) 1619-1623.
- [15] C. Smith, D. Norton, Dimethylketene, *Organic Syntheses*, (1963) 29-29.
- [16] C.C. McCarney, R.S. Ward, An improved method for the preparation of monoalkylketens, *Journal of the Chemical Society, Perkin Transactions 1*, (1975) 1600-1603.

- [17] A. Kostyuk, Z.G. Boyadzhan, G. Zaitseva, V. Sergeev, N. Savel'eva, Y.I. Baukov, I. Lutsenko, Halides and anhydrides of silyl- and germylacetic acid and γ -silyl- β -oxodiazalkanes, *Chemischer Informationsdienst*, 10 (1979) no-no.
- [18] W.T. Brady, R.M. Lloyd, Halogenated ketenes. 33. Cycloaddition of ketenes and trimethylsilyl enol ethers, *The Journal of Organic Chemistry*, 45 (1980) 2025-2028.
- [19] W.T. Brady, G.A. Scherubel, Halogenated ketenes. XXIII. Mechanism of the dehydrohalogenation of acid halides, *Journal of the American Chemical Society*, 95 (1973) 7447-7449.
- [20] C.D. Hurd, The ketenic decomposition of ketones. Ketene and methyl ketene, *Journal of the American Chemical Society*, 45 (1923) 3095-3101.
- [21] J.W. Williams, C.D. Hurd, An improved apparatus for the laboratory preparation of ketene and butadiene, *The Journal of Organic Chemistry*, 05 (1940) 122-125.
- [22] F. Wagner Jr, *Encyclopedia of chemical technology*, vol. 11, John Wiley & Sons, NY, USA, 1980.
- [23] J.C. Mackie, K.R. Doolan, High-temperature kinetics of thermal decomposition of acetic acid and its products, *International Journal of Chemical Kinetics*, 16 (1984) 525-541.
- [24] I.X. Green, W. Tang, M. Neurock, J.T. Yates, Localized partial oxidation of acetic acid at the dual perimeter sites of the Au/TiO_2 catalyst-formation of gold ketenylidene, *Journal of the American Chemical Society*, 134 (2012) 13569-13572.
- [25] C.L. Perrin, A. Flach, M.N. Manalo, Decomposition of malonic anhydrides, *Journal of the American Chemical Society*, 134 (2012) 9698-9707.
- [26] C.L. Perrin, T. Arrhenius, Malonic anhydride, *Journal of the American Chemical Society*, 100 (1978) 5249-5251.
- [27] G.J. Fisher, A. MacLean, A. Schnizer, Apparatus for the preparation of ketene by the pyrolysis of acetic anhydride, *The Journal of Organic Chemistry*, 18 (1953) 1055-1057.
- [28] N.T.M. Wilsmore, Clxxxviii.—keten, *Journal of the Chemical Society, Transactions*, 91 (1907) 1938-1941.
- [29] G. Pregaglia, M. Binaghi, *Encyclopedia of polymer science and technology*, vol. 8, (1968).
- [30] H. Egret, J.-P. Couvercelle, J. Belleney, C. Bunel, Cationic polymerization of dimethyl ketene, *European Polymer Journal*, 38 (2002) 1953-1961.
- [31] N. Hayki, N. Desilles, F. Burel, Aliphatic polyketone obtained by cationic polymerization of ethylketene, *Polymer Chemistry*, 2 (2011) 2350-2355.
- [32] C.D. Hurd, F.H. Blunck, The pyrolysis of esters, *Journal of the American Chemical Society*, 60 (1938) 2419-2425.
- [33] E.S. Rothman, Reactions of the stearylized enolic form of acetone, involving hexadecylketene as the reactive intermediate, *Journal of the American Oil Chemists Society*, 45 (1968) 189-193.
- [34] J.S. Witzeman, The transacetoacetylation: Mechanistic implications, *Tetrahedron Letters*, 31 (1990) 1401-1404.

- [35] J.S. Witzeman, W.D. Nottingham, Transacetoacetylation with tert-butyl acetoacetate: synthetic applications, *The Journal of Organic Chemistry*, 56 (1991) 1713-1718.
- [36] S. Andreades, H. Carlson, *Organic syntheses*, CV5, 1973.
- [37] H.W. Moore, D.S. Wilbur, Cyanoketenes. Mechanism of tert-butylcyanoketene cycloaddition to aldo- and ketoketenes, *The Journal of Organic Chemistry*, 45 (1980) 4483-4491.
- [38] R. Brown, F. Eastwood, K. Harrington, Methyleneketenes and methylenecarbenes. I. Formation of arylmethyleneketenes and alkylideneketenes by pyrolysis of substituted 2,2-Dimethyl-1,3-dioxan-4,6-diones, *Australian Journal of Chemistry*, 27 (1974) 2373-2384.
- [39] G.J. Baxter, R.F.C. Brown, F.W. Eastwood, K.J. Harrington, Pyrolytic generation of carbonylcyclopropane (dimethylene ketene) and its dimerization to dispiro-[2,1,2,1]-octane-4,8-dione, *Tetrahedron Letters*, 16 (1975) 4283-4284.
- [40] J.A.a.R. Hyatt, P. W., *Ketene Cycloadditions*, *Organic Reactions*, 2004.
- [41] F.A. Leibfarth, M. Kang, M. Ham, J. Kim, L.M. Campos, N. Gupta, B. Moon, C.J. Hawker, A facile route to ketene-functionalized polymers for general materials applications, *Nature Chemistry*, 2 (2010) 207.
- [42] N.J. Turro, P.A. Leermakers, H. Wilson, D. Neckers, G. Byers, G. Vesley, Photochemistry of 1, 3-cyclobutanediones. Decomposition modes and chemical intermediates, *Journal of the American Chemical Society*, 87 (1965) 2613-2619.
- [43] I. Haller, R. Srinivasan, Primary processes in the photochemistry of tetramethyl-1, 3-cyclobutanedione, *Journal of the American Chemical Society*, 87 (1965) 1144-1145.
- [44] A.P. Krapcho, B. Abegaz, Photochemistry of dispiro-1, 3-cyclobutanediones in methylene chloride and methanol solutions, *The Journal of Organic Chemistry*, 39 (1974) 2251-2255.
- [45] D.H.R. Barton, G. Quinkert, 1. Photochemical transformations. Part VI. Photochemical cleavage of cyclohexadienones, *Journal of the Chemical Society (Resumed)*, (1960) 1-9.
- [46] G. Quinkert, Light-induced formation of acids from cyclic ketones, *Angewandte Chemie International Edition in English*, 4 (1965) 211-222.
- [47] G. Quinkert, E. Kleiner, B.J. Freitag, J. Glenneberg, U.M. Billhardt, F. Cech, K.R. Schmieder, C. Schudok, H.C. Steinmetzer, J.W. Bats, Über dienketene aus o-chinolacetaten, *Helvetica chimica acta*, 69 (1986) 469-537.
- [48] G. Quinkert, En route to multisurface chemistry, *Angewandte Chemie International Edition in English*, 14 (1975) 790-800.
- [49] C. Araujo-Andrade, A. Gómez-Zavaglia, I.D. Reva, R. Fausto, Conformers, infrared spectrum and UV-induced photochemistry of matrix-isolated furfuryl alcohol, *The Journal of Physical Chemistry A*, 116 (2012) 2352-2365.
- [50] S. Tsutsui, K. Sakamoto, K. Ebata, C. Kabuto, H. Sakurai, Synthesis, structure, and photochemistry of 2, 3, 5, 6-tetrasilyl-1, 4-benzoquinones and related compounds, *Bulletin of the Chemical Society of Japan*, 75 (2002) 2571-2577.
- [51] L. Wolff, Ueber diazoanhydride, *Justus Liebigs Annalen der Chemie*, 325 (1902) 129-195.
- [52] L. Wolff, R. Krüche, Über diazoanhydride (1, 2, 3-oxydiazole oder diazoxyde) und diazoketone, *Justus Liebigs Annalen der Chemie*, 394 (1912) 23-59.

- [53] P. Haiss, K.-P. Zeller, The photochemical Wolff rearrangement of 3-diazo-1, 1, 1-trifluoro-2-oxopropane revisited, *Organic & biomolecular chemistry*, 1 (2003) 2556-2558.
- [54] P. Yates, T. Clark, The thermal decomposition of α -diazoacetophenone, *Tetrahedron Letters*, 2 (1961) 435-439.
- [55] R. Huisgen, G. Binsch, L. Ghosez, 1,3-dipolare cycloadditionen, vii. Abfangen der ketocarben-zwischenstufe bei der thermolyse von diazoketonen, *Chemische Berichte*, 97 (1964) 2628-2639.
- [56] P. Yates, G. Abrams, M.J. Betts, S. Goldstein, Base-induced rearrangement of γ -diketones. I. The rearrangement of 1, 2, 2-triphenyl-1, 4-pentanedione to 1, 3, 3-triphenyl-1, 4-pentanedione, *Canadian Journal of Chemistry*, 49 (1971) 2850-2860.
- [57] H. Meier, K.P. Zeller, The wolff rearrangement of α -diazo carbonyl compounds, *Angewandte Chemie International Edition in English*, 14 (1975) 32-43.
- [58] W. Jugelt, D. Schmidt, Struktur und reaktivität aliphatischer diazoverbindungen—IX: Kinetische untersuchung der thermischen Wolff-Umlagerung der aryl-aroyl-diazomethane, *Tetrahedron*, 25 (1969) 969-984.
- [59] M. Regitz, W. Bartz, Untersuchungen an diazoverbindungen, vii. Vergleichende kinetische untersuchungen zur thermischen stabilität aliphatischer diazoverbindungen, *Chemische Berichte*, 103 (1970) 1477-1485.
- [60] W. Bartz, M. Regitz, A. Liedhegener, Umlagerungsreaktionen, v. Eine kinetische studie zum mechanismus der Wolff-Umlagerung, *Chemische Berichte*, 103 (1970) 1463-1476.
- [61] J.T. Su, R. Sarpong, B.M. Stoltz, W.A. Goddard, Substituent effects and nearly degenerate transition states: rational design of substrates for the tandem wolff-cope reaction, *Journal of the American Chemical Society*, 126 (2004) 24-25.
- [62] S.G. Sudrik, T. Maddanimath, N.K. Chaki, S.P. Chavan, S.P. Chavan, H.R. Sonawane, K. Vijayamohanan, Evidence for the involvement of silver nanoclusters during the wolff rearrangement of α -diazoketones, *Organic letters*, 5 (2003) 2355-2358.
- [63] R.R. Julian, J.A. May, B.M. Stoltz, J. Beauchamp, Gas-phase synthesis of charged copper and silver Fischer carbenes from diazomalonates: Mechanistic and conformational considerations in metal-mediated Wolff rearrangements, *Journal of the American Chemical Society*, 125 (2003) 4478-4486.
- [64] R.R. Julian, J.A. May, B.M. Stoltz, J. Beauchamp, Molecular mousetraps: Gas-phase studies of the covalent coupling of noncovalent complexes initiated by reactive carbenes formed by controlled activation of diazo precursors, *Angewandte Chemie International Edition*, 42 (2003) 1012-1015.
- [65] R. Sarpong, J.T. Su, B.M. Stoltz, The development of a facile tandem Wolff/Cope rearrangement for the synthesis of fused carbocyclic skeletons, *Journal of the American Chemical Society*, 125 (2003) 13624-13625.
- [66] S.P. Marsden, W.-K. Pang, Efficient, general synthesis of silylketenes via an unusual rhodium mediated Wolff rearrangement, *Chemical Communications*, (1999) 1199-1200.
- [67] S.P. Marsden, J.T. Steer, B.S. Orlek, Synthesis of α -silylalkylbenzoxazoles and oxazoles from stable silylketenes, *Tetrahedron*, 65 (2009) 5503-5512.

- [68] S.M. Bucher, R. Brueckmann, G. Maas, Aryl Trialkylsilyl Ketenes: Acid-Catalyzed Synthesis from 1-Aryl-2-diazo-2-trialkylsilylethanones and Their Conversion into 3-Silyl-1-silyloxyallenes, *European Journal of Organic Chemistry*, 2008 (2008) 4426-4433.
- [69] L. Horner, E. Spietschka, Die präparative bedeutung der zersetzung von diazo-carbonylverbindungen im UV-licht, *Chemische Berichte*, 85 (1952) 225-229.
- [70] G. Burdzinski, Y. Zhang, J. Wang, M.S. Platz, Concerted wolff rearrangement in two simple acyclic diazocarbonyl compounds, *The Journal of Physical Chemistry A*, 114 (2010) 13065-13068.
- [71] G. Burdzinski, J. Réhault, J. Wang, M.S. Platz, A study of the photochemistry of diazo Meldrum's acid by ultrafast time-resolved spectroscopies, *The Journal of Physical Chemistry A*, 112 (2008) 10108-10112.
- [72] G. Natta, G. Mazzanti, G.F. Pregaglia, M. Binaghi, Crystalline polymers of dialkyl ketenes, *Die Makromolekulare Chemie*, 44 (1961) 537-549.
- [73] G. Natta, G. Mazzanti, G.F. Pregaglia, G. Pozzi, Alternating copolymers having a stereoregular polyester structure, *Journal of Polymer Science*, 58 (1962) 1201-1210.
- [74] E. Wedekind, Ueber das Verhalten einiger Säurechloride bei der Chlorwasserstoffentziehung, *Justus Liebigs Annalen Der Chemie*, 323 (1902) 246-257.
- [75] H. Staudinger, K. Clar, E. Czako, Über ketene. Xxiii. Über die reaktionsfähigkeit des halogenatoms gegen metalle, *Berichte der deutschen chemischen Gesellschaft*, 44 (1911) 1640-1647.
- [76] H. Staudinger, Ketene: L. Mitteilung. Über additions- und polymerisationsreaktionen des dimethylketens. 1. Über neue verbindungen des dimethylketens mit kohlendioxyd, *Helvetica Chimica Acta*, 8 (1925) 306-332.
- [77] H. Staudinger, Ueber ketene. 3. Mittheilung: Diphenylenketen, *Berichte der deutschen chemischen Gesellschaft*, 39 (1906) 3062-3067.
- [78] R.H. Hasek, R.D. Clark, E.U. Elam, J.C. Martin, The chemistry of dimethylketene dimer. IV. The polyester and β -lactone dimer of dimethylketene, *The Journal of Organic Chemistry*, 27 (1962) 60-64.
- [79] E.U. Elam, Ketenes. XI. Preparation of. beta.-lactone dimer by dimerization of dimethylketene in the presence of derivatives of trivalent phosphorus, *The Journal of Organic Chemistry*, 32 (1967) 215-216.
- [80] A. Rafai Far, Ketenes in polymer-assisted synthesis, *Angewandte Chemie International Edition*, 42 (2003) 2340-2348.
- [81] H. Wang, N. Desilles, F. Burel, Effect of tetra-n-butylammonium bromide salt on the cationic polymerization of dimethylketene and on the thermal properties of the obtained polyketones, *Journal of Polymer Science Part A: Polymer Chemistry*, 52 (2014) 1493-1499.
- [82] Y. Xiang, D.J. Burrill, K.K. Bullard, B.J. Albrecht, L.E. Tragesser, J. McCaffrey, D.S. Lambrecht, E. Pentzer, Polymerization of silyl ketenes using alkoxide initiators: a combined computational and experimental study, *Polymer Chemistry*, 8 (2017) 5381-5387.
- [83] X. Qi, P. Dong, Z. Liu, T. Liu, Q. Fu, Selective localization of multi-walled carbon nanotubes in bi-component biodegradable polyester blend for rapid electroactive shape memory performance, *Composites Science and Technology*, 125 (2016) 38-46.

- [84] Z. Chen, N. Lin, S. Gao, C. Liu, J. Huang, P.R. Chang, Sustainable composites from biodegradable polyester modified with camelina meal: synergistic effects of multicomponents on ductility enhancement, *ACS Sustainable Chemistry & Engineering*, 4 (2016) 3228-3234.
- [85] H. Wang, N. Desilles, N. Follain, S. Marais, F. Burel, Dimethylketene-based aliphatic polyketones: Copolymers and star-shaped polymers potentially useful in food packaging, *European Polymer Journal*, 85 (2016) 411-420.
- [86] N. Hayki, N. Desilles, F. Burel, Polyester Obtained by Anionic Polymerization of Ethylketene, *Macromolecular Chemistry and Physics*, 212 (2011) 375-382.
- [87] G. Pregaglia, M. Binaghi, Ketene polymers, *Enc. Polym. Sci. Technol*, 8 (1968) 18.
- [88] H. Wang, Synthèse et caractérisation de nouvelles polycétones aliphatiques à partir des cétones, Rouen, INSA, 2013.
- [89] Y. Yamashita, S. Nunomoto, Anionic polymerization of dimethylketene, *Die Makromolekulare Chemie: Macromolecular Chemistry and Physics*, 58 (1962) 244-246.
- [90] Y. Yamashita, S. Miura, M. Nakamura, Ambident nature of the polydimethylketene anion, *Die Makromolekulare Chemie*, 68 (1963) 31-47.
- [91] N. Kornblum, R.A. Smiley, R.K. Blackwood, D.C. Iffland, The mechanism of the reaction of silver nitrite with alkyl halides. The contrasting reactions of silver and alkali metal salts with alkyl halides. The alkylation of ambident anions 1, 2, *Journal of the American Chemical Society*, 77 (1955) 6269-6280.
- [92] H. Sugimoto, M. Kanai, S. Inoue, Lanthanoid alkoxide as a novel initiator for the synthesis of polyester via polymerization of ketenes, *Macromolecular Chemistry and Physics*, 199 (1998) 1651-1655.
- [93] P. Zarras, O. Vogl, Ketenes and bisketenes as polymer intermediates, *Progress in polymer science*, 16 (1991) 173-201.
- [94] D.E. Paul, D. Lipkin, S. Weissman, Reaction of sodium metal with aromatic hydrocarbons 1, 2, *Journal of the American Chemical Society*, 78 (1956) 116-120.
- [95] D. Lipkin, D. Paul, J. Townsend, S. Weissman, Observations on a class of free radicals derived from aromatic compounds, *Science*, 117 (1953) 534-535.
- [96] G. Natta, G. Mazzanti, G. Pregaglia, G. Pozzi, Alternating copolymers having a stereoregular polyester structure, *Journal of Polymer Science*, 58 (1962) 1201-1210.
- [97] J. Furukawa, T. Tsuruta, Catalytic reactivity and stereospecificity of organometallic compounds in olefin polymerization, *Journal of Polymer Science*, 36 (1959) 275-286.
- [98] B.J. Burger, M.E. Thompson, W.D. Cotter, J.E. Bercaw, Ethylene insertion and β -hydrogen elimination for permethylscandocene alkyl complexes. A study of the chain propagation and termination steps in Ziegler-Natta polymerization of ethylene, *Journal of the American Chemical Society*, 112 (1990) 1566-1577.
- [99] H.N. Friedlander, K. Oita, Organometallics in ethylene polymerization, *Industrial & Engineering Chemistry*, 49 (1957) 1885-1890.
- [100] T. Völker, F. Dempwolff, P.L. Graumann, E. Meggers, Progress towards bioorthogonal catalysis with organometallic compounds, *Angewandte Chemie International Edition*, 53 (2014) 10536-10540.

- [101] G.A. Molander, Application of lanthanide reagents in organic synthesis, *Chemical Reviews*, 92 (1992) 29-68.
- [102] H. Kagan, J. Namy, Tetrahedron report number 213: Lanthanides in organic synthesis, *Tetrahedron*, 42 (1986) 6573-6614.
- [103] T.M. Ford, S.J. McLain, Rare earth metal coordination compounds as lactone polymerization catalysts, U.S. Patent 5,208,297[P]. 1993-5-4.
- [104] H. Abe, S. Inoue, Lanthanoid complex as a novel carbon dioxide carrier for the carboxylation of active methylene compounds under mild conditions, *Journal of the Chemical Society, Chemical Communications*, (1994) 1197-1198.
- [105] N. Fukuwatari, H. Sugimoto, S. Inoue, Lanthanoid isopropoxide as a novel initiator for anionic polymerization of isocyanates, *Macromolecular rapid communications*, 17 (1996) 1-7.
- [106] G. Natta, G. Mazzanti, G.F. Pregaglia, M. Binaghi, M. Cambini, Polymers of dimethylketene having prevailing polyacetalic structure, *Die Makromolekulare Chemie*, 51 (1962) 148-153.
- [107] G.F. Pregaglia, M. Binaghi, M. Cambini, Polydimethylketene with carbon-oxygen backbone structure, *Die Makromolekulare Chemie*, 67 (1963) 10-30.
- [108] T. Tsunetsugu, K. Arimoto, T. Fueno, J. Furukawa, Polymerization of methylphenylketone and its copolymerization with benzaldehyde, *Die Makromolekulare Chemie: Macromolecular Chemistry and Physics*, 112 (1968) 210-219.
- [109] A. Sudo, S. Uchino, T. Endo, Development of a living anionic polymerization of ethylphenylketene: A novel approach to well-defined polyester synthesis, *Macromolecules*, 32 (1999) 1711-1713.
- [110] A. Sudo, S. Uchino, T. Endo, Living anionic polymerization of ethylphenylketene: A novel approach to well-defined polyester synthesis, *Journal of Polymer Science Part A: Polymer Chemistry*, 38 (2000) 1073-1082.
- [111] A. Sudo, S. Uchino, T. Endo, Application of ketenes to well-defined polyester synthesis. II. Synthesis of reactive polyester by living anionic polymerization of (4-halophenyl) ethylketene, *Journal of Polymer Science Part A: Polymer Chemistry*, 39 (2001) 2093-2102.
- [112] A. Sudo, S. Uchino, T. Endo, Application of ketenes to well-defined polyester synthesis. III. Living anionic polymerization of ethyl (4-methoxyphenyl) ketene—Development of polyester having masked phenol side chain, *Journal of Polymer Science Part A: Polymer Chemistry*, 39 (2001) 1596-1600.
- [113] G. Natta, G. Mazzanti, G. Pregaglia, M. Binaghi, Alternating copolymers of dimethylketene with ketones, *Journal of the American Chemical Society*, 82 (1960) 5511-5512.
- [114] M. Brestaz, N. Desilles, G. Le, C. Bunel, Polyester obtained from dimethylketene and acetone: synthesis and characterization, *Journal of Polymer Research*, 19 (2012) 12.
- [115] K. Hashimoto, H. Sumitomo, Anionic copolymerization of p-anisaldehyde with dimethylketene, *Journal of Polymer Science Part A-1: Polymer Chemistry*, 9 (1971) 1189-1196.
- [116] M. Brestaz, N. Desilles, G. Le, C. Bunel, Polyester from dimethylketene and acetaldehyde: Direct copolymerization and β -lactone ring-opening polymerization, *Journal of Polymer Science Part A: Polymer Chemistry*, 49 (2011) 4129-4138.

- [117] E. Dyer, E. Sincich, Anionic copolymerization of isocyanates with ketenes, *Journal of Polymer Science: Polymer Chemistry Edition*, 11 (1973) 1249-1260.
- [118] D. Nagai, A. Sudo, T. Endo, Anionic alternating copolymerization of ketene and aldehyde: Control of enantioselectivity by bisoxazoline-type ligand for synthesis of optically active polyesters, *Macromolecules*, 39 (2006) 8898-8900.
- [119] B.J. Lommerts, D.J. Sikkema, Synthesis and structure of a new polyalcohol, *Macromolecules*, 33 (2000) 7950-7954.
- [120] T. Higashimura, S. Aoshima, M. Sawamoto, New initiators for living cationic polymerization of vinyl compounds, *Makromolekulare Chemie. Macromolecular Symposia*, Wiley Online Library, 1988, pp. 457-471.
- [121] H. Egret, Synthèse et caractérisation des polymères du diméthylcétène. Application à la perméabilité aux gaz, Rouen, 1998.
- [122] R. Linemann, G. Le, Synthesis method for polydimethylketene by friedel-craft cationic polymerization of dimethylketene, U.S. Patent 7,105,615[P]. 2006-9-12.
- [123] G.A. Olah, E. Zadok, R. Edler, D.H. Adamson, W. Kasha, G.S. Prakash, Ionic polymerizations. 6. Friedel-Crafts dehydrohalogenative polymerization of acetyl and enolizable-substituted acetyl halides to polyketenes (poly (oxyacetylenes)), *Journal of the American Chemical Society*, 111 (1989) 9123-9124.
- [124] R. Oda, S. Munemiya, M. Okano, Polymerization of ketene and diketene, (1962).
- [125] G. Natta, G. Mazzanti, G. Pregaglia, M. Binaghi, M. Peraldo, Crystalline polymers of dimethylketene, *Journal of the American Chemical Society*, 82 (1960) 4742-4743.
- [126] J.I. Choi, S.K. Yoon, Polyketone resin composition having excellent gas barrier properties, U.S. Patent Application 15/524,536[P]. 2017-11-2.
- [127] M.M. Brubaker, D.D. Coffman, H.H. Hoehn, Synthesis and characterization of ethylene/carbon monoxide copolymers, a new class of polyketones, *Journal of the American Chemical Society*, 74 (1952) 1509-1515.
- [128] E. Drent, Polymeric polyalcohols, U.S. Patent 5,071,926[P]. 1991-12-10.
- [129] Y. Morishima, T. Takizawa, S. Murahashi, Synthesis, structure and some properties of a new polyalcohol, *European Polymer Journal*, 9 (1973) 669-675.
- [130] S.-Y. Lu, R.M. Paton, M.J. Green, A.R. Lucy, Synthesis and characterization of polyketoximes derived from alkene-carbon monoxide copolymers, *European polymer journal*, 32 (1996) 1285-1288.
- [131] K. Nozaki, N. Kosaka, V.M. Graubner, T. Hiyama, Methylenation of an optically active γ -polyketone: Synthesis of a new class of hydrocarbon polymers with main-chain chirality, *Macromolecules*, 34 (2001) 6167-6168.
- [132] D. Coffman, H. Hoehn, J. Maynard, Reductive amination of ethylene/carbon monoxide polyketones. A new class of polyamines, *Journal of the American Chemical Society*, 76 (1954) 6394-6399.
- [133] J.R. Johnson, Polymer containing extralinear hydantoin rings from monoolefin/carbon monoxide polymer, U.S. Patent 2,527,821[P]. 1950-10-31.
- [134] S.L. Scott, Polymeric polythiols, U.S. Patent 2,495,293[P]. 1950-1-24.

- [135] M.C. Walter, Reaction products of acrylonitrile with macromolecular ketones, U.S. Patent 2,396,963[P]. 1946-3-19.
- [136] R. Michel, W. Murphey, Intramolecular rearrangements of polyketones, *Journal of Polymer Science*, 55 (1961) 741-751.
- [137] C.W. Fitko, R. Abraham, Thermosetting polybisphenols, U.S. Patent 3,317,472 [P]. 1967-5-2.
- [138] T.E. Kiovsky, R.C. Kromer, Polymeric pyrrollic derivative, U.S. Patent 3,979, 374[P]. 1976-9-7.
- [139] Y. Zhang, A. Broekhuis, M.C. Stuart, F. Picchioni, Polymeric amines by chemical modifications of alternating aliphatic polyketones, *Journal of applied polymer science*, 107 (2008) 262-271.
- [140] Z. Jiang, S. Sangneria, A. Sen, Polymers incorporating backbone thiophene, furan, and alcohol functionalities formed through chemical modifications of alternating olefin–carbon monoxide copolymers, *Journal of Polymer Science Part A: Polymer Chemistry*, 32 (1994) 841-847.
- [141] Y. Zhang, A.A. Broekhuis, F. Picchioni, Thermally self-healing polymeric materials: the next step to recycling thermoset polymers?, *Macromolecules*, 42 (2009) 1906-1912.
- [142] B. Pedersen, S. Scheibye, N. Nilsson, S.O. Lawesson, Studies on organophosphorus compounds XX. Syntheses of thioketones, *Bulletin des Sociétés Chimiques Belges*, 87 (1978) 223-228.

2. Cationic Polymerization of Different Aliphatic and Aromatic Ketenes

As stated in Chapter 1, dimethylketene (DMK) and ethylketene (EK) are among the few monomers which were cationically polymerized to give polyketone-structured products [1, 2]. This result indicates a high possibility of success in the same reactions with other methyl- or ethyl-substituted ketenes.

Taking DMK and EK as references, two similar aliphatic ketenes, methylethylketene (MEK) and diethylketene (DEK), were first determined as our choices in this Chapter. Also, successful cationic polymerization of ketenes containing phenyl substitution has rarely been reported in the literature, but this is worthy to be further explored. So we also decided to study ethylphenylketene (EPK) and diphenylketene (DPK) in our experiments.

2.1 Monomer Synthesis

All these reactions schemes were taken from the literature.

2.1.1 Methylethylketene (MEK)

MEK was formed by decomposition of methyl ethyl malonic anhydride at high temperature under reduced pressure according to the previously reported procedure starting from the commercial diethyl-2-methylmalonate (Figure 2-1) [3]. The synthesis procedure was given in Annexes.

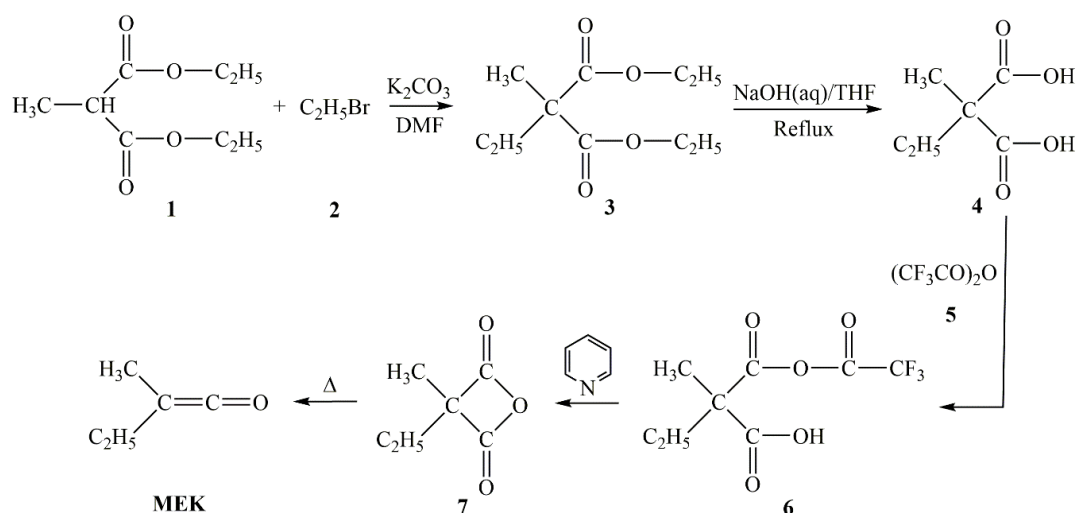


Figure 2-1. Synthesis route of MEK

Considering that the stability and potential danger of MEK have not been clearly mentioned in the literature, this freshly synthesized monomer was carefully handled and stored at 4°C under oxygen-free atmosphere, and used as soon as possible.

2.1.2 Diethylketene (DEK)

Similarly as MEK, DEK was prepared by a decomposition reaction of diethyl malonic anhydride at high temperature under reduced pressure starting from the commercial diethylmalonic acid (Figure 2-2) [4]. The synthesis procedure is detailed in Annexes.

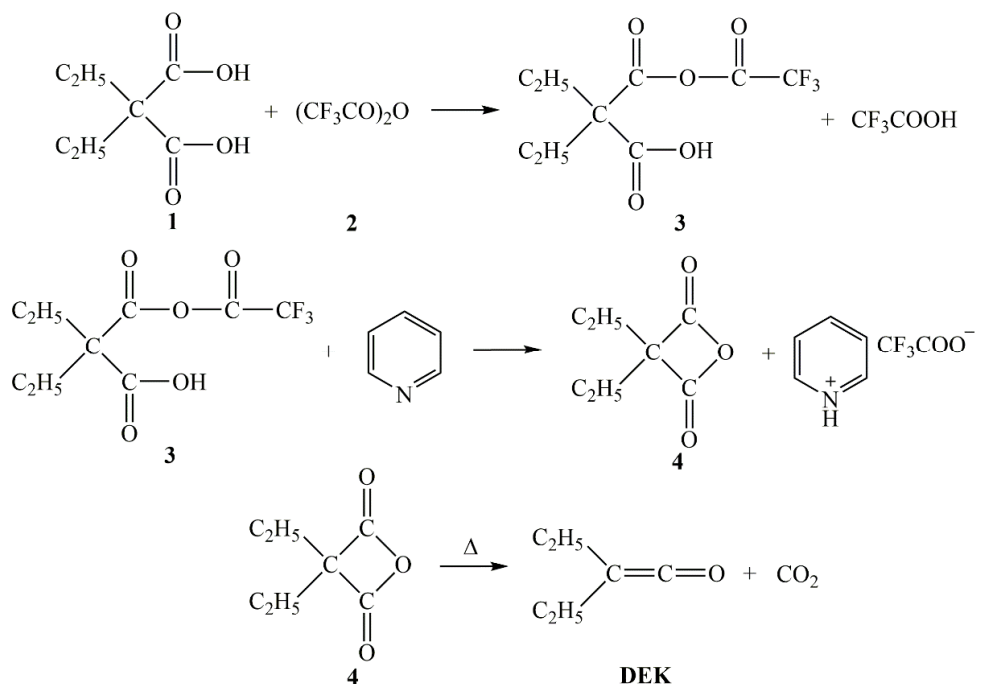


Figure 2-2. Synthesis and pyrolysis of diethyl malonic anhydride

The freshly distilled DEK monomer was stored in sealed bottles at 4°C under Alphagaz™ 2 nitrogen flow, and was used as soon as possible.

2.1.3 Ethylphenylketene (EPK)

EPK was prepared from 2-phenyl butanoyl chloride using a dehydrochlorination reaction (Figure 2-3) [5]. The synthetic procedure was detailed in Annexes.

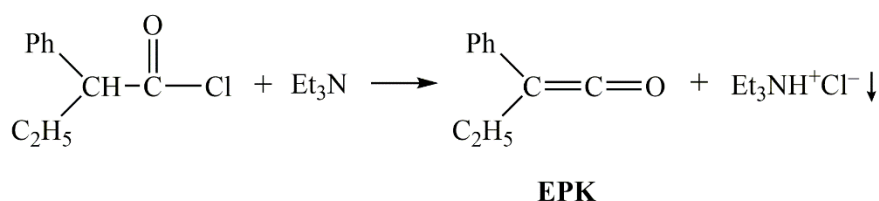


Figure 2-3. Synthesis of EPK by dehydrochlorination reaction

The prepared EPK remained to be stable for up to two months in the freezer under an argon atmosphere [5].

2.1.4 Diphenylketene (DPK)

DPK was synthesized similarly as EPK, by a dehydrochlorination reaction. The procedure includes an extra step for preparation of the corresponding acid chloride source compound (Figure 2-4) [6]. The synthetic procedure was detailed in Annexes.

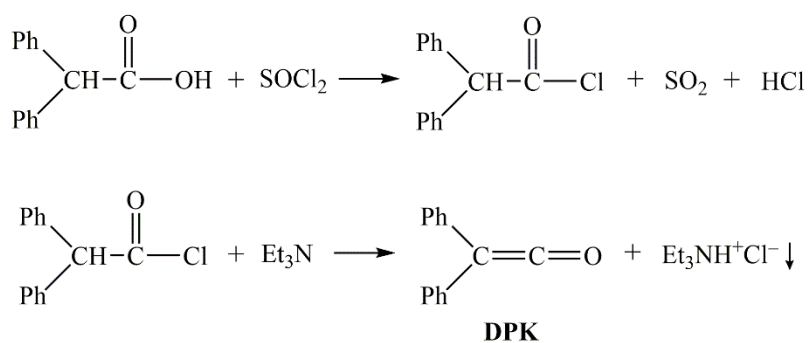


Figure 2-4. Synthesis of DPK by dehydrochlorination reaction

The DPK monomer was stored in sealed bottles in the fridge (at 4°C) under Alphagaz™ 2 nitrogen flow before use. The stability of DPK was monitored by IR spectra over time at 4°C (Figure 2-5). The decrease of signal at 2097 cm⁻¹ revealed side reactions; therefore all polymerizations of DPK were conducted on freshly prepared samples to avoid negative influence of monomer impurity.

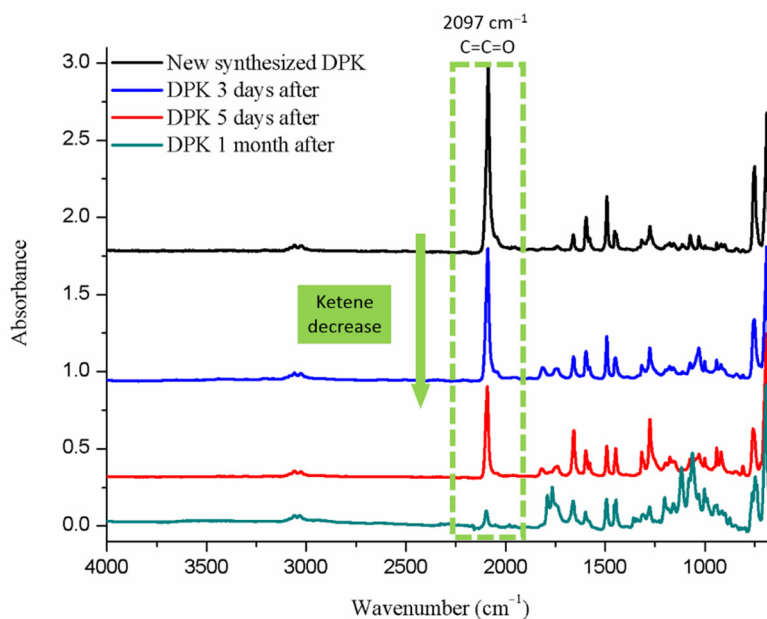


Figure 2-5. IR spectra of DPK tested at different storage times

2.2 Cationic Homopolymerization of Ketenes

All the recovered ketenes were stored in sealed bottles at 4°C under Alphagaz™ 2 nitrogen flow, and then quickly subjected to cationic polymerization after their synthesis. Otherwise stated, a general cationic polymerization set of conditions, optimized by the previous work, was adopted [1]: different reaction temperatures below 25°C, anhydrous dichloromethane as the solvent, $[\text{Monomer}]_0 = 3 \text{ mol} \cdot \text{L}^{-1}$, $[\text{Monomer}]_0 / [\text{Initiator}]_0 = 100$. The expected reaction should proceed as Figure 2-6:

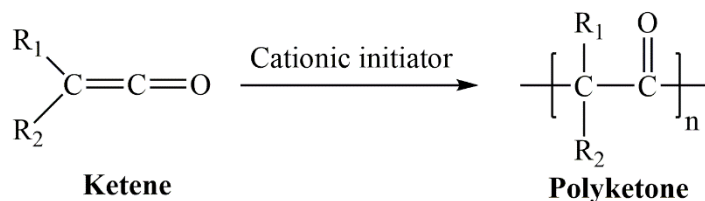


Figure 2-6. Desired cationic polymerization of the four ketenes

2.2.1 MEK

To reach $[\text{MEK}]_0 = 3 \text{ mol} \cdot \text{L}^{-1}$, anhydrous CH_2Cl_2 was first added into the freshly distilled MEK by a gas-tight syringe. After the reactor was stabilized at the desired temperature, $1 \text{ mol} \cdot \text{L}^{-1}$ initiator in anhydrous CH_2Cl_2 was added into the reaction system to trigger the polymerization, according to $[\text{Monomer}]_0 / [\text{Initiator}]_0 = 100$. The reactive medium was kept during 3 h at the required temperature and then allowed back to room temperature overnight before termination. Absolute ethanol was then injected into the reactor to neutralize residual ketenes and initiators. The polymerization conditions and results were summarized in Table 2-1.

Table 2-1. Summary of cationic polymerization conditions of methylethylketene

Run	Monomer	Initiating system	Solvent	Temperature (°C)	Remarks
23	MEK	AlBr_3	CH_2Cl_2	-78	reaction hardly proceeds
24		AlCl_3		-78	reaction hardly proceeds
25		AlCl_3 , $(\text{CH}_3)_3\text{CCl}$		0	reaction hardly proceeds
26		AlCl_3 , $(\text{CH}_3)_3\text{CCl}$		-78	reaction hardly proceeds
27		$\text{CF}_3\text{SO}_3\text{H}$		-78	reaction hardly proceeds

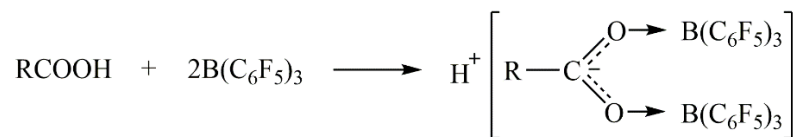
Unfortunately, no polymer was recovered from these polymerization experiments.

2.2.2 DEK

Numerous initiators, reaction temperatures and solvents were used. The detailed polymerization conditions and results were summarized in Table 2-2.

Table 2-2. Summary of cationic polymerization conditions of diethylketene

Run	Monomer	Initiating system	Solvent	Dielectric constant of solvent (ϵ)	Temp. (°C)	Remarks
1	DEK	AlBr ₃	CH ₂ Cl ₂	8.93	0	reaction hardly proceeds
2			Toluene	2.38	0	
3			Nitrobenzene / CCl ₄ (1 : 1)	-	-30	
4		AlCl ₃ , (CH ₃) ₃ CCl	CH ₂ Cl ₂	8.93	0	
54					-20	
11					-78	
8			DMF	36.7	-50	
9			NMP	32.2	-20	
10			Toluene	2.38	-78	
5			CH ₂ Cl ₂	8.93	0	
6					25	
7					-78	
12			CH ₂ Cl ₂	8.93	0	
13			CH ₂ Cl ₂	8.93	0	
14		CF ₃ SO ₃ H	CH ₂ Cl ₂	8.93	0	
15			CH ₂ Cl ₂	8.93	-78	
16			Toluene	2.38	-78	
44		HClO ₄	CH ₂ Cl ₂	8.93	0	
45			CH ₂ Cl ₂	8.93	-78	
64		Stearic acid, B(C ₆ F ₅) ₃	CHCl ₃	4.81	-78	
65			CH ₂ Cl ₂	8.93	-20	
66			CH ₂ Cl ₂	8.93	-78	

Figure 2-7. Preparation of a special Brønsted acid initiator by $n(\text{acid}) : n(\text{B}(\text{C}_6\text{F}_5)_3) = 1 : 2$

However, no polymer could be obtained using various solvents with distinct dielectric constants and several types of initiators (Lewis acids, with or without co-initiator and / or ligand, Brønsted acids).

GC-MS analysis (Figure in Annexes) of the reaction medium proved that DEK was effectively synthesized but could not be polymerized under these conditions. The ester with ethanol (main product) was solely obtained (Figure 2-8).

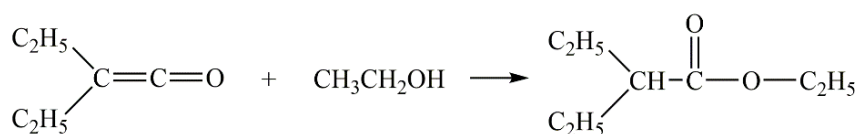


Figure 2-8. Products from DEK after polymerization procedure and precipitation in ethanol

2.2.3 EPK

The detailed polymerization conditions and results were summarized in Table 2-3.

Table 2-3. Summary of cationic polymerization conditions of ethylphenylketene

Run	Monomer	Initiating system	Solvent	Temperature (°C)	Remarks
50	EPK	AlBr_3	CH_2Cl_2	-78	reaction hardly proceeds
51		AlCl_3		-78	reaction hardly proceeds
29		AlCl_3 , $(\text{CH}_3)_3\text{CCl}$		0	reaction hardly proceeds
30		AlCl_3 , $(\text{CH}_3)_3\text{CCl}$		-78	reaction hardly proceeds
52		$\text{CF}_3\text{SO}_3\text{H}$		-78	reaction hardly proceeds

All these cationic polymerizations failed to give polymers. GC-MS analysis (Figure in Annexes) of the reaction medium only proved the presence of the ester and acid structure formed after neutralization with ethanol (Figure 2-9). This provided evidences to the successful synthesis of EPK monomer and ineffective cationic polymerization conditions.

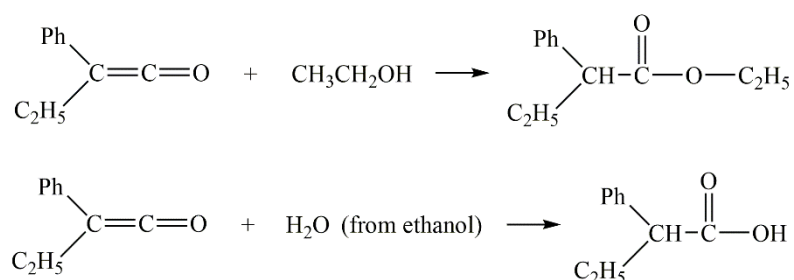


Figure 2-9. Product from EPK after polymerization procedure and precipitation in ethanol

2.2.4 DPK

The detailed polymerization conditions and results were summarized in Table 2-4.

Table 2-4. Summary of cationic polymerization conditions of diphenylketene

Run	Monomer	Initiating system	Solvent	Temperature (°C)	Remarks ^a
38	DPK	AlBr ₃	CH ₂ Cl ₂	-78	reaction hardly proceeds
53		AlCl ₃	CH ₂ Cl ₂	-78	reaction hardly proceeds
36		AlCl ₃ , (CH ₃) ₃ CCl	NMP	-20	reaction hardly proceeds
37			Toluene	-78	reaction hardly proceeds
34			CH ₂ Cl ₂	-78	reaction hardly proceeds
55				-20	reaction hardly proceeds
35				0	reaction hardly proceeds
39		CF ₃ SO ₃ H	CH ₂ Cl ₂	-78	83% yield oligoester

40			-20	48% yield oligoester
41			0	44% yield oligoester
42		Toluene	0	90% yield oligoester
43		DMF	0	reaction hardly proceeds
46	HClO ₄	CH ₂ Cl ₂	-78	reaction hardly proceeds
47			0	reaction hardly proceeds
68	Stearic acid, B(C ₆ F ₅) ₃	CH ₂ Cl ₂	-78	reaction hardly proceeds

a: yields were calculated by weight percent of obtained polymers (after precipitation) over feed monomers

As shown in the table, most of the cationic initiators failed to trigger the reaction. Like the other ketenes above, GC-MS analysis (Figure in Annexes) of the reaction media gave the ester and acid compound formed after neutralization with ethanol (Figure 2-10); some unreacted DPK monomer was identified.

However, when using CF₃SO₃H as initiator, in toluene and CH₂Cl₂ (solvents with low dielectric constant), polyesters with quite good yields (up to 90%) were obtained. This result was quite surprising since this initiator failed to give polymers for all other ketenes, and even for DMK [8].

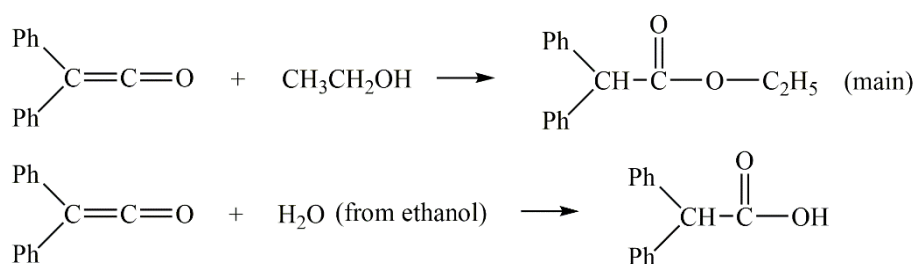


Figure 2-10. An undesired ester from DPK after polymerization procedure and precipitation in ethanol

The resulting polyester structure in Run 39~42 was supported by FT-IR spectra and ¹³C NMR (δ = 171.4 (C_a), 140.2 (C_b), 138.1 (C_c), 126~132 (benzene-C), 57.1 (C_i) ppm in CD₂Cl₂). A single strong absorption band at 1750 cm⁻¹ (Figure 2-11) and the peak at δ =

171.4 ppm on ^{13}C NMR (Figure 2-13) both proved the existence of polyester. In addition, ^1H NMR ($\delta = 7.23$ ($\text{H}_{1,2,3,4}$), 7.08 ($\text{H}_{5,6}$) ppm in CD_2Cl_2) spectrum was given in Figure 2-12.

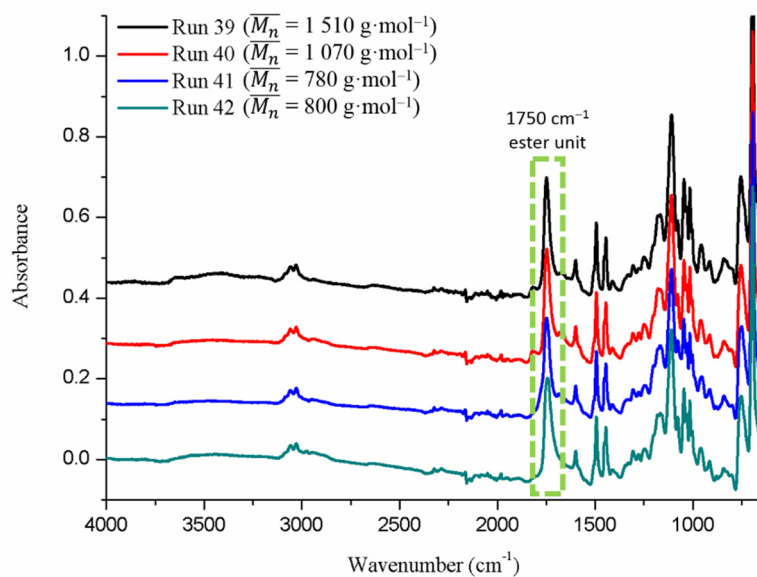


Figure 2-11. FT-IR monitoring of Run 39–42 (DPK-based polyesters)

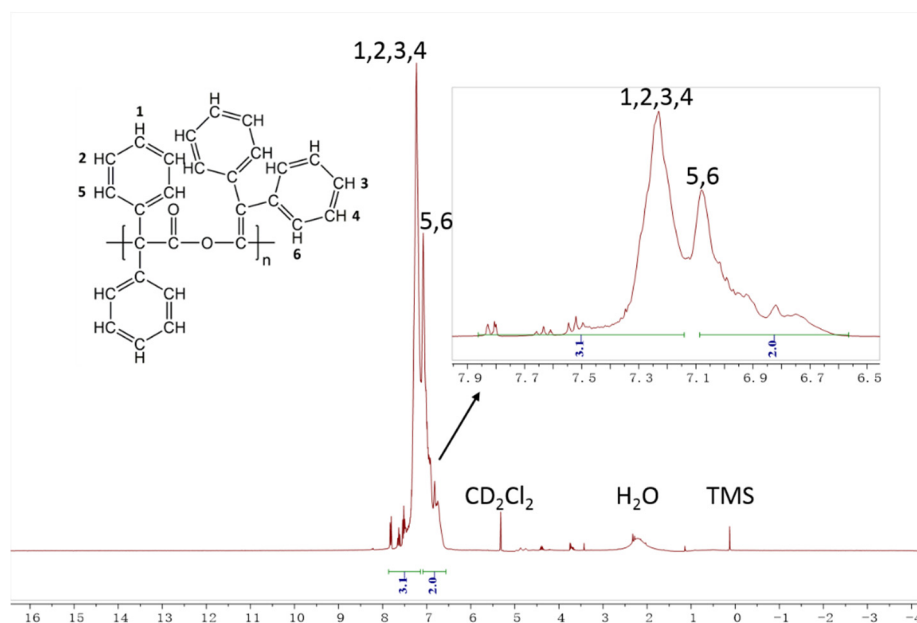


Figure 2-12. ^1H NMR spectrum (300 Mhz, 20°C, CD_2Cl_2) of Run 39 (DPK-based polyester)

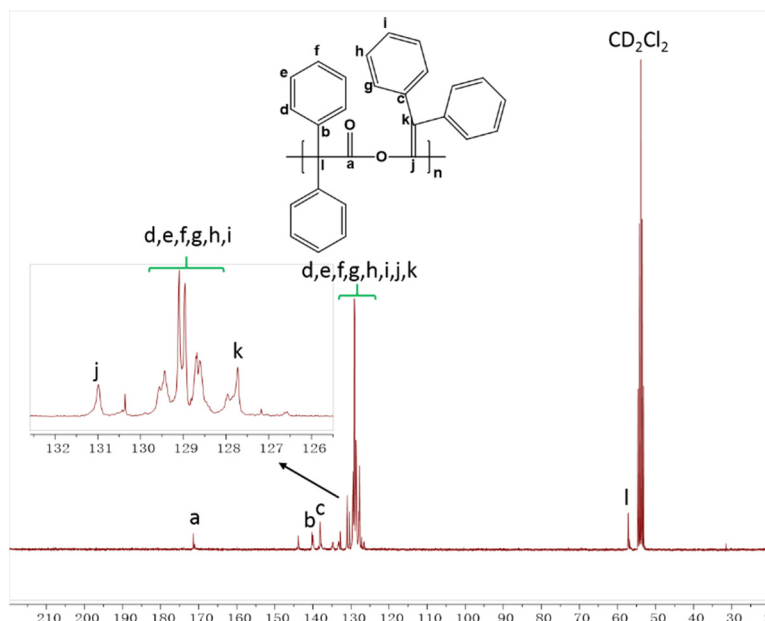


Figure 2-13. ^{13}C NMR spectrum (75 Mhz, 20°C, CD_2Cl_2) of Run 39 (DPK-based polyester)

\overline{M}_n and $\overline{M}_w/\overline{M}_n$ ratios determined by size exclusion chromatography (SEC) in CH_2Cl_2 were estimated (PMMA standards), and gave small molecular weights, lower than $2\,000\text{ g}\cdot\text{mol}^{-1}$ (see Table 2-5).

The thermal properties were also gathered in Table 2-5, TGA spectra were presented in Figure 2-14, and an exemple of DSC thermogram for Run 39 was given in Figure 2-15 (other DSC figures in Annexes).

Table 2-5. Properties of Run 39~42 (DPK-based polyesters)^a

Run	\overline{M}_w ($\text{g}\cdot\text{mol}^{-1}$)	\overline{M}_n ($\text{g}\cdot\text{mol}^{-1}$)	\mathcal{D}_M	T_g (°C) (2 nd heating)	$T_d^{5\%}$ (°C)	T_d^{Max} (°C)
39	1 940	1 510	1.28	88	284	372
40	1 400	1 070	1.31	59	225	326
41	1 040	780	1.33	58	227	291
42	1 080	800	1.35	46	203	277

a: calibration of \overline{M}_n and \overline{M}_w by SEC with poly(methylmethacrylate) standards

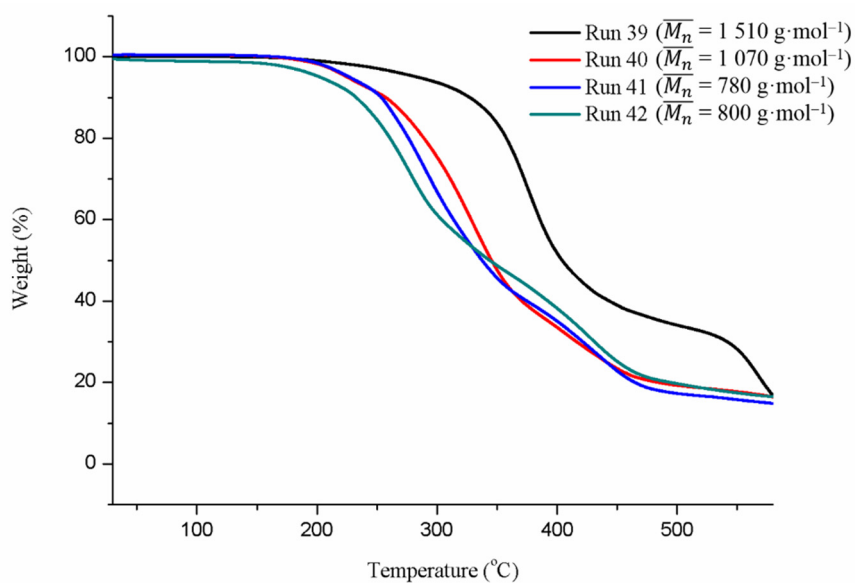
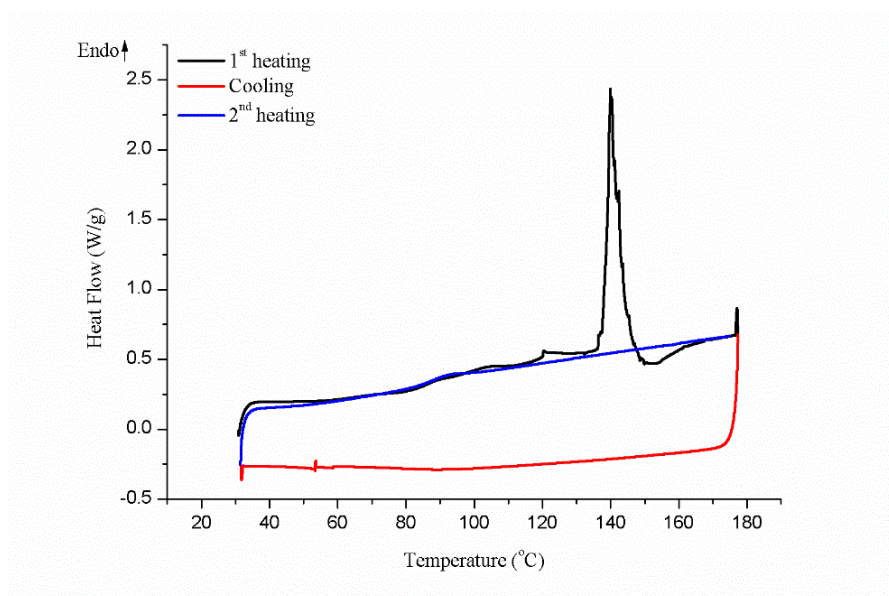


Figure 2-14. TGA spectra of Run 39~42 (DPK-based polyesters)

Figure 2-15. DSC analysis of Run 39 (DPK-based polyester $\overline{M}_n = 1\,510\text{ g}\cdot\text{mol}^{-1}$)

Except Run 39, these polymers exhibited poor thermal stability, probably owing to their short chains.

For the DSC of Run 39 (Figure 2-15), it should be stressed out that the first heating process offered an obvious melting point at 140°C, contrary to Run 40 to 42, which did not exhibit any endothermic transition. But this polyester did not manage to recrystallize upon cooling, as already observed with DMK-based polyester [9].

Run 39 also afforded a polymer with a relatively higher glass-transition temperature (T_g) than the other three products of Run 40 to 42, which could be addressed in the Flory-Fox equation, which relates molecular weight to the glass transition temperature of a polymer [10]:

$$T_g = T_{g,\infty} - \frac{K}{M_n}$$

where $T_{g,\infty}$ is the maximum glass transition temperature that can be reached at a theoretical infinite molecular weight and K is an empirical parameter that is related to the free volume present in the polymer sample.

Hence, Figure 2-16 illustrated this equation (for a sake of comparison, a plot of polystyrene was presented [10]). $T_{g,\infty} = 119\text{ }^{\circ}\text{C}$ and $K = 54\,453\text{ K}\cdot\text{g}\cdot\text{mol}^{-1}$ were obtained.

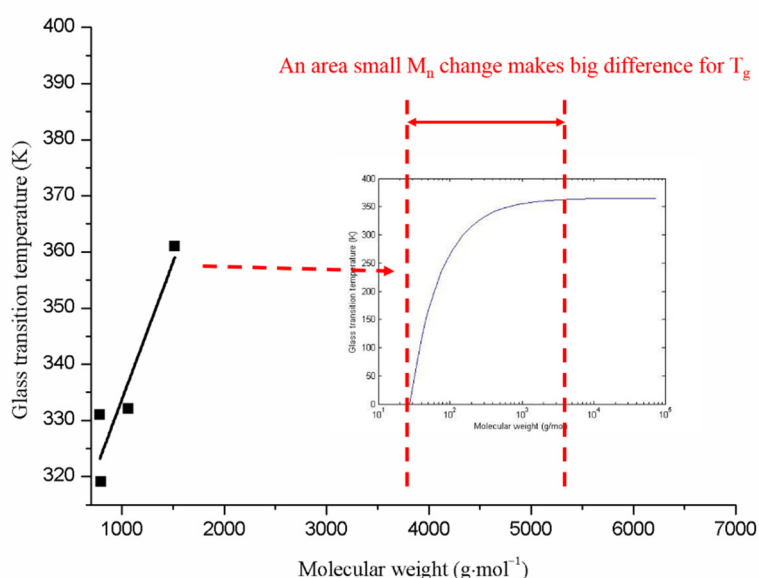


Figure 2-16. Glass transition temperature versus molecular weight for the obtained DPK-based polyesters

To conclude, two major facts can be highlighted:

- even if MEK [4], DEK [4] and EPK [11, 12] were already polymerized with anionic initiators to give polyesters, the numerous experimental conditions used in these cationic polymerizations never gave the expected polyketone structures
- DPK afforded a low molecular weight polyester using cationic initiators, whereas anionic initiators were unsuccessful in the literature [4].

Owing to the special HOMO and LUMO spatial orientations, we can suppose that the mechanisms involved in the ionic polymerizations of ketenes, not fully resolved yet, are fully affected by the steric hindrance which is different in an anionic compared to a cationic process.

2.3 Cationic copolymerization with Dimethylketene (DMK)

As all of the above four ketenes performed very poor reactivity in cationic polymerization conditions, it started to be interesting to study their copolymerization with DMK. Indeed, DMK is a monomer which has been well tested and verified to be able to polymerize to a polyketone structure in a cationic mechanism, using the typical mixture AlCl_3 / $(\text{CH}_3)_3\text{CCl}$ as the initiator. The aliphatic DEK and aromatic DPK were respectively picked up as the second monomer considering the price of raw materials and the substituents.

2.3.1 DMK Synthesis

Dimethylketene (DMK) was synthesized by pyrolysis of isobutyric anhydride (IBAN) (Figure 2-17).

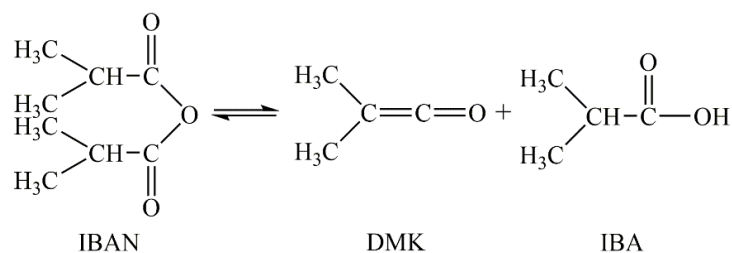


Figure 2-17. Synthesis of DMK by pyrolysis of isobutyric anhydride

The apparatus was illustrated in Figure 2-18, which was similar with the detailed description in our previous work [13]. The divided three segments of the experimental set-up referred to three different procedures: DMK synthesis by IBAN pyrolysis, DMK purification, and DMK collection. 50 g IBAN (0.632 mol) was carefully introduced into the pyrolysis oven **A** in a constant flow rate around $240 \text{ g}\cdot\text{h}^{-1}$ owing to a dosing pump. Furthermore, 625°C in oven **A** triggered the pyrolysis under a reduced 40 mbar nitrogen pressure. In conjunction, the resulting gaseous mixture mainly containing targeted DMK with unreacted IBAN and by-product IBA, was sequentially condensed by condenser **B** at 60°C , condenser **C** at -24°C and container **D'** at -30°C . Then gaseous DMK was further purified by bubbling through 5 g *n*-decane at -15°C in flask **F**, and finally trapped in collector **G** by liquid nitrogen (-196°C). Once the synthesis and purification steps were over, 13.55 g yellow liquid monomer DMK (194 mmol) was obtained by gently warming up to the desired temperature under atmospheric conditions. The overall synthesis yield, determined by mass balance, was 27%.

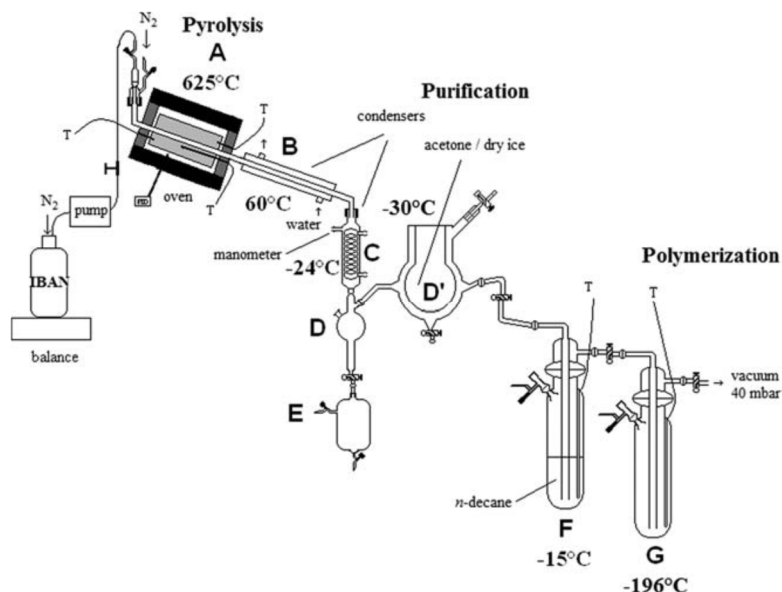


Figure 2-18. Apparatus of synthesis, purification and collection for DMK and reactor for copolymerization

2.3.2 Copolymerization of DEK / DMK

2.3.2.1 Experiments

The DEK and DMK monomers were prepared as previously mentioned. DEK was stored in sealed bottles at 0°C under Alphagaz™ 2 nitrogen flow before use, and DMK was used immediately after being freshly synthesized.

The cationic polymerization conditions optimized by the previous work were adopted in the present copolymerization [1]: reaction temperature at -20°C , anhydrous CH_2Cl_2 as the solvent, $\text{AlCl}_3 / (\text{CH}_3)_3\text{CCl}$ mixture as the cationic initiator, $[\text{Monomer}]_0 = 3 \text{ mol}\cdot\text{L}^{-1}$, and $[\text{Monomer}]_0 / [\text{Initiator}]_0 = 100$.

To reach that, the prepared DEK was directly added into the freshly prepared DMK in CH_2Cl_2 by a syringe according to the well calculated molar ratios ($n_{\text{DEK}} : n_{\text{DMK}} = 1 : 2, 1 : 8, 1 : 11$ and $1 : 35$). After the temperature of reactor was stabilized at the desired -20°C , $1 \text{ mol}\cdot\text{L}^{-1}$ $\text{AlCl}_3 / (\text{CH}_3)_3\text{CCl}$ equal molar ratio mixture in CH_2Cl_2 was further added into the

reaction system to trigger the polymerization, with $[\text{Monomer}]_0 / [\text{Initiator}]_0 = 100$. The reactive medium was kept during 3 h at -20°C and then allowed naturally back to room temperature for additional 2 days before the termination operation. Absolute ethanol was injected into the reactor to react with and neutralize residual ketenes and initiators. Then the mixture was poured into large amounts of absolute ethanol to afford precipitated polymers. The obtained polymers were filtered, washed several times with ethanol and dried under vacuum at 40°C for 2 days before weighing and testing. The yield was calculated by weight ratio of recovered copolymers to the monomer feed.

2.3.2.2 Copolymer Structures

The copolymerization results of DEK and DMK were listed in Table 2-6. The homopolymerizations of DEK and DMK are included for reference.

First of all, we can notice that a feed ratio $n_{\text{DMK}} : n_{\text{DEK}} = 2 : 1$ (Run 98) gave a yield as low as 3%, which well revealed the hindered polymerization of DEK. Increasing the feed ratio can reasonably improve the yield (for most Runs), thanks to the more reactive DMK.

Table 2-6. Results of DMK and DEK copolymerization

Run	Monomers	Feed of monomers $n_{\text{DMK}} : n_{\text{DEK}}$	Molar ratio in copolymer [DMK] : [DEK]	Yield ^a (%)
58	DMK	-	-	24
107	DMK and DEK	35 : 1	386 : 1	17
75	DMK and DEK	11 : 1	108 : 1	17
106	DMK and DEK	8 : 1	90 : 1	12
98	DMK and DEK	2 : 1	26 : 1	3
54	DEK	-	-	-

a: yields were calculated by weight percent of obtained polymers (after precipitation) over feed monomers

The structure of DMK / DEK copolymers was confirmed by ^1H NMR ($\delta = 2.1$ (H_1), 1.5 (H_2), 0.7 (H_3) ppm in CD_2Cl_2 and HFIP) and ^{13}C NMR ($\delta = 212.4$ (C_a), 211.7 (C_b), 65.4 (C_c), 65.3 (C_d), 24.6 (C_e), 24.2 (C_f), 9.3 (C_g) ppm in CD_2Cl_2 and HFIP), and the representative Run 98 was illustrated by Figure 2-19 and Figure 2-20 (other Runs were provided in Annexes).

The chemical shifts around 0.70 and 2.05 ppm in ^1H NMR spectra suggested the existence of DEK fractions in the copolymer chain, and the fraction ratios were calculated by integration and listed in the former table. The two single signals around 210 ppm in ^{13}C NMR were proof of the exclusive ketone repeating units in the backbone (no signal due to polyester, namely no carbonyl around 174 ppm).

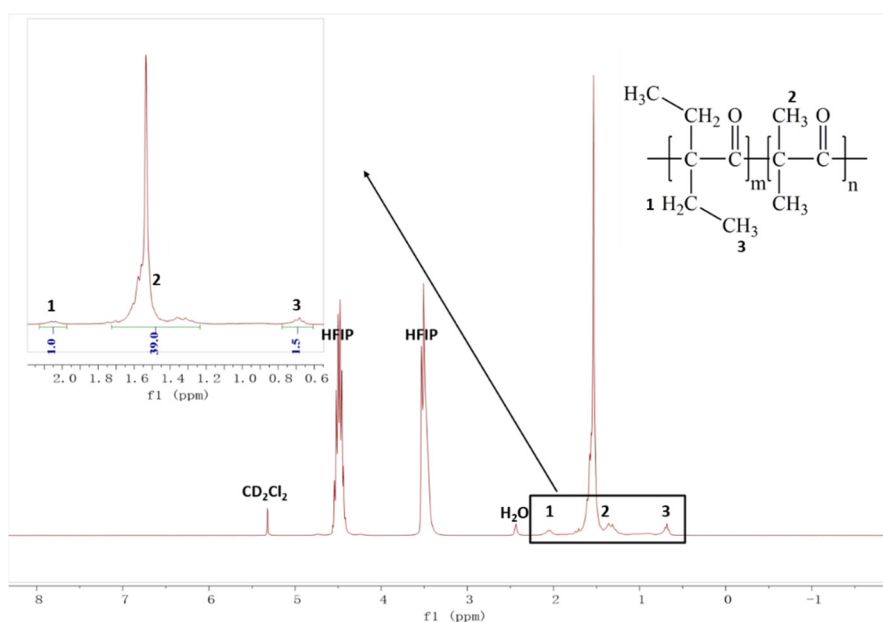


Figure 2-19. ^1H NMR spectrum (300 Mhz, 20°C , CD_2Cl_2 + HFIP) of Run 98 ([DMK] : [DEK] = 26 : 1)

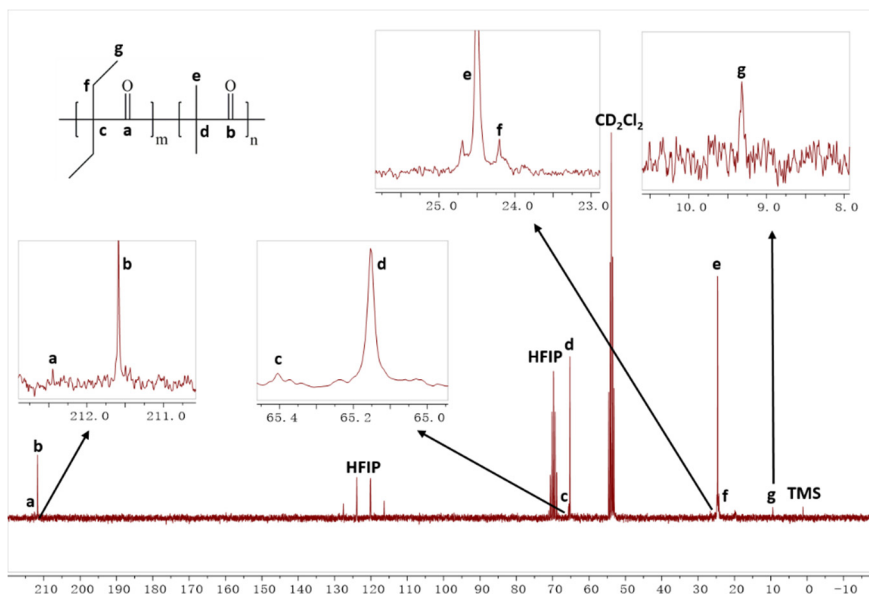


Figure 2-20. ^{13}C NMR spectrum (75MHz, 20°C, CD_2Cl_2 + HFIP) of Run 98 ([DMK] : [DEK] = 26 : 1)

Owing to very poor solubility in common and less common SEC solvents, no molecular weights could be determined.

2.3.2.3 Thermal Properties

To verify the thermal stabilities of these DMK / DEK copolymers, thermogravimetric analysis (TGA) was applied (Figure 2-21).

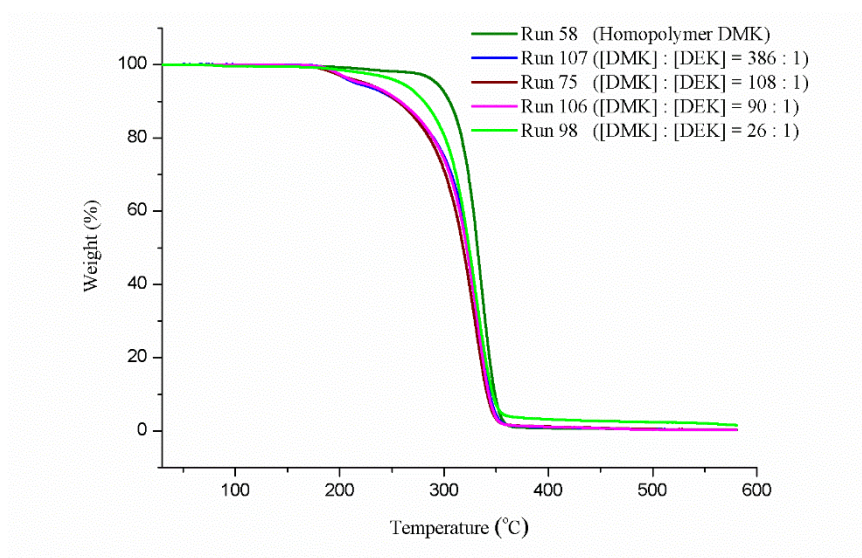


Figure 2-21. TGA spectra of DMK / DEK copolymers

Comparing with PDMK homopolymer, it can be concluded that the introduction of DEK isolated units into the main chain causes degradation to happen at lower temperature, even if all the copolymers still remain stable up to $T_d^{5\%} = 220^\circ\text{C}$. However, T_d^{Max} remained unchanged around 330°C when compared to the reference homopolymer PDMK. All these temperatures were gathered in Table 2-7. We addressed it by the influence of DEK fractions on the spatial configuration of the polymer chain, which is discussed in the next paragraph. Surprisingly, the product of Run 98, possessing more DEK isolated units, exhibited a relatively better thermal stability than the others, which was hard to explain.

Table 2-7. Summary of thermal properties of DMK / DEK copolymers

Run	Molar ratio in copolymer [DMK] : [DEK]	T_m ($^\circ\text{C}$) (1 st heating)	ΔH_m ($\text{J}\cdot\text{g}^{-1}$) (2 nd heating)	$T_d^{5\%}$ ($^\circ\text{C}$)	T_d^{Max} ($^\circ\text{C}$)
		T_m ($^\circ\text{C}$) (2 nd heating)			
58	DMK Homopolymer	231 175 / 233	72.6	285	338
107	386 : 1	194 / 241 234	59.0	216	331

75	108 : 1	187 / 224 168 / 220	45.7	222	327
106	90 : 1	180 / 237 211 / 222 / 234	24.2	221	331
98	26 : 1	203 155 / 164	15.8	259	331

A closer look showed that the thermal degradation can be divided into two stages. Due to the small amount of DEK in the copolymers, we supposed these units were isolated in a main DMK chain (discussion in detail below along with the reactivity ratio estimation), and acted like drawing points of intersection on a straight line. These points on the line can be better thought of to become ‘joints’ of the polymer ‘arm’, which plays a role of the weakest link in the polymer Great Wall. When exposed to heat, the molecular chain starts to move whereas these more bulky ‘joints’ become shackles of the movement. Therefore in a requirement of freedom, the polymer chain breaks at some of these ‘joints’, then a quick degradation of smaller chains between the break joints occurs, which could explain why the stability of the copolymers performs worse than the homopolymer (Figure 2-22).

After the chain have already been broken into segments in which no freedom obstacle exists, the difference of movement freedom between DMK / DEK copolymers and DMK homopolymer disappear. The second degradation stage then occurs to them without distinction along with the rising temperature.

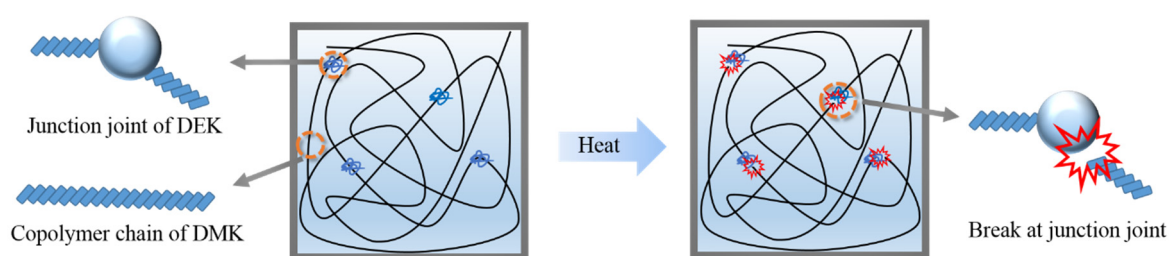


Figure 2-22. Thermal degradation of DMK / DEK copolymers at the ‘junction points’

Then, differential scanning calorimetry (DSC) tests were conducted. The T_m (melting point) and more particularly ΔH_m (melting enthalpy) of all the copolymers proved to be decreased by the introduction of DEK units (details see Table 2-7), which was attributed to the DEK rigid ‘joints’, seen as defects by the PDMK crystalline structure. Run 98 behaved differently from other Runs, as shown in Figure 2-23 (where Run 75 was chosen as representative, other Runs are presented in Annexes). Indeed, a thermal crystallization peak around 65°C can be seen clearly upon heating.

All the T_g of these series of polymers could not be reliably measured by DSC.

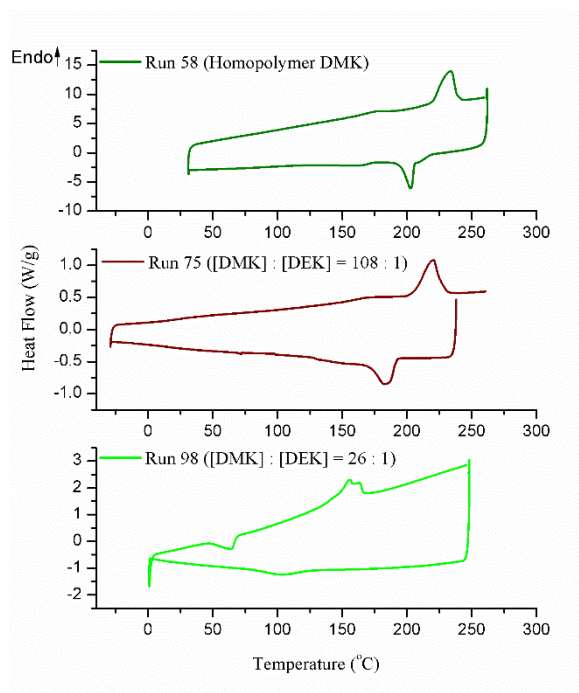


Figure 2-23. Comparison of DSC spectra of Run 58, Run 75 and Run 98

Even if homopolymerization of DEK could not be achieved, its copolymerization with DMK was a success. The ΔH_m and $T_d^{5\%}$ of the obtained copolymers were lowered, but a specific copolymer (Run 98 with a unit ratio of [DMK] : [DEK] = 26 : 1) with a broad processing window was obtained ($T_m = 164^\circ\text{C}$, $T_d^{5\%} = 259^\circ\text{C}$). This copolymer broadens the family of more processable PDMKs, since an ethylketene / DMK copolymer containing a

unit ratio of [DMK] : [EK] = 93 : 7, synthesized in our previous work, exhibited $T_m = 180^\circ\text{C}$ and $T_d^{5\%} = 300^\circ\text{C}$ [14].

2.3.3 Copolymerization of DPK / DMK

2.3.3.1 Experiments

The DPK and DMK monomers were prepared as described above, with the same polymerization conditions. Similar molar feed ratios were used, which were $n_{DPK} : n_{DMK} = 1 : 1, 1 : 6, 1 : 13$ and $1 : 36$.

2.3.3.2 Copolymer Structures

The copolymerization results of DPK and DMK were listed in Table 2-8. The poor reactivity of DPK generated declining yields, even more with the decreasing feed ratio, reaching a minimum of 3% (Run 95).

Table 2-8. Results of DMK and DPK copolymerization

Run	Monomers	Feed of monomers $n_{DMK} : n_{DPK}$	Molar ratio in copolymer [DMK] : [DPK]	Yield ^a (%)
58	DMK	-	-	24
69	DMK and DPK	36 : 1	436 : 1	28
93	DMK and DPK	13 : 1	196 : 1	20
103	DMK and DPK	6 : 1	84 : 1	16
95	DMK and DPK	1 : 1	6 : 1	3
55	DPK	-	-	-

a: yields were calculated by weight percent of obtained polymers (after precipitation) over feed monomers

The copolymer structure was determined by ^1H ($\delta = 6.8\sim 7.5$ (benzene-H), 1.5 (H_4) ppm in CD_2Cl_2 and HFIP) and ^{13}C NMR ($\delta = 212.2$ (C_a), 208.4 (C_b), 127~130 (benzene-C), 65.4 (C_g), C_h should be around 70 (peak is too small to be observed), 24.6 (C_i) ppm in CD_2Cl_2 and HFIP) spectra, the typical Run 95 was illustrated by Figure 2-24 and Figure 2-25 (other

Runs are in Annexes). According to the ^{13}C NMR spectrum, both the presence of signal around 210 ppm (polyketone) and the absence of signal around 170 ppm (polyester) demonstrated that only neat ketone structure without ester resulted during the copolymerization, thanks to the cationic initiators. The existence of DPK fraction can be confirmed by the signal around 7 ppm ($\text{H}_{1,2,3}$) for ^1H NMR and signals around 130 ppm ($\text{C}_{c,d,e,f}$) for ^{13}C NMR. The DMK / DPK molar ratios in different copolymers listed in the former table were calculated according to the integration ratio of methyl-assigned to phenyl-assigned H area for ^1H NMR from different Runs. Comparing the feed of monomers and the molar ratio in copolymer, it can be concluded that the DPK was much less reactive than the DMK monomers. The reactivity ratios of these two monomers are discussed later.

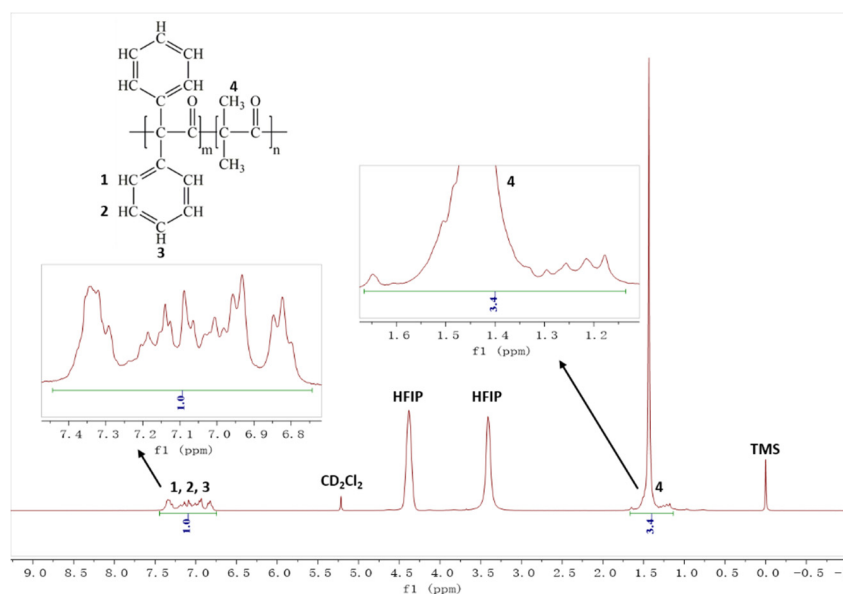


Figure 2-24. ^1H NMR spectrum (300 Mhz, 20°C , CD_2Cl_2 + HFIP) of Run 95 ([DMK] : [DPK] = 6 : 1)

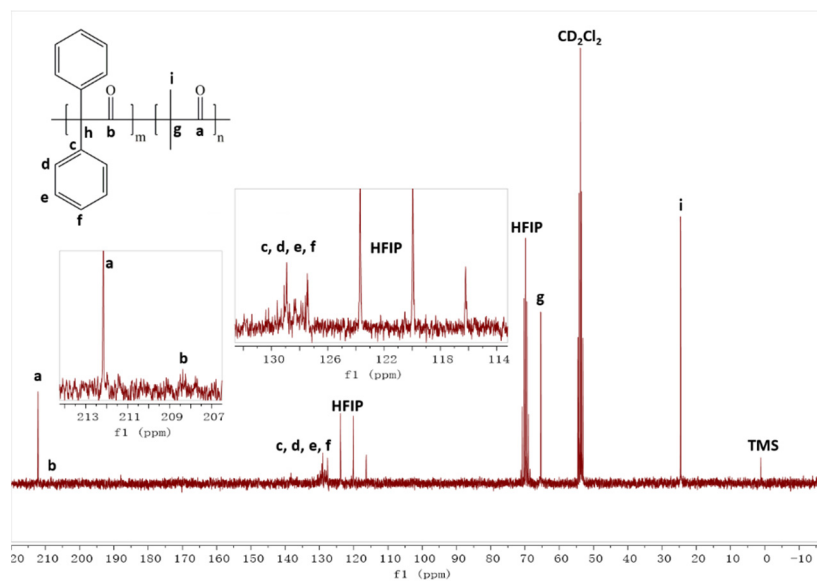


Figure 2-25. ^{13}C NMR spectrum (75 Mhz, 20°C , CD_2Cl_2 + HFIP) of Run 95 ([DMK] : [DPK] = 6 : 1)

2.3.3.3 Thermal Properties

TGA spectra of DMK / DPK copolymers and the DMK homopolymer are compared in Figure 2-26.

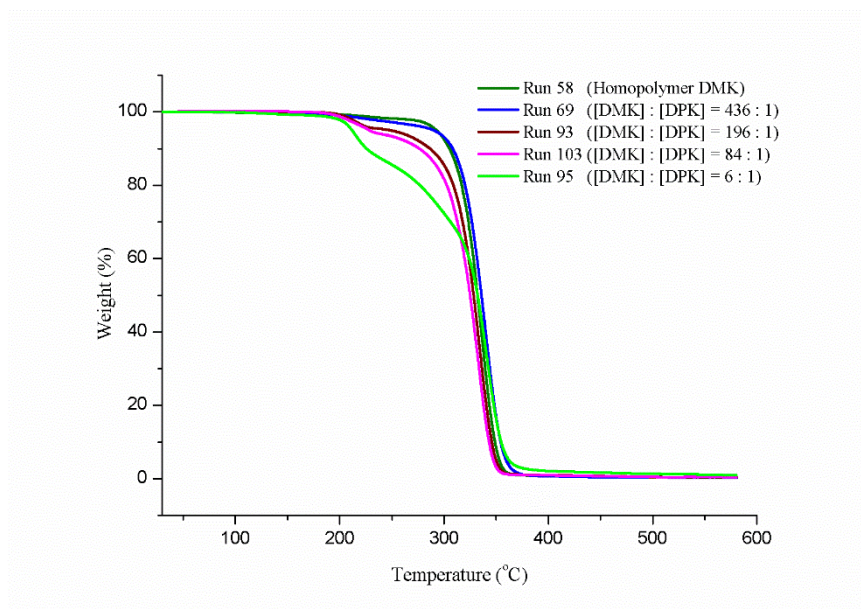


Figure 2-26. TGA spectra of DMK / DPK copolymers

Introducing DPK units into the copolymer clearly reduced its stability ($T_d^{5\%}$), while T_d^{Max} constantly remains around 330~340°C (details see Table 2-9). This behaviour can be explained similarly by the steric influence of the phenyl group on the spatial configuration of the polymer chain. As a fact that the volume of the phenyl group is much bigger than the ethyl, the ‘joints’ in DMK / DPK copolymers become more sensitive to heat, which can be given proof by the significant weight loss around 230°C.

Table 2-9. Summary of thermal properties of DMK / DPK copolymers

Run	Fraction ratio [DMK] : [DPK]	T_g (°C)	T_m (°C) $\frac{(1^{st} \text{ heating})}{(2^{nd} \text{ heating})}$	ΔH_m (J·g ⁻¹) (2 nd heating)	$T_d^{5\%}$ (°C)	T_d^{Max} (°C)
58	PDMK	-	231 175 / 233	72.6	285	338
69	436 : 1	-	191 / 235 164 / 231	46.4	290	340
93	196 : 1	-	188 / 247 239 / 252	27.6	248	334
103	84 : 1	-	188 / 238 224 / 231	22.1	229	333
95	6 : 1	21	196 185	18.8	212	341

DMK / DPK copolymers were also analyzed by DSC. The most DPK rich copolymer from Run 95 was illustrated by Figure 2-27 together with the homopolymer from Run 58, the detailed data was given in Table 2-9. Similarly to DEK / DMK copolymers, even worse sometimes, T_m and ΔH_m of all the DMK / DPK copolymers decrease a lot comparing to

PDMK. This also gives evidence to the successful copolymerization and the steric hindrance influence of DPK isolated units on the copolymers and their crystallinity. But the melting of the richer DPK copolymers (Run 93, 103 and 95) quite always happened along with degradation.

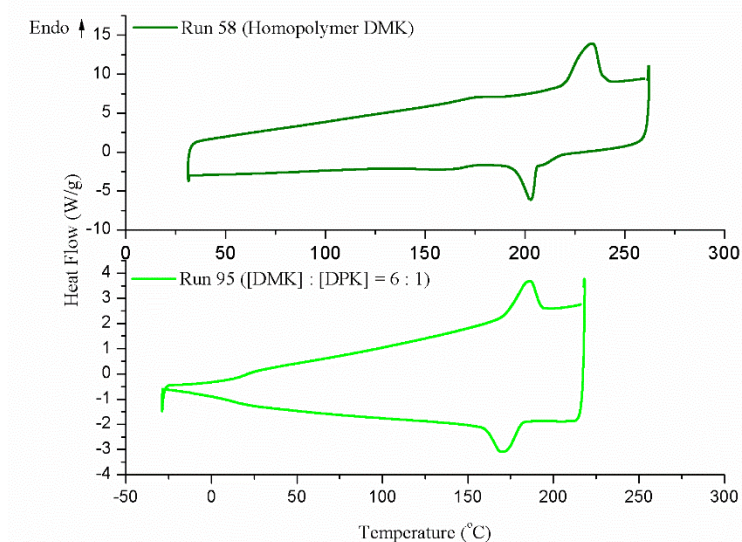


Figure 2-27. Comparison of DSC spectra of Run 58 and Run 95

In conclusion, the copolymerization of DPK with DMK was evidenced, but the thermal properties of the obtained copolymers were dramatically decreased, with a melting concomitant to degradation.

2.3.4 Monomer reactivity ratios

To further assess the different copolymerizing abilities of DPK and DEK with DMK, their reactivity ratios were respectively estimated.

2.3.4.1 Bibliography

Copolymerization reactivity ratios have been estimated for a wide variety of systems by various methods (Table 2-10) [15], although most involve free-radical processes [16].

Table 2-10. Listing of the various methods used to estimate the reactivity ratios

Method	Description	Reference
BF	Barson-Fenn	Barson and Fenn [17]
EVM	error-in-variables model	Dube et al. [18]
ex-KT	extended Kelen-Tudos	Tudos et al. [19]
FR	Fineman-Ross	Fineman and Ross [20]
KT	Kelen-Tudos	Kelen and Tudos [21]
MH	Mao-Huglin	Mao and Huglin [22]
ML	Mayo-Lewis	Mayo and Lewis [23]
TM	Tidwell-Mortimer	Tidwell and Mortimer [24]
YBR	Yezrielev-Brokhina-Roskin	Yezrielev et al. [25]

Among these methods, the linear extended Kelen-Tudos method was chosen for our systems regarding its confidence for both low and high conversions and its reliability with cationic copolymerization systems [21, 26]. All the elements for calculation were explained in the following equations [19].

Deriving from the Mayo and Lewis equation, as provided in Equation (2.1), a simple linear equation was rearranged by Fineman and Ross (Equation (2.2)).

$$\frac{dM_1}{dM_2} = \frac{r_1 M_1^2 + M_1 M_2}{r_2 M_2^2 + M_1 M_2} \quad (2.1)$$

In the above equation, r_1 and r_2 are the monomer reactivity ratios and M_1 and M_2 are the concentration of monomers in the feed. The fraction dM_1/dM_2 is the ratio of monomer instantaneous incorporation into the polymer.

$$\frac{X(1-Y)}{Y} = r_2 - \frac{X^2}{Y} r_1 \quad (2.2)$$

In the above equation, $X = M_1/M_2$ and $Y = m_1/m_2$ are the molar ratios of monomer in the feed and concentrations in the copolymer, respectively.

After that, Kelen and Tudos refined the linearization method by adding an arbitrary positive constant ' α ' into the Fineman-Ross equation and by redefining η and ξ using partial molar conversion of the monomers. The resulting Equation (2.3) is a more useful and widely accepted method for the estimation of reactivity ratios with data obtained even at high conversions. A plot of η as ordinate and ξ as abscissa is a straight line with slope as $(r_1 + r_2/\alpha)$ and intercept as $-r_2/\alpha$.

$$\eta = \left(r_1 + \frac{r_2}{\alpha} \right) \xi - \frac{r_2}{\alpha} \quad (2.3)$$

In the above equation, all the elements were detailed as below:

$$\eta = \frac{G}{(\alpha + F)} \quad (2.4)$$

$$\xi = \frac{F}{(\alpha + F)} \quad (2.5)$$

$$\alpha = (F_{max} F_{min})^{1/2} \quad (2.6)$$

$$F = \frac{Y}{Z^2} \quad (2.7)$$

$$G = \frac{Y-1}{Z} \quad (2.8)$$

These equations may be derived by computing the partial molar monomer conversions ζ_1 and ζ_2 and the integral Z .

$$Z = \frac{\log(1 - \zeta_1)}{\log(1 - \zeta_2)} \quad (2.9)$$

$$\zeta_1 = \frac{\zeta_2 Y}{X} \quad (2.10)$$

$$\zeta_2 = \frac{W(\mu + X)}{(\mu + Y)} \quad (2.11)$$

Where W is the weight yield, and μ is the ratio of molecular weights (molecular weight of M_2 / molecular weight of M_1).

2.3.4.2 Estimation of Reactivity Ratios

Extended Kelen-Tudos method parameters of DEK / DMK and DPK / DMK systems were calculated and are presented in Table 2-11 and Table 2-12. DMK was always set as Monomer 1, DEK and DPK were respectively set as Monomer 2.

Table 2-11. Data for the copolymerization of DMK and DEK including Kelen-Tudos parameters

Run	X	Y	W	ζ_2	ζ_1	Z	F	G	η	ξ
107	34.86	385.83	0.171	0.016	0.177	12.082	2.643	31.852	9.613	0.798
75	11.53	108.16	0.172	0.020	0.190	10.300	1.019	10.404	6.158	0.603
106	7.91	89.84	0.121	0.012	0.140	12.182	0.606	7.306	5.723	0.475
98	2.14	25.83	0.027	0.004	0.042	12.311	0.170	2.017	2.400	0.203
$\alpha = (F_{max}F_{min})^{1/2} = 0.67$										

Table 2-12. Data for the copolymerization of DMK and DPK including Kelen-Tudos parameters

Run	X	Y	W	ζ_2	ζ_1	Z	F	G	η	ξ
69	36.37	435.67	0.282	0.025	0.302	14.080	2.198	30.871	11.035	0.786
93	13.26	195.83	0.201	0.016	0.239	16.742	0.699	11.637	8.961	0.538
103	6.05	84.16	0.163	0.016	0.230	15.672	0.343	5.306	5.629	0.364
95	1.05	6.27	0.031	0.013	0.079	6.180	0.164	0.853	1.116	0.215
$\alpha = (F_{max}F_{min})^{1/2} = 0.60$										

By plotting parameter η vs. ξ shown in the two tables, two straight lines were obtained (Figure 2-28).

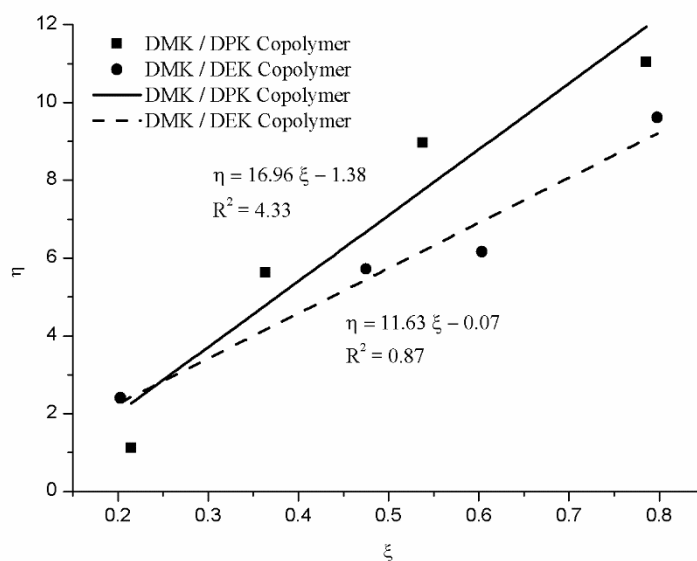


Figure 2-28. Kelen-Tudos method applied to DEK / DMK and DPK / DMK copolymers

Based on the slope and intercept of these lines, reactivity ratios were calculated by Equation (2.3):

- for DMK and DEK system: $r_1 = 11.55$, $r_2 = 0.05$;
- for DMK and DPK system: $r_1 = 15.58$, $r_2 = 0.83$.

It can be concluded by the distinct r_1 and r_2 for the two systems that DMK is far more reactive than DEK and DPK, which may result from the steric hindrance of the bulky ethyl- and phenyl- substituted groups (Figure 2-29). Both r_2 remain below 1, confirming that DEK and DPK can probably not be self-polymerized into a polyketone.

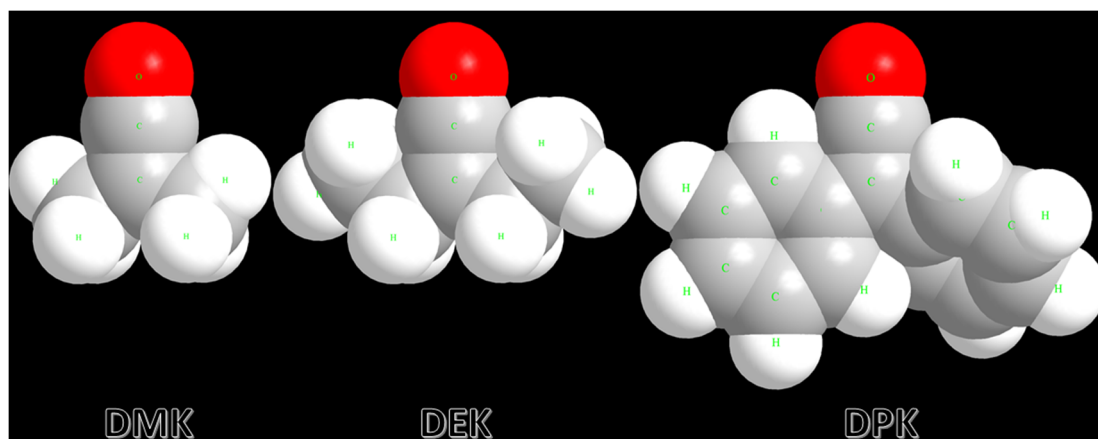
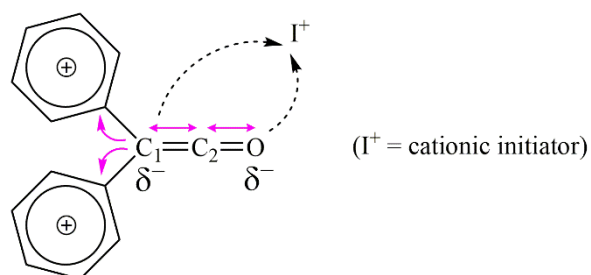


Figure 2-29. 3D predicted space filling structures of DMK, DEK and DPK

However, comparing $r_2 = 0.05$ of DEK with $r_2 = 0.83$ of DPK suggests that DPK was more reactive than DEK, which is difficult to understand. Indeed, from the viewpoint of electric charge, phenyl, as an electron withdrawing group, balances the electric charge between the C=C and C=O double bonds, and further reduces the negative charge of C₁, which should normally weaken the reactivity of DPK in the cationic system (Figure 2-30). The real reason for this has not been figured out.

Figure 2-30. Phenyl as electron withdrawing group decreases the electronegativity of C₁ and O

Taking these elements into account, we considered it reasonable to regard these resulting polyketones as intercalated copolymers, which remained mainly homopolymerized DMK ketone chains with very short DEK or DPK isolated units, due to their large differences of r_1 and r_2 (Figure 2-31).

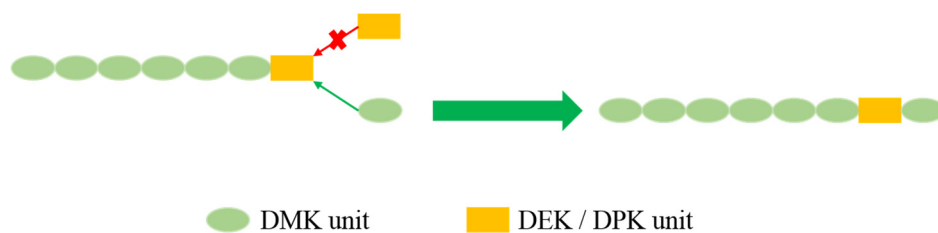


Figure 2-31. Formation of the intercalated copolymer

2.4 Conclusion

In this chapter, cationic polymerization abilities of four different ketene monomers substituted by methyl-, ethyl- and phenyl-groups were tested under various initiating systems. Among them, metylethylketene (MEK), diethylketene (DEK) and ethylphenyl-ketene (EPK) never gave any polymers even though different initiators, solvents and reaction temperatures were applied. Diphenylketene (DPK) performed similarly in most cationic processes, except with the $\text{CF}_3\text{SO}_3\text{H}$ initiator, where a fully new polyester of very small molecular weight was obtained: $\overline{M}_n = 1\,500\text{ g}\cdot\text{mol}^{-1}$, $T_g = 88^\circ\text{C}$, $T_m = 140^\circ\text{C}$ (first heating) and $T_d^{5\%} = 284^\circ\text{C}$.

After that, attempts to copolymerize DEK, as a typical aliphatic ketene, and DPK, as a typical aromatic ketene, with DMK, which have proved much more reactive in cationic mechanisms and able to dominately form polyketone structures, were performed. The experiments demonstrated successful copolymerizations for both DEK / DMK and DPK / DMK, even if the reactivity ratios (r_1 , r_2) present large distinctions. The resulting polyketones are considered to be intercalated copolymers, with a main DMK chain comprising small DEK or DPK isolated units, of which the thermal properties are obviously affected by the embedded units: for DPK / DMK copolymers, melting often means degradation, while an interesting DEK / DMK copolymer with a broad processing window was still obtained ($T_m = 164^\circ\text{C}$, $T_d^{5\%} = 259^\circ\text{C}$).

In summary, DMK can definitely be considered as a very special ketene monomer, of which the behavior in cationic polymerization can hardly be transposed to other ketenes.

2.5 References

- [1] H. Egret, J.-P. Couvercelle, J. Belleney, C. Bunel, Cationic polymerization of dimethyl ketene, *European Polymer Journal*, 38 (2002) 1953-1961.
- [2] N. Hayki, N. Desilles, F. Burel, Aliphatic polyketone obtained by cationic polymerization of ethylketene, *Polymer Chemistry*, 2 (2011) 2350-2355.
- [3] M.J. Konz, Herbicidal isoxazolidine-3, 5-diones, U.S. Patent 4,302,238[P]. 1981-11-24.
- [4] H. Sugimoto, M. Kanai, S. Inoue, Lanthanoid alkoxide as a novel initiator for the synthesis of polyester via polymerization of ketenes, *Macromolecular Chemistry and Physics*, 199 (1998) 1651-1655.
- [5] J. Douglas, J.E. Taylor, G. Churchill, A.M.Z. Slawin, A.D. Smith, NHC-Promoted Asymmetric β -Lactone Formation from Arylalkylketenes and Electron-Deficient Benzaldehydes or Pyridinecarboxaldehydes, *The Journal of Organic Chemistry*, 78 (2013) 3925-3938.
- [6] J.M. Goll, E. Fillion, Tuning the Reactivity of Palladium Carbenes Derived from Diphenylketene, *Organometallics*, 27 (2008) 3622-3625.
- [7] K. Calvin, A. Penciu, P.J. McInenly, K.R. Kumar, M.J. Drewitt, M.C. Baird, Isobutene homo- and isobutene-isoprene copolymerization initiated by protic initiators associated with a series of novel, weakly coordinating counteranions, *European polymer journal*, 40 (2004) 2653-2657.
- [8] H. Egret, Synthèse et caractérisation des polymères du diméthylcétène. Application à la perméabilité aux gaz, Rouen, 1998.
- [9] M. Brestaz, Synthèse et caractérisation de polyesters à partir du diméthylcétène et de composés carbonylés, INSA de Rouen, 2009.
- [10] T.G.F. Jr., P.J. Flory, Second-Order Transition Temperatures and Related Properties of Polystyrene. I. Influence of Molecular Weight, *Journal of Applied Physics*, 21 (1950) 581-591.
- [11] A. Sudo, S. Uchino, T. Endo, Development of a living anionic polymerization of ethylphenylketene: A novel approach to well-defined polyester synthesis, *Macromolecules*, 32 (1999) 1711-1713.
- [12] A. Sudo, S. Uchino, T. Endo, Living anionic polymerization of ethylphenylketene: A novel approach to well-defined polyester synthesis, *Journal of Polymer Science Part A: Polymer Chemistry*, 38 (2000) 1073-1082.
- [13] H. Wang, N. Desilles, F. Burel, Effect of tetra-n-butylammonium bromide salt on the cationic polymerization of dimethylketene and on the thermal properties of the obtained polyketones, *Journal of Polymer Science Part A: Polymer Chemistry*, 52 (2014) 1493-1499.
- [14] H. Wang, Synthèse et caractérisation de nouvelles polycétones aliphatiques à partir des cétones, Rouen, INSA, 2013.
- [15] A. Polic, T. Duever, A. Penlidis, Case studies and literature review on the estimation of copolymerization reactivity ratios, *Journal of Polymer Science Part A: Polymer Chemistry*, 36 (1998) 813-822.
- [16] D.M. Sarzotti, J.B.P. Soares, A. Penlidis, Ethylene/1-hexene copolymers synthesized with a single-site catalyst: Crystallization analysis fractionation, modeling, and reactivity ratio estimation, *Journal of Polymer Science Part B: Polymer Physics*, 40 (2002) 2595-2611.

- [17] C. Barson, D. Fenn, A method for determining reactivity ratios when copolymerizations are influenced by the penultimate group effects of both monomers, *European polymer journal*, 25 (1989) 719-720.
- [18] M. Dube, R.A. Sanayei, A. Penlidis, K.F. O'Driscoll, P.M. Reilly, A microcomputer program for estimation of copolymerization reactivity ratios, *Journal of Polymer Science Part A: Polymer Chemistry*, 29 (1991) 703-708.
- [19] F. Tüdös, T. Kelen, T. Földes-bereznich, B. Turcsányi, Analysis of Linear Methods for Determining Copolymerization Reactivity Ratios. III. Linear Graphic Method for Evaluating Data Obtained at High Conversion Levels, *Journal of Macromolecular Science: Part A—Chemistry*, 10 (1976) 1513-1540.
- [20] M. Fineman, S.D. Ross, Linear method for determining monomer reactivity ratios in copolymerization, *Journal of Polymer Science*, 5 (1950) 259-262.
- [21] J.P. Kennedy, T. Kelen, F. Tüdös, Analysis of the linear methods for determining copolymerization reactivity ratios. II. A critical reexamination of cationic monomer reactivity ratios, *Journal of Polymer Science: Polymer Chemistry Edition*, 13 (1975) 2277-2289.
- [22] R. Mao, M.B. Huglin, A new linear method to calculate monomer reactivity ratios by using high conversion copolymerization data: terminal model, *Polymer*, 34 (1993) 1709-1715.
- [23] F.R. Mayo, F.M. Lewis, Copolymerization. I. A basis for comparing the behavior of monomers in copolymerization; the copolymerization of styrene and methyl methacrylate, *Journal of the American Chemical Society*, 66 (1944) 1594-1601.
- [24] P.W. Tidwell, G.A. Mortimer, An improved method of calculating copolymerization reactivity ratios, *Journal of Polymer Science Part A: General Papers*, 3 (1965) 369-387.
- [25] A. Yezrielev, E. Brokhina, Y.S. Roskin, An analytical method for calculating reactivity ratios, *Polymer Science USSR*, 11 (1969) 1894-1907.
- [26] T. Kelen, F. Tüdös, B. Turcsányi, Confidence intervals for copolymerization reactivity ratios determined by the Kelen-Tüdös method, *Polymer Bulletin*, 2 (1980) 71-76.

3. Modification of Dimethylketene-based Polyketone

This short chapter gives several useful information about postpolymerization modification of aliphatic polyketones to approach functional materials. Thus, we tested some possible reaction pathways using different modification reagents upon our well investigated and reliable polyketone (PDMK) based on dimethylketene (DMK) monomer.

3.1 Superiority and Limitation of PDMK

After the copolymerization trials in the previous chapter, it appears that adding other type of ketene units into the polymer chain is not attractive to improve the thermal properties and processing performances of PDMK. In contrast, it more or less reduces the T_g and T_{deg} , which relates to the utilisation temperature.

As was mentioned in Chapter 1.2, PDMK became a rising star in the area of packaging owing to its impressively low dioxygen permeability (P_{O_2}) in the condition of both low and high relative humidity, which was superior to the three other types of conventional barrier polymers: polyamide, EVOH (copolymer of ethylene and vinyl alcohol) and PVDC.

For industrial applications of barrier materials, three main properties are necessary:

- the permeability of corresponding gas (oxygen, water vapor, carbon dioxide...),
- the service temperature,
- the ease and mode of fabrication.

Despite of the excellent oxygen barrier property (thanks to a crystallinity of 0.29~0.45) and satisfying service temperature (thanks to T_g of 65~75°C), the narrow processing window (less than 50°C depending on T_m of 220~250°C, $T_d^{5\%}$ around 280°C) of PDMK unfortunately limits its industrial application [1]. Besides, its poor solubility in common solvents impeded its characterization. Thus the following functional modification pathways were conducted in our experiments.

3.2 Generalities on Modification Pathways

3.2.1 Conversion to Polypyrazole from Polyketones

A successful approach to the postpolymerization modification of polyketones containing 1,3-diketone units was performed using the hydrazine hydrate ($\text{NH}_2\text{NH}_2 \cdot \text{H}_2\text{O}$) as the modification reagent. It is regarded as a very efficient chemical conversion reaction to polypyrazoles from aliphatic polyketones, in association with that the carbonyl groups are converted to imine groups [2, 3].

Cafeo et al [2] reported that the cyclic polyketones can react with hydrazine hydrate to afford macrocycles containing isopyrazole units, since the pair of nucleophilic nitrogen atoms of hydrazine have the potential to react with pairs of carbonyl units placed in 1,3-diketones within the polyketonic macroring. It was also mentioned in the publication that these polyketones can be subjected to the Paal-Knorr reaction with AcONH_4 to give pyrrole-units involved macrocycles [4, 5] (Figure 3-1).

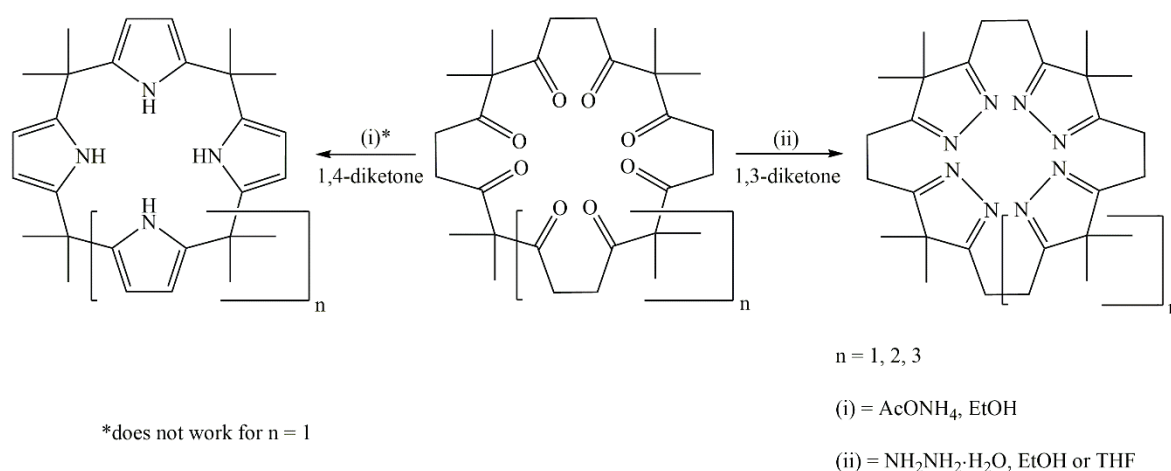


Figure 3-1. From cyclic polyketones to heterocyclophanes containing isopyrazole or pyrrole units [2]

Uesaka et al [3] developed diketone conversion reactions to linear aliphatic polyketones of short chain lengths. They studied two different efficient chemical conversions of diketone

units which were achieved chemoselectively on aliphatic polycarbonyl chains composed of an alternating 1,3- and 1,4-diketone sequence. The chemical modification reactions proved feasible to polyketone chains of various lengths up to tetracontane (C40) with 16 carbonyl groups (Figure 3-2).

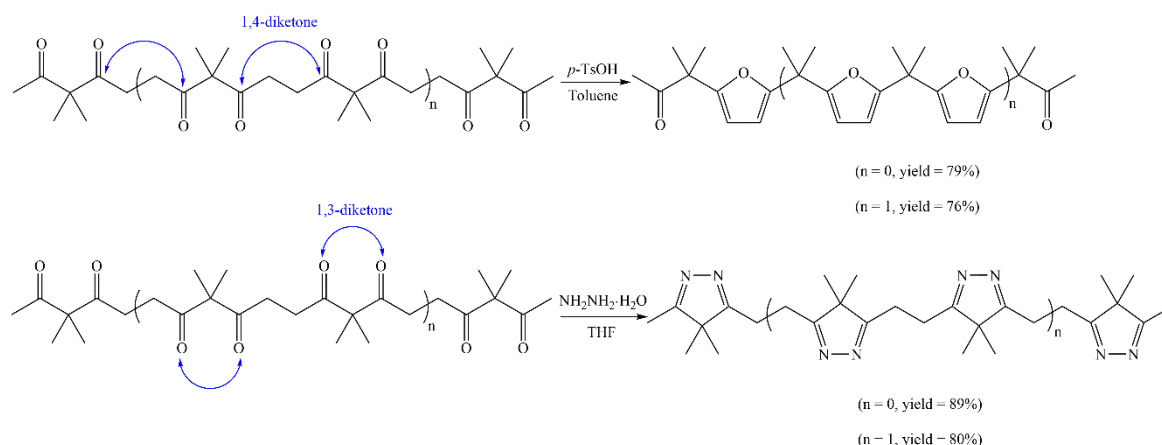


Figure 3-2. Conversion of 1,3- and 1,4-diketone in the aliphatic flexible polyketone chain into isopyrazole or furan subunits [3]

However, the above 1,3-diketone-to-pyrazole conversion reaction was only effective on ketone oligomers. Therefore, in this chapter, the feasibility of this modification pathway was verified on the DMK-based polyketone of long carbonyl chains containing regularly alternating 1,3-diketones.

3.2.2 One-step Beckmann Rearrangement

As is well known, the Beckmann type rearrangement forms amides from corresponding ketones. The transformation normally undergoes two steps, one step from a ketone to an oxime and the other from the oxime to a substituted amide (Figure 3-3) [6].

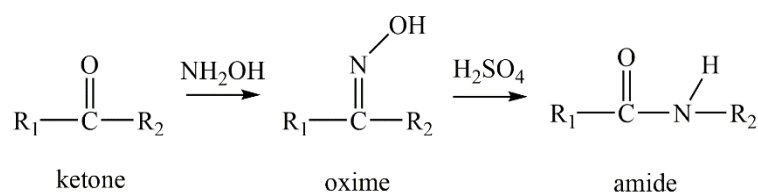


Figure 3-3. General transformation from a ketone to an amide via Beckmann rearrangement

Sharghi and Sarvari [7] developed a one-pot Beckmann rearrangement using alumina / methanesulfonic acid (AMA) to simplify this procedure; several approaches were reported with various aldehydes and ketones (Figure 3-4).

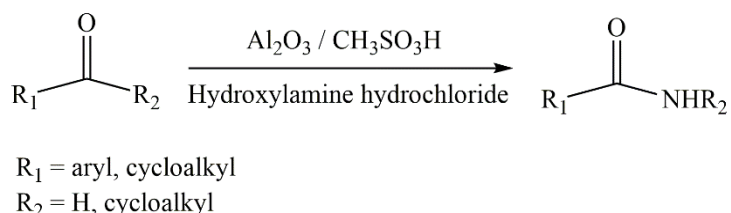
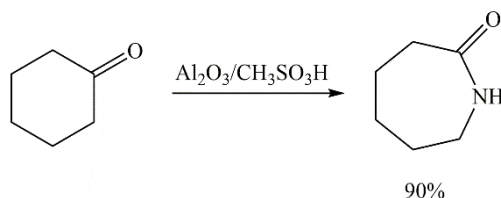


Figure 3-4. General Beckmann rearrangement reaction [7]

In particular, satisfying conversion (90% yield) and selectivity were obtained for the transformation of cyclohexanone into ϵ -caprolactam using AMA (Figure 3-5), presenting the advantage to prepare directly amides in good yields from the corresponding aldehydes and ketones without previous need to prepare the corresponding aldo- and keto-ximes.

Figure 3-5. Conversion of cyclohexanone oxime into ϵ -caprolactam using AMA [7]

However, to our knowledge, the Beckmann rearrangement reaction never successfully applied to polymers which can potentially convert polyketones to polyamides. In our experiments, we approached to validate the feasibility of the one-pot Beckmann rearrangement reaction upon the DMK-based polyketone using AMA catalysts.

3.2.3 Dithioketal Functionalized Reaction

For the DMK-based polyketone, its high crystallinity is a double-edge sword, which on one hand affords excellent thermomechanical stability and resistance to solvent attack, on the other one makes itself insoluble in conventional organic solvents. The insolubility causes inconvenience to its processing and characterization [1].

The dithioacetalisation reaction, which already successfully modified the very high crystallinity polymers of the PEEK family, was tested [8, 9].

Indeed, Colquhoun et al [9] discovered that crystalline aromatic poly(ether ketone)s such as PEEK and PEK can be cleanly and reversibly derivatized by dithioketalization of the carbonyl groups with 1,2-ethanedithiol (EDT) or 1,3-propanedithiol (PDT) under strong acid conditions (trifluoroacetic acid, TFA). The resulting 1,3-dithiolane and 1,3-dithiane polymers are hydrolytically stable, amorphous, and readily soluble in organic solvents such as chloroform and THF and thus can be (unlike their parent polymers) easily characterized. Furthermore, the obtained polymers can be quantitatively deprotected by prolonged reaction with a mixture of 2-iodo-2-methylpropane and dimethyl sulfoxide at high temperature to regenerate the starting poly(etherketone)s without loss of molecular weight (Figure 3-6).

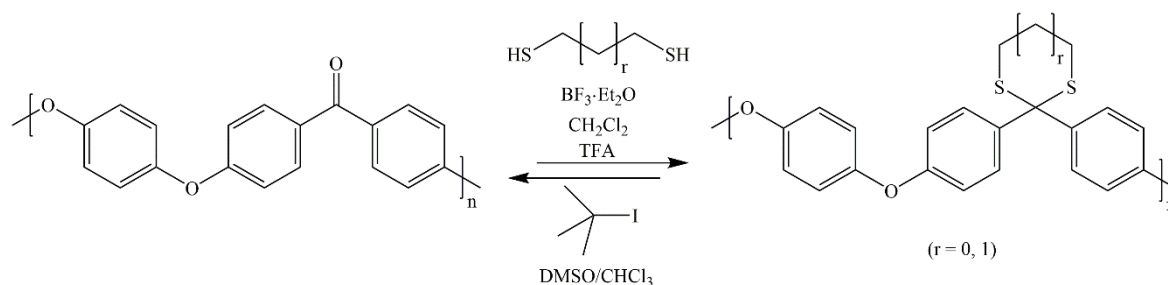


Figure 3-6. Dithioketalization and deprotection of PEEK with EDT ($r = 0$) and PDT ($r = 1$), respectively

The dithioketalization in fact provides a completely general solution to the problem of achieving nondegradative derivatization and solubilization of semi-crystalline aromatic PEEK and its derives.

So is it possible to apply dithioketalization to our DMK-based polyketone to solve the solubility problem ? That is the question we want to answer in this chapter.

3.3 Experimental Modification on PDMK

3.3.1 Experimental Procedure

All the DMK-based polyketones involved in the following postpolymerization modification reactions were obtained in Run 58 (Chapter 2.3). For convenience, the DMK-based polyketone was named as PDMK.

3.3.1.1 Conversion to Polypyrazole from Polyketones

The procedure was conducted similarly to what was described in literature [2]. A dispersion of PDMK in the solvent indicated in Table 3-1, prepared by vigorous stirring of a mixture of 0.2 g PDMK and 5 mL solvent with the various quantity of hexafluoro-2-propanol (if necessary), was placed in a 25 mL three-necked flask equipped with a reflux condenser, a stirrer and a dropping funnel; the medium was then kept at the refluxing

temperature. The reaction was carried out by adding 2 or 10 mmol of $\text{N}_2\text{H}_4 \cdot \text{H}_2\text{O}$ (0.2 or 1 mL) to the flask through the dropping funnel, for as much as 3 days at the refluxing temperature. After 3 days, the reaction mixture was cooled to room temperature, and then poured into a large amount of ethanol; the resulting solid was filtered and washed several times with ethanol.

3.3.1.2 One-step Beckmann Rearrangement

The procedure was conducted similarly to what was described in literature [6]. 10 mL $\text{CH}_3\text{SO}_3\text{H}$ (0.15 mol) and 1.5 g Al_2O_3 (15 mmol) were charged into a 5 mL round-bottomed flask equipped with a magnetic stirrer. Then 0.35 g PDMK was added with vigorous stirring at 80°C. After a few minutes, 1.05 g hydroxylamine hydrochloride (15 mmol) was added and the temperature was kept at 80°C for 3 days. After 3 days the reaction mixture was cooled to room temperature, and then was poured into a large amount of ethanol, the resulting solid was filtered and washed several times with ethanol.

3.3.1.3 Dithioketal Functionalized Reaction

The procedure was conducted similarly with what was described in literature [9]. To a 50 mL round-bottomed flask charged with 0.28 g PDMK in a mixture of 20 mL dichloromethane and 5 mL trifluoroacetic acid, was added 0.752 g 1,2-ethanedithiol (7.99 mmol), followed by 0.571 g boron trifluoride diethyl etherate (4.02 mmol) under an atmosphere of nitrogen with stirring. After a reaction period indicated in Table 3-1, the reaction mixture was cooled to room temperature, and then was poured into a large amount of ethanol, the resulting solid was filtered and washed several times with ethanol.

3.3.2 Experimental Results and Discussion

The three different postpolymerization modification were carried out according to the above details, the main data and results for the reaction systems were summarized in Table 3-1.

Table 3-1. Postpolymerization modification and results

Run	PDMK	Reagent	Solvent	Temp. (°C)	Remark
Conversion to Polypyrazole from Polyketones					
100	0.2 g	0.2 mL N ₂ H ₄ ·H ₂ O	5 mL THF	70	No change
101	0.2 g	0.2 mL N ₂ H ₄ ·H ₂ O	CH ₂ Cl ₂ / HFIP (5 mL : 0.1 mL)	50	No change
103	0.2 g	1 mL N ₂ H ₄ ·H ₂ O	CH ₂ Cl ₂ / HFIP (5 mL : 0.5 mL)	50	No change
104	0.2 g	1 mL N ₂ H ₄ ·H ₂ O	CH ₂ Cl ₂ / HFIP (5 mL : 2.5 mL)	50	No change
105	0.2 g	0.2 mL N ₂ H ₄ ·H ₂ O	5 mL Toluene	115	No change
One-step Beckmann Rearrangement					
97	0.35 g	10 mL CH ₃ SO ₃ H 1.5 g Al ₂ O ₃ 1.05 g NH ₂ OH·HCl	-	80	No change
Dithioketal Functionalized Reaction					
99	0.28 g	5 mL CF ₃ COOH 0.046 mL EDT 0.51 mL BF ₃ ·Et ₂ O	20 mL CH ₂ Cl ₂	80 (3 h)	0.18 g polymer soluble in CH ₂ Cl ₂
102	0.28 g	5 mL CF ₃ COOH 0.046 mL EDT 0.51 mL BF ₃ ·Et ₂ O	20 mL CH ₂ Cl ₂	80 (3 days)	Nothing precipitates in ethanol

All the trials of conversion to polypyrazole and Beckmann rearrangement from PDMK were unsuccessful. All the polymers collected after these reactions were identical to the initial ones.

For the dithioketal functionalized reaction of PDMK in Run 99, the powders obtained after precipitation in ethanol presented partial solubility in CH_2Cl_2 , which was different from the complete insolubility of original PDMK. Moreover, increasing the reaction time in Run 102 afforded no precipitate in ethanol. We analyzed the structure of the product collected in Run 99, its ^1H and ^{13}C spectra were illustrated respectively by Figure 3-7 and Figure 3-8.

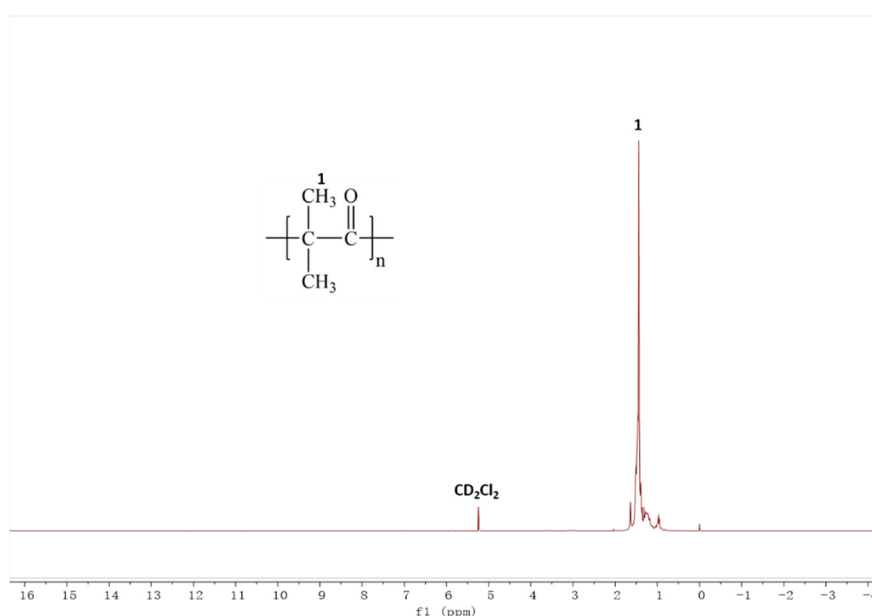


Figure 3-7. ^1H spectrum (300 Mhz, 20°C , CD_2Cl_2) of Run 99 in CD_2Cl_2 (dithioketal functionalized reaction)

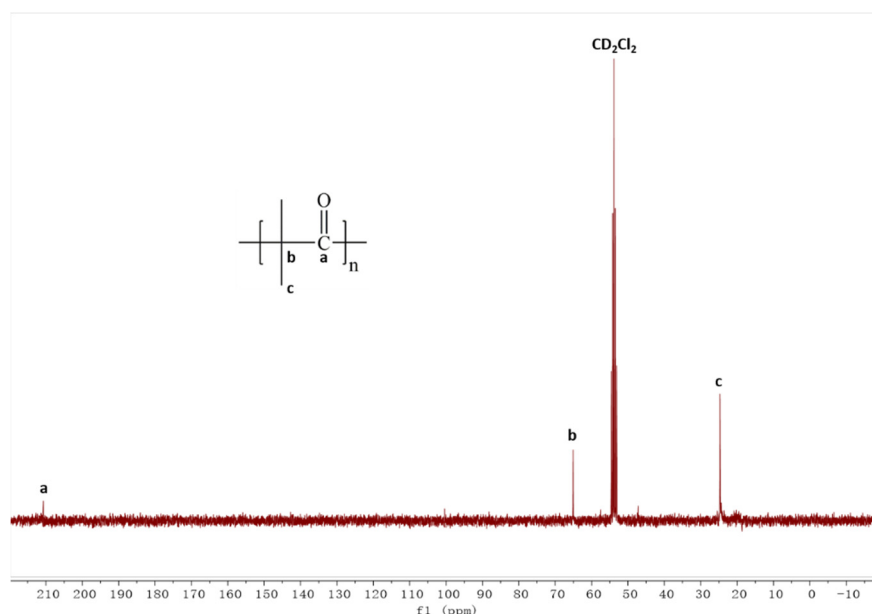


Figure 3-8. ^{13}C spectrum (75 Mhz, 20°C , CD_2Cl_2) of Run 99 in CD_2Cl_2 (dithioketal functionalized reaction)

It can be seen that the structure of the new polymer is the same as the original PDMK, whereby the same signals were found in the ^1H (1.5 (H_1) ppm in CD_2Cl_2) and ^{13}C NMR ($\delta = 212.2$ (C_a), 65.4 (C_b), 24.6 (C_c) ppm in CD_2Cl_2) spectra. We then measured its molecular weight by SEC analysis in CH_2Cl_2 using PMMA standards (figure in Annexes): the extremely low molecular weight ($\overline{M}_n = 2\,500\text{ g}\cdot\text{mol}^{-1}$, $\overline{M}_w = 3\,400\text{ g}\cdot\text{mol}^{-1}$, $D_M = 1.4$) suggested some chain-cut reactions, resulting an oligomer soluble in CH_2Cl_2 .

The TGA spectrum given in Figure 3-9 offered another proof to the above reasoning. The 5% weight loss temperature of the polymer in Run 99 decreased more than 50°C from the original PDMK, while their maximum weight loss temperature remained nearly the same (around 335°C). The melting point T_m and the melting enthalpy ΔH_m also decreased according to the DSC spectrum (in the Annexes).

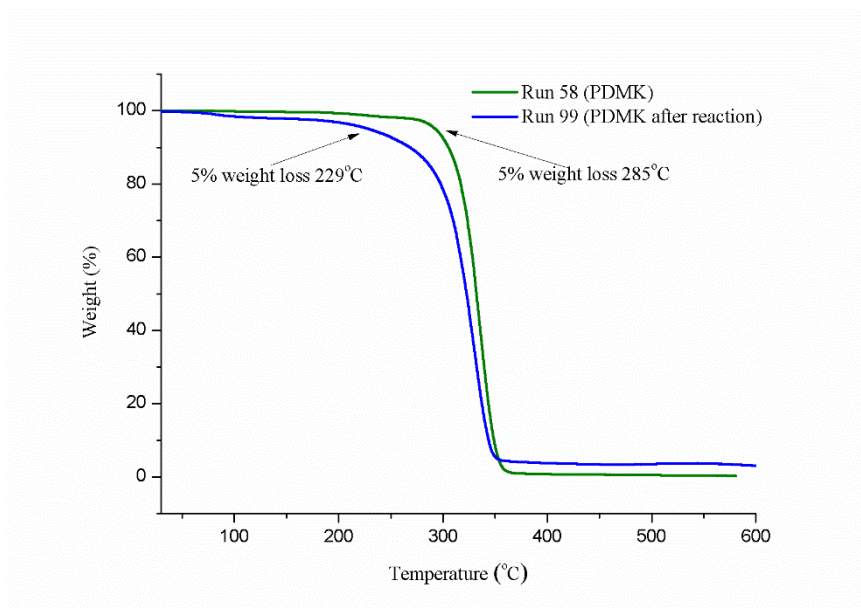


Figure 3-9. TGA spectra of Run 99 (dithioketal functionalized reaction) and original PDMK

In summary, the dithioketal functionalized reaction did not succeed to bring functional groups to PDMK, but a chain-cut procedure.

For a small conclusion, PDMK possesses a very special and extremely stable molecular structure, which is different from 1,3-diketone polyketones or other similar polyketones. Except the possibility of chain-cut, the functional modification was inaccessible or very hard to apply to PDMK with the aforementioned methods.

3.4 Conclusion

In this chapter, three different postpolymerization modification reactions (conversion of polypyrazole from polyketone, one-pot Beckmann rearrangement and dithioketal functionalized reaction) were presented and tested upon our DMK-based polyketone (PDMK), with the aim to functionalize PDMK and to broaden its chemical and physical properties.

However, it proved the 1,3-diketone structure of PDMK remains very special from other polyketones, which ensures PDMK of an excellent chemical stability behaving inert to even most of the modification reagents: all the three proposed modification pathways failed. The dithioketal functionalized reaction afforded by 1,2-ethanedithiol and boron trifluoride diethyl etherate in the strong acid condition caused a chain-cut reaction to PDMK, which gave a $\overline{M}_n = 2\,500\text{ g}\cdot\text{mol}^{-1}$ PDMK oligomer of worse thermal stability but soluble in CH_2Cl_2 .

3.5 References

- [1] H. Wang, Synthèse et caractérisation de nouvelles polycétones aliphatiques à partir des cétones, Rouen, INSA, 2013.
- [2] G. Cafeo, D. Garozzo, F.H. Kohnke, S. Pappalardo, M.F. Parisi, R.P. Nascone, D.J. Williams, From calixfurans to heterocyclophanes containing isopyrazole units, *Tetrahedron*, 60 (2004) 1895-1902.
- [3] M. Uesaka, Y. Saito, S. Yoshioka, Y. Domoto, M. Fujita, Y. Inokuma, Oligoacetylacetones as shapable carbon chains and their transformation to oligoimines for construction of metal-organic architectures, *Communications Chemistry*, 1 (2018) 23.
- [4] G. Cafeo, F.H. Kohnke, G.L. La Torre, M.F. Parisi, R. Pistone Nascone, A.J. White, D.J. Williams, Calix [6] pyrrole and Hybrid Calix [n] furan [m] pyrroles ($n + m = 6$): Syntheses and Host-Guest Chemistry, *Chemistry—A European Journal*, 8 (2002) 3148-3156.
- [5] G. Cafeo, F.H. Kohnke, M.F. Parisi, R. Pistone Nascone, G.L. La Torre, D.J. Williams, The Elusive β -unsubstituted calix [5] pyrrole finally captured, *Organic letters*, 4 (2002) 2695-2697.
- [6] A.H. Blatt, The Beckmann Rearrangement, *Chemical Reviews*, 12 (1933) 215-260.
- [7] H. Sharghi, M.H. Sarvari, One-step Beckmann rearrangement from carbonyl compounds and hydroxylamine hydrochloride in $\text{Al}_2\text{O}_3/\text{CH}_3\text{SO}_3\text{H}$ (AMA) as a new reagent, (2001).
- [8] H.M. Colquhoun, F.P. Paoloni, M.G. Drew, P. Hodge, Dithioacetalisation of PEEK: a general technique for the solubilisation and characterisation of semi-crystalline aromatic polyketones, *Chemical Communications*, (2007) 3365-3367.
- [9] H.M. Colquhoun, P. Hodge, F.P. Paoloni, P.T. McGrail, P. Cross, Reversible, nondegradative conversion of crystalline aromatic poly (ether ketone) s into organo-soluble poly (ether dithioacetal) s, *Macromolecules*, 42 (2009) 1955-1963.

4. Novel Initiators Approach to Cationic Polymerization of Ketene Monomers

Until now, the few studies on cationic polymerization of ketenes was limited to the use of classical initiators, mainly Lewis acids. This chapter describes three different types of updated cationic initiators and their catalytic performance on our ketene monomers.

4.1 Generalities on Novel Initiators

In comparison to ‘classic’ initiators for cationic polymerizations, researches on novel types of initiators focus on developing environmentally friendly, nontoxic, easily handled and highly effective compounds. To follow these development trends, we successively tested the solid, photo and metallocene initiators on the ketene monomers.

4.1.1 Montmorillonitic Clay

During recent years, either by acting as initiators itself or initiator carriers, different solid catalysts such as zeolites [1], heteropoly acid salts [2], clays [3], porous polymer powders [4] and miscellaneous supports [5] have been studied in the polymerization of olefins. Among them, clay catalysts, especially montmorillonitic clays, have drawn great attention thanks to their wide availability, eco-friendly processing, easy recyclability and high catalytic efficiency [6-8]. Using clay catalysts can be done both at industrial level and laboratory scale [9].

4.1.1.1 The Nature of Montmorillonitic Clays

Clays are solid acidic catalysts which can serve as both Brønsted and Lewis acids in their natural and ion-exchanged form, which behave according to the mechanism of cationic polymerization [6-8, 10]. They are also known to act as radical catalysts, making them useful in radical polymerization reactions [11].

Clays are a class of soil with a particle size of less than 2 mm in diameter, which implies a considerable number of about 7.2×10^{11} particles per gram of clay and a huge surface area up to 23 000 cm² per gram [12]. At the macroscopic level, they are sticky and plastic when moist, but hard and solid when dry. At the microscopic level, they are crystalline hydrous aluminosilicates containing various cations. On the basis of their chemical components and crystal structures, clays can be divided into four main groups such as illite, smectite, vermiculite and kaolinite. Among these, the one that is found to be most useful as a catalyst to the synthetic organic chemist is a subgroup of the smectite clay, called montmorillonite (Figure 4-1), which is the main constituent of bentonites and Fuller's earth [9, 13].



Figure 4-1. Montmorillonite samples

The montmorillonite lattice is composed of a sheet of octahedrally coordinated gibbsite ($\text{Al}_2(\text{OH})_6$) sandwiched between two sheets of tetrahedrally coordinated silicate ($[\text{SiO}_4]^{4-}$) sheets. The three-sheet layer repeats itself, and the interlayer space holds the key to the chemical and the physical properties of the clay. An important and useful property of montmorillonite stems from its high degree of efficiency for metal cation exchange. This happens because of charge imbalances in its structure caused by exchange of Al^{3+} for Si^{4+} in the tetrahedral sheets, and of Mg^{2+} for Al^{3+} cations in the octahedral sheets (Figure 4-2).

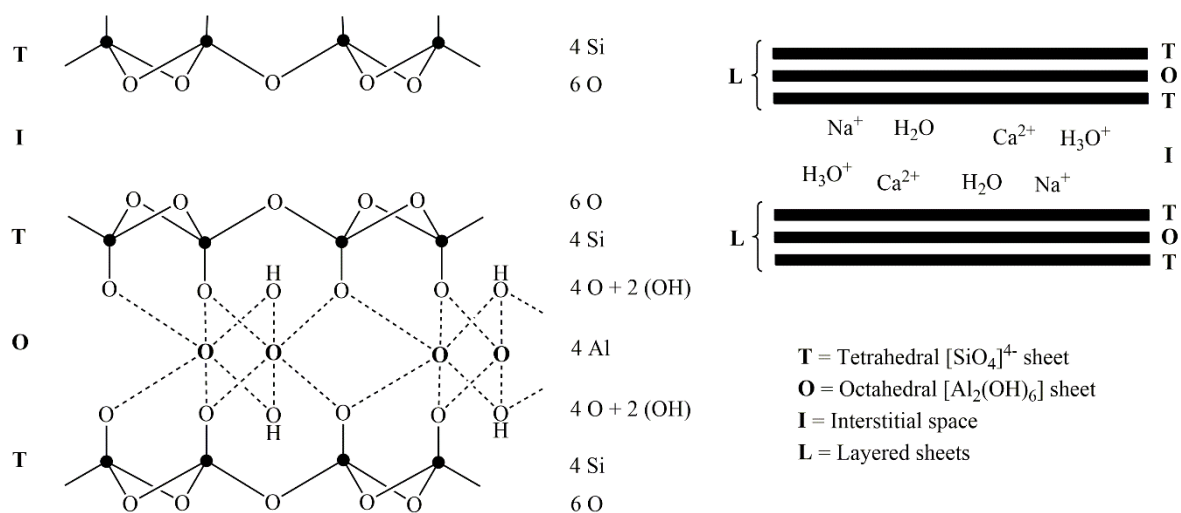


Figure 4-2. Structure of montmorillonite [9]

The interlayer in montmorillonite clay normally contains Na^+ , Ca^{2+} and Mg^{2+} as compensatory cations for the charge imbalance. When the clay is dry these cations reside in the hexagonal cavities of the silica sheets. However, when it is treated with water or other solvents, the cations relocate themselves in the interlamellar region and become exchangeable by a variety of both metallic and nonmetallic cations, such as H_3O^+ , NH_4^+ , Al^{3+} , Fe^{3+} , R_4N^+ , R_4P^+ , etc. The most useful properties of clay minerals lie in this fact [9].

4.1.1.2 Aluminum-Exchanged Montmorillonite Clay

As is mentioned above, the crystalline sheets of negatively charged aluminosilicates are balanced by hydrated cations (Na^+ , K^+ or Ca^{2+}) in the interlayer spaces of montmorillonite and these interlayer cations can be freely exchanged by other metal cations. When smectite clay is immersed into a solution of metal cations, the intercalation and swelling as well as exchange of both water molecule and cations occur, which can improve the catalytic properties of the clay [14]. The substitution of exchangeable cations, by highly polarizing species of small radius such as aluminum, zinc or iron, results in the activation of Brønsted and Lewis acid sites [15].

Considering that aluminum based Lewis acids such as AlCl_3 and AlBr_3 performed well in the catalytic procedure of ketenes, aluminum-exchanged montmorillonite clays (Al-Montmorillonite) have been of particular interest to us. Al-Montmorillonite have been found to be very effective acid catalysts for reactions such as dimerization of ethylene oxide to dioxygen heterocycles [16], for α,ω -dicarboxylic acids to cyclic anhydrides [17] and ether synthesis [18]. However, to our knowledge, no successful study has been reported on the polymer synthesis using Al-Montmorillonite.

4.1.1.3 Proton-Exchanged Montmorillonite Clay

As an efficient initiator for cationic polymerization of many vinylic and heterocyclic monomers, 'H-Maghnite' is produced from the montmorillonite sheet silicate clay by exchanging with protons [7, 19-26]. Comparing with other cationic initiators, the non-toxic H-Maghnite retains advantages in the easy separation procedure from the polymer products and regeneration capacity by heating to a temperature above 100°C [21]. Moreover, no inorganic residual species from the initiators can be entrapped into the polymer, which gives access to a free-metal trace polymer [20].

Bennabi et al [20] explored the synthesis of poly(ethylglyoxylate) (PEtG) using the H-Maghnite in bulk conditions at three temperatures (-40°C , 25°C , 80°C) and in THF solutions at room temperature (25°C). It was observed that an optimum ratio of 5 wt% of initiator leads to molecular weights up to $22\,000\text{ g}\cdot\text{mol}^{-1}$ in THF solutions at 25°C (Figure 4-3).

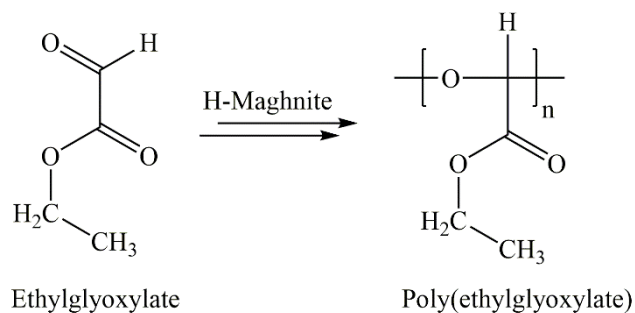


Figure 4-3. Synthesis of PETG [20]

Meghabar et al [7] investigated the polymerization of N-vinyl-2-pyrrolidone (NVP) catalyzed by the H-Maghnite. The main conclusion is that the polymerization rate increases with increase of the temperature and the loading of initiator, and it is more pronounced in nitrobenzene than in toluene (Figure 4-4).

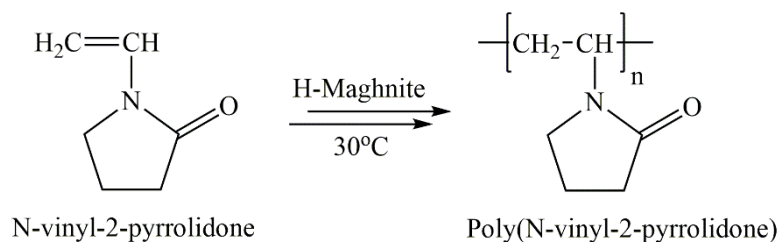


Figure 4-4. Polymerization of N-vinyl-2-pyrrolidone [7]

The polymerization was considered to be initiated by the proton addition from H-Maghnite to monomer and the propagation proceeds with Maghnite as counter-ion (Figure 4-5).

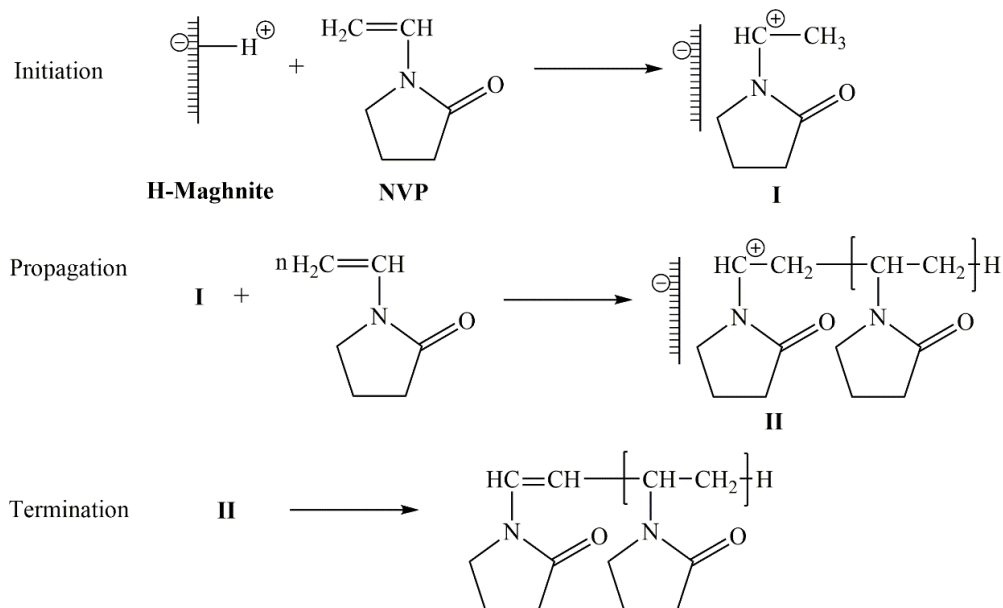


Figure 4-5. Mechanism of polymerization of N-vinyl-2-pyrrolidone using H-Maghnite [7]

The H-Maghnite initiator has never been applied to ketene monomers, although it is efficient in the polymerization of various vinylic and heterocyclic monomers.

4.1.2 Photoinitiators

Photopolymerizations are typically chain-growth reactions in which the propagating active centers (usually free radicals or cations) are formed by absorbing the exciting light as a photochemical step, which initiates the polymerization [27, 28].

Photopolymerization represents significant advantages over the relatively conventional polymerizations in the production cost, process control, environmental friendliness and reaction rates [29-33]. The spatial and temporal control of initiation, afforded by the use of light, provides cure-on-demand, since the light can be easily directed to a location of interest and shuttered on or off at will. As a result, photopolymerization typically exhibits high-speed reaction rates, and it can be exploited for heat-sensitive substrates without risk of thermal deformation. In addition, photocurable compositions are generally solvent-free, so they do

not contribute to emissions of volatile organic compounds, which makes photopolymerization eco-friendly. Comparing with the thermally-cured systems, photocurable systems are considered low-cost, since they consume a fraction of the energy required in conventional reactions [34].

A variety of photoinitiator systems are available that produce free radicals and/or cations upon absorption of ultraviolet and / or visible light [35]. In free-radical systems, light-sensitive photoinitiator molecules present within a liquid monomer (typically an acrylate or a methacrylate) react with photons of light to generate highly reactive free radicals. These radicals initiate the polymerization process, attacking reactive double bonds on monomer molecules and converting them to a polymer [28]. In cationic polymerization, the use of cationic photoinitiators, such as diaryliodonium, triarylsulfonium and ferrocene salts, provides a convenient method of generating powerful Brønsted acids under irradiation [31, 36-38].

4.1.2.1 Diaryliodonium Salts

Diaryliodonium salts ($\text{Ar}_2\text{I}^+\text{MX}_n^-$) possessing complex metal halide anions such as BF_4^- , AsF_6^- , PF_6^- , and SbF_6^- are active photoinitiators of cationic polymerization. As a type of compounds which can be readily isolated and purified by conventional techniques, diaryliodonium salts are considered indefinitely stable in the absence of light and in the presence of even such highly reactive cationically polymerizable monomers like cycloaliphatic olefin oxides [39].

On irradiation with ultraviolet (UV) light, diaryliodonium salts which bear complex metal halide anions undergo photolysis during which the organic cation is destroyed and a powerful Brønsted acid (HMX_n) is liberated (Figure 4-6). The strong protonic acid, in subsequent steps, efficiently initiates the polymerization of cationically polymerizable monomers.

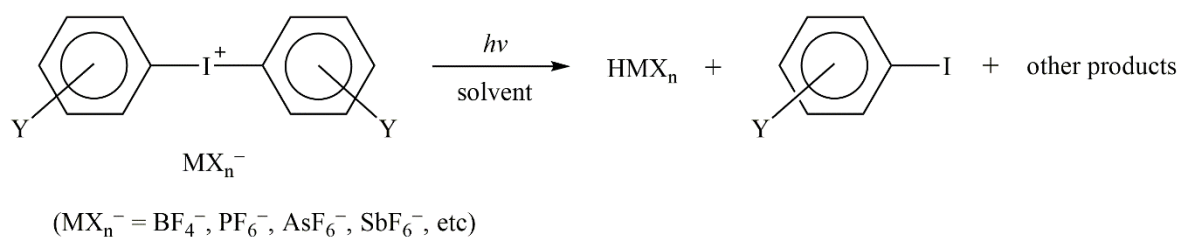


Figure 4-6. General photolysis of diaryliodonium salts [40]

Diaryliodonium salts are especially desirable in industrial applications as they do not contain heavy metals, do not cleave into toxic byproducts, and they can be prepared with a range of substituents to aid solubility [41].

IRGACURE 250 is a new type of substituted diaryliodonium salt for cationic photocuring of epoxy, oxetane, and vinyl ether formulations (Figure 4-7). A big advantage is that the product is active even at low concentrations and can be combined with a photosensitizer. Other benefits of IRGACURE 250 are the high line speeds that can be attained, even in highly pigmented applications, and the absence of hazardous cleavage products [42].

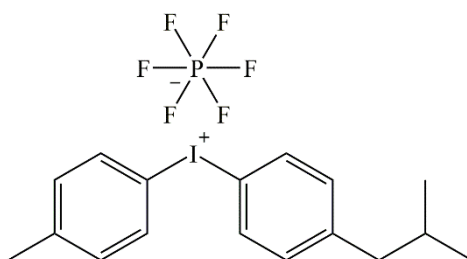


Figure 4-7. Structure of IRGACURE 250 [42]

The UV absorbance spectra of IRGACURE 250 in methanol at various concentrations are given in Figure 4-8. It can be seen that the main absorption bands range from 200 to 250 nm.

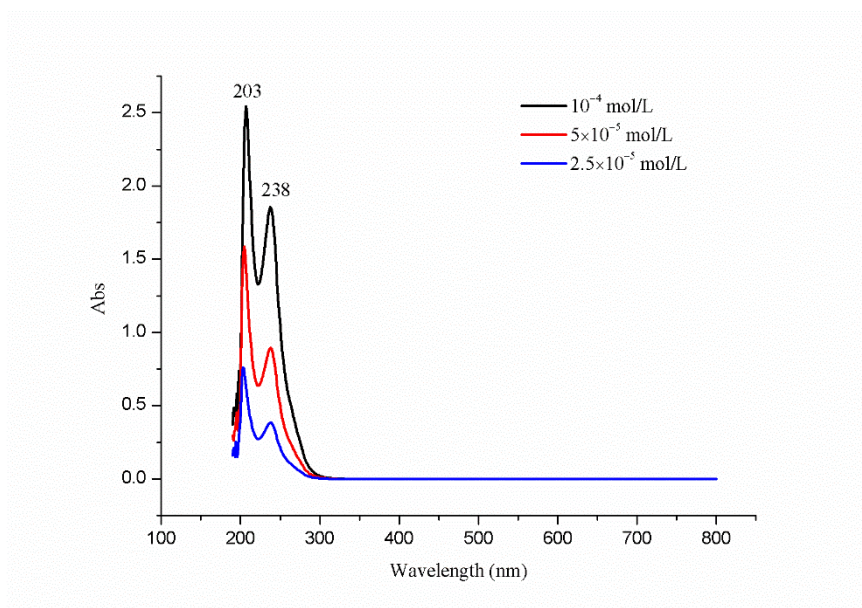


Figure 4-8. UV absorbance spectra of IRGACURE 250 in methanol

4.1.2.2 Ferrocene Salts

Ferrocene (Cp_2Fe , $\text{Cp} = \text{h}_5\text{-cyclopentadienyl}$) is usually believed to be a light-stable compound, but in organic halide solvents it decomposes upon exposure to light, resulting in the formation of active sites [43-45]. It is also believed that ferrocene does work as a sensitizer only when it has some interaction with monomer or additive (halide solvents) in the polymerization system upon various absorption band in the wavelength region of 250~490 nm [46]. The UV absorbance spectra of ferrocene in organic solvents show a maximum absorption near 440 nm along with a smaller band at 325 nm (Figure 4-9).

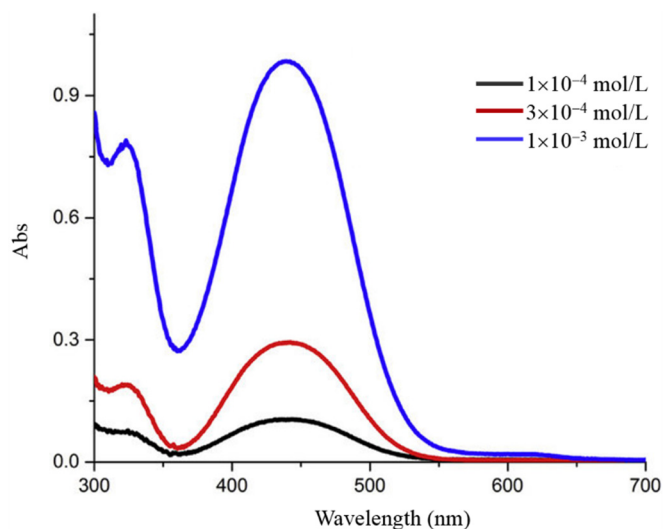


Figure 4-9. UV absorbance spectra of ferrocene in 1-methyl-3-nonylimidazolium bis[(trifluoromethane)sulfonyl]amide [47]

The primary process of photochemical initiation of the polymerization is the absorption of light by the ferrocene chlorinated solvent complex, and the initiating species is formed by the photochemical dissociation of this latter complex (Figure 4-10).

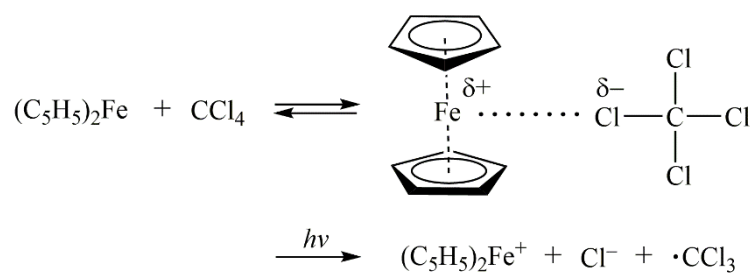


Figure 4-10. Photochemical dissociation of ferrocene carbon tetrachloride complex [48]

Normally the formed ferricenium cation is demonstrated to be the active centre for example in the cases of polymerization of pyrrole and epoxy [49, 50]. However, in some works these initiating species are also considered as radicals (trichloromethyl radical in the example), which are reactive in free radical photopolymerization or free radical promoted

cationic polymerization reactions, as for example in the case of polymerization of methyl methacrylate (MMA) [48].

In addition, absorption of substituted ferrocenes was investigated by Yavorskii [51] and Nesmeyanov [52]. It was concluded that effective absorption of bands range broadens to 220~600 nm.

In our experiments, an updated type of substituted ferrocene called 1,1'-bis(dimethylsilyl)ferrocene was applied (Figure 4-11).

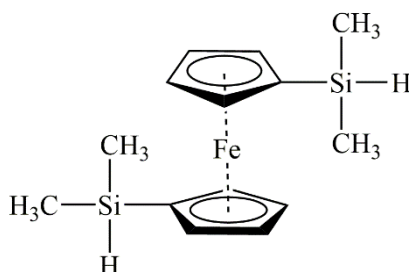


Figure 4-11. Structure of 1,1'-bis(dimethylsilyl)ferrocene

It has already been found that ferrocene salts can photoinitiate polymerization of pyrrole, epoxy and vinyl compounds such as methyl methacrylate (MMA), methyl acrylate (MA), vinyl acetate (VAc), acrylonitrile (AN), and methacrylonitrile (MAN) in the presence of halogenated solvents, such as $\text{CH}_2\text{CH}_2\text{Cl}_2$, CH_2Cl_2 , CHCl_3 and CCl_4 [46, 48-50, 53].

4.1.2.3 Three-component Initiator Systems

The major absorption bands of cationic photoinitiators like onium salts fall in the deep UV region (200~250 nm), thus the absence of overlap of these bands with the emission spectra of medium and low pressure mercury lamps and light-emitting diode (LED) limits their application [36, 54]. As a result, photosensitizers are often used with the initiator in the aim of broadening the spectral sensitivity of onium salts to longer wavelengths [54-58].

In contrast to the above mentioned separate photoinitiators which were used for the free-radical and cationic polymerizations, a three-component initiator system containing photosensitizers was investigated by Oxman and collaborators [59-62]. The three-component initiator systems generally contain a light absorbing photosensitizer (ketone sensitizers, dyes, etc.), a proton donor (typically an amine), and a third component (often a diaryliodonium or sulfonium salt) [63]. In addition to using initiating wavelengths in the visible region of the spectrum, the three-component photoinitiating systems have consistently been found to yield rapid polymerizations at lower light intensities than traditional ones or two-component photoinitiators [64, 65].

At first, these three-component systems were only applied in free-radical polymerizations because most of the amine H-donors that are used in these systems are too basic and will terminate a cationic active center, and the diaryliodonium salts used are often nucleophilic. However, it was discovered later that these three-component systems can be used for cationic photopolymerization if they are carefully designed. It was proved that cationic photopolymerization can smoothly proceed using electron donors with low basicity and iodonium salts with non-nucleophilic anions [57].

A proposed mechanism of photosensitization of the three-component photoinitiating system is illustrated in Figure 4-12. In this figure, camphorquinone (2,3-bornanedione, CQ) is a 1,2-diketone that has a broad UV-visible spectral absorption which extends into the visible region with a prominent band at 468 nm (Figure 4-13) [66]. The use of camphorquinone as a visible light photosensitizer in the iodonium-initiated cationic polymerization of epoxy and vinyl ethers has already been reported in numerous studies [34, 58, 67].

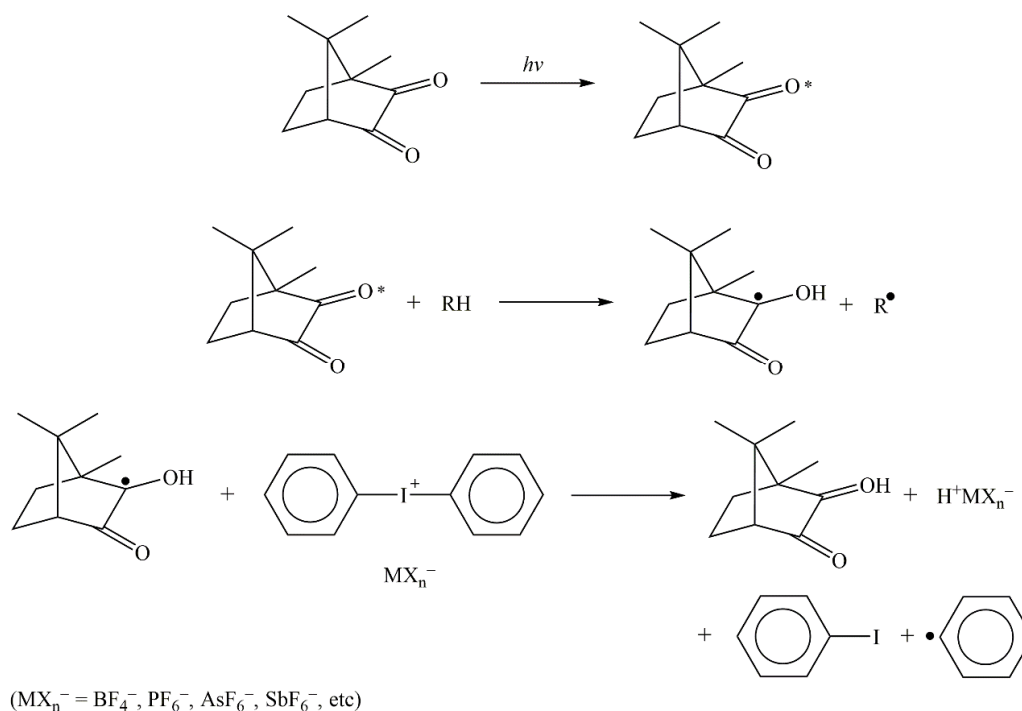


Figure 4-12. Proposed photosensitization mechanism of three-component initiator which accounts for the regeneration of CQ during irradiation with visible light [68]

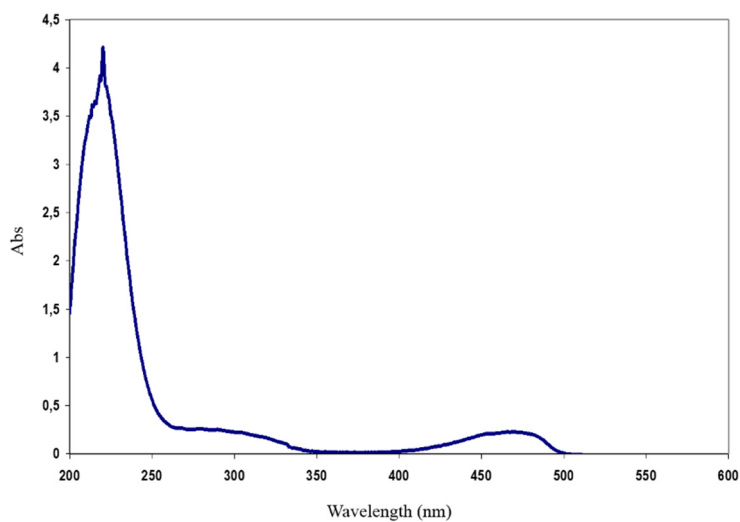


Figure 4-13. UV absorbance spectrum of camphorquinone (CQ) in ethanol ($9.6 \times 10^{-3} \text{ mol} \cdot \text{L}^{-1}$)

Taking all above factors in consideration, in our experiments, CQ was used as the photosensitizer, which acts as the first component. H-donors of toluene, *N,N*-dimethylaniline

and $\text{CF}_3\text{SO}_3\text{H}$ were respectively tested as the second component. The third component was the substituted diaryliodonium salt IRGACURE 250.

4.1.3 Metallocene

A typical metallocene initiator consists of a transition metal atom sandwiched between two cyclopentadienyl (Cp) or Cp-derivative rings (Figure 4-14) [69]. The transition metal atom usually belongs to group IV and is mostly zirconium (leading to zirconocenes), titanium (leading to titanocenes), or hafnium (leading to hafnocenes). Metallocenes are soluble in hydrocarbons and show only one type of active site upon activation, thus they are generally known as “single-site” initiators [70, 71].

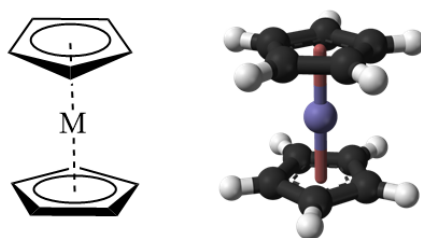


Figure 4-14. Sandwich structure of the metallocene

The single-site metallocenes generally derive from the metallorganic complex activated by methylaluminoxane (MAO), aluminum alkyls, borates, fluoroarylanes, trityl and ammonium borate, aluminate salts and other similar compounds [72]. Numerous metallocenes of different structures have been found, as examples depicted in Figure 4-15.

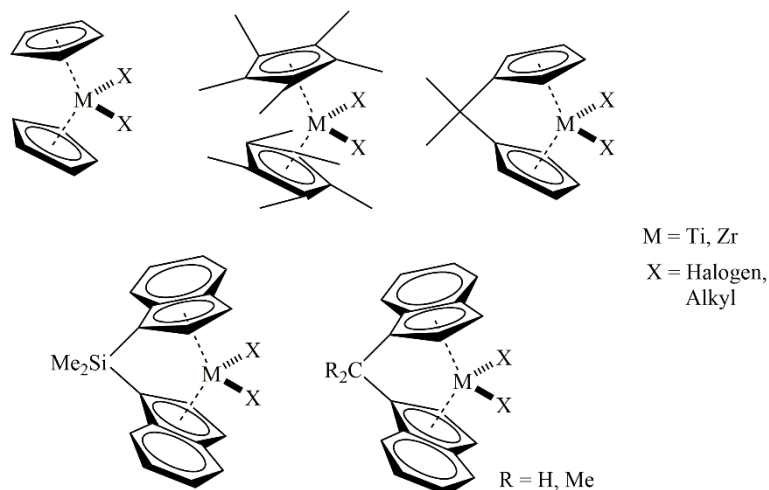


Figure 4-15. Several metallocene initiators [72]

Among these metallocenes, the simple bis(Cp) initiators containing alkyl single-sites were widely used with polymerization of olefins and they can be easily activated by activators or coinitiators such as methylaluminoxane (MAO), alkyl aluminum halides, tris(pentafluorophenyl)borane, tetra(penta-fluorophenyl)borate, etc (Figure 4-16) [73, 74]. Fukui and co-workers demonstrated that the alkyl metallocene activated with $B(C_6F_5)_3$ was capable of the living polymerization of propylene at -78°C in the presence of $Al(n\text{-Oct})_3$ as scavenger [75].

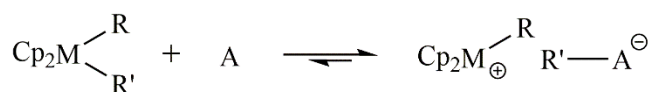


Figure 4-16. Formation of alkyl metallocene (Cp = cyclopentadienyl ligand; M = Ti, Zr, Hf; R = alkyl;

R' = alkyl or halide; A = Activator)

Polymerizations of other olefins such as ethylene, butene, hexene, octene using metallocenes were also reported, among which different grades of PE were already fulfilled in the commercial production [70]. Similar with conventional Ziegler-Natta initiators, polymerizations using metallocene initiators were believed based on a living Ziegler-Natta

chain growth mechanism (Figure 4-17), which is featured by the orderly monomer insertion between the growing chain and the active center [76]. However, as an obvious advantage over conventional Ziegler-Natta initiators, the precise control over the dispersity makes metallocenes very useful in terms of tailoring polymer properties (short and long chain branching, polymer tacticity, etc) [77, 78].

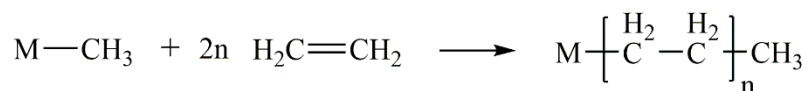


Figure 4-17. Insertion (Ziegler-Natta) polymerization of ethylene

In our research, bis(cyclopentadienyl) dimethylzirconium (Cp_2ZrMe_2) as a simple bis(Cp) initiator activated by tris(penta-fluorophenyl)borane ($\text{B}(\text{C}_6\text{F}_5)_3$) was chosen, motivated by a desire to simplify the experimental model at the very beginning of a new initiator test.

4.2 Polymerization with Montmorillonite Clays

4.2.1 Preparation of Clay Initiators

4.2.1.1 Al-Montmorillonite

The initiators were prepared by cation-exchange process according to the method reported in the literature [79].

In a typical preparation, 5 g of montmorillonite clay was slowly added to 80 mL of 0.3 mol·L⁻¹ aluminum nitrate ($\text{Al}(\text{NO}_3)_3$) aqueous solution. The resulting mixture was stirred for 4 h at room temperature. The final product was filtered, washed 2 times with 80 mL of distilled water and then dried in vacuum oven at 100°C for 2 h. ‘As prepared’ initiators were powdered and then calcined in a furnace at 300°C for 3 h. The yield was over 95%.

4.2.1.2 H-Maghnite

The preparation of the H-Maghnite was carried out by using a method similar to that described by Belbachir et al [21].

Briefly, 20 g of montmorillonite clay was dried for 2 h at 105°C in the oven before use. In a second time, a Maghnite / water (500 mL) mixture was stirred and combined with 0.25 mol·L⁻¹ sulfuric acid solution to remove calcite traces. Saturation was achieved over 2 days at room temperature. In a last step, H-Maghnite was washed with distilled water to eliminate sulfate species and then dried at 105°C during 24 h. The yield was over 95%.

4.2.2 Polymerization

Ketene monomers were prepared as described in Chapter 2. General polymerization conditions were set as follows: in CH₂Cl₂ (or in bulk for run 85), with [Monomer] = 3 mol·L⁻¹ (if solvent was needed); for the initiator, 5 wt% of solid with respect to the monomer was added into the system, according to the average value of 1~10% found in literature [7, 8, 20]; for temperature, -20~0°C was set to ensure a relatively high reactivity of the initiator. The reactive medium was kept during 5 h at this temperature and then, allowed to reach room temperature. After the 2 day reaction time, the system was neutralized and poured into a large amount of ethanol. The experimental details and results were summarized in Table 4-1.

It can be concluded that for these three ketene monomers in these conditions of solvent and temperatures, clay initiators of Al-Montmorillonite and H-Maghnite presented no catalytic activity.

Table 4-1. Polymerization summary of ketenes using clay initiators

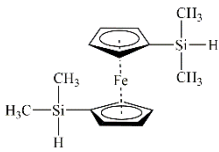
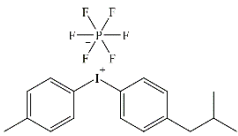
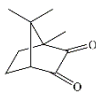
Run	Monomer	Initiator	Solvent	Temperature (°C)	Remarks
79	DMK	Al-Montmorillonite	CH ₂ Cl ₂	-20	reaction hardly proceeds
83		H-Maghnite	CH ₂ Cl ₂	-20	reaction hardly proceeds
80	DPK	Al-Montmorillonite	CH ₂ Cl ₂	-20	reaction hardly proceeds
82		H-Maghnite	CH ₂ Cl ₂	-20	reaction hardly proceeds
85		H-Maghnite	-	0	reaction hardly proceeds
70	DEK	Al-Montmorillonite	CH ₂ Cl ₂	-20	reaction hardly proceeds
96		H-Maghnite	CH ₂ Cl ₂	-20	reaction hardly proceeds

4.3 Polymerization with Photoinitiators

The five different photoinitiating systems involved were listed in Table 4-2. For all the experiments, the addition of photoinitiator followed $[\text{Monomer}]_0 / [\text{Initiator}]_0 = 100 / 1$, the photosensitizer and H-donor were added according to molar ratio $[\text{sensitizer}]_0 : [\text{Initiator}]_0 : [\text{H-donor}]_0 = 1 : 1 : 2$ (except when toluene served as H-donor and solvent). The UV process lasted for 30 min. Two different light sources were used, depending on the initiating system:

- Hamamatsu LC8: a 500 W power Hg-Xe lamp ($706 \text{ mW} \cdot \text{cm}^{-2}$ measured at 365 nm); the emission spectrum, illustrated in Figure 4-18, showed that this lamp could be suitable for all initiators (however at a much lower extent for IRGACURE 250 (B))
- 460 nm LED: used only for the third-component initiators (C, D, E); the real intensity could not be measured (no measuring cell centered on 460 nm).

Table 4-2. Photoinitiator systems involved

Mark	Photoinitiator	Photosensitizer	H-donor	Solvent	Absorption peak (nm)
A	1,1'-bis(dimethylsilyl)ferrocene 	-	-	CH ₂ Cl ₂	325 440
B	IRGACURE 250 	-	-	CH ₂ Cl ₂	203 238
C	IRGACURE 250	Camphorquinone (CQ) 	Toluene	Toluene	468
D	IRGACURE 250	CQ	<i>N,N</i> -Dimethylaniline	CH ₂ Cl ₂	468
E	IRGACURE 250	CQ	CF ₃ SO ₃ H	CH ₂ Cl ₂	468

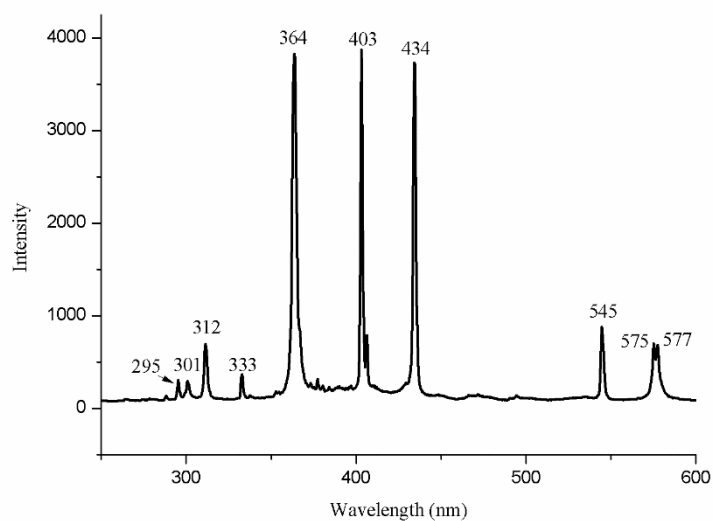


Figure 4-18. UV Emission spectral distribution of Hamamatsu lamp

The reactive medium was kept during 5 h at the desired temperature and then, allowed to reach room temperature. After additional two days with stirring, it was neutralized by ethanol and then poured into ten times volume of ethanol. The polymerization conditions and results were summarized in Table 4-3.

Table 4-3. Photopolymerization of ketenes

Run	Monomer	Initiator system	Temperature	Light source	Remarks
28	MEK	A	−78°C	Hamamatsu LC8	reaction hardly proceeds
19	DEK	A	−78°C	Hamamatsu LC8	reaction hardly proceeds
20		A	0°C	Hamamatsu LC8	reaction hardly proceeds
21		B	−78°C	Hamamatsu LC8	reaction hardly proceeds
22		B	0°C	Hamamatsu LC8	reaction hardly proceeds
32	EPK	A	−78°C	Hamamatsu LC8	reaction hardly proceeds
56	DPK	A	−78°C	Hamamatsu LC8	reaction hardly proceeds
76	DMK	A	−20°C	Hamamatsu LC8	reaction hardly proceeds
77		B	−20°C	Hamamatsu LC8	reaction hardly proceeds
89		C	−20°C	460 nm LED	reaction hardly proceeds
90		D	−20°C	460 nm LED	reaction hardly proceeds
92		E	−20°C	460 nm LED	reaction hardly proceeds

Unfortunately, whatever the initiating system and light source used, no polymer could be retrieved. The reason why all these Runs failed to give polymers probably addressed to the UV spectra of ketenes (for the typical DMK see Figure 4-19), which widely overlap the absorption spectra of initiators and thus makes their photodecomposition almost impossible. Indeed, let's not forget that our reactive media are $[\text{DMK}]_0 = 3 \text{ mol}\cdot\text{L}^{-1}$ compared to the

$8.3 \times 10^{-4} \text{ mol} \cdot \text{L}^{-1}$ used for measuring the UV spectrum, and as a consequence the absorption of DMK is tremendous even at 460 nm.

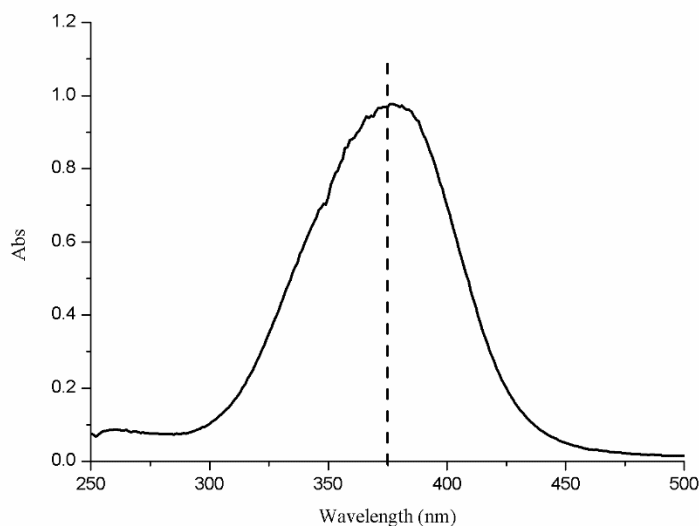


Figure 4-19. UV absorbance spectrum of DMK in ethyl acetate ($8.3 \times 10^{-4} \text{ mol} \cdot \text{L}^{-1}$)

In conclusion, the five applied cationic photoinitiator systems using different initiators proved to be ineffective for photopolymerization of the ketene monomers used in our experiments.

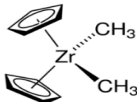
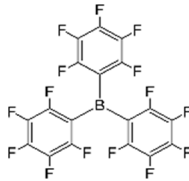
4.4 Polymerization with Metallocene

4.4.1 Polymerization Procedure and Results

Ketene monomers were prepared as described in Chapter 2 and used as soon as possible. All experiments were conducted with $[\text{Monomer}]_0 = 3 \text{ mol} \cdot \text{L}^{-1}$ and $[\text{Monomer}]_0 / [\text{Initiator}]_0 = 1\,000 / 1$ under oxygen and water free conditions. The initiator was added as a prepared solution of bis(cyclopentadienyl)dimethyl zirconium (Cp_2ZrMe_2) and tris(pentafluorophenyl)borane ($\text{B}(\text{C}_6\text{F}_5)_3$) in the corresponding solvent ($[\text{Cp}_2\text{ZrMe}_2]_0 = [\text{B}(\text{C}_6\text{F}_5)_3]_0 = 0.125 \text{ mol} \cdot \text{L}^{-1}$) after the reaction system stabilized at the targeted temperature. The reactive

medium was kept stirred during 5 h at this temperature and then, allowed to reach room temperature. Time of polymerization lasted always overnight. After that, a sufficient quantity of absolute ethanol was poured into the reactor to react with and neutralize residual monomers and initiators. Then the mixture was precipitated in large amounts of absolute ethanol. The obtained polymer (if there existed) was filtered, washed several times with ethanol and dried under vacuum at 40°C. A summary of the polymerization conditions and results was presented in Table 4-4.

Table 4-4. Summary of ketene polymerization using metallocene initiators

Run	Monomer	Initiator system	Solvent	Temperature (°C)	Remarks ^a
57	MEK	Bis(cyclopentadienyl) dimethylzirconium 	CH ₂ Cl ₂	0	reaction hardly proceeds
17	DEK		CH ₂ Cl ₂	−78	reaction hardly proceeds
18			CH ₂ Cl ₂	0	reaction hardly proceeds
31	EPK		CH ₂ Cl ₂	0	yield < 3% polyester
48	DPK	Tris(pentafluorophenyl) borane 	CH ₂ Cl ₂	0	reaction hardly proceeds
59	DMK		CH ₂ Cl ₂	−20	24% yield polyester
60			CH ₂ Cl ₂	−78	58% yield polyester
86			Toluene	−78	31% yield polyester
88			Diethyl ether	−78	68% yield polyester

a: yields were calculated by weight percent of obtained polymers (after precipitation) over feed monomers

From the table, it can be concluded that the metallocene initiators were effective only in the polymerization of DMK, although a very small quantity was obtained for EPK. The structure, molecular weights and other properties of the polymers were discussed in the following part.

4.4.2 Polyester from EPK

4.4.2.1 Molecular weights and structure

The FT-IR spectrum of Run 31 (Figure 4-20) showed only one bond around 1745 cm^{-1} , which generally attributes to the carbonyl of the polyester structure.

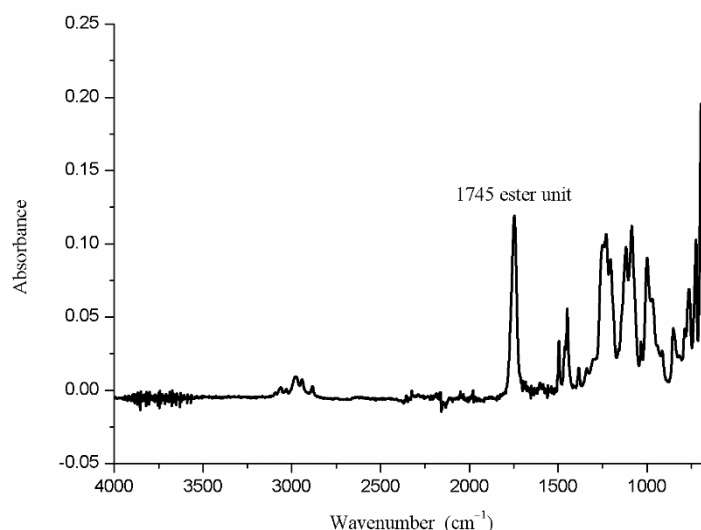


Figure 4-20. IR spectrum of Run 31 (EPK-based polyester)

Furthermore, ^1H ($\delta = 6.6\sim 7.8$ ($\text{H}_{1\sim 6}$), $2.2\sim 2.8$ ($\text{H}_{7,8}$), $0.1\sim 0.8$ ($\text{H}_{9,10}$) ppm in CD_2Cl_2 , see Figure 4-21) and ^{13}C ($\delta = 174.7$ (C_a), 139.7 (C_b), $126\sim 129$ (benzene-C), 86.8 (C_c), 52.1 (C_d), 27.1 ($\text{C}_{e,f}$), 12.3 (C_g), 7.2 (C_h) ppm in CD_2Cl_2 , see Figure 4-22) NMR spectra also proved that only polyester was present, however besides unidentified signals. The absence of signal

around 210 ppm excluded the presence of polyketone structure. However, the signals of ^{13}C NMR were not very clear because of the little quantity obtained (very low 3% yield).

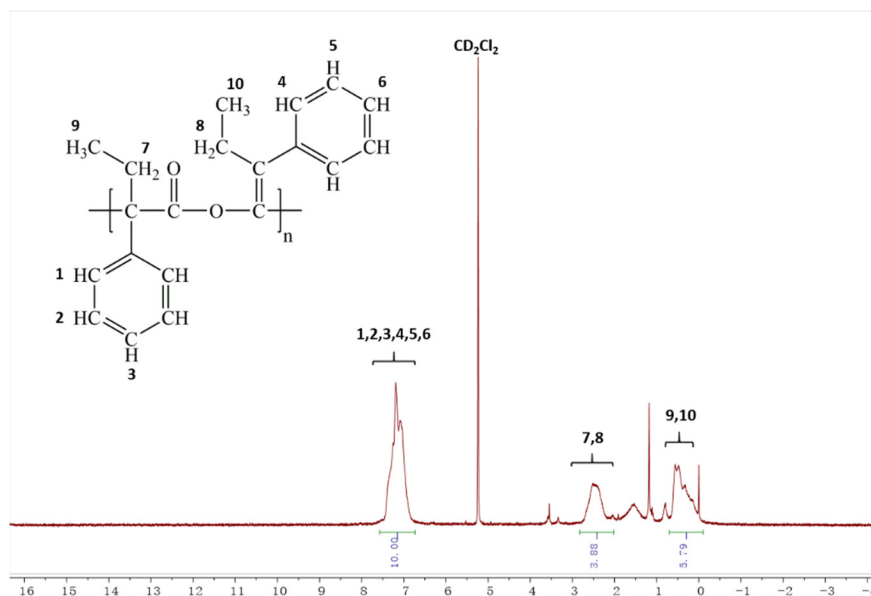


Figure 4-21. ^1H NMR (300 Mhz, 20°C , CD_2Cl_2) spectrum of Run 31 (EPK-based polyester)

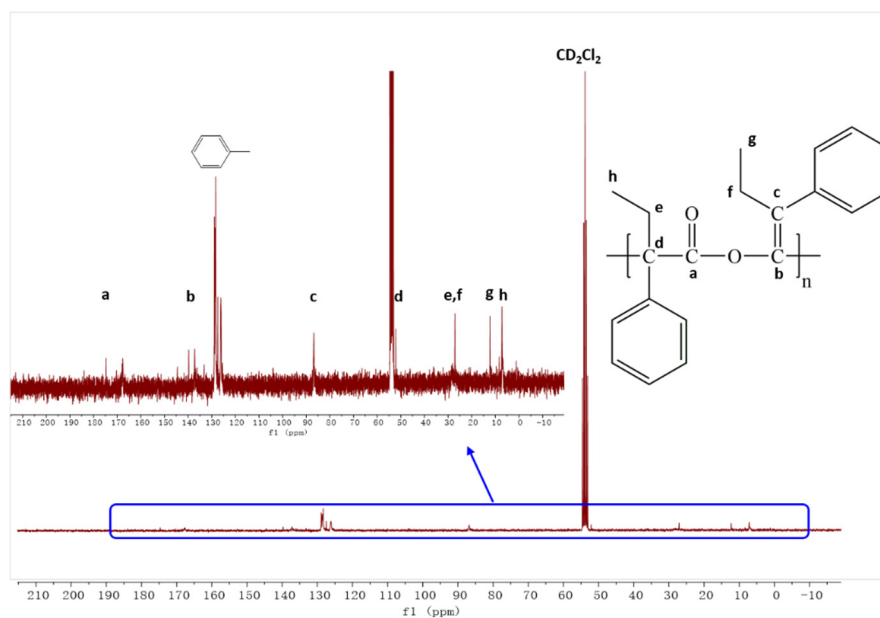


Figure 4-22. ^{13}C NMR spectrum (75 Mhz, 20°C , CD_2Cl_2) of Run 31 (EPK-based polyester)

\overline{M}_n and \overline{M}_w determined by SEC in CH_2Cl_2 (PMMA standards) respectively reached $\overline{M}_n = 3\,500\text{ g}\cdot\text{mol}^{-1}$ and $\overline{M}_w = 5\,800\text{ g}\cdot\text{mol}^{-1}$, with $D_M = 1.66$ (chromatograms have been put in Annexes). The extremely low yield, and the unsatisfying molecular weight and complex structure could be explained by the steric hindrance of the bulky side phenyl group on the polymer chain growth process.

4.4.2.2 Thermal properties

TGA analysis of Run 31 (Figure 4-23) showed that the 5% weight loss temperature is far below 200°C , which would be a big limitation of this material.

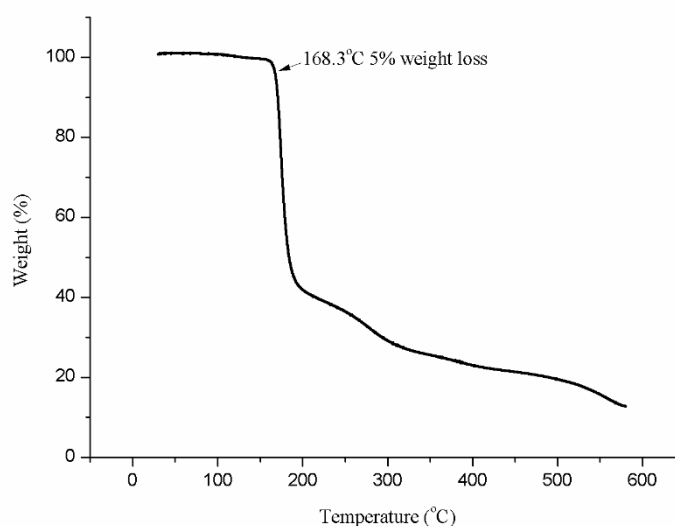


Figure 4-23. TGA analysis of Run 31 (EPK-based polyester)

Unfortunately, the sample quantity was not enough for the DSC measurement.

In conclusion, comparing with the already reported polyesters using conventional initiators like *n*-BuLi in the literature [80, 81], the polyester from EPK initiated with metallocene initiators does not seem very interesting, because of its extremely low yield (less than 3%), short polymer chains ($\overline{M}_n = 3\,500\text{ g}\cdot\text{mol}^{-1}$) and poor thermal stability ($T_d^{5\%} = 168^\circ\text{C}$).

4.4.3 Polyester from DMK

4.4.3.1 Structure Determination

The polymer structures (example of Run 88) were investigated by FT-IR (Figure 4-24), ^1H NMR (Figure 4-25) and ^{13}C NMR (Figure 4-26) analyses (spectra of Run 59, 60, 86 were put in Annexes, and were exactly the same as Run 88).

For FT-IR, a single strong absorption band at 1733 cm^{-1} ($\text{C}=\text{O}$) shown in Figure 4-24 indicated a pure and clean ester structure of the obtained polymers, which exactly matched what was reported in the literature [82].

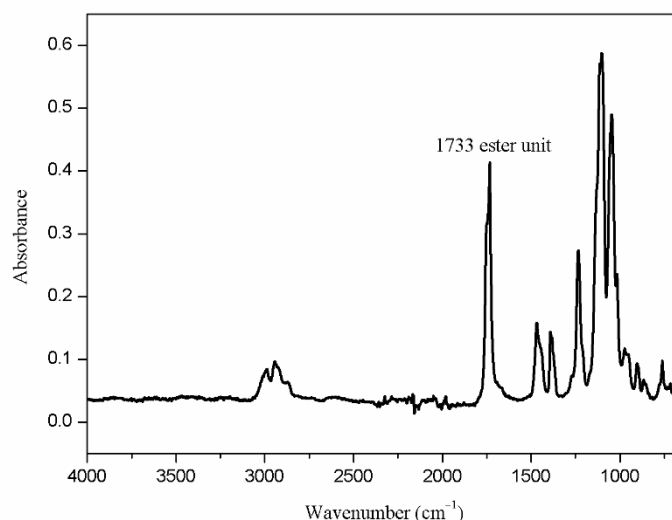


Figure 4-24. IR spectrum of Run 88 (DMK-based polyester)

The ^1H NMR in Figure 4-25 presented every H atoms from $-\text{CH}_3$ ($\delta = 1.72$ (H_1), 1.52 (H_2), 1.47 (H_3) ppm in CD_2Cl_2) which are characteristic of a polyester structure. But as already stated [83], the other possible polymer structures (ketone, ester and acetal) give signals in the same range. Therefore, ^{13}C NMR analysis ($\delta = 173.8$ (C_a), 142.8 (C_b), 123.4 (C_c), 47.2 (C_d), 25.4 (C_e), 20.2 (C_f), 19.5 (C_g) ppm in CD_2Cl_2) was undertaken (Figure 4-26) to further confirm the polymer repeating units. The presence of the peak at $\delta = 173.8$ ppm proved the existence of polyester, while the absence of the acetal (around 100 ppm) and

ketone (around 210 ppm) peaks further verified its absolute structure specificity and purity. The complete assignment of the other signals were well attributed to the repeating ester unit, which definitely demonstrated that only the polyester structure was obtained.

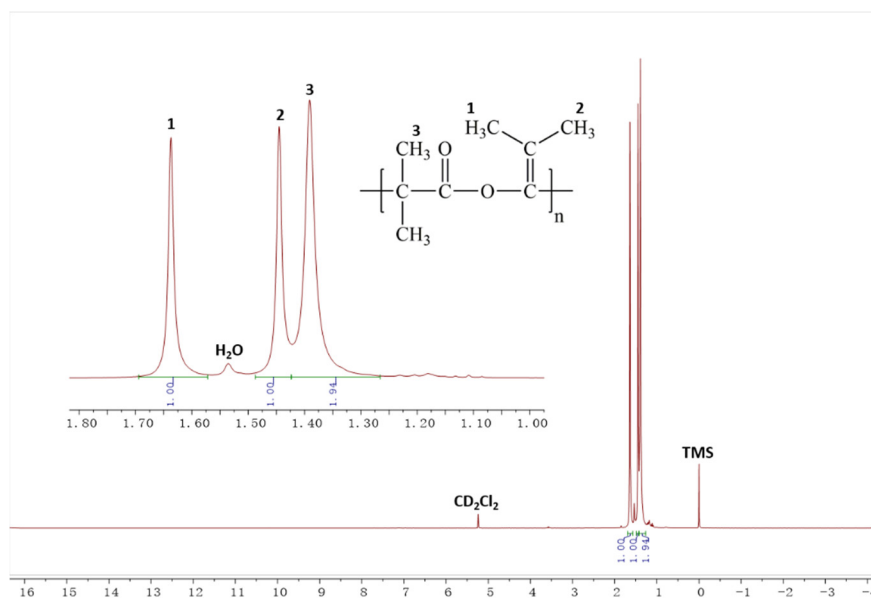


Figure 4-25. ^1H NMR spectrum (300 Mhz, 20°C , CD_2Cl_2) of Run 88 (DMK-based polyester)

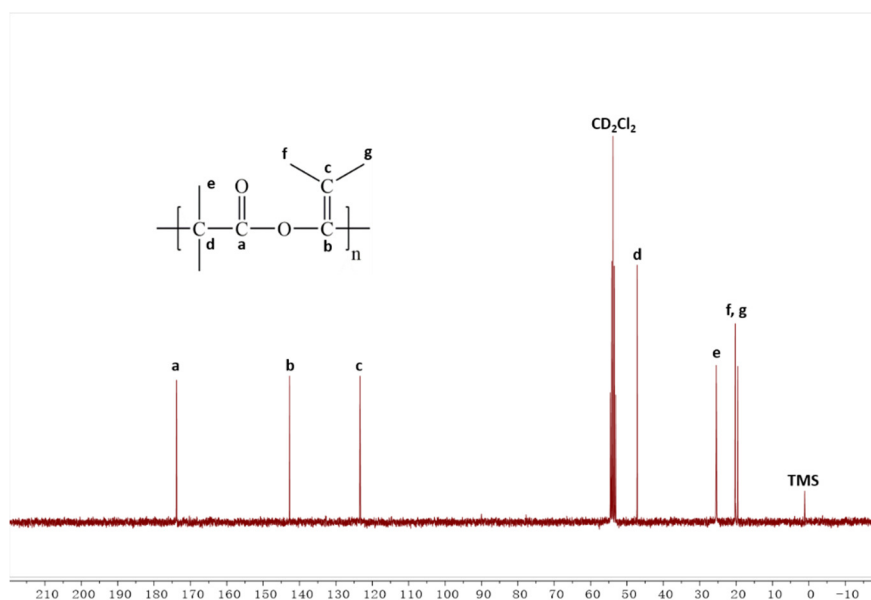


Figure 4-26. ^{13}C NMR spectrum (75 Mhz, 20°C , CD_2Cl_2) of Run 88 (DMK-based polyester)

4.4.3.2 Solvent and Temperature Effects on Molecular Weights and Yields

The various experimental conditions and results were presented in Table 4-5. It should be stressed that all the Runs proceeded very smoothly without remarkable exotherm. The obtained polymers were fully soluble in CH_2Cl_2 and toluene, but precipitated in diethyl ether along with the proceeding of the insertion reaction (Run 88).

Table 4-5. Polymerization conditions of dimethylketene and results using metallocene initiators

Run	Solvent	$\epsilon_{\text{solvent}}$	Temperature (°C)	\overline{M}_w ($\text{g}\cdot\text{mol}^{-1}$)	\overline{M}_n ($\text{g}\cdot\text{mol}^{-1}$)	\overline{D}_M	Yield ^a (%)
59	CH_2Cl_2	8.93	−20	33 800	16 000	2.11	24
60	CH_2Cl_2	8.93	−78	128 900	76 600	1.68	58
86	Toluene	2.38	−78	236 500	120 100	1.97	31
88	Diethyl ether	4.33	−78	359 700	306 000	1.19	68

a: yields were calculated by weight percent of obtained polymers (after precipitation) over feed monomers

The polymerization realized at -20°C in CH_2Cl_2 (Run 59) afforded relatively low molecular weights and yield compared to using a temperature of -78°C (Run 60), maybe because the higher temperature led to more side reactions giving cyclic dimer or trimer compounds of ketenes [84], which were incapable of inserting into the living chains.

At the chosen reaction temperature of -78°C , all the Runs resulted in products that possessed much higher molecular weights, narrower polydispersities and increased yields (except for Run 86 in toluene which was quite underwhelming). This suggested a large superiority of metallocene initiators compared to the traditional anionic initiators, for which polyesters with \overline{M}_n close to $20\,000\text{ g}\cdot\text{mol}^{-1}$ and \overline{D}_M close to 1.9 were already reported [85].

Top yield and molecular weights were reached in diethyl ether, relatively up to 68% and 300 000 g·mol⁻¹, with a very low polydispersity of 1.19. No evident relevance could be concluded between the molecular weight and dielectric constant of the solvent.

4.4.3.3 Insertion Mechanism

Different from olefins, both of the negatively-charged C and O gained the opportunity to be attacked by the positively-charged zirconium, owing to the two isoelectronic structures occurring to the ketene, which was responsible for the diverse linkage mode between monomers.

The positively-charged Zr, deriving from Cp₂ZrMe⁺MeB(C₆F₅)₃⁻ (described as the following equation in Figure 4-27), was stabilized by the α-agostic association bond from a shared hydrogen at the very beginning of the insertion.

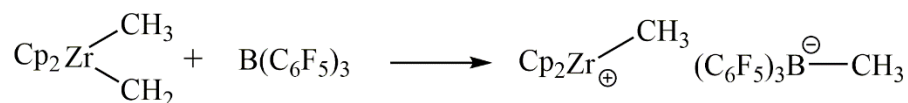


Figure 4-27. Activate reaction of metallocenes

When a ketene approached to the electron-deficient active center, the Zr⁺ first chose to link with the O⁻ regarding that a carbon was already in the hand. Interstitial rearrangement then happened associating with the electron moving. For the second coming ketene, the C⁻ was preferred by the Zr⁺, attributing to the existing of Zr-O linkage. Thus, an ester unit appeared since another rearrangement motivated by the movement of electrons. Similarly, other ketene fragments alternatively inserted into the living growing chain with headfirst and tailfirst styles, and a polyketene chain of repeating ester units was finally obtained via this insertion polymerization (see Figure 4-28).

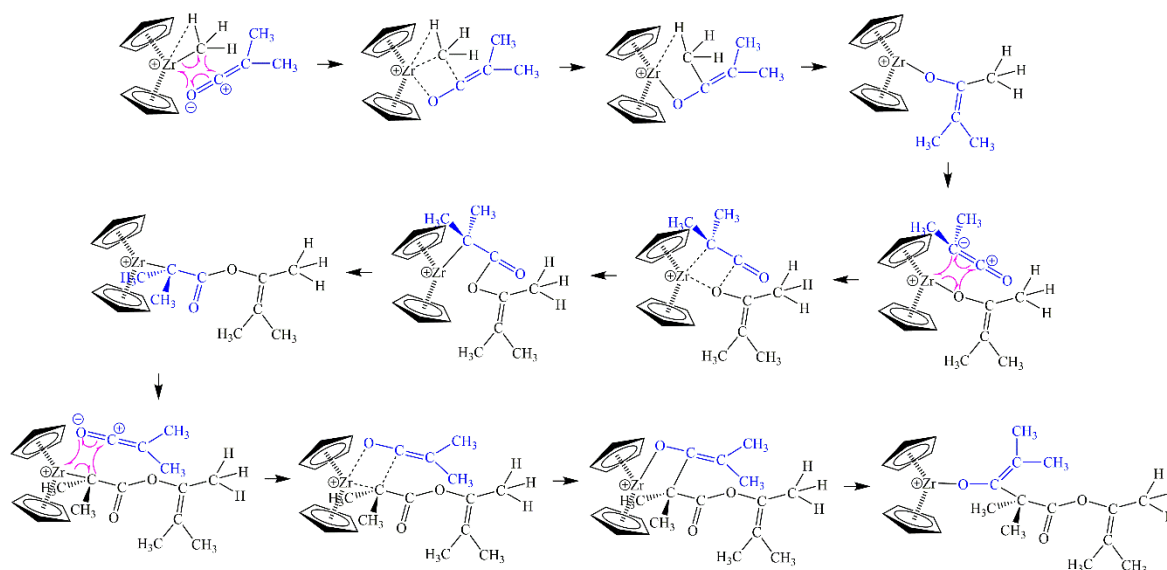


Figure 4-28. Insertion polymerization mechanism of DMK

The whole insertion polymerization procedure can be summarized in Figure 4-29.

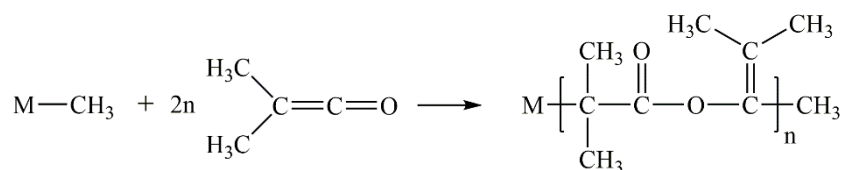


Figure 4-29. Insertion polymerization of DMK

To express this insertion mechanism more vividly, we preferred to infer it to a mechanism we named an ‘Obsessive-Compulsive Snake’ (Figure 4-30). The active center of metallocene initiators, positively-charged Zr in the ‘sandwich’, can be regarded as the head of a hungry snake. The ketene monomer, which can be possibly rearranged to two different units in the chain, can be a fish with the negatively-charged O as the head and C as the tail. A headfirst-to-tailfirst alternative fish eating habit make the snake grow to a ester-structured polymer.

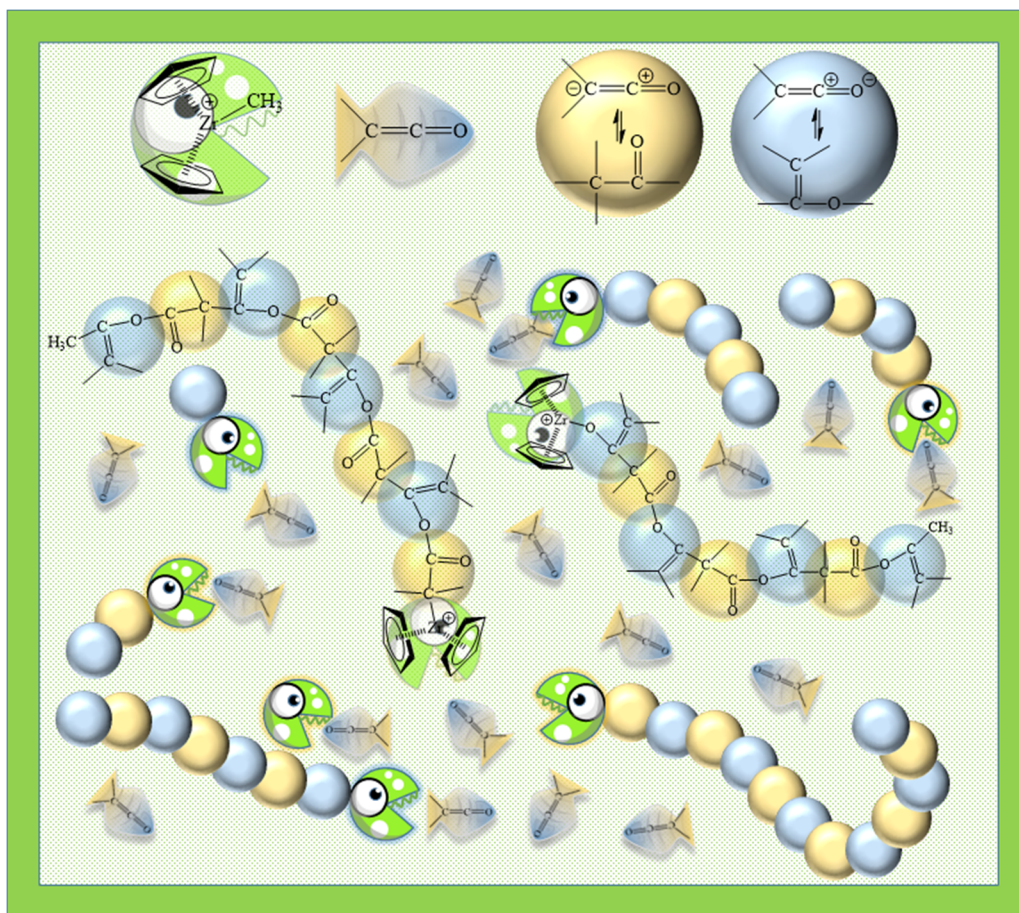


Figure 4-30. Association of 'Obsessive-Compulsive Snake' with ketene insertion mechanism

4.4.3.4 Thermal Properties

The thermal stability of these DMK-based polyesters was determined by TGA (Figure 4-31). The detailed $T_d^{5\%}$ and T_d^{Max} values were given in Table 4-6. It was logical that the polymers of Run 60, 86 and 88, possessing higher molecular weights ($\overline{M}_w > 100\,000$ g·mol⁻¹), had a better heat resistance, of which all the $T_d^{5\%}$ exceeded 320°C, while the shorter chains (Run 59) presented a worse temperature stability with a $T_d^{5\%}$ around 250°C. The unexpected slightly decrease before 300°C occurring to Run 86 probably owed to the relatively wide molecular distribution, which indicated a polymer with mixed short and long chains.

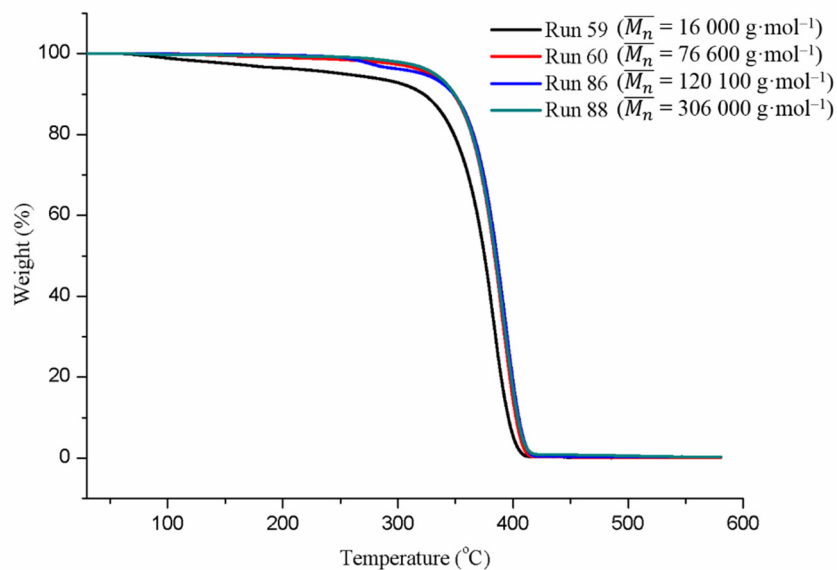


Figure 4-31. TGA spectra of DMK-based polyesters

Table 4-6. Thermal properties of DMK-based polyesters

Run	\overline{M}_w	\overline{M}_n	\mathcal{D}_M	T_g	T_m	ΔH_m	$T_d^{5\%}$	T_d^{Max}		
	(g·mol ⁻¹)	(g·mol ⁻¹)		(°C)	(°C)	(J·g ⁻¹)			(°C)	(°C)
	(2 nd heating)									
59	33 800	16 000	2.11	35	-	-	254	383		
60	128 900	76 600	1.68	51	-	-	328	390		
86	236 500	120 100	1.97	76	198	21.2	322	392		
88	359 700	306 000	1.19	69	200	22.2	332	391		

The DSC spectra of a normally heating-cooling-heating rate at 10°C / min were put in Annexes. It seemed that at this cooling rate it is difficult for these polyesters to crystallize well, as already observed in literature for polyesters of \overline{M}_n around 20 000 g·mol⁻¹ [85]: ΔH_m of Run 86 was 17.4 J·g⁻¹ while ΔH_m of Run 88 was only 5.6 J·g⁻¹, certainly due to long polymer chains, meanwhile no melting was detected for Run 59 and Run 60.

Considering that the DMK-based polyesters were hard to crystallize, therefore after the first heat at the rate of 10°C / min, a cooling process at 0.5°C / min was conducted to ensure a better crystallization (if possible). Then the spectra during the second heating procedure with a rate of 10°C / min were collected in Figure 4-32 and details were organised in Table 4-6.

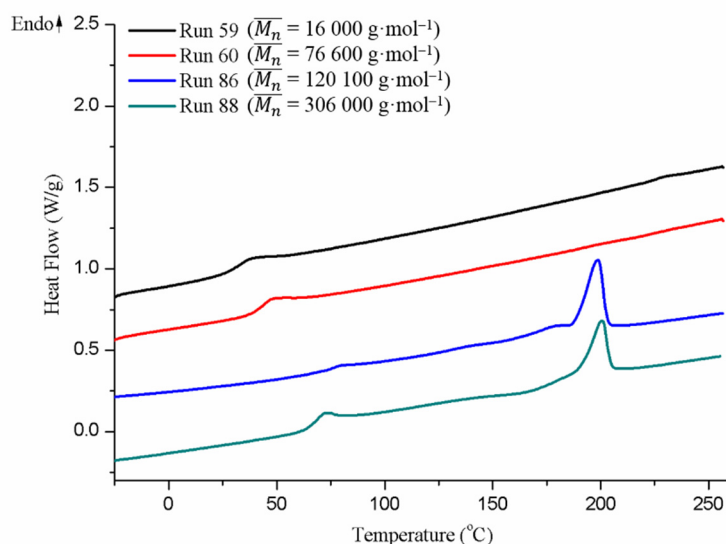


Figure 4-32. DSC spectra of DMK-based polyesters (heat at 10°C / min after a cooling at 0.5°C / min)

From Figure 4-32, T_g of massive polyesters ($\overline{M}_w > 200\,000\text{ g}\cdot\text{mol}^{-1}$) was found around 70°C associated with general T_m of 200°C and ΔH_m ranging 21~22 J·g⁻¹, whereas T_g range 30~60°C was assigned to the obtained products of a molecular weight (\overline{M}_w) less than $2\times 10^5\text{ g}\cdot\text{mol}^{-1}$, with no melting behavior detected. This also suggested a large superiority of metallocene initiators compared to the traditional anionic initiators, for which polyesters with T_m of 206°C and ΔH_m close to 13 J·g⁻¹ without detected T_g (at a cooling rate of 0.2°C / min comparing to 0.5°C / min in our experiments) were already reported [85].

These results are logical at the point of Flory-Fox equation [86]: a polymer with long chains has less free volume than one with short chains. Thus, low molecular weights gives lower values of T_g , and higher molecular weights causes T_g stabilize in an asymptotic

approach to the theoretical infinite T_g . In the same manner, the massive polyester crystallized whereas the less massive did not, because longer chains made less crystal defects.

4.4.3.5 Degradation Properties

It was interesting to notice that, after several months of storage (six months on average) in the air at room temperature from the first synthesis of these DMK-based polyesters, obvious degradation was observed, changing several properties (Table 4-7).

Table 4-7. Summary of property changes of DMK-based polyesters after 6 month-storage

Run	SEC ^a			MAL S	T_g	T_m	ΔH_m	$T_d^{5\%}$	T_d^{Max}
	\overline{M}_w	\overline{M}_n	\mathcal{D}_M		(°C)	(°C)	(J·g ⁻¹)		
	(g·mol ⁻¹)	(g·mol ⁻¹)		(g·mol ⁻¹)	(2 nd heating after cooling at 0.5°C / min)			(°C)	(°C)
59 (t₀)	33 800	16 000	2.11	-	35	-	-	254	383
59 (t₁)	7 000	2 200	3.16	4 500	25	-	-	143	385
60 (t₀)	128 900	76 600	1.68	-	51	-	-	328	390
60 (t₁)	6 100	2 500	2.47	31 000	25	-	-	143	389
86 (t₀)	236 500	120 100	1.97	-	76	198	21.2	322	392
86 (t₁)	33 200	12 500	2.66	44 000	44	187	2.5	264	390
88 (t₀)	359 700	306 000	1.19	-	69	200	22.2	332	391
88 (t₁)	135 800	43 800	3.10	210 100	66	199	6.0	326	389

t₁ = t₀ + 180 days;

a: calibration of \overline{M}_n and \overline{M}_w by SEC with poly(methylmethacrylate) standards

From the SEC comparison in Figure 4-33 and detailed data in Table 4-7, it can be easily concluded that all the polymer chains were cut into shorter ones as time went on. The \overline{M}_w

of the polyesters determined by SEC analysis decline to $1/20 \sim 1/3$ of their origins. We also applied MALS analysis to the degraded polymers to verify the true \overline{M}_w values. Except Run 86, it proved that the \overline{M}_w values from SEC kept the same order of magnitude with the values from light scattering, which confirmed the occurring of degradation. In addition, molecular weight distributions were broadened by the degradation.

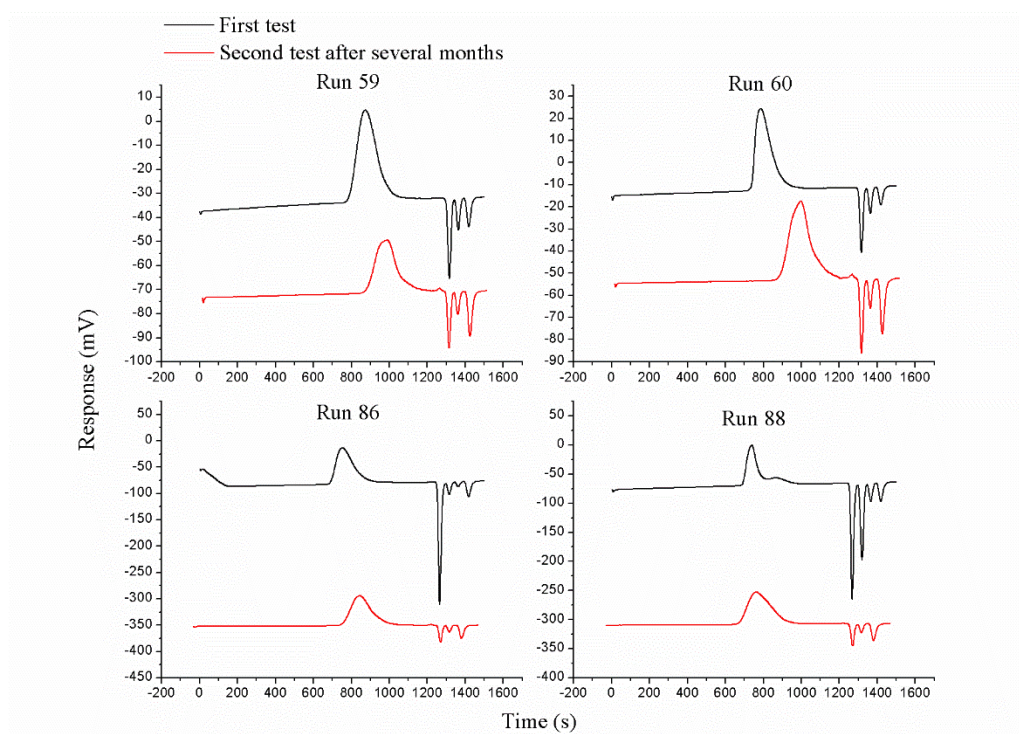


Figure 4-33. SEC comparison of DMK-based polyesters before and after degradation

All the T_g also declined in various degrees, as shown in Figure 4-34 and Table 4-7. Among all runs, T_g of Run 88 only decreased from 69°C to 66°C , which was logical because its \overline{M}_w still remained more than $10^5 \text{ g}\cdot\text{mol}^{-1}$. Furthermore, the crystallization ability of Run 86 and Run 88 was also negatively affected by the shortening of the molecular chains, associating with the pronounced falling of their ΔH_m .

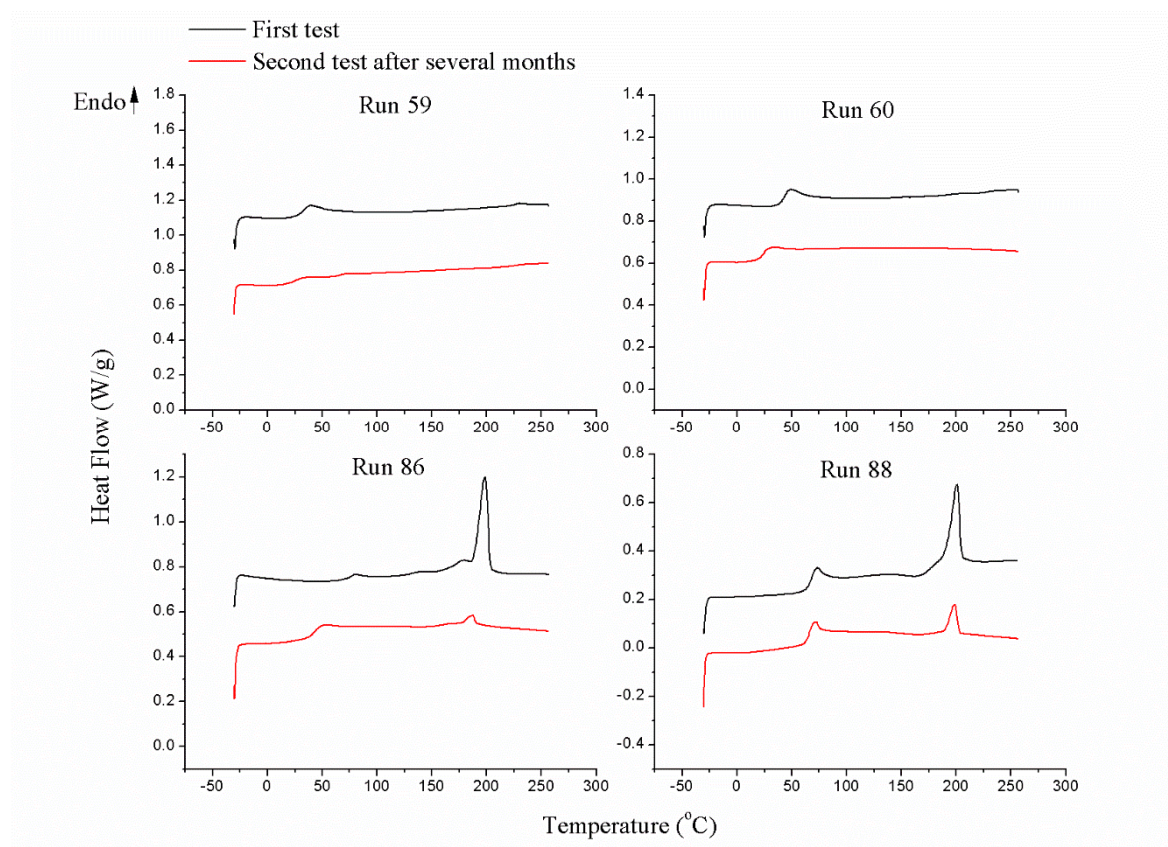


Figure 4-34. DSC comparison of DMK-based polyesters before and after degradation

The TGA spectra between the original and after-degradation were compared in Figure 4-35 along with the exhaustive information in Table 4-7. It appeared that except Run 88, which remained a relatively high molecular weight polymer even degradation happened, other degraded products with shortened polymer chains lost their thermal stabilities in a considerable degree, to be specific, at a general falling range of 50~110°C for $T_d^{5\%}$.

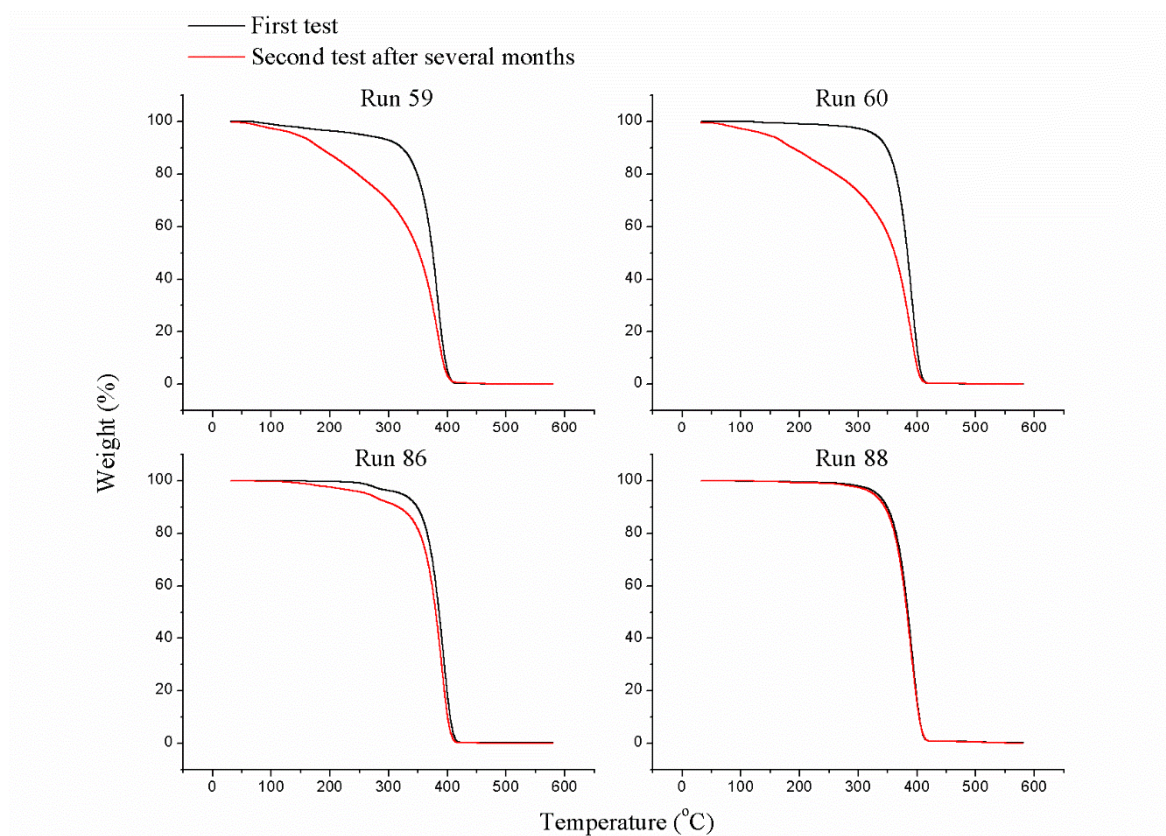


Figure 4-35. TGA comparison of DMK-based polyesters before and after degradation

Regarding that aliphatic polyesters are all more or less sensitive to hydrolytic degradation [87], a possible degradation mechanism could be hydrolysis. But we really have doubts since these polymers were only exposed to atmospheric moisture at ambient temperature. A much more likely explanation could be the presence of unstable acetal units in the chains, well known to be very heat sensitive [83], but in so small amounts they could not be detected by NMR. These two possible degradation reason were illustrated by Figure 4-36.

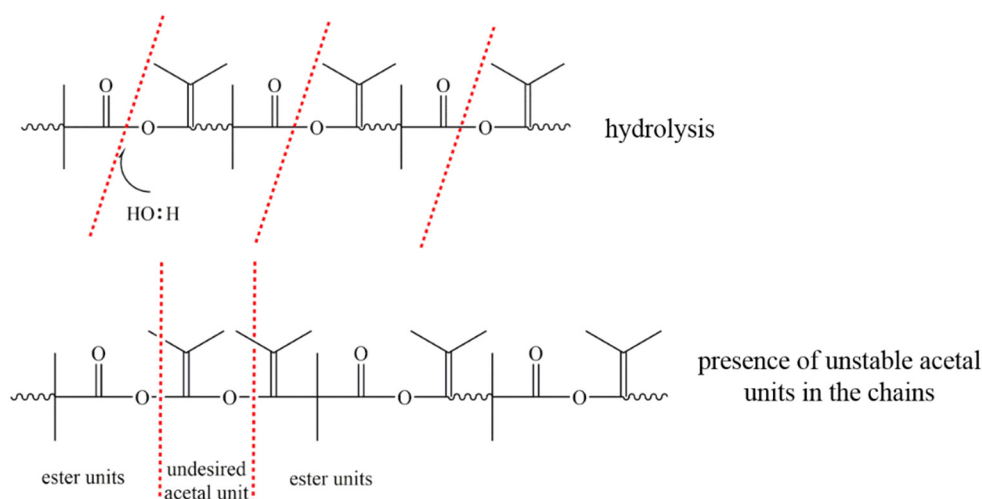


Figure 4-36. Possible reasons for the degradation

In a small conclusion, a structure-specific, crystalline and high molecular weight ($\overline{M}_n > 300\,000 \text{ g}\cdot\text{mol}^{-1}$) polyester possessing interesting thermal properties (T_g around 70°C , T_m around 200°C , $T_d^{5\%}$ more than 330°C) has been synthesized on the basis of dimethylketene in the application of the new metallocene initiators.

4.5 Conclusion

In this chapter, three special types of initiators (solid, photo, metallocene) compared to the conventional Lewis acids were tested in the cationic polymerization of various ketene monomers including methylethylketene (MEK), diethylketene (DEK), ethylphenylketene (EPK), diphenylketene (DPK) and the very special and active ketene monomer dimethylketene (DMK).

Both the Al^{3+} and proton exchanged montmorillonitic clay as the solid initiators and the diaryliodonium salt (IRGACURE 250), ferrocene salt (1,1'-bis(dimethylsilyl)ferrocene) and three-component photoinitiators comprising of camphorquinone (CQ) photosensitizer revealed without catalytic activity upon these ketene monomers in the conditions used. However, the sandwich-structured metallocene initiators deriving from the reaction of

bis(cyclopentadienyl)-dimethylzirconium (Cp_2ZrMe_2) with tris(penta-fluorophenyl)borane ($\text{B}(\text{C}_6\text{F}_5)_3$) behaved effective to both EPK and DMK monomers, although in the case of EPK only a polyester with low yield (less than 3% in weight yield), short polymer chains ($\overline{M}_n = 3\,500\text{ g}\cdot\text{mol}^{-1}$) and poor thermal stability ($T_d^{5\%} = 168^\circ\text{C}$) was obtained.

For DMK, the metallocene in contrast performed highly effective in a insertion polymerization mechanism, affording a type of crystallized, degradable and regularly ester-structured aliphatic polymer. The optimized conditions (diethyl ether as the solvent at -78°C) gave the DMK-based polyester possessing excellent properties ($\overline{M}_n \sim 300\,000\text{ g}\cdot\text{mol}^{-1}$, $T_g \sim 70^\circ\text{C}$, $T_m \sim 200^\circ\text{C}$, $T_d^{5\%} \sim 330^\circ\text{C}$), with a satisfying 68% yield. It is the first time that metallocene initiators, on the basis of an insertion chain growth mechanism, were successfully broadened to a non-olefin monomer.

4.6 References

- [1] M. Michelotti, A. Altomare, F. Ciardelli, E. Roland, Zeolite supported polymerization catalysts: Copolymerization of ethylene and α -olefins with metallocenes supported on HY zeolite, *Journal of Molecular Catalysis A: Chemical*, 129 (1998) 241-248.
- [2] V. Touchard, R. Spitz, C. Boisson, M.-F. Llauro, Highly Active Yttrium and Lanthanide Catalysts for Polymerization of Isobutene, *Macromolecular Rapid Communications*, 25 (2004) 1953-1957.
- [3] Y. Suga, Y. Uehara, Y. Maruyama, E. Isobe, Y. Ishihama, T. Sagae, Patent 5,928,982, 1999, *Chem. Abstr*, 1996, pp. 118289.
- [4] G.G. Hlatky, Heterogeneous Single-Site Catalysts for Olefin Polymerization, *Chemical Reviews*, 100 (2000) 1347-1376.
- [5] D.H. Lee, K.B. Yoon, W.S. Huh, Metallocene/MAO polymerization catalysts supported on cyclodextrin, *Macromolecular Symposia*, Wiley Online Library, 1995, pp. 185-193.
- [6] S. Aoshima, S. Kanaoka, A renaissance in living cationic polymerization, *Chemical Reviews*, 109 (2009) 5245-5287.
- [7] R. Meghabar, A. Megherbi, M. Belbachir, Maghnite-H⁺, an ecocatalyst for cationic polymerization of N-vinyl-2-pyrrolidone, *Polymer*, 44 (2003) 4097-4100.
- [8] A. Moulkheir, A. Harrane, M. Belbachir, Maghnite-H⁺, a solid catalyst for the cationic polymerization of α -methylstyrene, *Journal of applied polymer science*, 109 (2008) 1476-1479.
- [9] G. Nagendrappa, Organic synthesis using clay catalysts: Clays for "green chemistry", *Resonance*, 7 (2002) 64-67.
- [10] A. Jha, A. Garade, M. Shirai, C. Rode, Metal cation-exchanged montmorillonite clay as catalysts for hydroxyalkylation reaction, *Applied Clay Science*, 74 (2013) 141-146.
- [11] A. Blumstein, Polymerization of adsorbed monolayers. I. Preparation of the clay-polymer complex, *Journal of Polymer Science Part A: General Papers*, 3 (1965) 2653-2664.
- [12] F. Uddin, Clays, nanoclays, and montmorillonite minerals, *Metallurgical and Materials Transactions A*, 39 (2008) 2804-2814.
- [13] P.F. Luckham, S. Rossi, The colloidal and rheological properties of bentonite suspensions, *Advances in colloid and interface science*, 82 (1999) 43-92.
- [14] T. Cseri, S. Békássy, F. Figueras, E. Cseke, L.-C. de Menorval, R. Dutartre, Characterization of clay-based K catalysts and their application in Friedel-Crafts alkylation of aromatics, *Applied Catalysis A: General*, 132 (1995) 141-155.
- [15] M. Kawai, M. Qnaka, Y. Izumi, Solid acid-catalyzed allylation of acetals and carbonyl compounds with allylic silanes, *Chemistry Letters*, 15 (1986) 381-384.
- [16] J. Adams, D. Clement, S. Graham, Reactions of alcohols with alkenes over an aluminum-exchanged montmorillonite, *Clays and clay minerals*, 31 (1983) 129-136.
- [17] G. Nagendrappa, Organic synthesis using clay catalysts, *Resonance*, 7 (2002) 64-77.
- [18] J. Adams, D. Clement, S. Graham, Synthesis of methyl-t-butyl ether from methanol and isobutene using a clay catalyst, *Clays Clay Miner*, 30 (1982) 129-134.

- [19] N. Kaur, D. Kishore, Montmorillonite: An efficient, heterogeneous and green catalyst for organic synthesis, *J. Chem. Pharm. Res.*, 4 (2012) 991-1015.
- [20] S. Bennabi, N. Sahli, M. Belbachir, C.-H. Brachais, G. Boni, J.-P. Couvercelle, New approach for synthesis of poly (ethylglyoxylate) using Maghnite-H⁺, an Algerian proton exchanged montmorillonite clay, as an eco-catalyst, *Journal of Macromolecular Science, Part A*, 54 (2017) 843-852.
- [21] M. Belbachir, A. Bensaoula, Composition and method for catalysis using bentonites: U.S. Patent 6,274,527[P]. 2001-8-14.
- [22] F. Reguieg, N. Sahli, M. Belbachir, P.J. Lutz, One-step synthesis of bis-macromonomers of poly(1,3-dioxolane) catalyzed by Maghnite-H⁺, *Journal of Applied Polymer Science*, 99 (2006) 3147-3152.
- [23] K. Beloufa, N. Sahli, M. Belbachir, Synthesis of copolymer from 1,3,5-trioxane and 1,3-dioxolane catalyzed by Maghnite-H⁺, *Journal of Applied Polymer Science*, 115 (2010) 2820-2827.
- [24] S. Bennabi, M. Belbachir, In situ polymerization of the metal-organic framework 5 (MOF-5) by the use of maghnite-H⁺ as a green solid catalyst, *Adv. Mater. Lett.*, 6 (2015) 271-277.
- [25] Z. Draoua, A. Harrane, M. Belbachir, Amphiphilic Biodegradable Poly (ε-caprolactone)-Poly (ethylene glycol)-Poly (ε-caprolactone) Triblock Copolymer Synthesis by Maghnite-H⁺ as a Green Catalyst, *Journal of Macromolecular Science, Part A*, 52 (2015) 130-137.
- [26] F. Hennaoui, M. Belbachir, A Green One-pot Synthesis of PDMS Bis-Macromonomers Using an Ecologic Catalyst (Maghnite-H⁺), *Journal of Macromolecular Science, Part A*, 52 (2015) 992-1001.
- [27] R.S. Davidson, The chemistry of photoinitiators—some recent developments, *Journal of Photochemistry and Photobiology A: Chemistry*, 73 (1993) 81-96.
- [28] S. Jonsson, P.-E. Sundell, J. Hultgren, D. Sheng, C.E. Hoyle, Radiation chemistry aspects of polymerization and crosslinking. A review and future environmental trends in 'non-acrylate' chemistry, *Progress in organic coatings*, 27 (1996) 107-122.
- [29] V. Narayanan, A.B. Scranton, Photopolymerization of composites, *Trends in Polymer Science*, 12 (1997) 415-419.
- [30] J.-P. Fouassier, Photoinitiation, photopolymerization, and photocuring: fundamentals and applications, Hanser 1995.
- [31] J.V. Crivello, The discovery and development of onium salt cationic photoinitiators, *Journal of Polymer Science Part A: Polymer Chemistry*, 37 (1999) 4241-4254.
- [32] J. Fouassier, Photochemical reactivity of UV radical photoinitiators of polymerization: A general discussion, *Recent research developments in photochemistry and photobiology*, (2000) 51-74.
- [33] H. Gruber, Photoinitiators for free radical polymerization, *Progress in polymer Science*, 17 (1992) 953-1044.
- [34] J.D. Oxman, D.W. Jacobs, M.C. Trom, V. Sipani, B. Ficek, A.B. Scranton, Evaluation of initiator systems for controlled and sequentially curable free-radical/cationic hybrid photopolymerizations, *Journal of Polymer Science Part A: Polymer Chemistry*, 43 (2005) 1747-1756.

- [35] C.I. Vallo, S.V. Asmussen, Methacrylate and epoxy resins photocured by means of visible Light-Emitting Diodes (LEDs), *Photocured Materials*, (2014) 321.
- [36] Y. Yağci, I. Reetz, Externally stimulated initiator systems for cationic polymerization, *Progress in Polymer Science*, 23 (1998) 1485-1538.
- [37] Y. Yagci, S. Jockusch, N.J. Turro, Photoinitiated polymerization: advances, challenges, and opportunities, *Macromolecules*, 43 (2010) 6245-6260.
- [38] C. Decker, T. Nguyen Thi Viet, H. Pham Thi, Photoinitiated cationic polymerization of epoxides, *Polymer International*, 50 (2001) 986-997.
- [39] J.V. Crivello, J. Lam, Photoinitiated cationic polymerization with triarylsulfonium salts, *Journal of Polymer Science Part A: Polymer Chemistry*, 34 (1996) 3231-3253.
- [40] J.V. Crivello, J. Lam, Diaryliodonium salts. A new class of photoinitiators for cationic polymerization, *Macromolecules*, 10 (1977) 1307-1315.
- [41] E.A. Merritt, B. Olofsson, Diaryliodonium salts: a journey from obscurity to fame, *Angewandte Chemie International Edition*, 48 (2009) 9052-9070.
- [42] S. Seo, Y. Kim, J. You, B.D. Sarwade, P.P. Wadgaonkar, S.K. Menon, A.S. More, E. Kim, Electrochemical Fluorescence Switching from a Patternable Poly (1, 3, 4-oxadiazole) Thin Film, *Macromolecular rapid communications*, 32 (2011) 637-643.
- [43] A. Tarr, D. Wiles, Electronic absorption spectra and photodecomposition of some substituted ferrocenes, *Canadian Journal of Chemistry*, 46 (1968) 2725-2731.
- [44] J. Brand, W. Snedden, Electron-transfer spectra of ferrocene, *Transactions of the Faraday Society*, 53 (1957) 894-900.
- [45] O. Traverso, F. Scandola, Photooxidation of ferrocene in halocarbon solvents, *Inorganica Chimica Acta*, 4 (1970) 493-498.
- [46] K. Tsubakiyama, S. Fujisaki, Photosensitized initiation of vinyl polymerization by a system of ferrocene and carbon tetrachloride, *Journal of Polymer Science Part B: Polymer Letters*, 10 (1972) 341-344.
- [47] M. Thakurathi, E. Gurung, M.M. Cetin, V.D. Thalangamaarachchige, M.F. Mayer, C. Korzeniewski, E.L. Quitevis, The Stokes-Einstein equation and the diffusion of ferrocene in imidazolium-based ionic liquids studied by cyclic voltammetry: Effects of cation ion symmetry and alkyl chain length, *Electrochimica Acta*, 259 (2018) 245-252.
- [48] R. Bozak, Photochemistry in the Metallocenes, *Advances in photochemistry*, 8 (1971) 227-244.
- [49] J. Rabek, J. Lucki, M. Zuber, B. Qu, W. Shi, Photopolymerization of pyrrole initiated by the ferrocene-and iron-arene salts-chlorinated solvents complexes, *Journal of Macromolecular Science—Pure and Applied Chemistry*, 29 (1992) 297-310.
- [50] T. Wang, B.S. Li, L.X. Zhang, Carbazole-bound ferrocenium salt as an efficient cationic photoinitiator for epoxy polymerization, *Polymer international*, 54 (2005) 1251-1255.
- [51] B.M. Yavorskii, N.S. Kochetkova, G. Zaslavskaya, A.N. Nesmeyanov, Absorption spectrum of some ferrocene derivatives, *Doklady Akademii Nauk, Russian Academy of Sciences*, 1963, pp. 111-113.

- [52] A.N. Nesmeyanov, B.M. Yavorskii, G. Zaslavskaya, N.S. Kochetkova, Absorption spectra of some ferrocene derivatives, *Doklady Akademii Nauk, Russian Academy of Sciences*, 1965, pp. 837-840.
- [53] S. Tazuke, S. Okamura, Photo and thermal polymerization sensitized by donor-acceptor interaction. I. N-vinyl-carbazole-acrylonitrile and related systems, *Journal of Polymer Science Part A-1: Polymer Chemistry*, 6 (1968) 2907-2920.
- [54] B. Aydogan, B. Gacal, A. Yildirim, N. Yonet, Y. Yuksel, Y. Yagci, Wavelength Tunability In Photoinitiated Cationic Polymerization, (2006).
- [55] Y. He, M. Xiao, F. Wu, J. Nie, Photopolymerization kinetics of cycloaliphatic epoxide-acrylate hybrid monomer, *Polymer international*, 56 (2007) 1292-1297.
- [56] J. Crivello, J. Lam, Dye-sensitized photoinitiated cationic polymerization, *Journal of Polymer Science: Polymer Chemistry Edition*, 16 (1978) 2441-2451.
- [57] Y. Bi, D.C. Neckers, A visible light initiating system for free radical promoted cationic polymerization, *Macromolecules*, 27 (1994) 3683-3693.
- [58] J.V. Crivello, M. Sangermano, Visible and long-wavelength photoinitiated cationic polymerization, *Journal of polymer science part A: polymer chemistry*, 39 (2001) 343-356.
- [59] J.D. Oxman, D.W. Jacobs, Ternary photoinitiator system for curing of epoxy/polyol resin compositions: U.S. Patent 5,998,495[P]. 1999-12-7.
- [60] M.C. Palazzotto, A.F. Ubel III, J.D. Oxman, Z.M. Ali, Ternary photoinitiator system for addition polymerization, U.S. Patent 5,545,676[P]. 1996-8-13.
- [61] J.D. Oxman, D.W. Jacobs, Ternary photoinitiator system for curing of epoxy resins, U.S. Patent 6,025,406[P]. 2000-2-15.
- [62] J.D. Oxman, M.C. Trom, D.W. Jacobs, Compositions featuring cationically active and free radically active functional groups, and methods for polymerizing such compositions, U.S. Patent 6,187,836[P]. 2001-2-13.
- [63] E. Takahashi, F. Sanda, T. Endo, Photocationic and radical polymerizations of epoxides and acrylates by novel sulfonium salts, *Journal of Polymer Science Part A: Polymer Chemistry*, 41 (2003) 3816-3827.
- [64] M.L. Gómez, H.A. Montejano, M. del Valle Bohorquez, C.M. Previtali, Photopolymerization of acrylamide initiated by the three-component system safranine / triethanolamine / diphenyliodonium chloride: The effect of the aggregation of the salt, *Journal of Polymer Science Part A: Polymer Chemistry*, 42 (2004) 4916-4920.
- [65] J. Yang, D.C. Neckers, Cobaltic accelerator for the methylene blue photoinitiation system in aqueous acrylate solution, *Journal of Polymer Science Part A: Polymer Chemistry*, 42 (2004) 3836-3841.
- [66] G. Ullrich, D. Herzog, R. Liska, P. Burtscher, N. Moszner, Photoinitiators with functional groups. VII. Covalently bonded camphorquinone—amines, *Journal of Polymer Science Part A: Polymer Chemistry*, 42 (2004) 4948-4963.
- [67] J.V. Crivello, A new visible light sensitive photoinitiator system for the cationic polymerization of epoxides, *Journal of Polymer Science Part A: Polymer Chemistry*, 47 (2009) 866-875.

- [68] W.F. Schroeder, S.V. Asmussen, M. Sangermano, C.I. Vallo, Visible light polymerization of epoxy monomers using an iodonium salt with camphorquinone/ethyl-4-dimethyl aminobenzoate, *Polymer International*, 62 (2013) 1368-1376.
- [69] J.B. Soares, T.F. McKenna, *Polyolefin reaction engineering*, John Wiley & Sons 2013.
- [70] W. Kaminsky, Discovery of methylaluminoxane as cocatalyst for olefin polymerization, *Macromolecules*, 45 (2012) 3289-3297.
- [71] W. Kaminsky, J. Kopf, H. Sinn, H.J. Vollmer, Extrem verzerrte Bindungswinkel bei Organozirconium-Verbindungen, die gegen Ethylen aktiv sind, *Angewandte Chemie*, 88 (1976) 688-689.
- [72] E.Y.-X. Chen, T.J. Marks, Cocatalysts for metal-catalyzed olefin polymerization: activators, activation processes, and structure-activity relationships, *Chemical Reviews*, 100 (2000) 1391-1434.
- [73] X. Yang, C.L. Stern, T.J. Marks, Cationic Zirconocene Olefin Polymerization Catalysts Based on the Organo-Lewis Acid Tris(pentafluorophenyl)borane. A Synthetic, Structural, Solution Dynamic, and Polymerization Catalytic Study, *Journal of the American Chemical Society*, 116 (1994) 10015-10031.
- [74] M.C. Baier, M.A. Zuideveld, S. Mecking, Post-Metallocenes in the Industrial Production of Polyolefins, *Angewandte Chemie International Edition*, 53 (2014) 9722-9744.
- [75] Y. Fukui, M. Murata, K. Soga, Living polymerization of propylene and 1-hexene using bis - Cp type metallocene catalysts, *Macromolecular rapid communications*, 20 (1999) 637-640.
- [76] K.C. Jayaratne, L.R. Sita, Stereospecific living Ziegler-Natta polymerization of 1-hexene, *Journal of the American Chemical Society*, 122 (2000) 958-959.
- [77] W. Kaminsky, Highly active metallocene catalysts for olefin polymerization, *Journal of the Chemical Society, Dalton Transactions*, (1998) 1413-1418.
- [78] J.R. Severn, J.C. Chadwick, R. Duchateau, N. Friederichs, "Bound but Not Gagged" Immobilizing Single-Site α -Olefin Polymerization Catalysts, *Chemical reviews*, 105 (2005) 4073-4147.
- [79] J. Wang, Y. Masui, M. Onaka, Synthesis of α -Amino Nitriles from Carbonyl Compounds, Amines, and Trimethylsilyl Cyanide: Comparison between Catalyst-Free Conditions and the Presence of Tin Ion-Exchanged Montmorillonite, *European Journal of Organic Chemistry*, 2010 (2010) 1763-1771.
- [80] A. Sudo, S. Uchino, T. Endo, Development of a living anionic polymerization of ethylphenylketene: A novel approach to well-defined polyester synthesis, *Macromolecules*, 32 (1999) 1711-1713.
- [81] A. Sudo, S. Uchino, T. Endo, Living anionic polymerization of ethylphenylketene: A novel approach to well-defined polyester synthesis, *Journal of Polymer Science Part A: Polymer Chemistry*, 38 (2000) 1073-1082.
- [82] M. Brestaz, N. Desilles, G. Le, C. Bunel, Polyester obtained from dimethylketene and acetone: synthesis and characterization, *Journal of Polymer Research*, 19 (2012) 12.
- [83] H. Egret, J.-P. Couvercelle, J. Belleney, C. Bunel, Cationic polymerization of dimethyl ketene, *European polymer journal*, 38 (2002) 1953-1961.

[84] H. Egret, Synthèse et caractérisation des polymères du diméthylcétène. Application à la perméabilité aux gaz, Rouen, 1998.

[85] A. Bienvenu, Modification et perfectionnement du procédé de synthèse et de polymérisation du diméthylcétène. Caractérisation et propriétés des polydiméthylcétènes et de leurs mélanges, INSA de Rouen, 2004.

[86] T.G.F. Jr., P.J. Flory, Second-Order Transition Temperatures and Related Properties of Polystyrene. I. Influence of Molecular Weight, Journal of Applied Physics, 21 (1950) 581-591.

[87] M. Vert, Aliphatic polyesters: great degradable polymers that cannot do everything, Biomacromolecules, 6 (2005) 538-546.

General Conclusions

The objective of this study focused on the cationic homo- and co-polymerizations of various ketene monomers, using different more or less traditional initiators, and on post-polymerization modification reactions upon dimethylketene-based polyketone, in order to obtain high performance, easily synthesized and easy to process ketene-based materials.

In the first part, four different ketenes (methylethylketene (MEK), diethylketene (DEK), ethylphenylketene (EPK) and diphenylketene (DPK)) were involved in the trials of cationic homopolymerizations using classic Brønsted Acids, Lewis Acids or Friedel-Craft initiators at the temperature of $-78\sim 25^{\circ}\text{C}$ in various solvents. Except the polymerization of EPK initiated by $\text{CF}_3\text{SO}_3\text{H}$ which afforded polyesters of very small molecular weight ($\overline{M}_n = 1\,500\text{ g}\cdot\text{mol}^{-1}$, $T_g = 88^{\circ}\text{C}$, $T_m = 140^{\circ}\text{C}$ (first heating) and $T_d^{5\%} = 284^{\circ}\text{C}$), no polymer was formed by MEK, DEK and DPK. This unexpected result, which was quite different from DMK and its dominance to polyketone structure by cationic polymerization, indicated that DMK has a very special reactivity in the aspect of the polymer synthesis that could hardly be copied by other ketenes.

Since homopolymerization of these four ketenes did not succeed to give the desired polyketone structures, the copolymerization of DEK and DPK with DMK was taken into consideration. Although the reactivity ratio estimation respectively presents large distinctions for DMK / DEK ($r_1 = 11.55$, $r_2 = 0.05$) and DMK / DPK systems ($r_1 = 15.58$, $r_2 = 0.83$), two series of intercalated copolymers of ketone structures, containing a main DMK chain comprising small DEK or DPK isolated units, were successfully obtained. Despite the fact that the thermal properties were always lowered comparing to DMK-based polyketone (PDMK), an exception occurred to the most DEK-embedded DEK / DMK copolymer, which successfully broadened the processing window ($T_m = 164^{\circ}\text{C}$, $T_d^{5\%} = 259^{\circ}\text{C}$).

In the second part, the ketone group conversion reactions were tested on the 1,3-diketone structured PDMK. Three different modification pathways including the conversion reaction of polypyrazole from polyketone using $\text{N}_2\text{H}_4\cdot\text{H}_2\text{O}$, one-pot Beckmann rearrangement using $\text{CH}_3\text{SO}_3\text{H} / \text{Al}_2\text{O}_3 / \text{NH}_2\text{OH}\cdot\text{HCl}$ and dithioketal functionalized

reaction using 1,2-ethanedithiol / $\text{BF}_3 \cdot \text{Et}_2\text{O}$ / CF_3COOH , were applied to PDMK. However, all of these pathways failed to give new polymers, the reason of which can be addressed to the specific 1,3-diketone units stability. The only chance of chain revolution was offered by dithioketal functionalized reaction, which caused a chain-cut reaction to PDMK, potentially giving a \overline{M}_n around 2 500 $\text{g} \cdot \text{mol}^{-1}$ of worse thermal stability.

In the third part, three novel types of cationic initiators (solid, photo and metallocene) were for the first time tested upon ketene-based polymerizations in the seek of catalytic efficiency and selectivity. The Al^{3+} and proton exchanged montmorillonitic clay as the solid initiators behaved ineffective, under the conditions used, to three ketenes (DMK, DEK and DPK). For the five ketenes, the same conclusion was drawn for three photoinitiators including the diaryliodonium salt (IRGACURE 250), the ferrocene salt (1,1'-bis(dimethylsilyl)ferrocene) and the three-component photosystem comprising camphorquinone (CQ) as the photosensitizer.

Surprises came from the metallocene initiators, which derived from the reaction of bis(cyclopentadienyl)-dimethylzirconium (Cp_2ZrMe_2) with tris(penta-fluorophenyl)borane ($\text{B}(\text{C}_6\text{F}_5)_3$), and successfully initiated both EPK and DMK to form polyesters. In the case of EPK, a 3% yield and short polymer ($\overline{M}_n = 3\,500 \text{ g} \cdot \text{mol}^{-1}$) with poor thermal stability ($T_d^{5\%} = 168^\circ\text{C}$) presented no advantage over the anionic resulting ones from the literature. In the case of DMK, the optimized conditions ($[\text{Monomer}]_0 / [\text{Initiator}]_0 = 1\,000 / 1$, diethyl ether as the solvent at -78°C) afforded a type of crystallized, degradable and neat polyester, which could be potentially used in industry thanks to its excellent properties ($\overline{M}_n \sim 300\,000 \text{ g} \cdot \text{mol}^{-1}$, $T_g \sim 70^\circ\text{C}$, $T_m \sim 200^\circ\text{C}$, $T_d^{5\%} \sim 330^\circ\text{C}$) and a satisfying yield (68%).

The perspectives envisaged for this work are mainly focused on the outstanding results afforded by the metallocene on DMK polymerization. Indeed, other different metallocenes (for example Cp_2ZrCl_2 with the co-initiator MAO) could be very interesting if the same structured polymer could be obtained; the catalytic efficiency and polymer properties could also be further improved. Finally, a full degradation study devoted to the metallocene polyester would further improve the knowledge on these little known polymers.

Annexes

List of Annexes

Annex 1. Experimental section

Annex 2. Apparatus

Annex 3. NMR Spectra

Annex 4. IR Spectra

Annex 5. GC-MS Analysis

Annex 6. SEC Analysis

Annex 7. DSC Thermograms

Annex 8. Chemicals Used

Annex 9. List of GHS Hazard and Precautionary Statements

1. Experimental section

Synthesis of MEK:

Synthesis of MEK was carried out according to Figure 1.

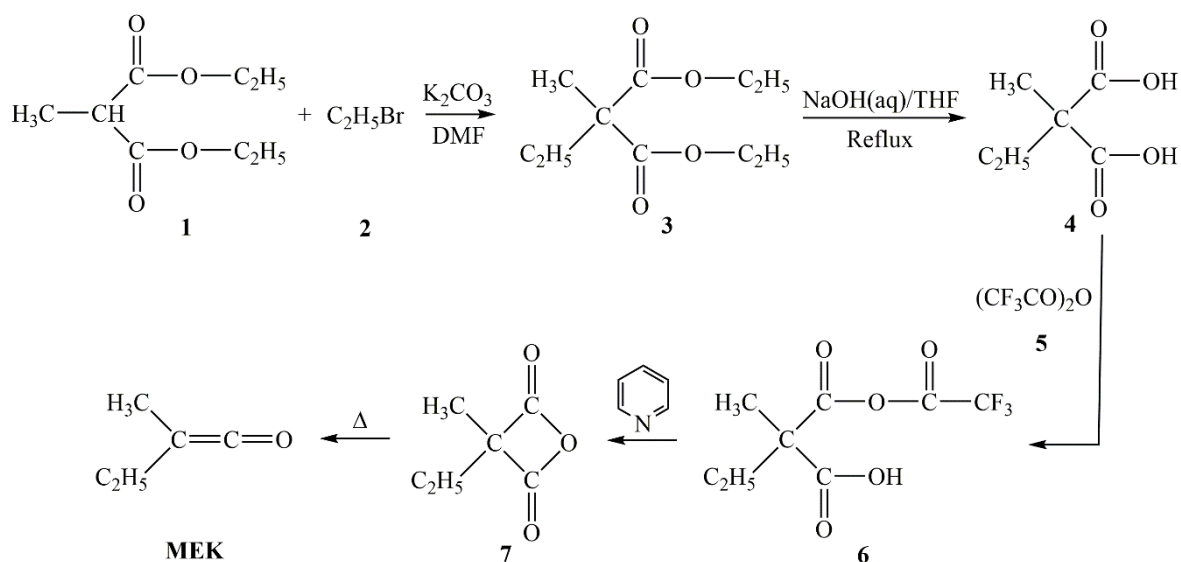


Figure 1. Synthesis route of MEK

To a stirring solution of 40.0 g (0.23 mol) diethyl 2-methylmalonate **1** and 50.2 g (0.46 mol) bromomethane **2** in 200 mL anhydrous dimethylformide (DMF), 79.5 g (0.58 mol) potassium carbonate was added. The reaction was carried out at ambient temperature for 16 hours, and the resulting mixture was a white solution. Another 50.2 g bromomethane was then added into the mixture before the reaction proceeded for additional 3 days at ambient temperature. After that, the temperature was raised to 50°C to complete the first step reaction.

The obtained mixture was filtered and the filter cake was washed with 200 mL methylene chloride (CH_2Cl_2). The filtrate was further diluted with 500 mL CH_2Cl_2 and the combination was washed with three portions of 500 mL each of water. The organic layer was dried with MgSO_4 and filtered. A residual oil was obtained after the filtrate was concentrated under reduced pressure. This oil was distilled under 10 mbar and 125°C to give 41.5 g diethyl 2-ethyl-2-methylmalonate **3** (boiling point: 109~112°C / 25 mmHg). If the

product was still combined with DMF, saturated sodium chloride solution can be used to wash it several times before the above purification procedures were repeated.

As the second step, a solution of 76.0 g (1.90 mol) sodium hydroxide in 70 mL water was dropwisely added into a stirring solution of 38.5 g (0.19 mol) diethyl 2-ethyl-2-methylmalonate **3** in 175 mL tetrahydrofuran (THF). The temperature of the reaction mixture was well controlled between 27~31°C at the same time. Upon completion of addition, the mixture was heated under reflux for 16 hours.

After refluxing, the mixture was diluted with 500 mL water and washed with 200 mL diethyl ether to wash THF off. The obtained aqueous layer was cooled in an ice bath and acidified with concentrated hydrochloric acid to a pH of 1~2. The mixture was then saturated with sodium chloride and extracted with six portions of 150 mL each of CH₂Cl₂. The extracts were further combined, dried with magnesium sulfate (MgSO₄) and filtered. The filtrate was concentrated under reduced pressure to give the light yellow solid (melting point: 119~123°C).

Then, to improve the yield, additional sodium chloride was added to the original aqueous layer and the mixture extracted with ten portions of 150 mL diethyl ether. The combined extracts were dried with MgSO₄, filtered and concentrated under reduced pressure to give the light yellow solid (Figure 2).

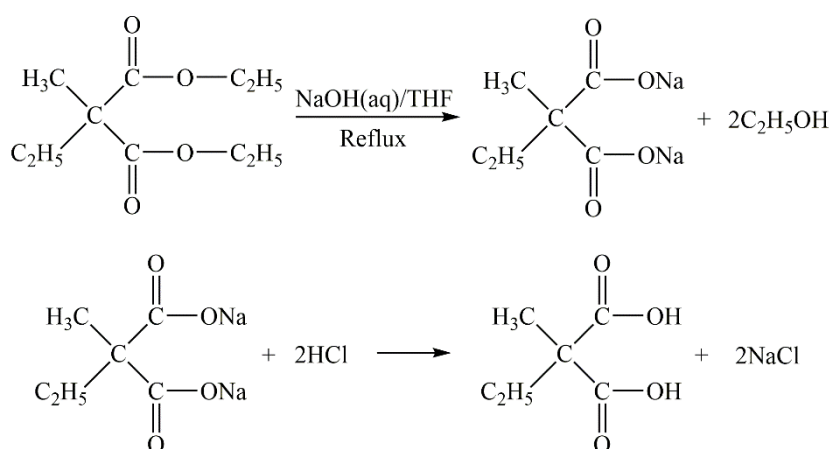


Figure 2. Synthesis of methylethyl malonic acid

The solids were combined giving about 20 g (yield 70%) of methylethyl malonic acid **4**, as evidenced by ^1H -NMR ($\delta = 12.6$ (H_{COOH}), 1.7 (H_1), 1.2 (H_2), 0.8 (H_3) ppm in d^6 -DMSO, see Figure 3).

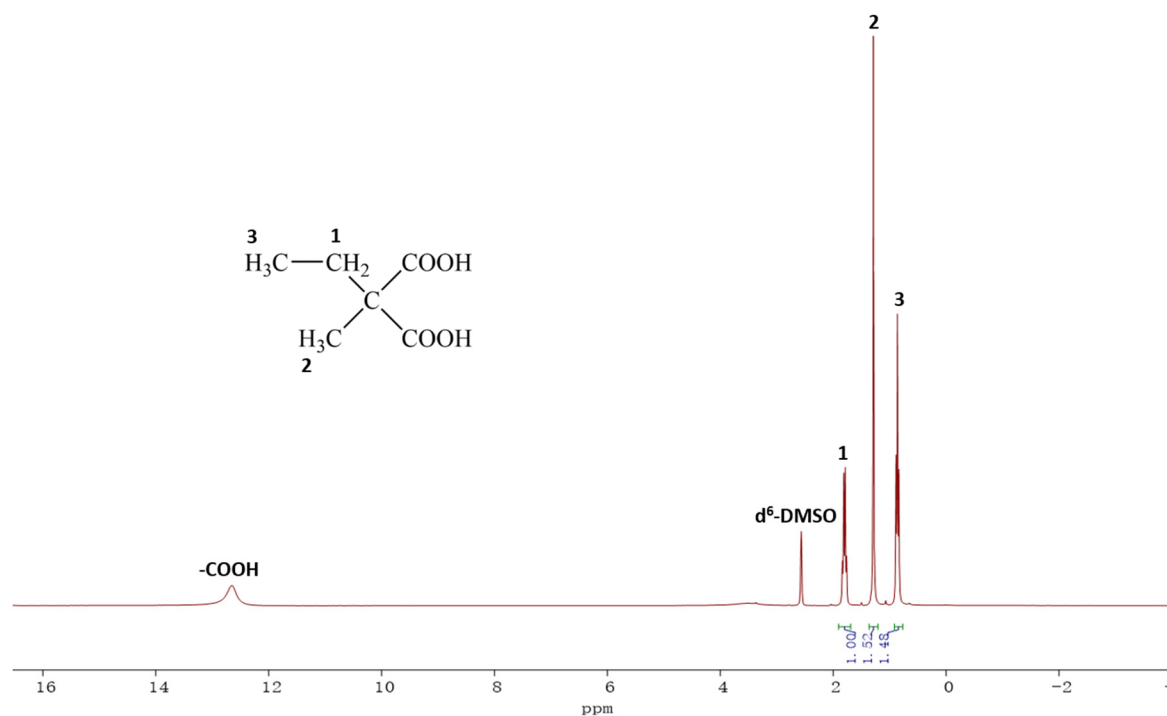


Figure 3. ^1H NMR spectrum (300 Mhz, 20°C, d^6 -DMSO) of the synthesized methylethyl malonic acid

Furthermore, 6.9 mL trifluoroacetic anhydride **5** (0.048 mol) was added dropwise to a solution of 7.5 g methylethyl malonic acid **4** (0.051 mol) in 51 mL hexane at room temperature. The mixture (2-methyl-2-((2,2,2-trifluoroacetoxy)carbonyl)butanoic acid **6** solution) was stirred for 10 min, then was diluted to 250 mL with diethyl ether, to which was added 7.9 mL pyridine (0.098 mol) under stirring at room temperature. After the reaction was settled for 1h, the precipitated pyridinium salt was filtered off quickly. Evaporation of the filtrate gave methylethyl malonic anhydride **7** as a pale-orange viscous liquid. The resulting anhydride was heated under reduced pressure (80 mbar) at 120°C for 20 min, and led to 0.91 g of MEK (yield 32%) as a yellow liquid.

Considering that the stability and potential danger of MEK have not been clearly mentioned in the literature, this freshly synthesized monomer was carefully handled and stored at 4°C under oxygen-free atmosphere, and used as soon as possible.

Synthesis of DEK:

Synthesis of DEK was carried out according to Figure 4.

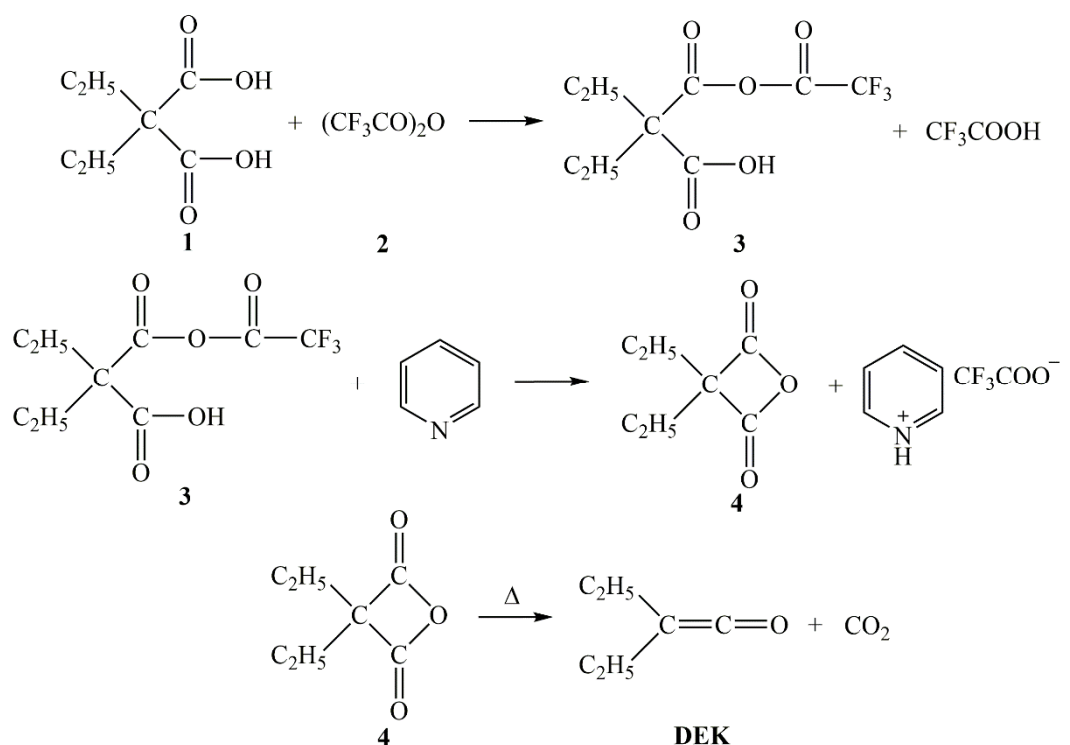


Figure 4. Synthesis and pyrolysis of diethyl malonic anhydride

With stirring at room temperature, 12.6 mL trifluoroacetic anhydride **2** (0.089 mol) was added dropwise to a solution of 15.0 g diethylmalonic acid **1** (0.094 mol) in 100 mL anhydrous *n*-hexane. After 10 min, the mixture (2-ethyl-2-((2,2,2-trifluoroacetoxy)carbonyl)butanoic acid **3** solution) was diluted to 480 mL with *n*-hexane. Furthermore, 14.4 mL pyridine (0.178 mol) was directly added and the reaction remained another 1 h at room temperature. Immediately following filtration of the precipitated pyridinium salt, diethylmalonic anhydride **4** as a pale-orange viscous liquid was then concentrated by

evaporation of the filtrate. The thermal decomposition and distillation of diethylmalonic anhydride **4** by a two-step heating procedure (120°C for 10 min and 170°C for 20 min), finally afforded 2.2 g DEK (yield 25%).

The freshly distilled DEK monomer was stored in sealed bottles at 4°C under Alphagaz™ 2 nitrogen flow, and was used as soon as possible.

Synthesis of EPK:

Synthesis of DEK was carried out according to Figure 4.

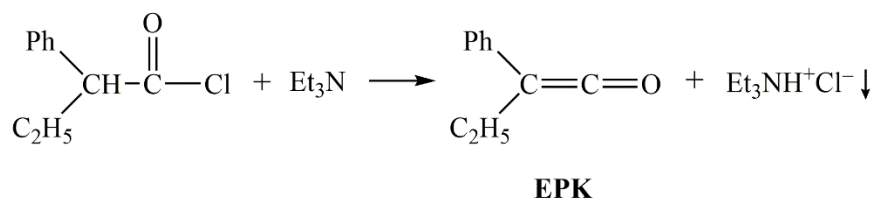


Figure 5. Synthesis of EPK by dehydrochlorination reaction

A two-neck round bottom flask under an inert gas atmosphere was charged with 3.00 g of 2-phenylbutanoyl chloride (16.4 mmol, 1.0 equiv) in 45 mL of anhydrous diethyl ether and cooled to 0°C. Dropwise addition over 30 min of 2.52 mL triethylamine (18.1 mmol, 1.1 equiv) formed a bright yellow solution and a white precipitate that was stirred overnight at 0°C. The solution was then warmed to room temperature after which the further filtration and concentration gave a bright yellow oil. The filtrated solution was transferred to flame dried Kugelrohr flask and 110~120°C distillation under 5 mbar pressure gave 0.5 g of a light yellow oil (yield 22%), which was supposed to be EPK.

The prepared EPK remained to be stable for up to two months in the freezer under an argon atmosphere.

Synthesis of DPK:

Synthesis of DPK was carried out according to Figure 5.

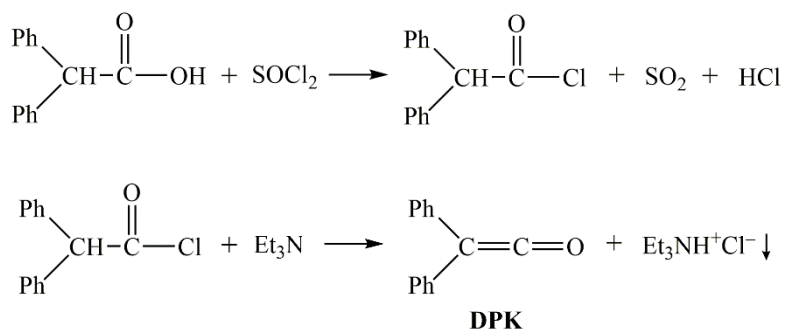


Figure 6. Synthesis of DPK by dehydrochlorination reaction

A 500 mL three-necked flask equipped with a dropping funnel and a reflux condenser carrying a calcium chloride drying tube was charged with 30 g diphenylacetic acid (0.142 mol) and 90 mL toluene. The mixture was then heated to 80°C, to which 78.6 g thionyl chloride (0.67 mol) was added dropwise over 30 min. The reaction continued for additional 7 h before the toluene and excess thionyl chloride was removed by rotary evaporation. 3 times 50 mL toluene were added and evaporated repetitively to ensure removal of thionyl chloride and HCl. The resulting purple residue was recrystallized by *n*-hexane and activated charcoal to afford 22.1 g diphenylacid chloride (yield 68%).

4.075 g diphenylacid chloride (19.9 mmol) in 35 mL diethyl ether was cooled by an ice bath to 0°C. 2.77 mL of freshly distilled triethylamine (19.9 mmol) was then added dropwise to the mixture over 30 min. The reaction was settled overnight at 0°C after completion of addition. The reaction mixture was then warmed to room temperature, followed by filtration of the salts. The filtrate was concentrated by evaporation and the residue was distilled via Kugelrohr distillation to afford 1.0 g DPK as an orange oil (yield 26%).

The DPK monomer was stored in sealed bottles in the fridge (at 4°C) under Alphagaz™ 2 nitrogen flow before use.

2. Apparatus

Differential Scanning Calorimetry (DSC):

The device used is a TA Instruments DSC Q2000 (Figure 1). The diagram of the system is given in Figure 2. The principle of measurement of the DSC heat flux is based on the measurement of the difference of the heat flows exchanged between the sample, the reference, and the outside.



Figure 1. DSC Q2000

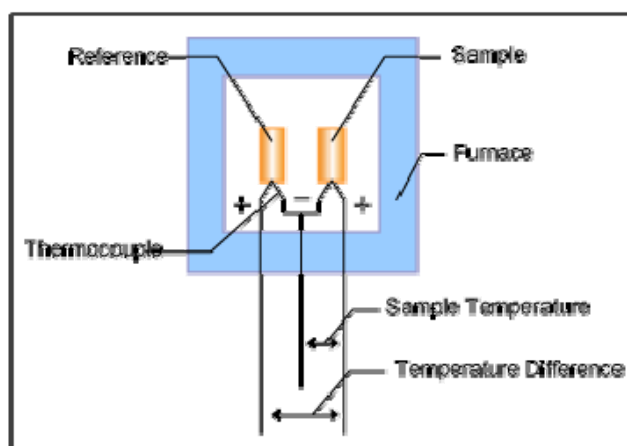


Figure 2. Principle of DSC devices

When the furnace undergoes a linear ramp upward or downward in temperature, the sample temperature and reference temperature are measured by means of thermocouples

fixed below the trays supporting the cups in reference with the temperature of the oven which is measured by means of a thermocouple placed between the two cups. Heat flows between the furnace and respectively the reference and the sample are thus calculated. The output signal is obtained by the difference of the heat flows between the furnace and the reference calculated from the temperature difference.

The cooling of the block is ensured by a system allowing to fall to -80°C . The temperature and energy calibration was carried out with indium ($\Delta T_m = 156.6^{\circ}\text{C}$ and $\Delta H_m = 28.45 \text{ J}\cdot\text{g}^{-1}$).

Analysis conditions:

All the analyzes were carried out under nitrogen ($50 \text{ mL}\cdot\text{min}^{-1}$) with test portions ranging from 6 to 15 mg. The temperature programs used are:

- For polyesters of DMK using metallocenes:

- from -30°C to 260°C at $10^{\circ}\text{C} / \text{min}$;
- from 260°C to -30°C at $0.5^{\circ}\text{C} / \text{min}$;
- from -30°C to 260°C at $10^{\circ}\text{C} / \text{min}$;

- For others:

- from -30°C (or 0, 30°C) to 260°C (or a temperature before degradation) at $10^{\circ}\text{C} / \text{min}$;
- from 260°C to -30°C at $10^{\circ}\text{C} / \text{min}$;
- from -30°C to 260°C at $10^{\circ}\text{C} / \text{min}$;

Thermogravimetric Analysis (TGA):

A TA Instrument Q500 was used (Figure 3). It consists of two main elements: a very sensitive microbalance coupled to a temperature controlled oven.

The microbalance is capable of detecting a variation of 0.1 μg for a maximum capacity of 1.3 g. The sample is placed in a platinum cup and the the plate is maintained in equilibrium via a current proportional to the mass supported.

The temperature is regulated between 30°C and 1000°C with a maximum temperature rising rate of 200°C / min. A thermocouple near the sample monitors the temperature and regulates the heating power.

Calibration was performed with nickel of which the Curie point is 358°C.



Figure 3. TGA Q500

Analysis conditions:

All the analyzes were carried out between 30 and 600°C with a heating rate of 10°C / min, under nitrogen (50 mL / min), with test samples ranging from 5 to 15 mg.

Fourier Transform Infrared (FTIR):

The FTIR spectra were recorded using a Perkin Elmer Spectrum 2000 Fourier Transform Spectrometer (Figure 4) equipped with an ATR (Attenuated Total Reflection) monoreflexion system (MKII type, Specac). Products are placed on a platen with a 2 mm square diamond cell. An adjustable screw keeps the powder against the measuring cell. A blank measurement of the air is performed before each analysis. A dozen scans are performed from 4000 to 650 cm^{-1} for each FTIR spectrum.



Figure 4. Perkin Elmer Spectrum 2000

Size Exclusion Chromatography (SEC):

The steric exclusion chromatography (SEC) analyzes were carried out on a Varian PL-GPC 50 equipped with two PLgel MIXED-C 5 μm (300 \times 7.5 mm) columns, and a Refractive Index detector (Figure 5). The mobile phase used is the CH_2Cl_2 previously filtered, and the temperature was set to 27.5°C. Calibration was established with PMMA standards. Before being injected, the samples are filtered on 0.45 μm pre-filters. The solvent flow rate is 1 mL / min.



Figure 5. Varian PL-GPC 50

Gas Chromatography Mass Spectrometry (GC-MS):

The analyzes are carried out on a Varian 3900 chromatograph, equipped with an on-column injector, a capillary column (HP-5 (5% phenyl) of 30 m, internal diameter 0.25 mm and film thickness 0.25 μm) coupled to a Saturn 2000 ion trap mass spectrometer ($T = 150^\circ\text{C}$, transfer line = 250°C , manifold = 50°C).

Product identification was performed by comparing mass spectra with the NIST02 National Institute of Science and Technology (NIST) spectra library.

Analysis conditions:

- T injector: 250°C in splitless mode;
- Injection volume: 1 μL ;
- Helium flow rate: 1 mL / min;
- Programming in temperature: 130°C during 2 min then rise at $6^\circ\text{C} / \text{min}$ up to 250°C , further then rise at $25^\circ\text{C} / \text{min}$ up to 300°C , isothermal for 10 min;

Nuclear Magnetic Resonance (NMR):

The proton and carbon NMR spectra were recorded using a Bruker 300 MHz spectrometer (Figure 6). The chemical shifts (δ) are indicated in ppm with respect to the deuterated solvents and the singlet of the TMS used in the samples for internal commercial reference ($\delta = 0$).

The polyketone samples are prepared in deuterated dichloromethane, to which a very small amount of HFIP is added in order to allow the solubilization of the polymer. Other samples are prepared in classical deuterated solvents (d_6 -DMSO, CDCl_3 , CD_2Cl_2 , etc).



Figure 6. Bruker 300 MHz

Multi-Angle Light Scattering (MALS):

The Multi-Angle static Light Scattering (MALS) was measured on a Wyatt Dawn Heleos 8 (Figure 7) combined with a Shimadzu RID-20A differential refractive index detector (Figure 8).

Analysis conditions:

- The solvent used is dichloromethane, at a temperature of 30°C;
- The concentration of mother solution of the polyester is 5 g·L⁻¹ (for lower molecular weights polymers like Run 59, it was 10 g·L⁻¹).

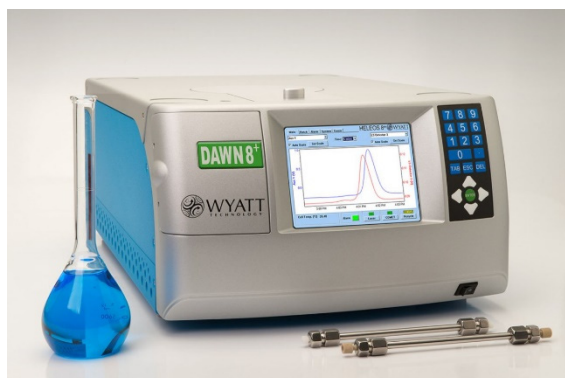


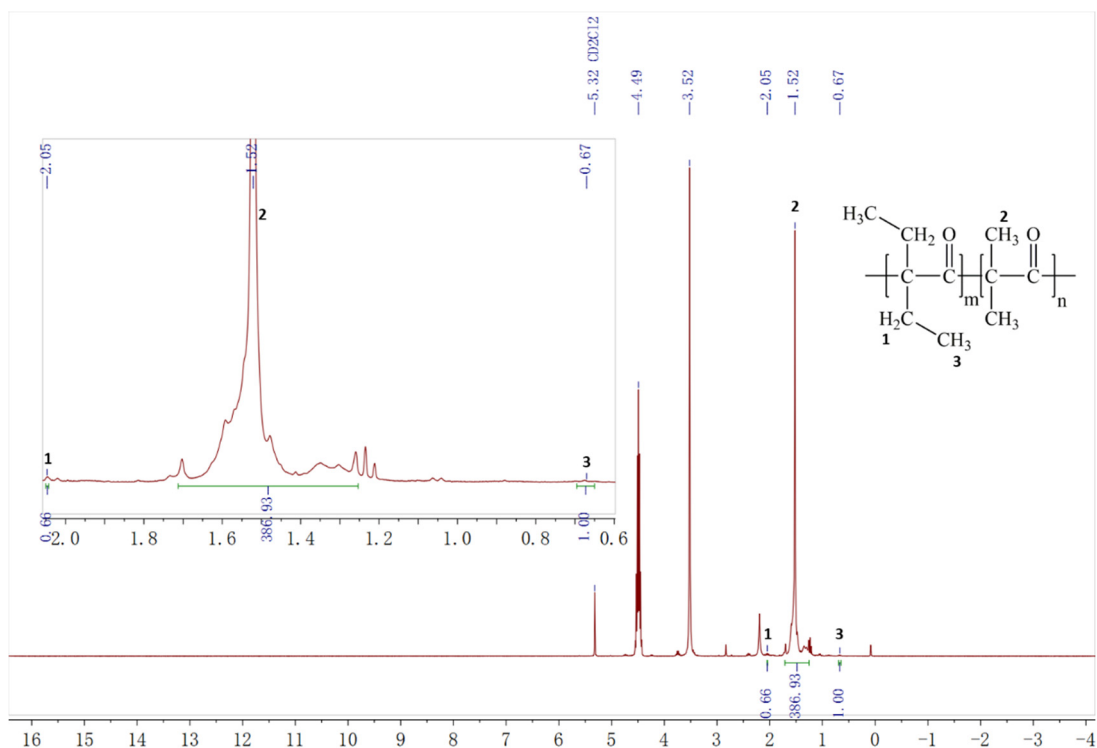
Figure 7. Wyatt Dawn Heleos 8 Multi-Angle static Light Scattering



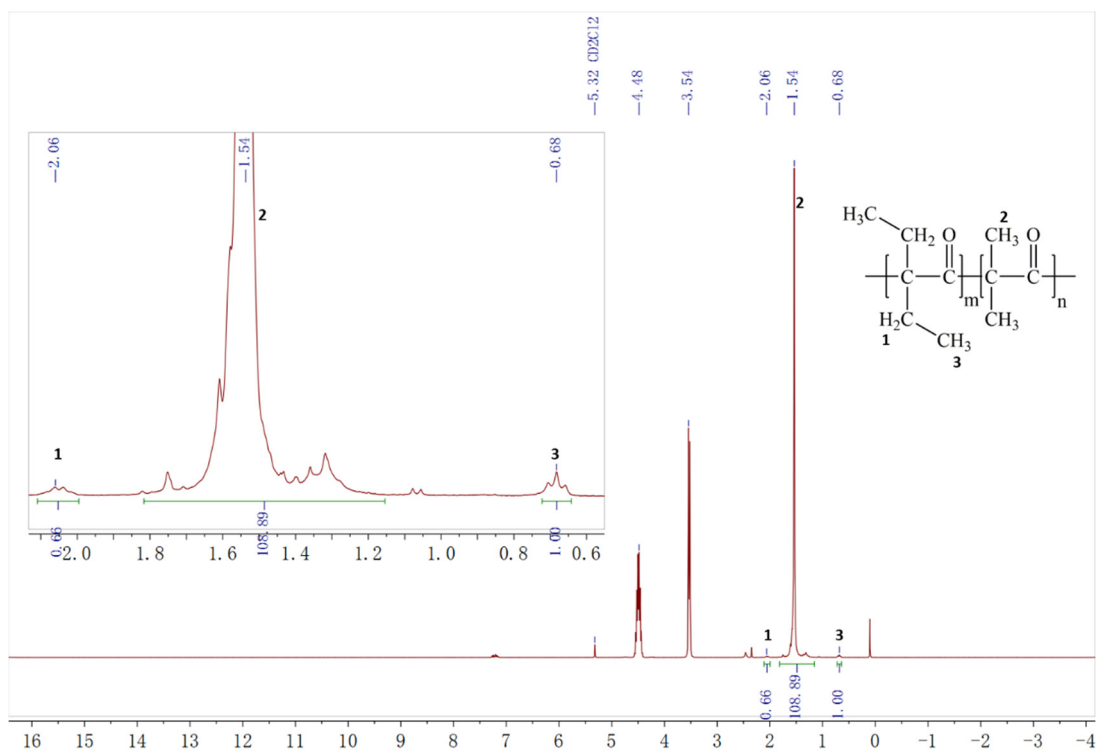
Figure 8. Shimadzu RID-20A differential refractive index detector

3. NMR Spectra

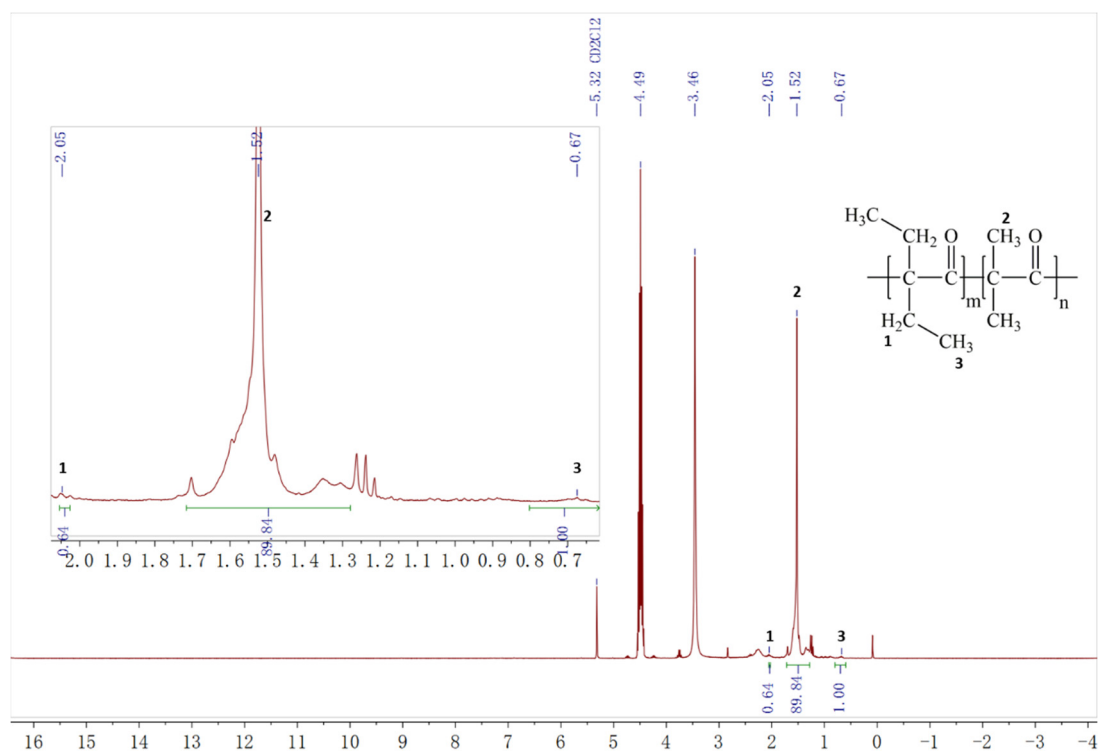
2.3.2 Copolymerization of DEK / DMK



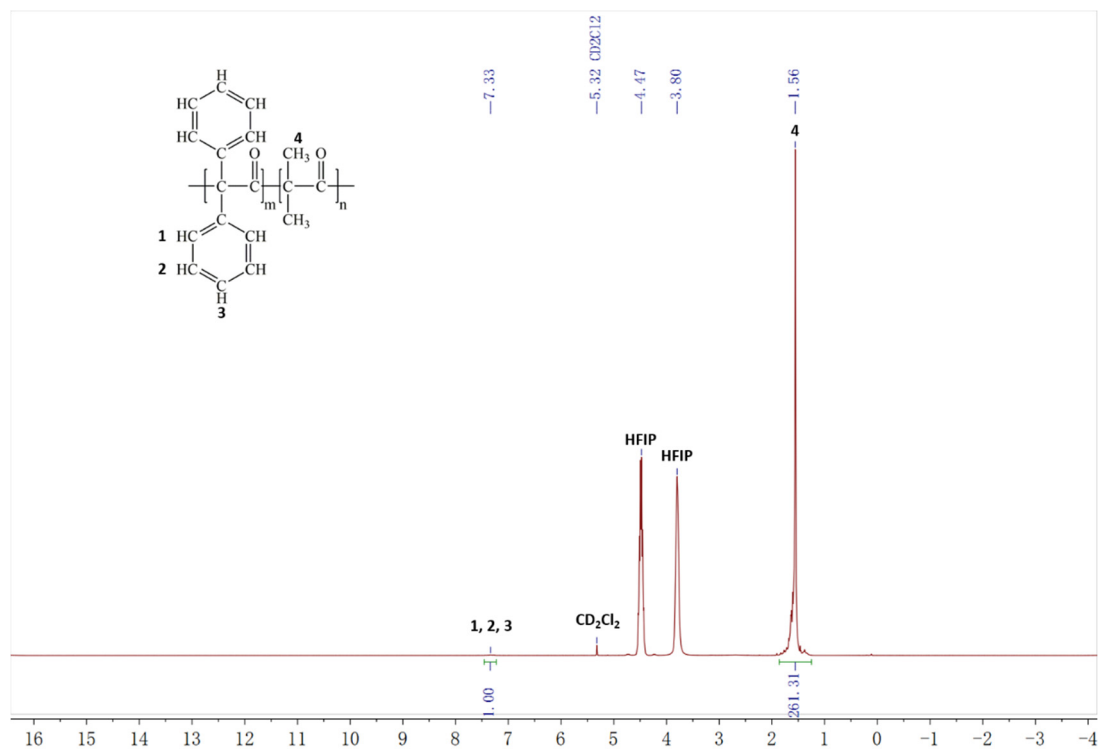
Run 107 ^1H NMR (CD_2Cl_2 $\delta = 5.32$ ppm, HFIP $\delta = 4.49, 3.52$ ppm)

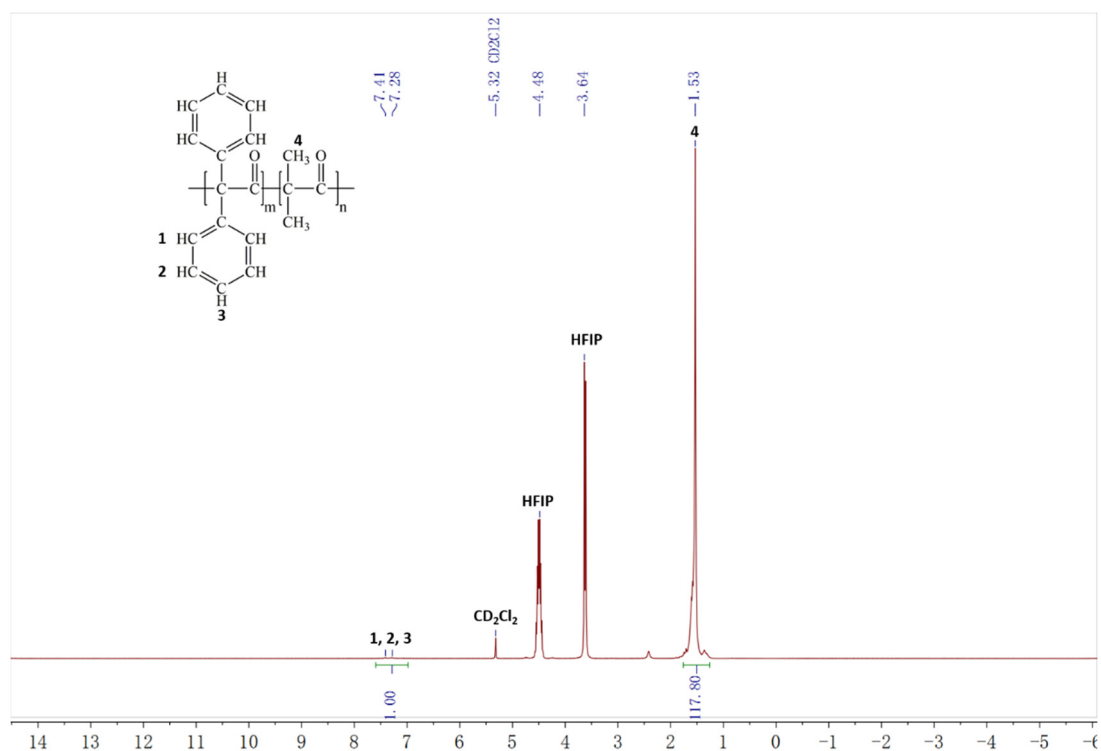
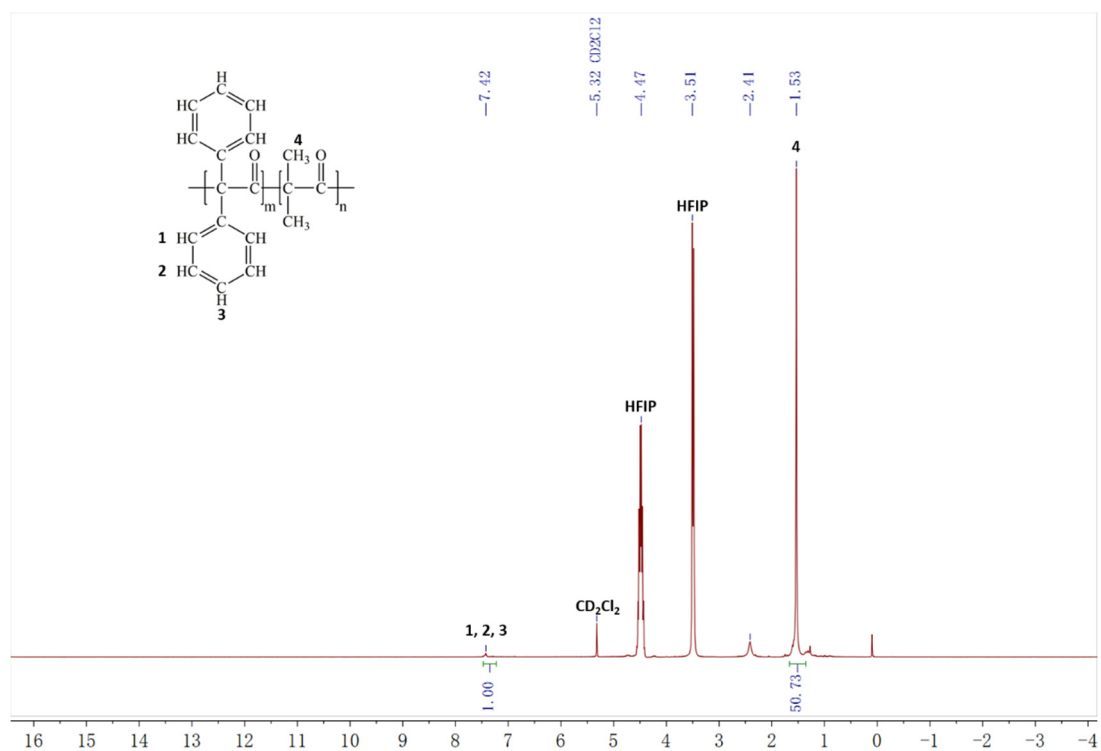


Run 75 ^1H NMR (CD_2Cl_2 $\delta = 5.32$ ppm, HFIP $\delta = 4.48, 3.54$ ppm)

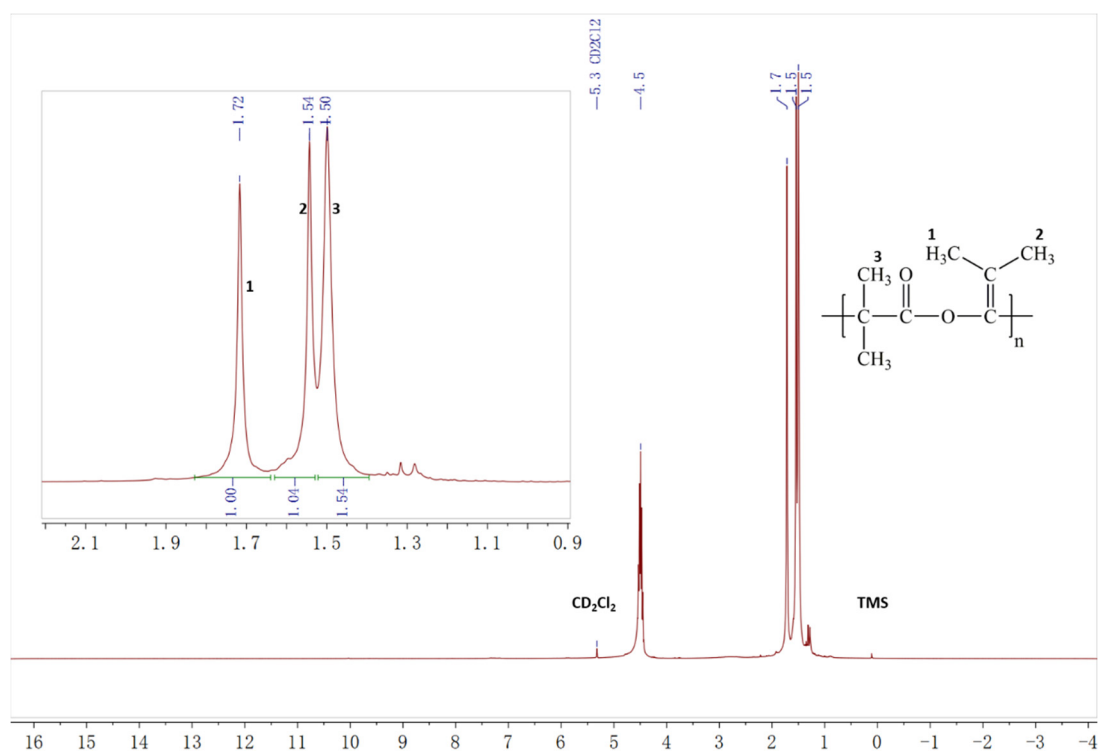
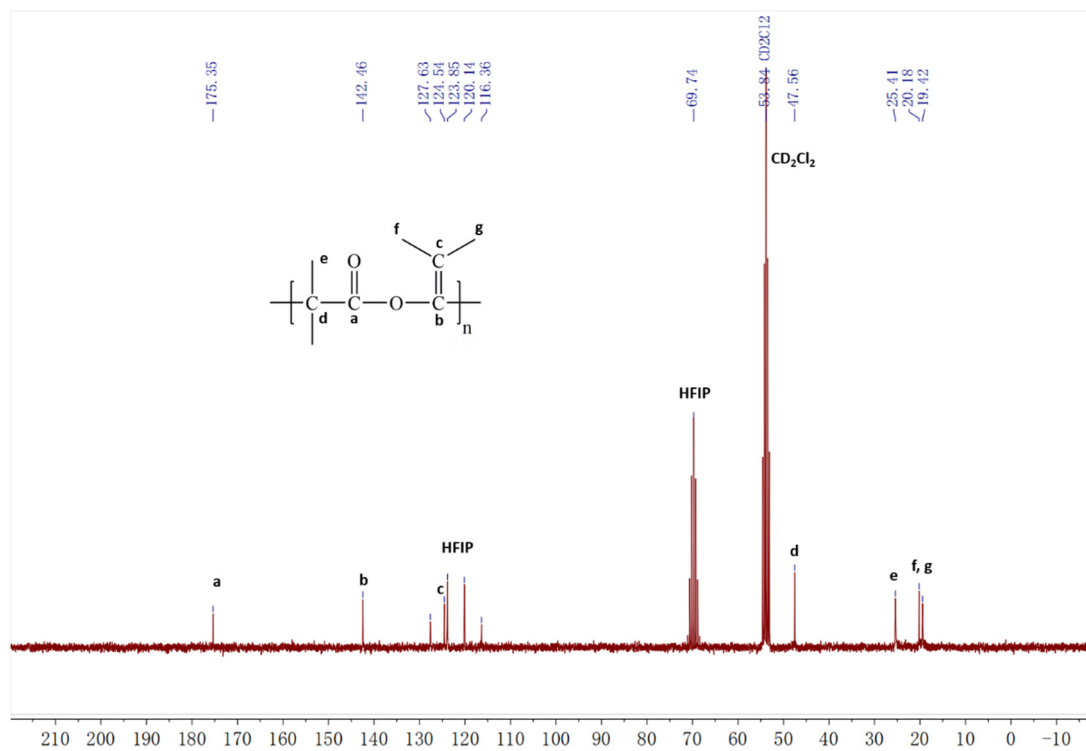
Run 106 ¹H NMR (CD₂Cl₂ δ = 5.32 ppm, HFIP δ = 4.49, 3.46 ppm)

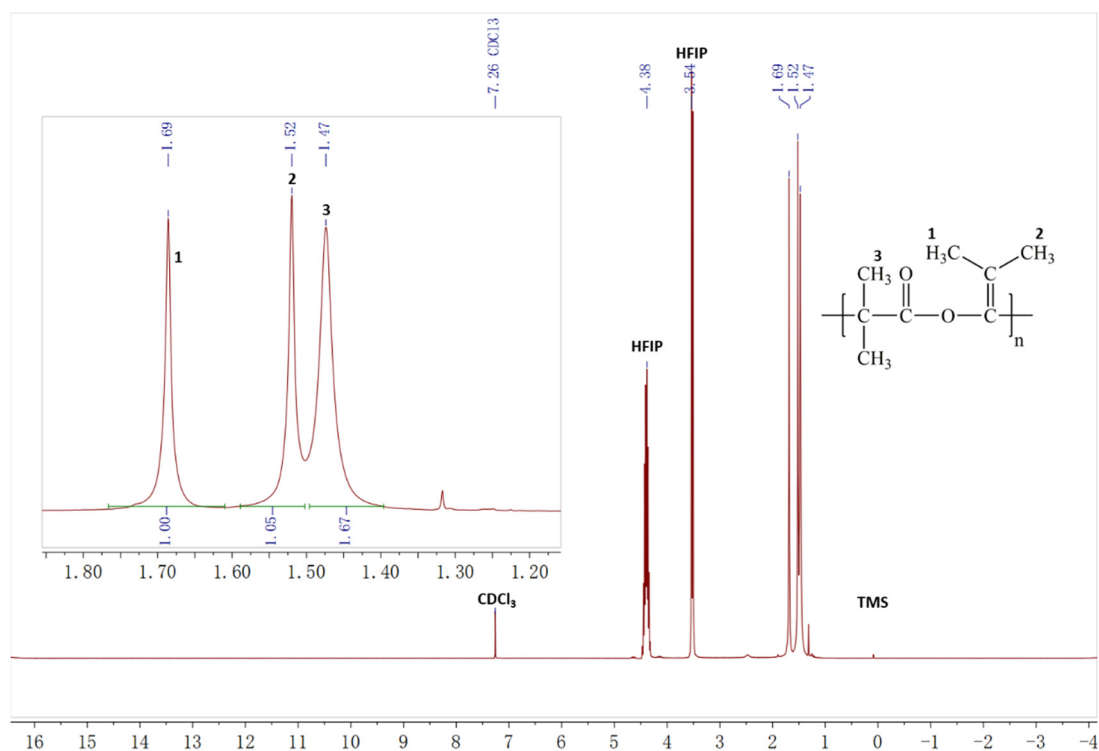
2.3.3 Copolymerization of DPK / DMK

Run 69 ¹H NMR (CD₂Cl₂ δ = 5.32 ppm, HFIP δ = 4.47, 3.80 ppm)

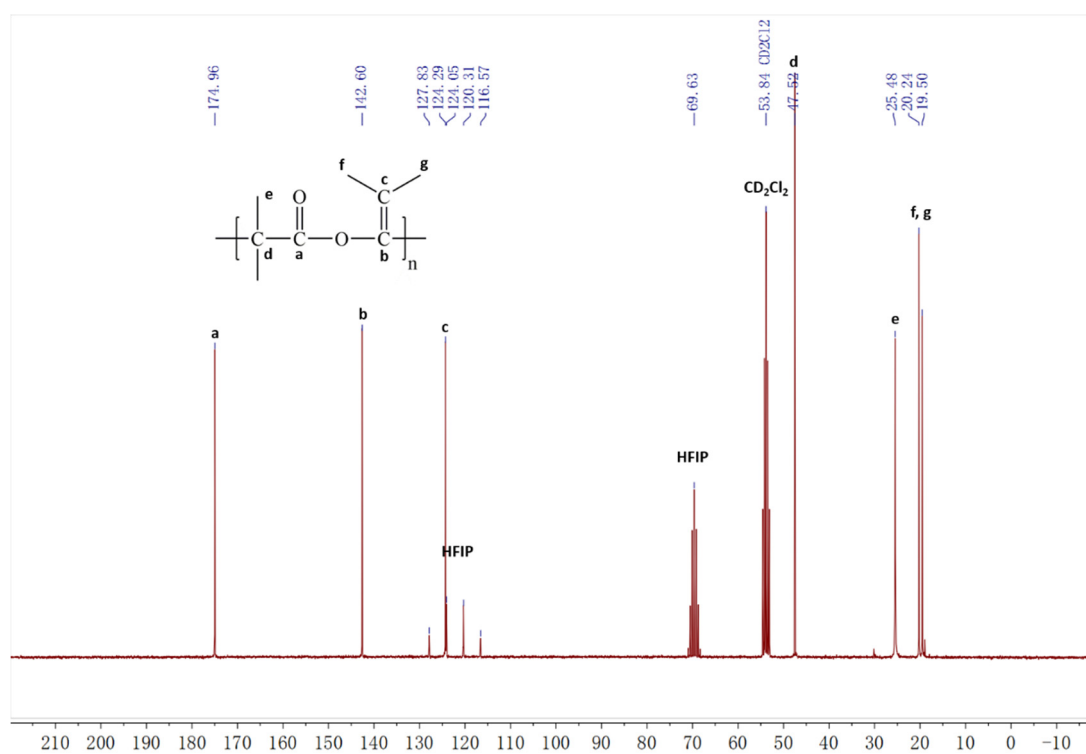
Run 93 ¹H NMR (CD₂Cl₂ $\delta = 5.32$ ppm, HFIP $\delta = 4.48, 3.64$ ppm)Run 103 ¹H NMR (CD₂Cl₂ $\delta = 5.32$ ppm, HFIP $\delta = 4.47, 3.51$ ppm)

4.4.3.1 Structure Determination

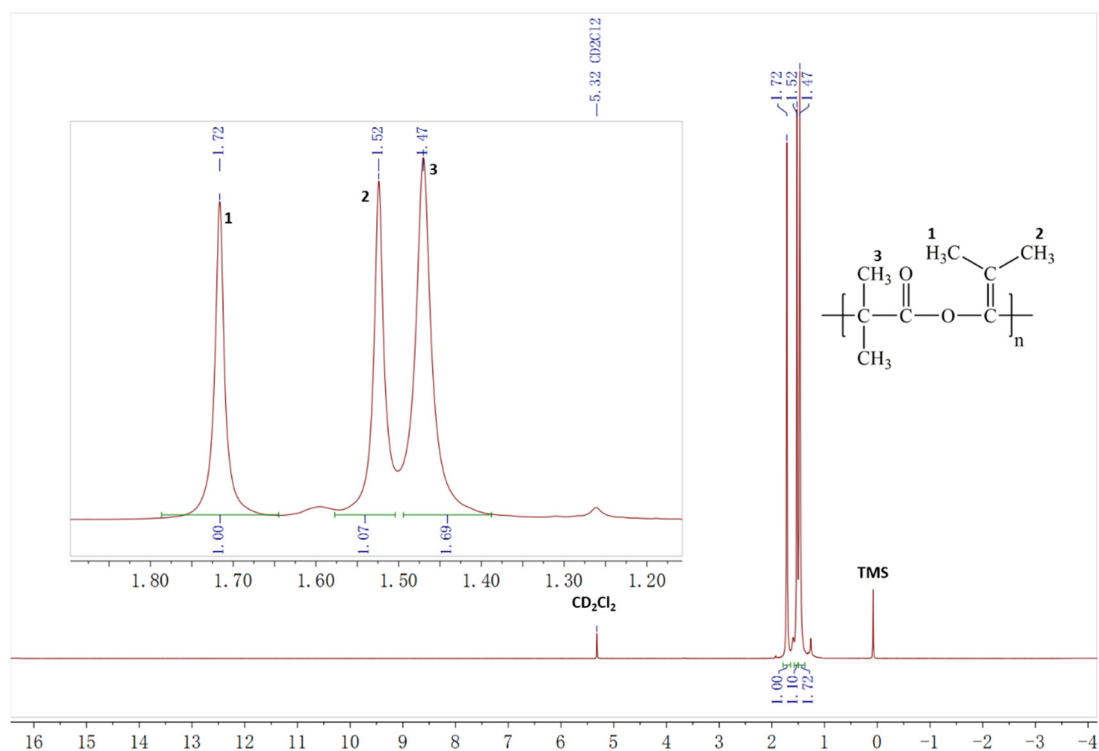
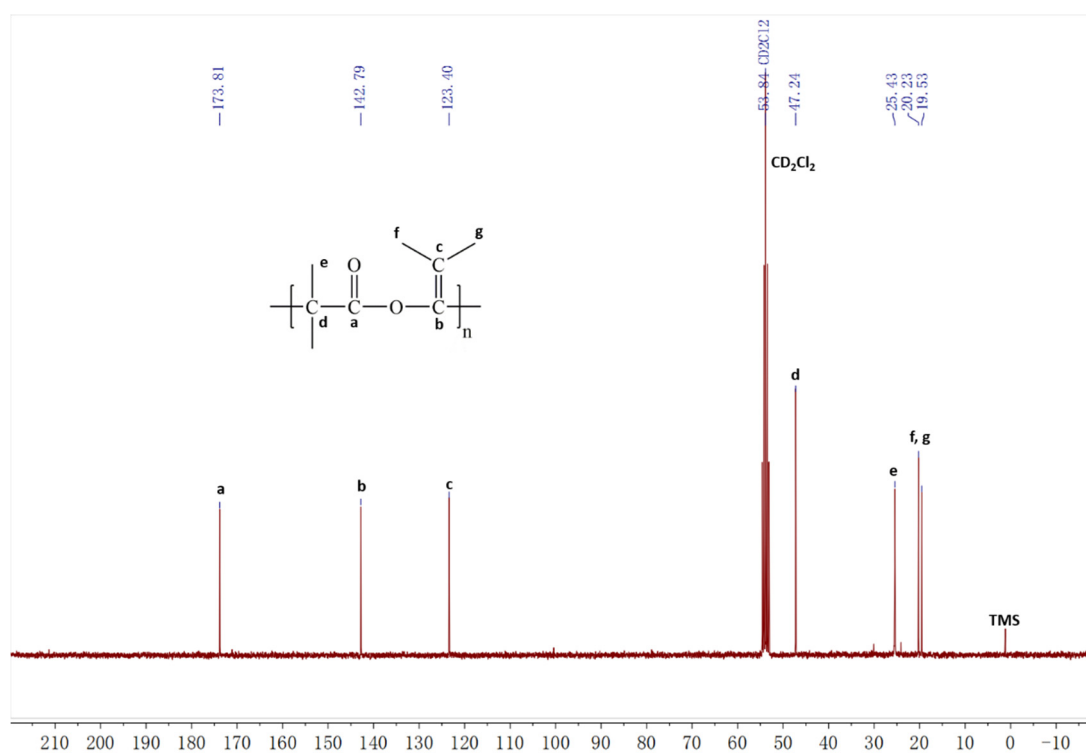
Run 59 ^1H NMR (CD_2Cl_2 $\delta = 5.32$ ppm, HFIP $\delta = 4.49$ ppm)Run 59 ^{13}C NMR (CD_2Cl_2 $\delta = 53.84$ ppm, HFIP $\delta = 127.63, 123.58, 120.14, 116.36$ ppm)



Run 60 ¹H NMR (CDCl₃ δ = 7.26 ppm, HFIP δ = 4.38, 3.54 ppm)

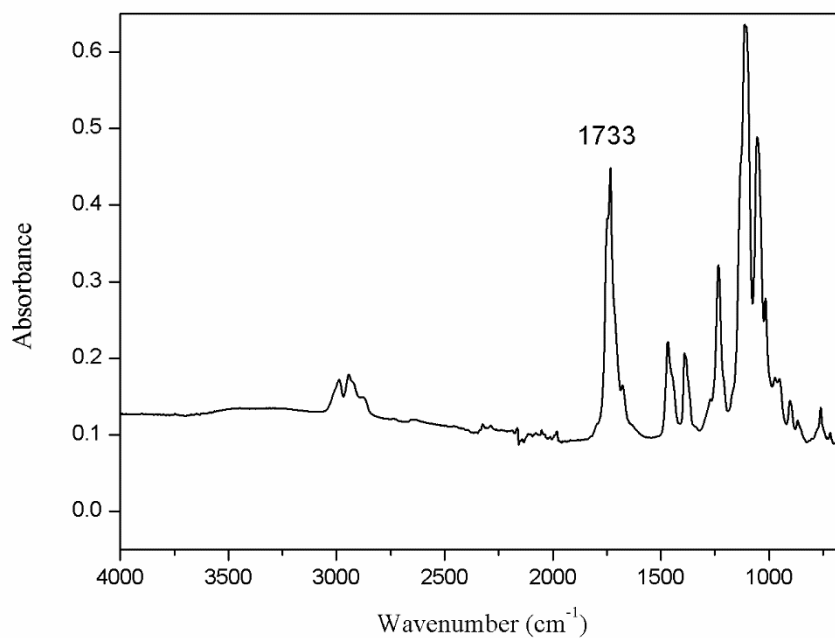


Run 60 ¹³C NMR (CD₂Cl₂ δ = 53.84 ppm, HFIP δ = 127.83, 124.05, 120.31, 116.57 ppm)

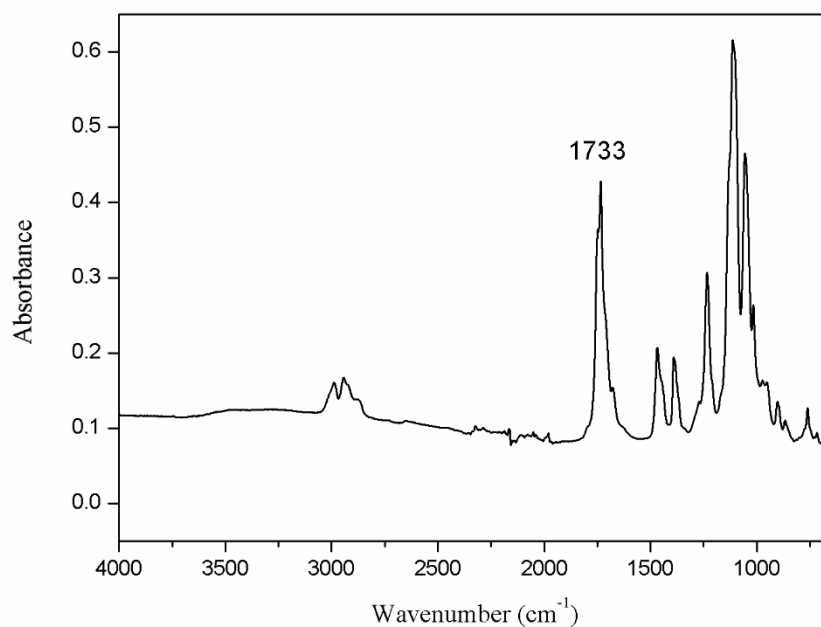
Run 86 ^1H NMR (CD₂Cl₂ δ = 5.32 ppm)Run 86 ^{13}C NMR (CD₂Cl₂ δ = 53.84 ppm)

4. FT-IR Spectra

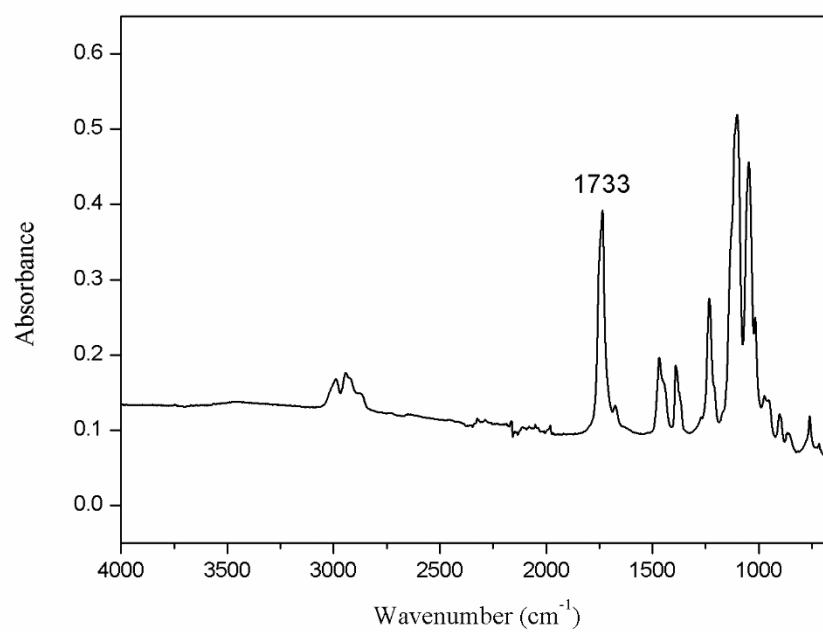
4.4.3 Polyester from DMK



Run 59



Run 60



Run 86

5. GC-MS Analysis

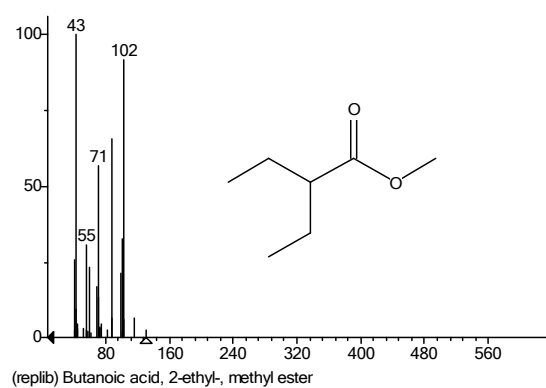
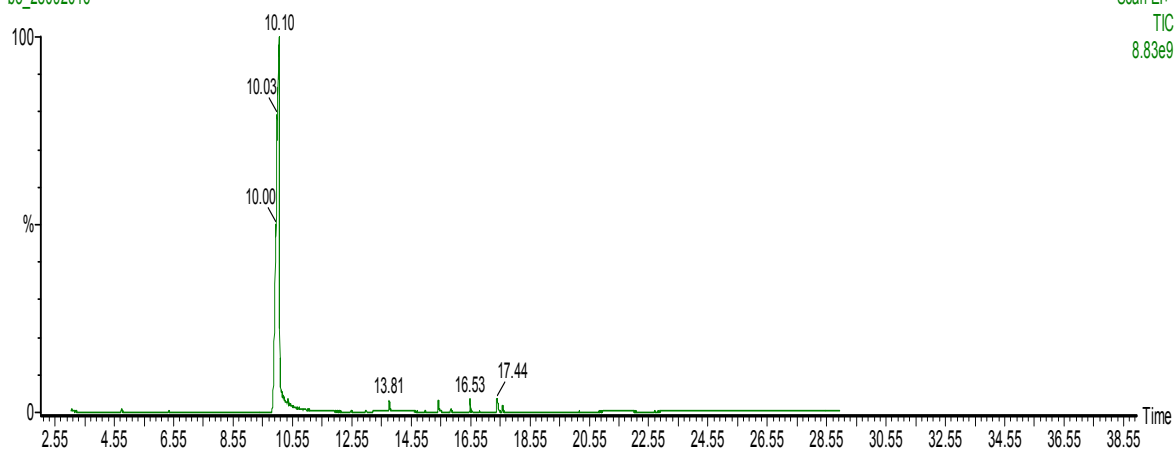
2.2.2 DEK

Peak at 10.1 min:

, 28-Sep-2016 + 16:48:45

bo_28092016

Scan E1+
TIC
8.83e9



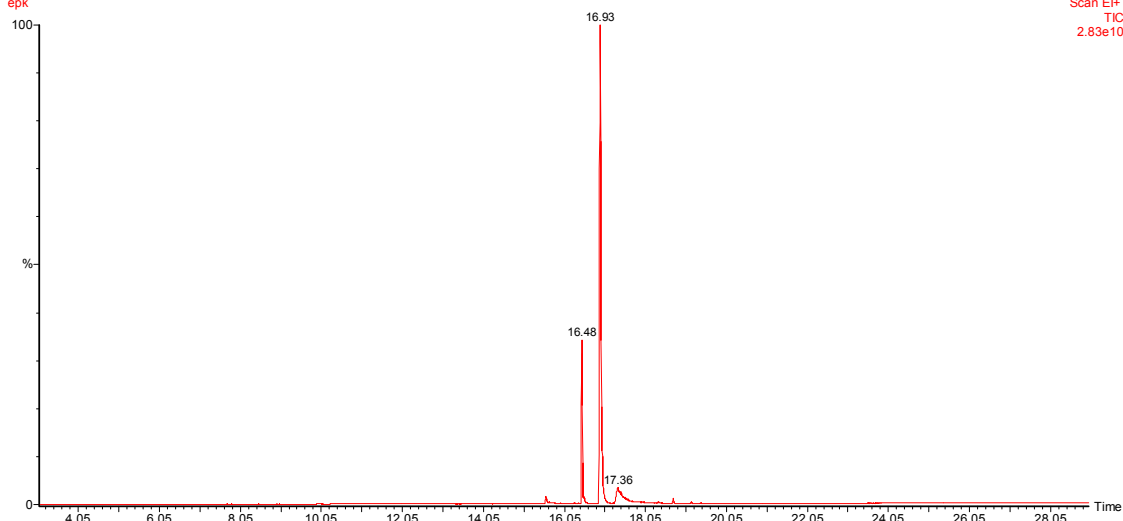
(replib) Butanoic acid, 2-ethyl-, methyl ester

2.2.3 EPK

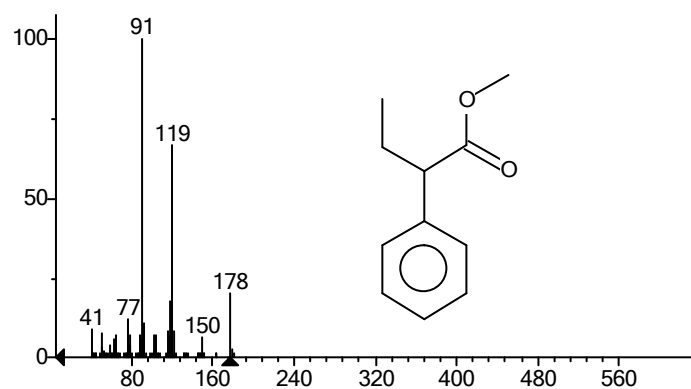
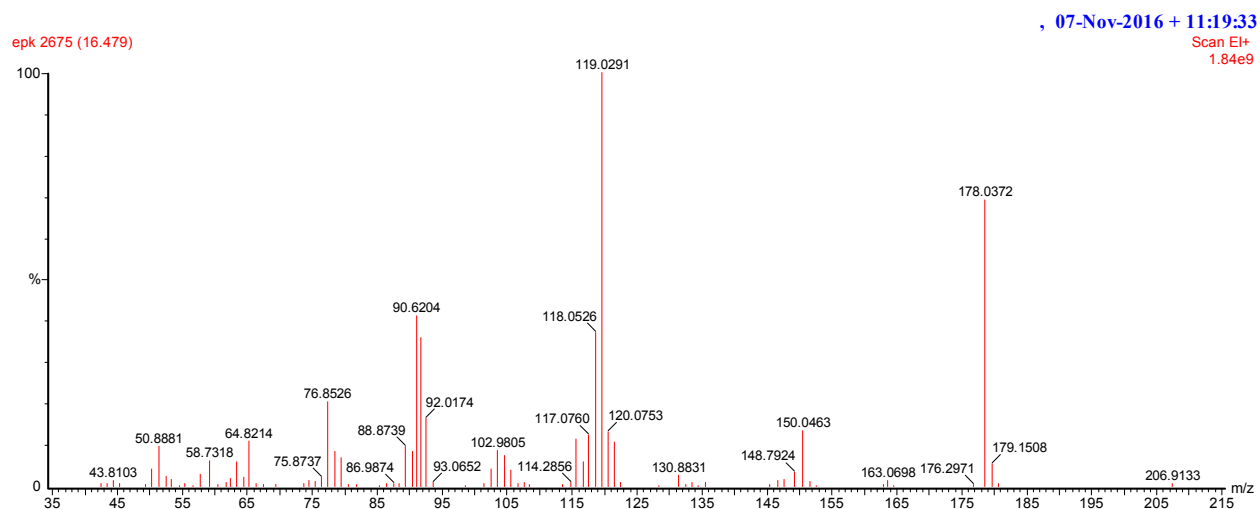
, 07-Nov-2016 + 11:19:33

epk

Scan E1+
TIC
2.83e10

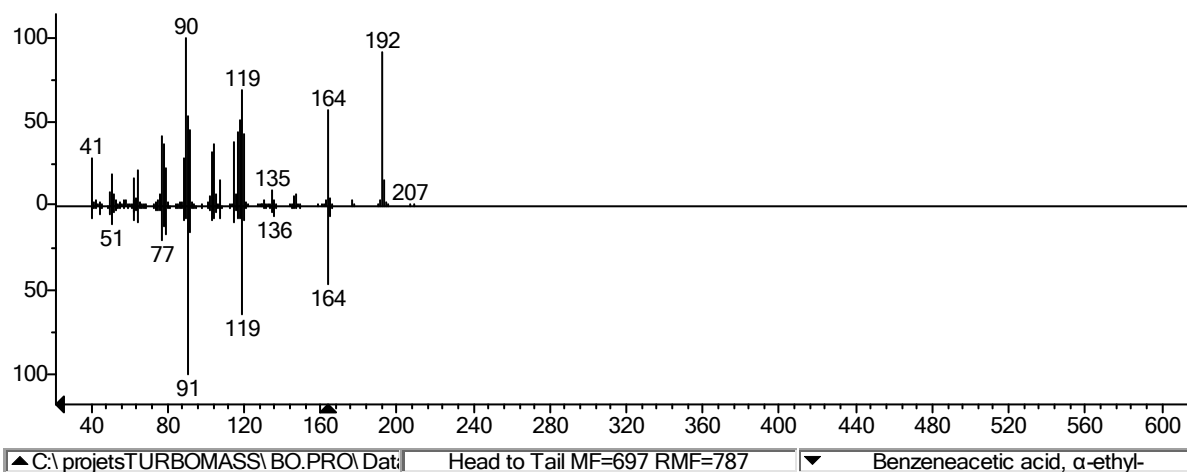


Peak at 16.9 min:

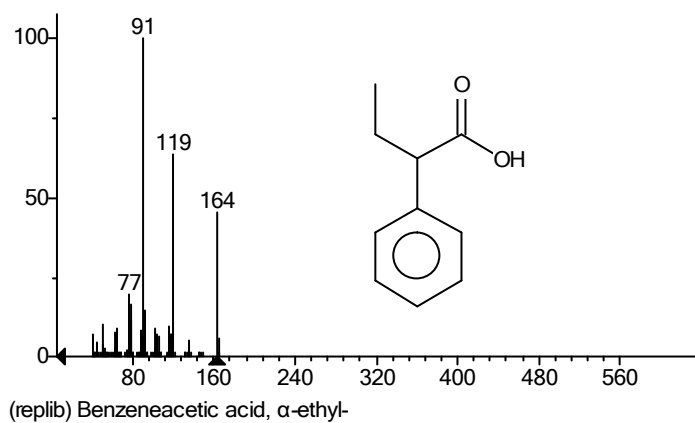


(mainlib) Benzeneacetic acid, α-ethyl-, methyl ester

Peak at 16.5 min:

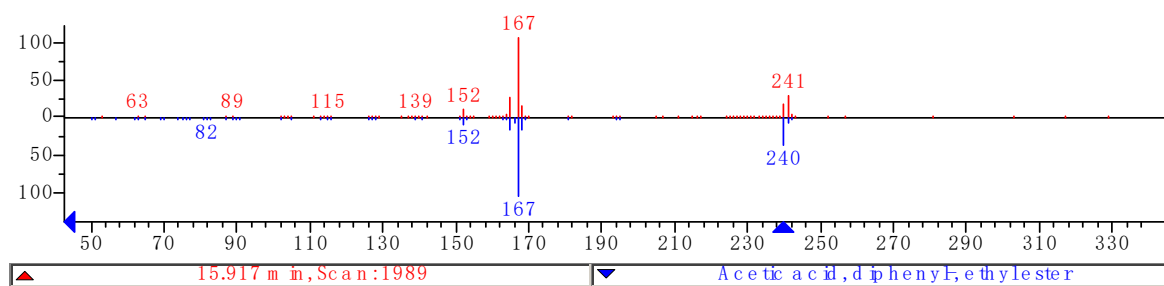
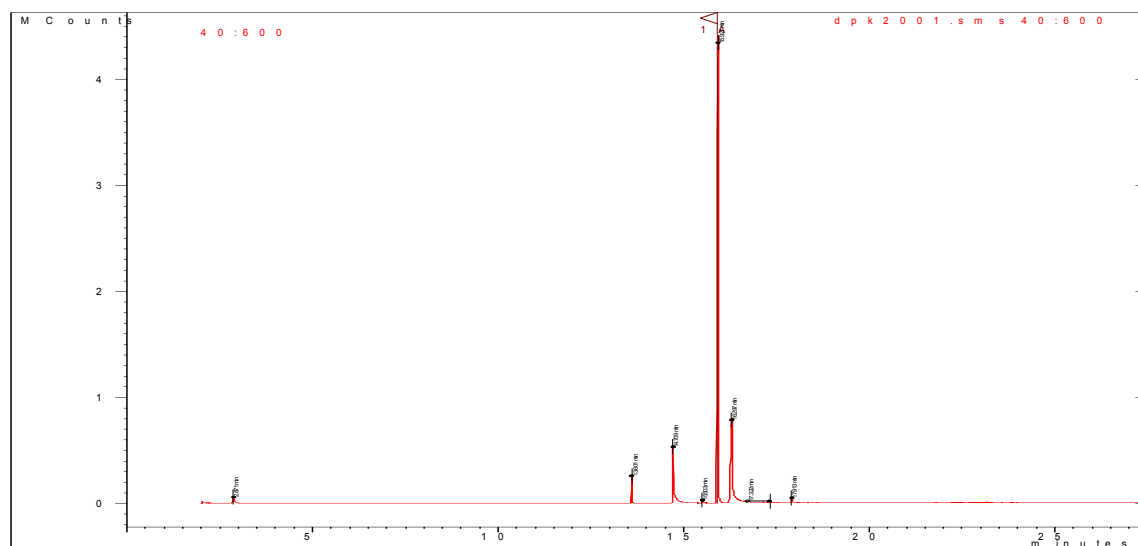


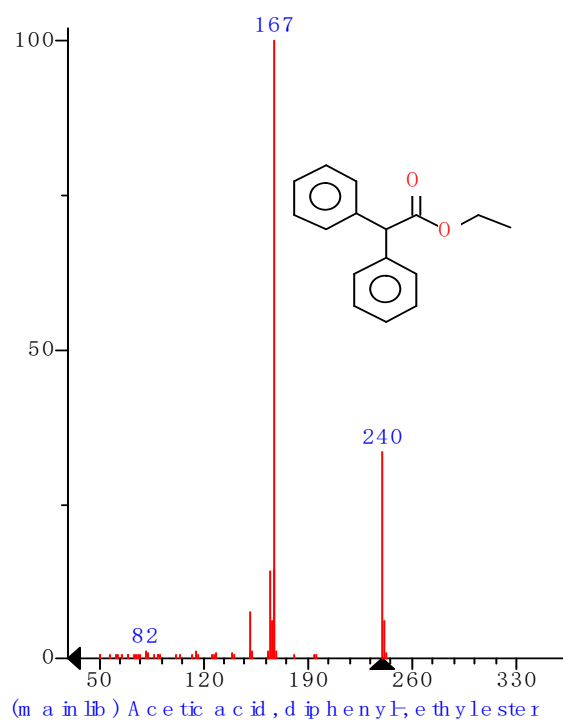
▲ C:\projetsTURBOMASS\BO.PRO\Dat\ Head to Tail MF=697 RMF=787 ▼ Benzeneacetic acid, α-ethyl-



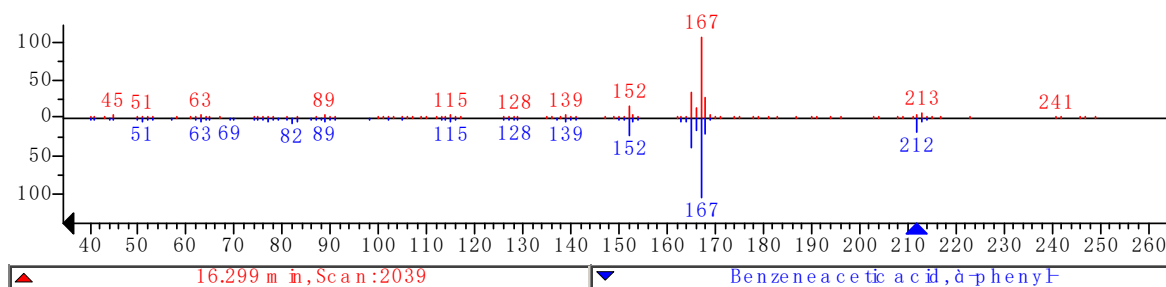
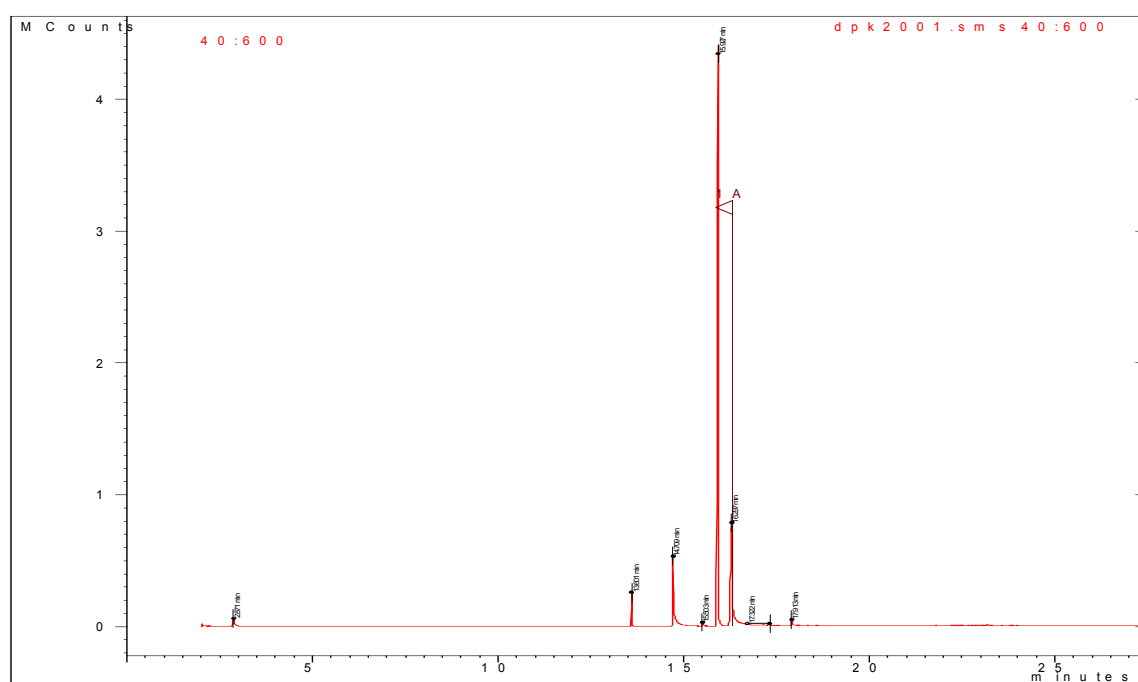
2.2.4 DPK

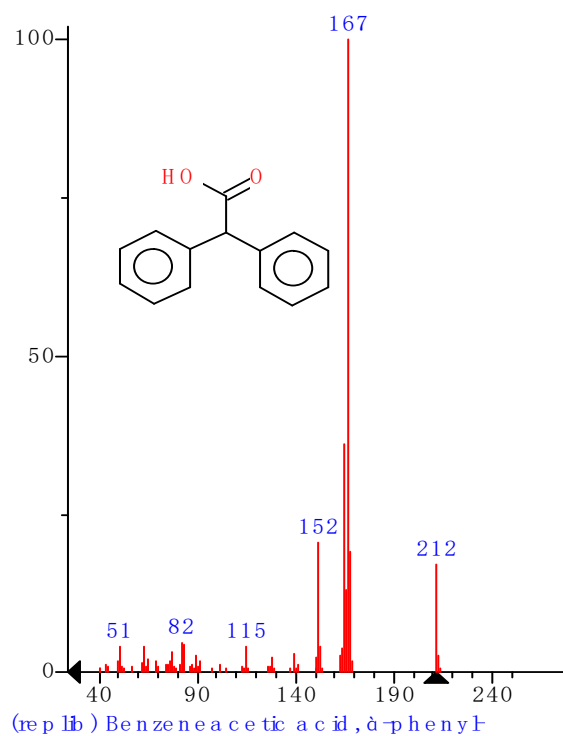
Bigger Peak at 15.9 min



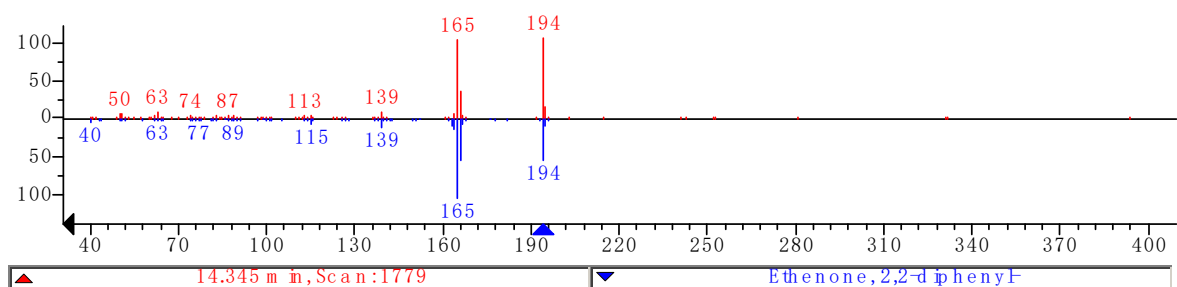
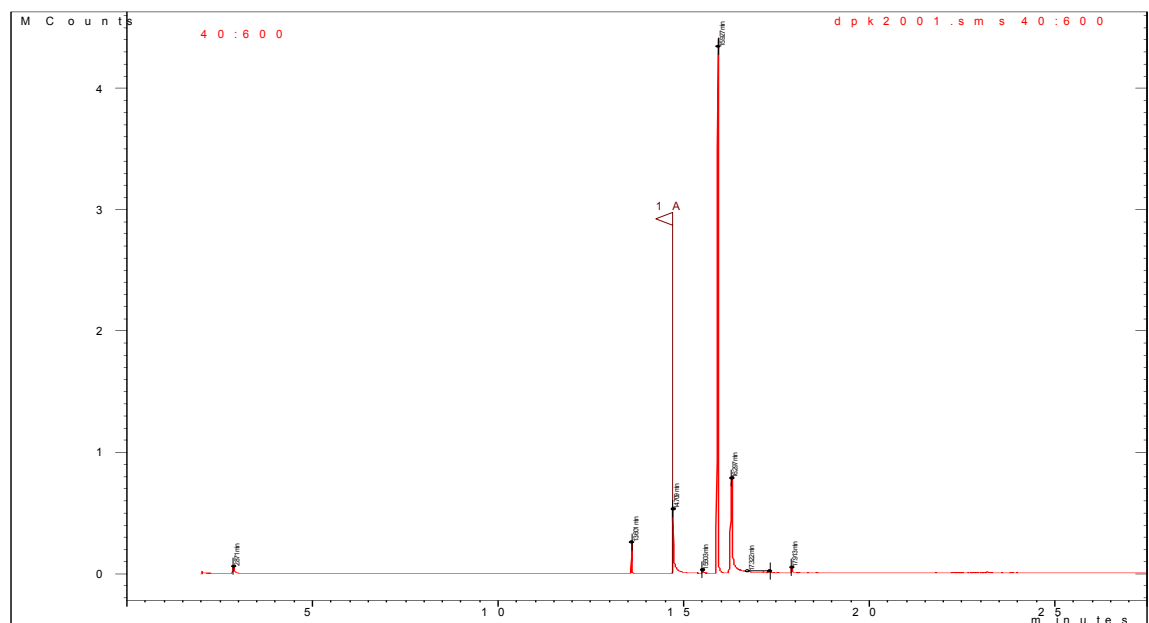


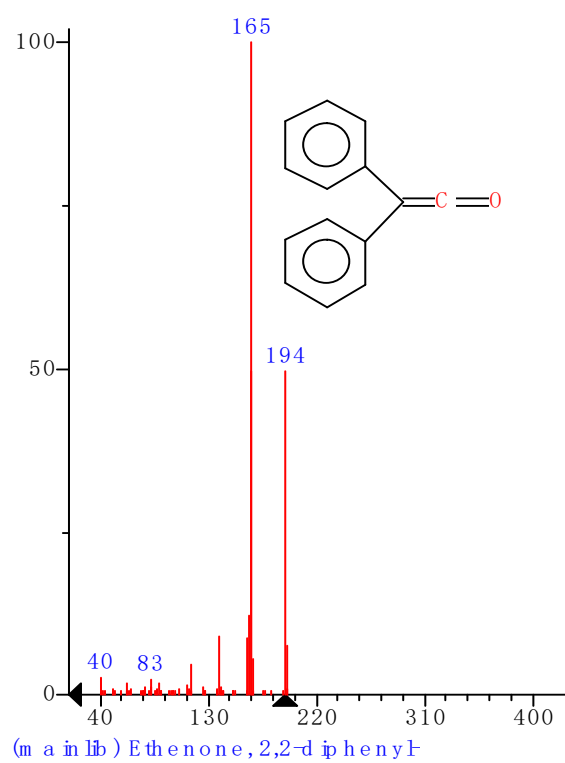
Peak at 16.3 min:





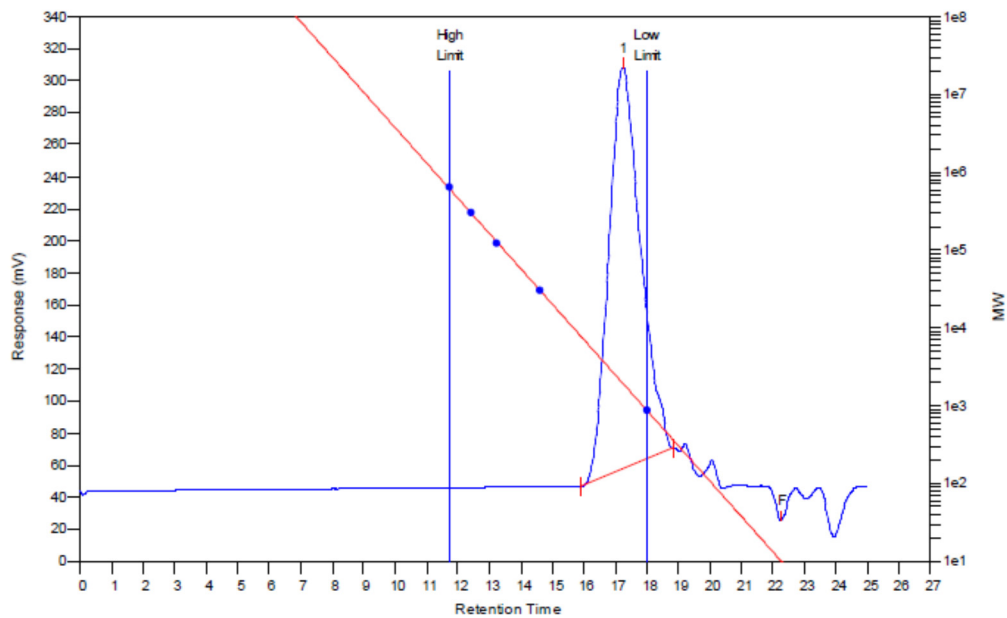
Peak at 14.3 min:





6. SEC Analysis

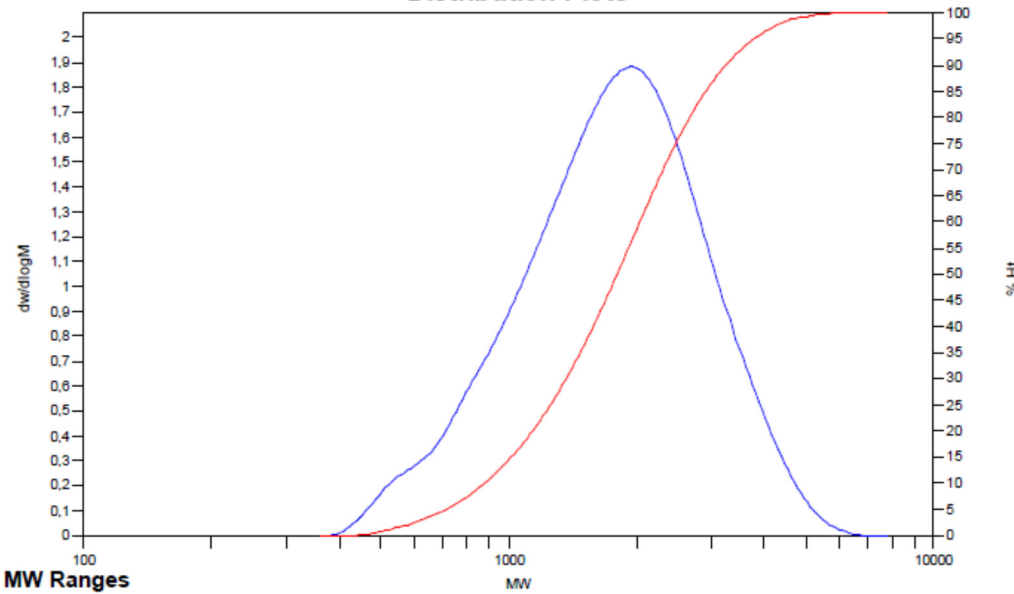
2.2.4 DPK



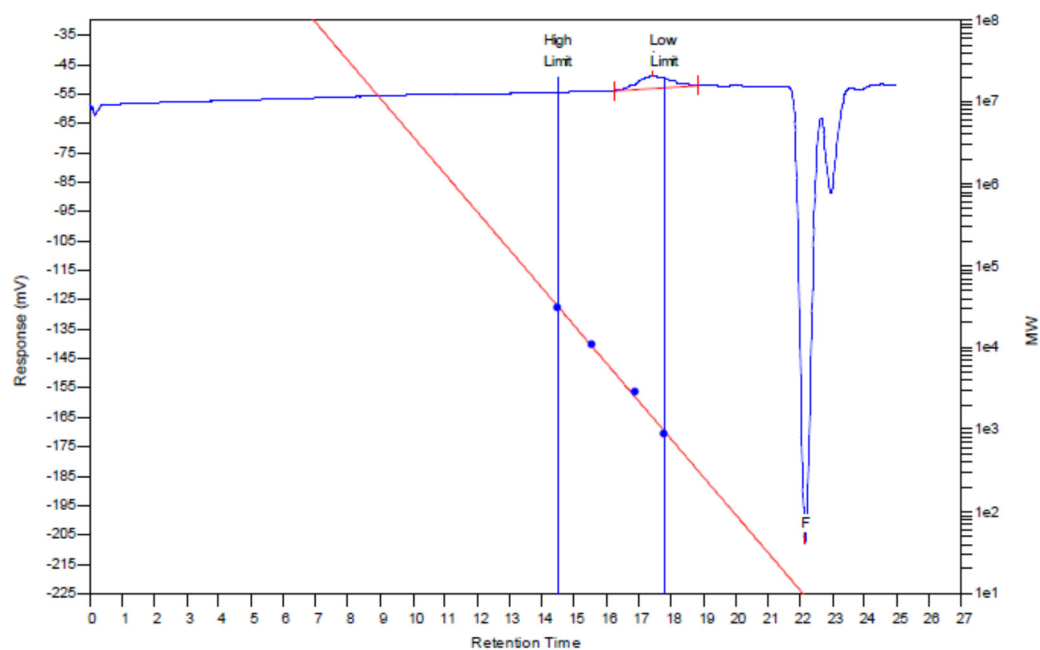
MW Averages

Mp: 1930	Mn: 1516	Mv: 1875	Mw: 1940
Mz: 2391	Mz+1: 2838	PD: 1.2797	

Distribution Plots



Run 39

**MW Averages**

Mp: 1404

Mn: 1066

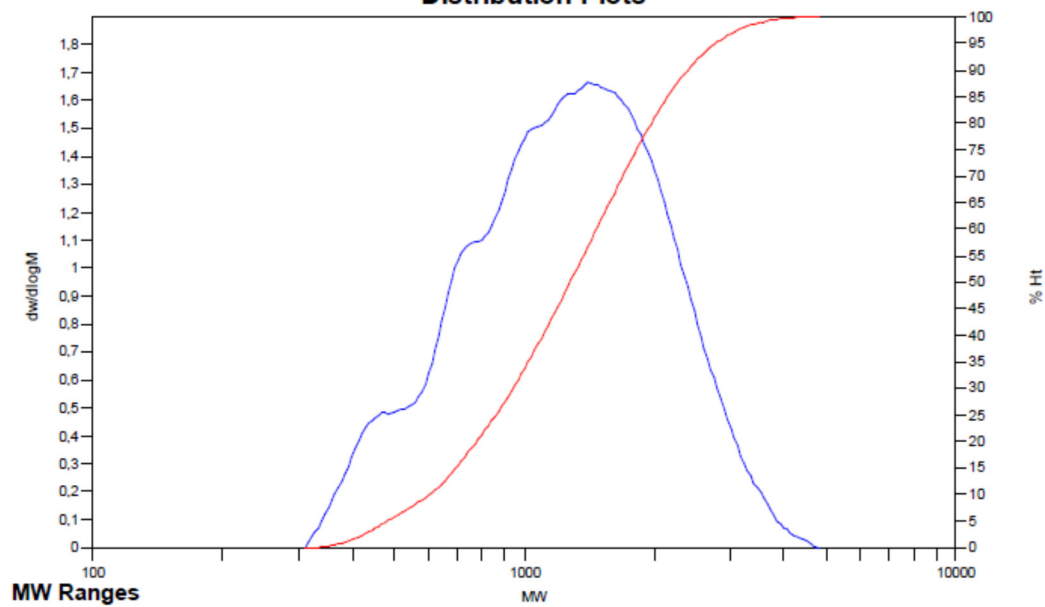
Mv: 1344

Mw: 1396

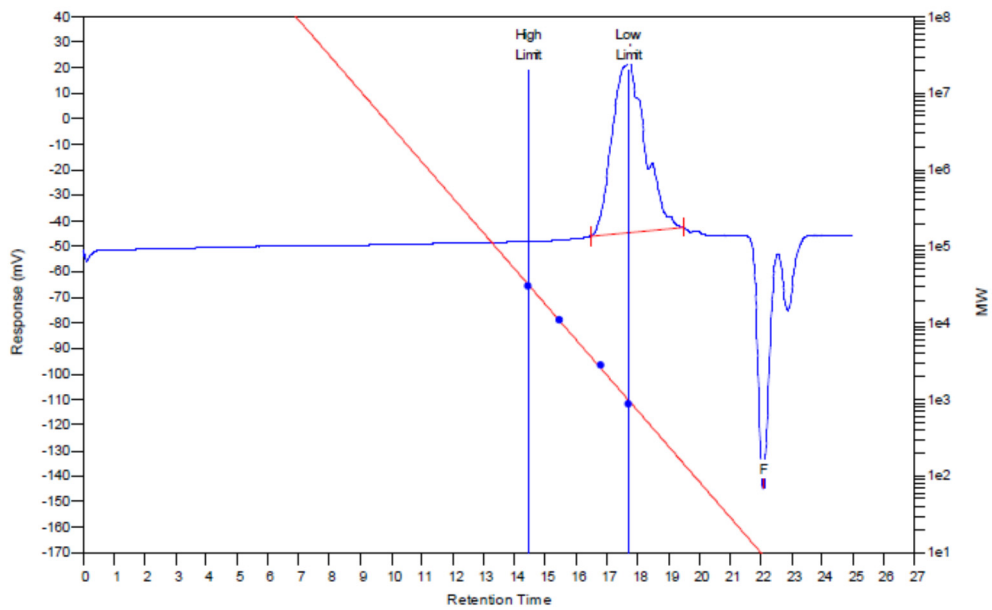
Mz: 1754

Mz+1: 2103

PD: 1.3096

Distribution Plots

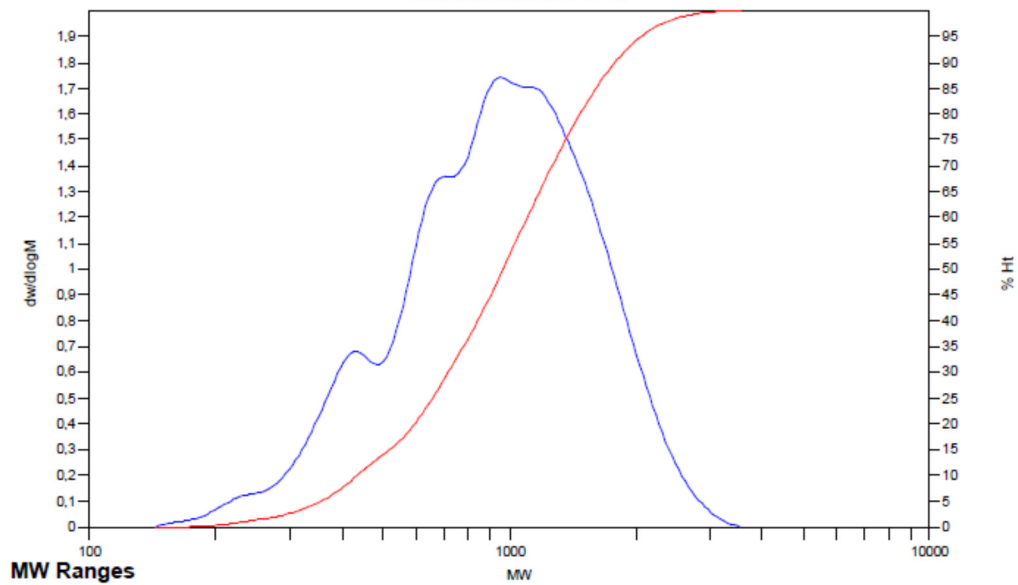
Run 40



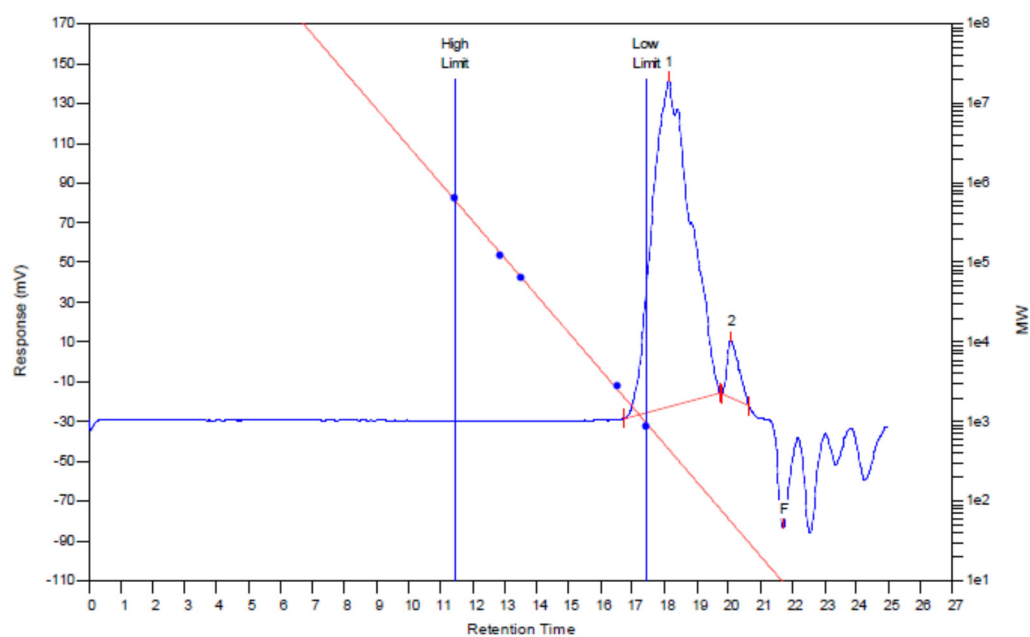
MW Averages

Mp: 950	Mn: 785	Mv: 1004	Mw: 1042
Mz: 1305	Mz+1: 1552	PD: 1.3274	

Distribution Plots



Run 41

**MW Averages**

Mp: 1084

Mn: 796

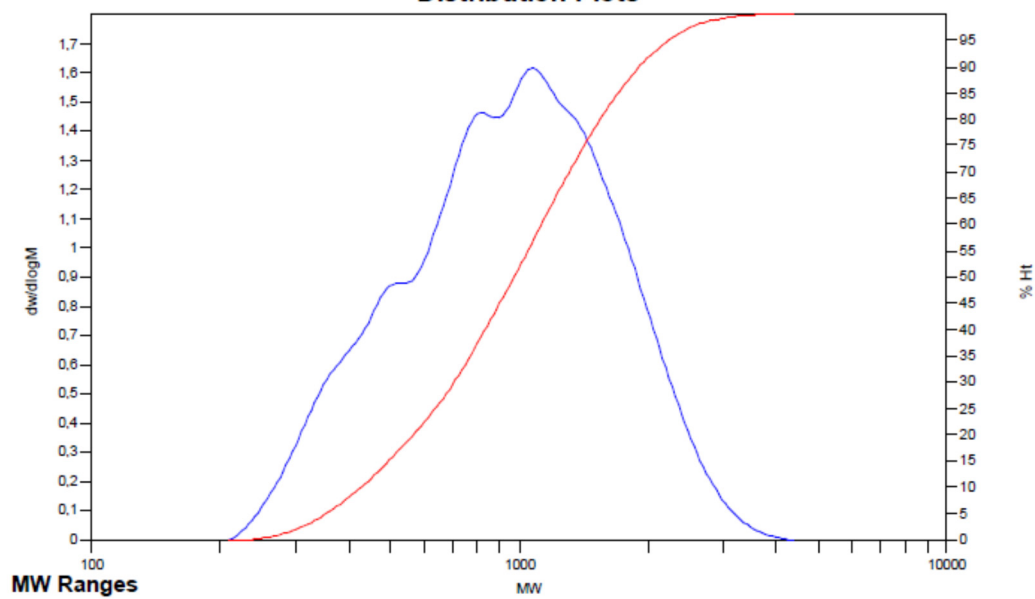
Mv: 1035

Mw: 1080

Mz: 1399

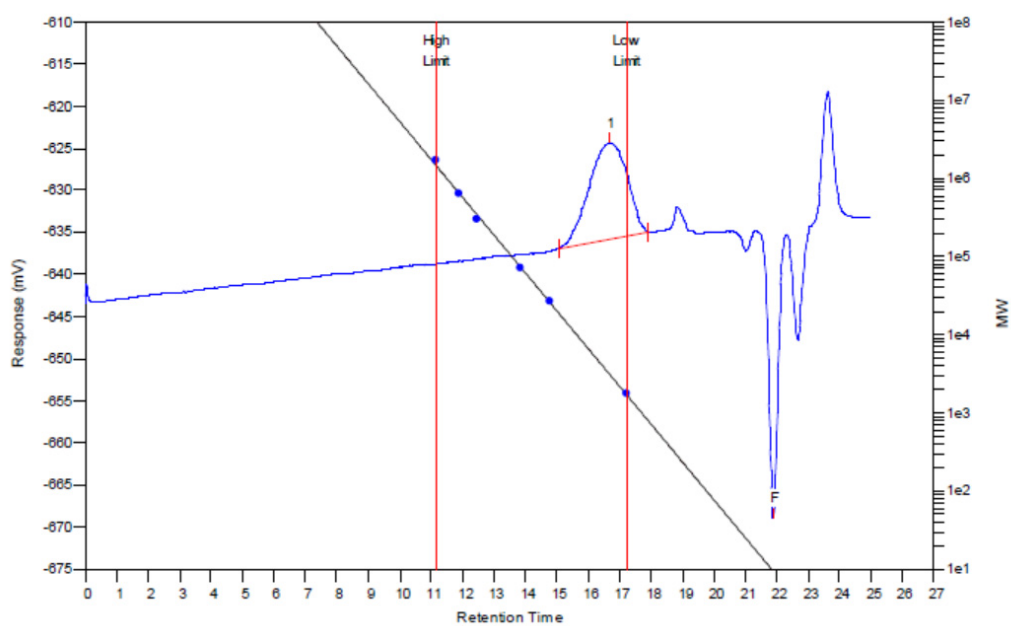
Mz+1: 1712

PD: 1.3568

Distribution Plots

Run 42

3.3.2 Experimental Results and Discussion



MW Averages

Mp: 2781

Mn: 2523

Mv: 3319

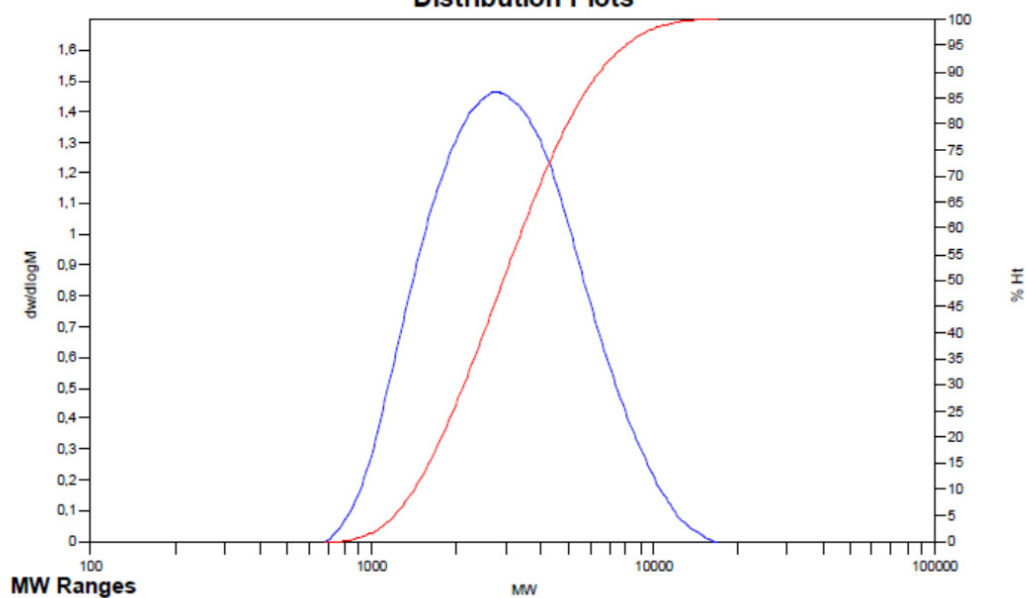
Mw: 3490

Mz: 4825

Mz+1: 6357

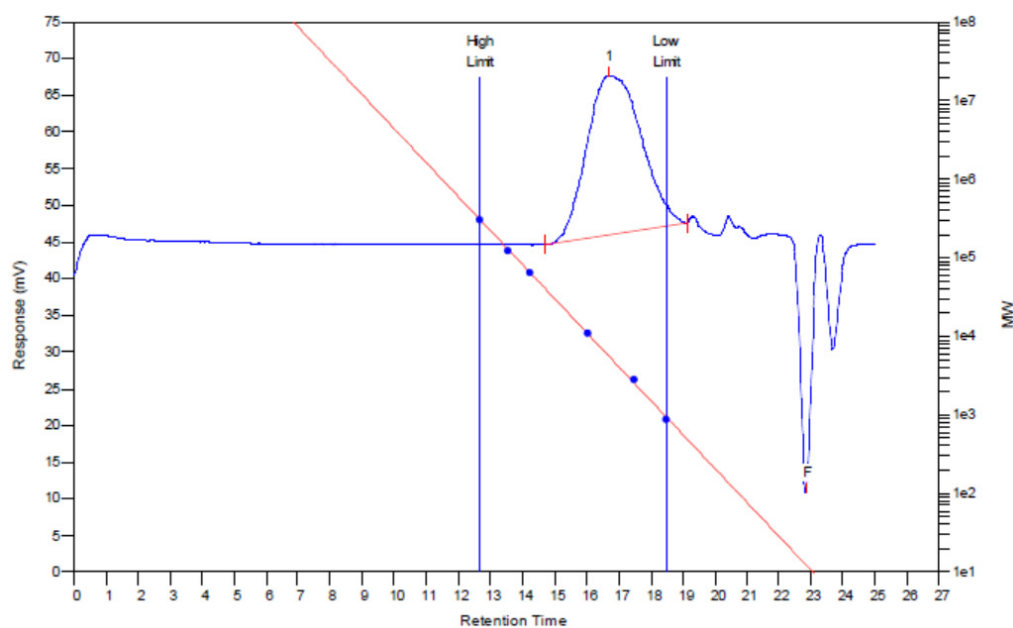
PD: 1.3833

Distribution Plots



Run 99

4.4.2 Polyester from EPK



MW Averages

Mp: 5744

Mn: 3475

Mv: 5378

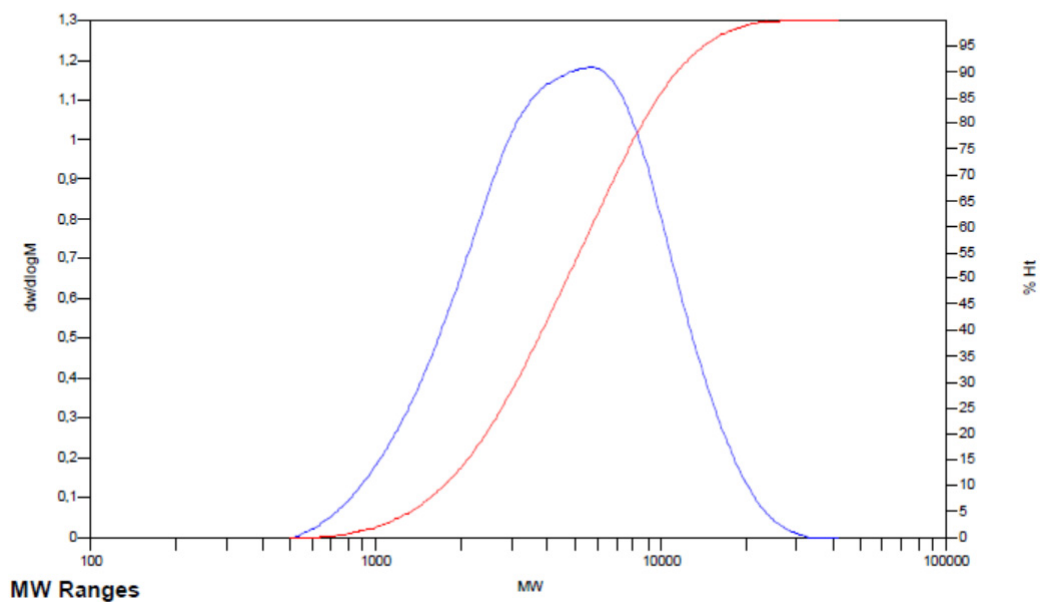
Mw: 5766

Mz: 8737

Mz+1: 11876

PD: 1.6593

Distribution Plots

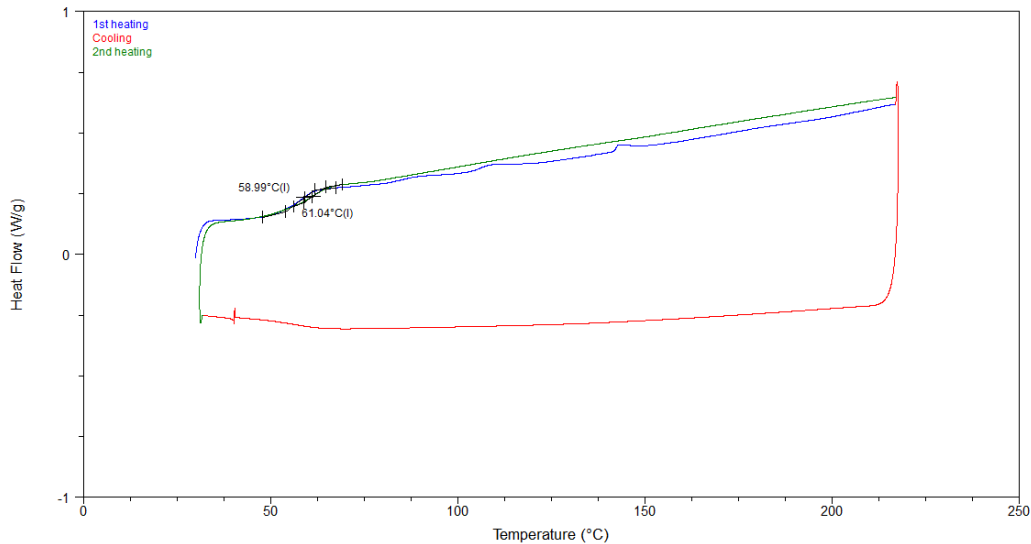


Run 31

7. DSC Thermograms

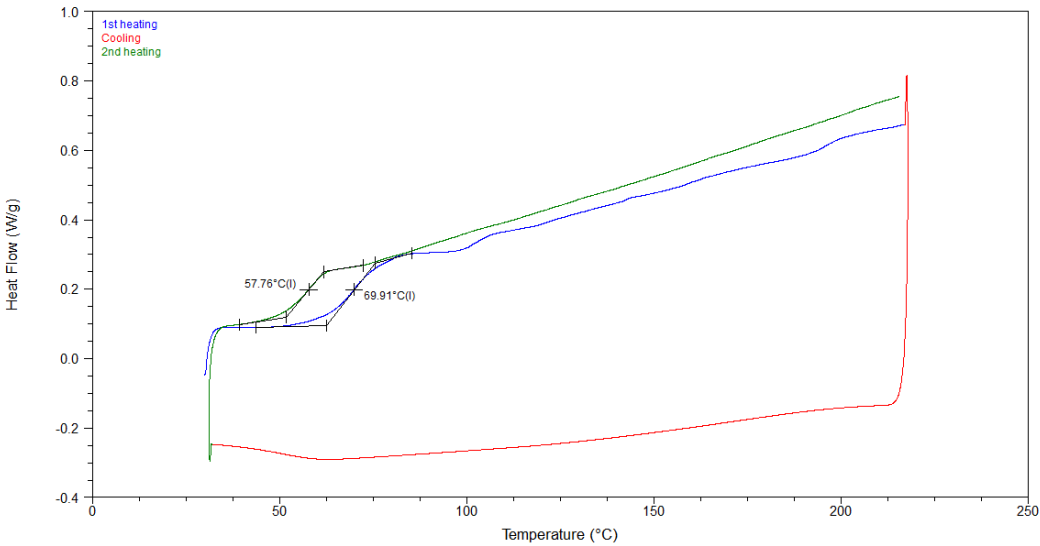
2.2.4 DPK

Run 40



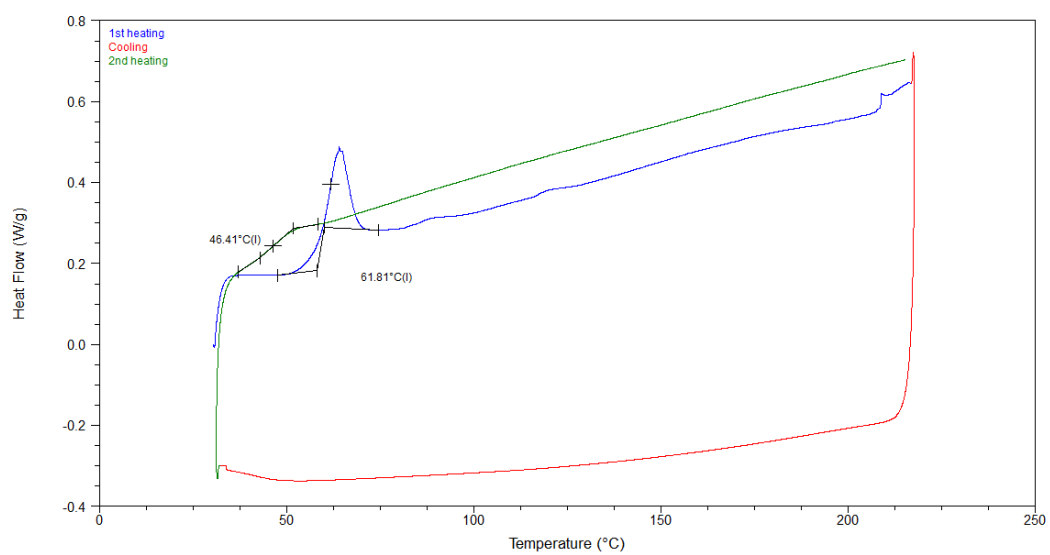
Run 40

Run 41



Run 41

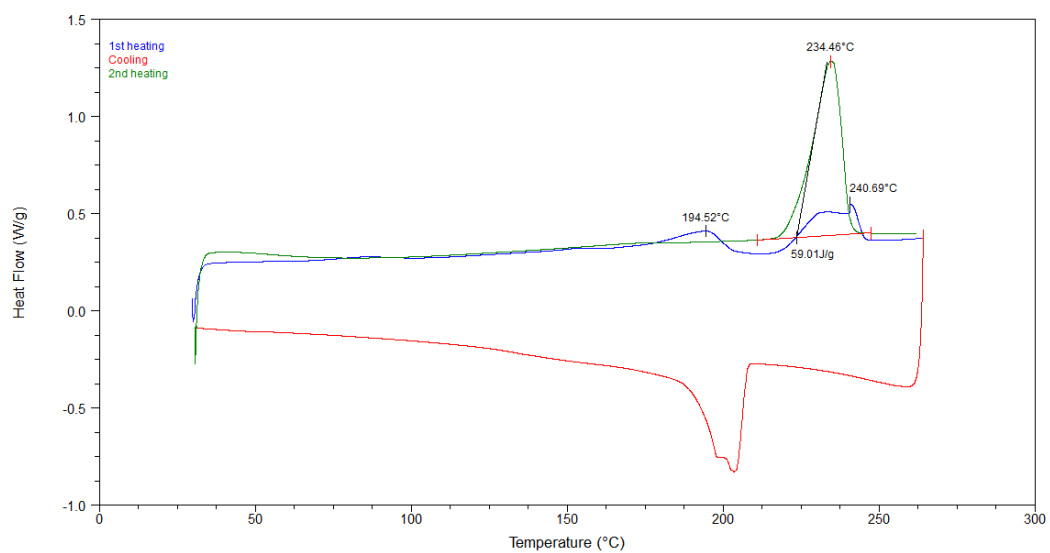
Run 42



Run 42

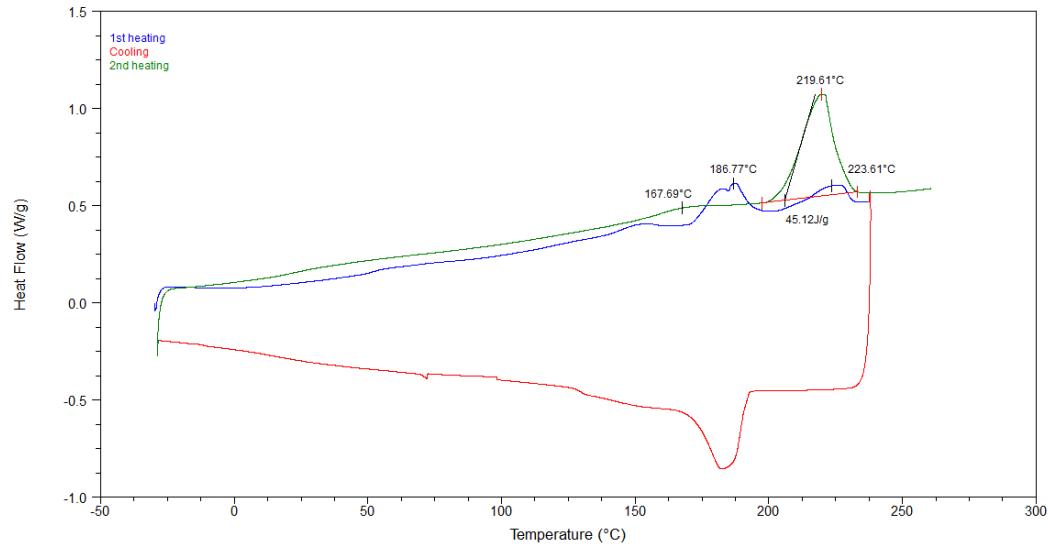
2.3.2 Copolymerization of DEK / DMK

Run 107



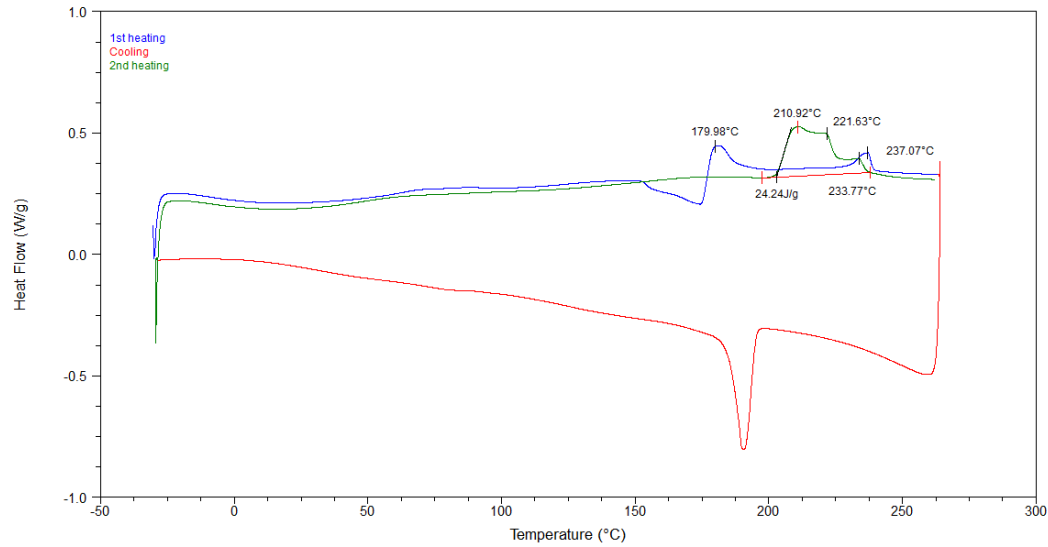
Run 107

Run 75



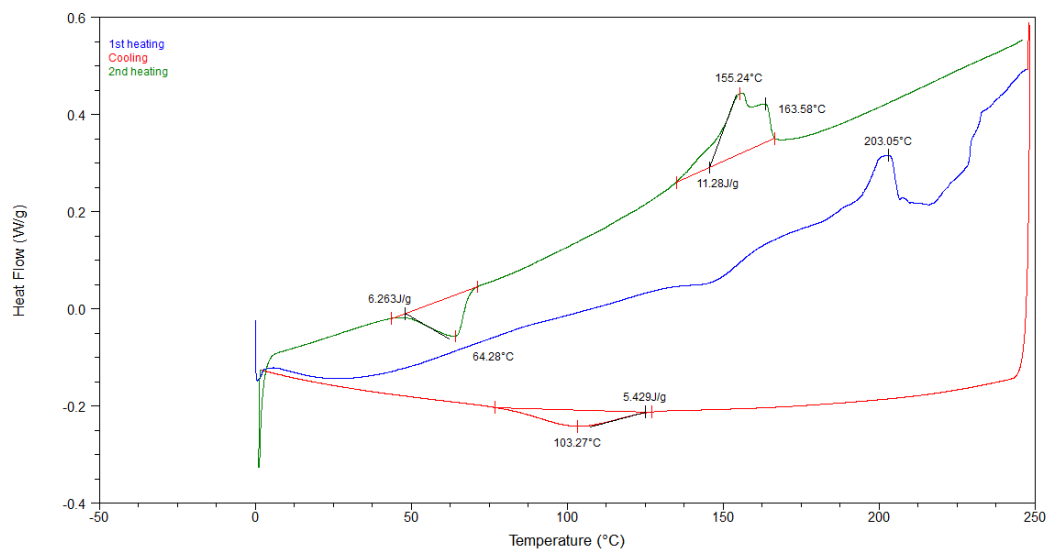
Run 75

Run 106



Run 106

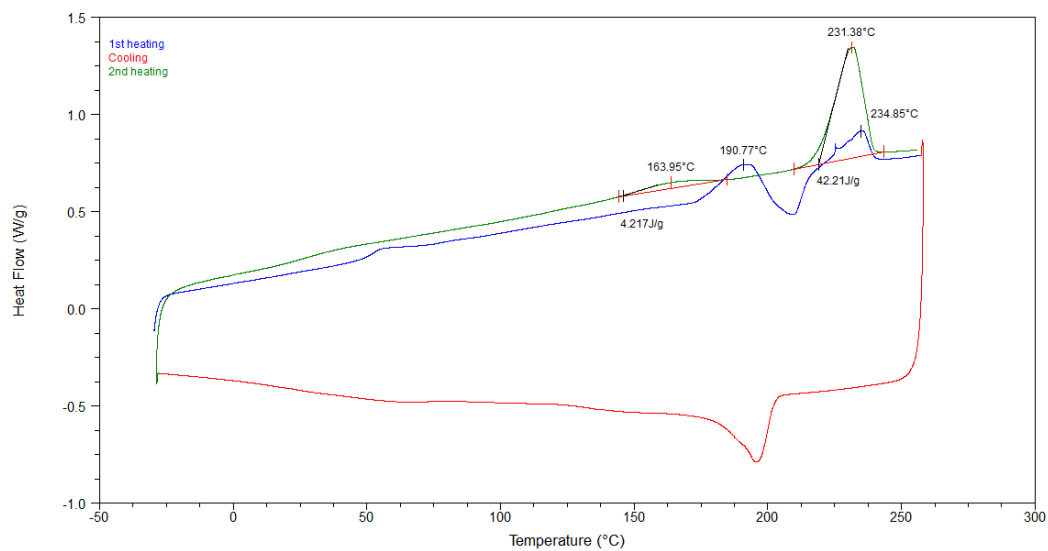
Run 98



Run 98

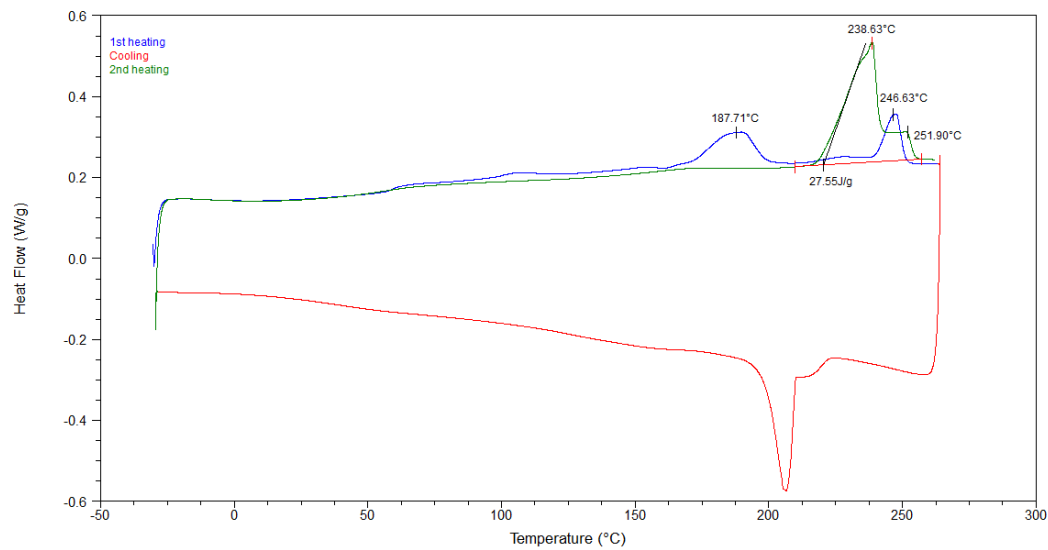
2.3.3 Copolymerization of DPK / DMK

Run 69



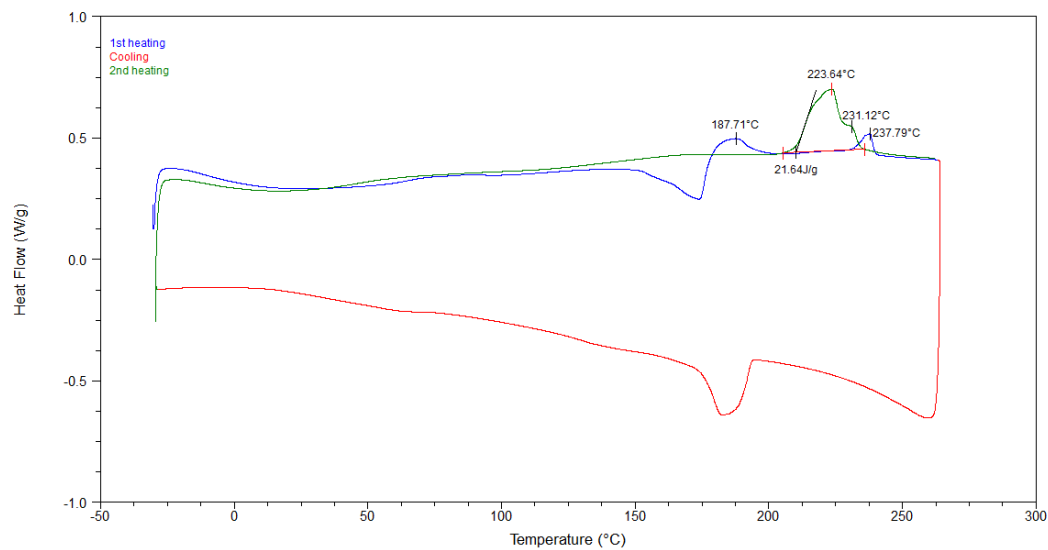
Run 69

Run 93



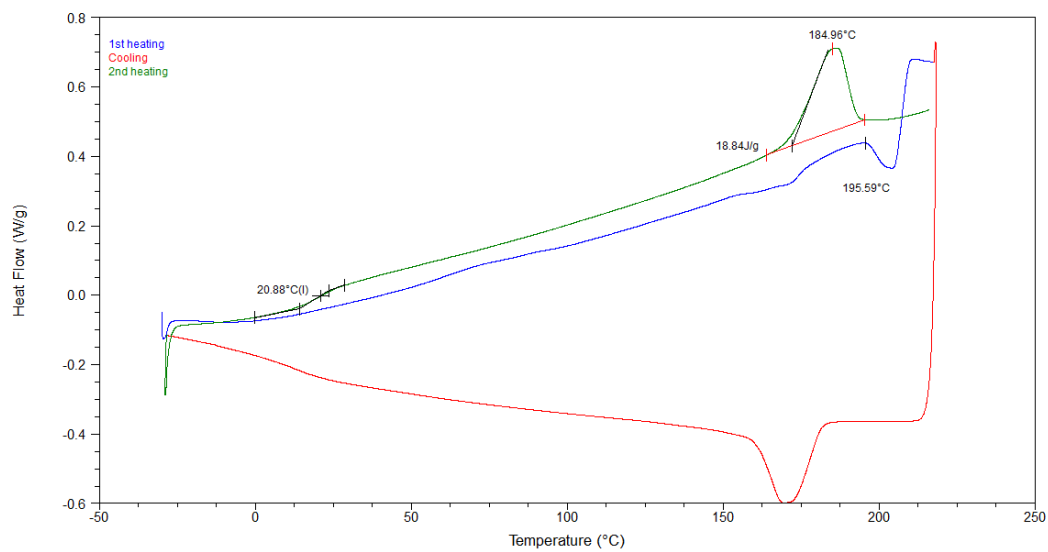
Run 93

Run 103



Run 103

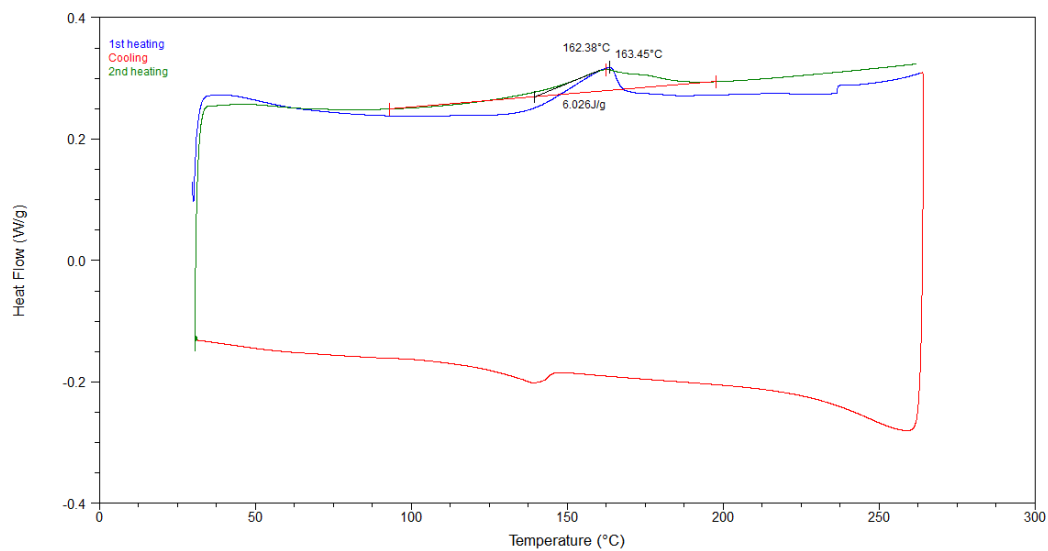
Run 95



Run 95

3.3.2 Experimental Results and Discussion

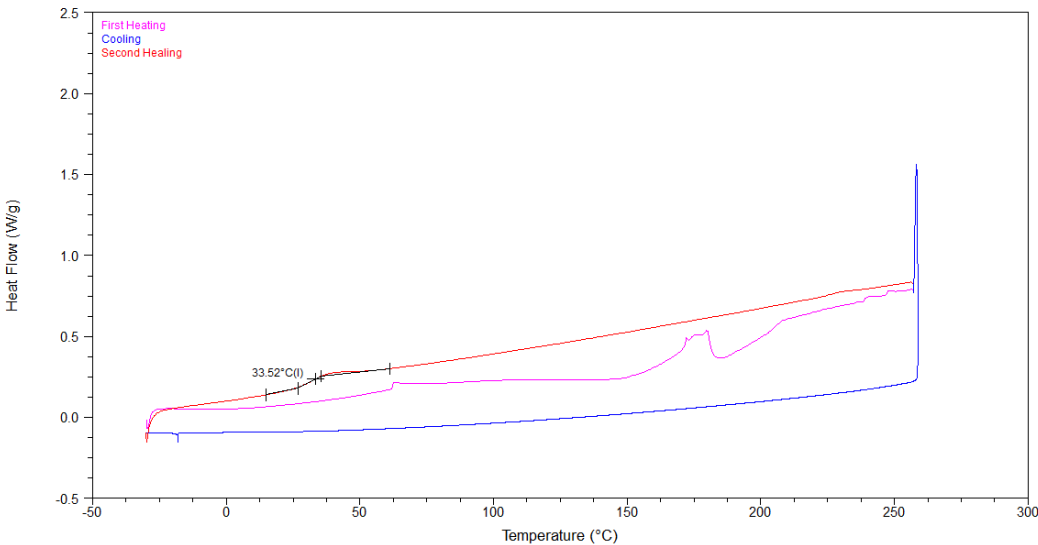
Run 99



Run 99

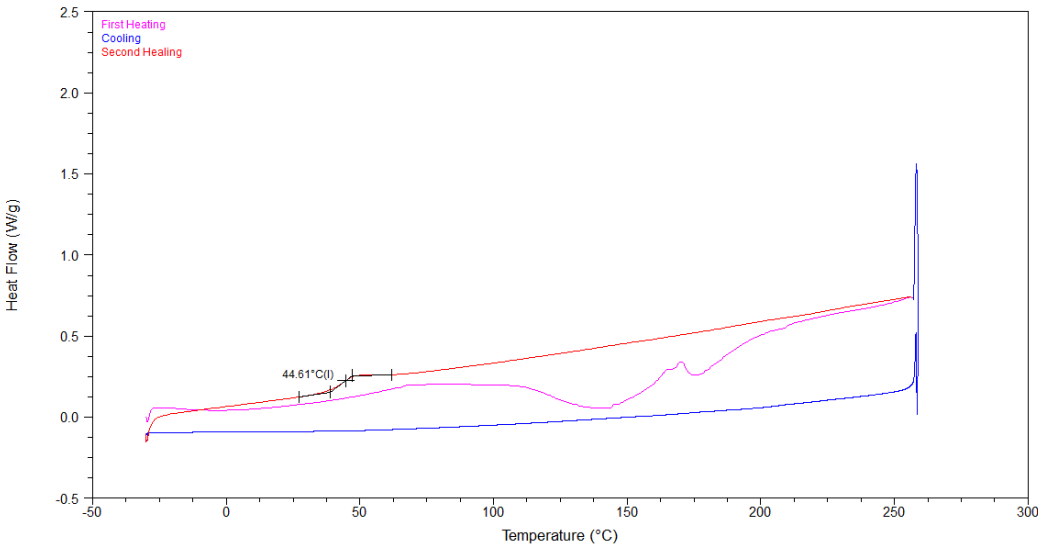
4.4.3 Polyester from DMK

Run 59



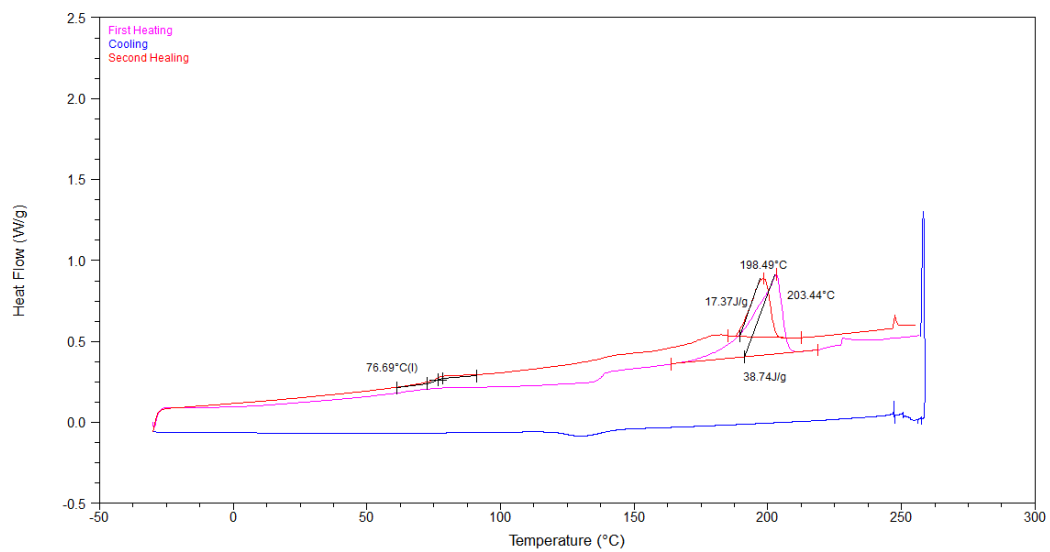
Run 59

Run 60



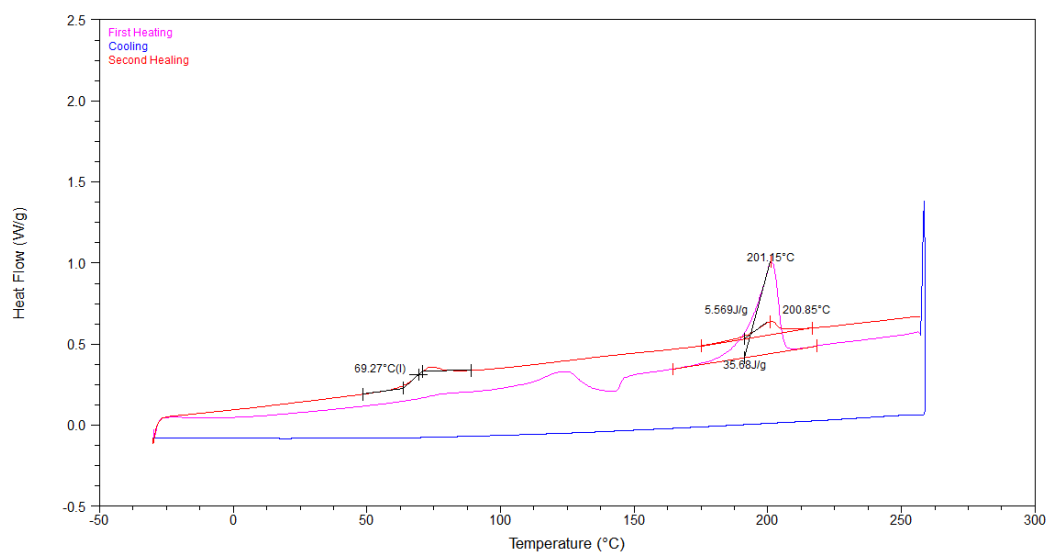
Run 60

Run 86



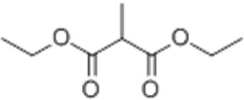
Run 86

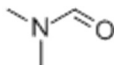
Run 88

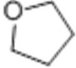


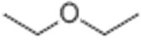
Run 88

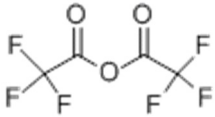

8. Chemicals Used

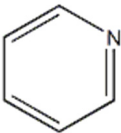
Name	Formula	GHS Keyword	M (g·mol ⁻¹)	T_m (°C)	T_b (°C)	d (g·cm ⁻³)	H Statement	P Statement
Dimethylketene	Me ₂ C=C=O		70.08					
Methylethylketene	MeEtC=C=O		84.12					
Diethylketene	Et ₂ C=C=O		98.14					
Ethylphenylketene	EtPhC=C=O		146.19					
Diphenylketene	Ph ₂ C=C=O		194.23					
Diethyl 2-methylmalonate		Flammable	174.19	-	198-199	1.0	H227	P210, P280, P370+P378, P403+P235, P501
Bromomethane	CH ₃ Br	Flammable Compressed gas Harmful Environmental hazard	94.94	-94	4	3.3	H225, H280, H315, H319, H335, H336, H341, H370, H373, H400, H420	P210, P261, P273, P280, P281, P311, P301+P310, P305+P351+P338, P370+P378, P403+P235

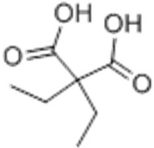
Name	Formula	GHS Keyword	M (g·mol ⁻¹)	T_m (°C)	T_b (°C)	d (g·cm ⁻³)	H Statement	P Statement
		Health hazard						
Dimethylformide		Flammable Toxic Harmful Corrosive Health hazard	73.09	-61	153	0.9	H226, H302, H312, H318, H319, H331, H332, H341, H360, H370, H372	P201, P202, P210, P233, P240, P260, P261, P264, P270, P271, P280, P303+P361+P353, P305+P351+P338, P307+P311, P308+P313, P370+P378, P405, P403+P233, P501
Potassium carbonate	K ₂ CO ₃	Toxic	138.21	891	decomposes	2.4	H302, H315 H319, H335	P261, P264, P280, P304+P340, P305+P351+P338, P337+P313, P405
Methylene chloride	CH ₂ Cl ₂	Flammable	84.93	-97	39.8-40	1.3	H225, H302, H314, H315,	P201, P202, P210, P260,

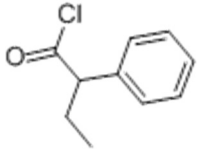
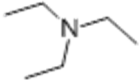
Name	Formula	GHS Keyword	M (g·mol ⁻¹)	T_m (°C)	T_b (°C)	d (g·cm ⁻³)	H Statement	P Statement
		Toxic Harmful Corrosive Health hazard					H319, H335, H336, H351, H370, H371, H373, H412	P261, P280, P281, P311 P301+P310, P303+P361+P3 53, P305+P351, P338, P308+P313, P405
Sodium hydroxide	NaOH	Corrosive	39.99	318	1388	2.1	H290, H314, H318	P260, P280, P310, P301+P330+ P331, P303+P36 1+P353, P305+ P351+P338, P405
Tetrahydrofuran		Flammable Harmful Health hazard	72.11	33- 36	66	0.9	H225, H302, H319, H333, H335, H351	P201, P210, P280, P303+P361+P3 53, P305+P351+P3 38, P370+P378, P405, P403+P235

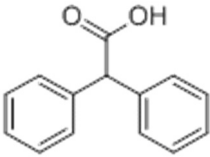
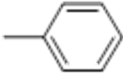
Name	Formula	GHS Keyword	M (g·mol ⁻¹)	T_m (°C)	T_b (°C)	d (g·cm ⁻³)	H Statement	P Statement
Magnesium sulfate	MgSO ₄	Harmful	120.37	1124	-	1.1	H302, H312, H332	P261, P264, P270, P271, P280, P301+P312, P302+P352, P304+P312, P304+P340, P312, P322, P330, P363, P501
Diethyl ether		Flammable Harmful	74.12	-116	34.6	0.7	H224, H302, H336	P210, P233, P240, P241, P242, P243, P261, P264, P270, P271, P280, P301+P312, P303+P361+P353, P304+P340, P312, P330, P370+P378, P403+P233, P403+P235, P405, P501

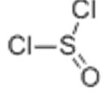
Name	Formula	GHS Keyword	M (g·mol ⁻¹)	T_m (°C)	T_b (°C)	d (g·cm ⁻³)	H Statement	P Statement
Trifluoroacetic anhydride		Corrosive Harmful	210.03	-64	39.5-40	1.5	H314, H332, H412	P260, P261, P264, P271, P273, P280, P301+P330+P3 31, P303+P361+P3 53, P304+P312, P304+P340, P305+P351+P3 38, P310, P312, P321, P363, P405, P501
Hexane		Flammable Harmful Health hazard Environmental hazard	86.18	-95	68.95	0.7	H225, H304, H315, H317, H319, H336, H361, H373, H411, H412	P201, P202, P210, P233, P240, P241, P242, P243, P260, P261, P264, P271, P272, P273, P280, P281, P301+P310, P302+P352, P303+P361+P3 53, P304+P340, P305+P351+P3 38, P308+P313,

Name	Formula	GHS Keyword	M (g·mol ⁻¹)	T_m (°C)	T_b (°C)	d (g·cm ⁻³)	H Statement	P Statement
								P312, P314, P321, P331, P332+P313, P333+P313, P337+P313, P362, P363, P370+P378, P391, P403+P233, P403+P235, P405, P501
Pyridine		Flammable Harmful Corrosive Health hazard Environmental hazard	79.1	-42	96-98	1.0	H225, H302, H304, H312, H314, H318, H332, H335, H336, H351, H370, H372, H400, H410	P201, P202, P210, P233, P240, P241, P242, P243, P260, P261, P264, P270, P271, P273, P280, P281, P301+P310, P301+P312, P301+P330+P3 31, P302+P352, P303+P361+P3 53, P304+P312, P304+P340,

Name	Formula	GHS Keyword	M (g·mol ⁻¹)	T_m (°C)	T_b (°C)	d (g·cm ⁻³)	H Statement	P Statement
								P305+P351+P338, P307+P311, P308+P313, P310, P312, P314, P321, P322, P330, P331, P363, P370+P378, P391, P403+P233, P403+P235, P405, P501
Diethylmalonic acid		Harmful	160.17	129-131	328.8	1.4	H315, H319, H335	P261, P264, P271, P280, P302+P352, P304+P340, P305+P351+P338, P312, P321, P332+P313, P337+P313, P362, P403+P233, P405, P501

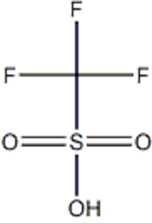
Name	Formula	GHS Keyword	M (g·mol ⁻¹)	T_m (°C)	T_b (°C)	d (g·cm ⁻³)	H Statement	P Statement
2-phenylbutanoyl chloride		Corrosive	182.65	-	122-125	1.1	H314	P260, P264, P280, P301+P330+P331, P303+P361+P53, P304+P340, P305+P351+P338, P310, P321, P363, P405, P501
Triethylamine		Flammable Harmful Corrosive Toxic	101.19	-115	90	0.7	H225, H302, H311, H312, H314, H318, H331, H332, H335	P210, P233, P240, P241, P242, P243, P260, P261, P264, P270, P271, P280, P301+P312, P301+P330+P331, P302+P352, P303+P361+P53, P304+P312, P304+P340, P305+P351+P338, P310, P311, P312, P321, P322, P330,

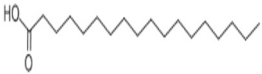
Name	Formula	GHS Keyword	M (g·mol ⁻¹)	T_m (°C)	T_b (°C)	d (g·cm ⁻³)	H Statement	P Statement
								P361, P363, P370+P378, P403+P233, P403+P235, P405, P501
Diphenylacetic acid		Toxic Harmful Environmental hazard	212.24	147- 149	195	1,3	H302, H311, H315, H319, H331, H332, H335, H400, H412	P261, P264, P270, P271, P273, P280, P301+P312, P302+P352, P304+P312, P304+P340, P305+P351+P3 38, P311, P312, P321, P322, P330, P332+P313, P337+P313, P361, P362, P363, P391, P403+P233, P405, P501
Toluene		Flammable Harmful	92.14	-95	111	0.9	H225, H304, H315, H336,	P201, P202, P210, P233, P240, P241,

Name	Formula	GHS Keyword	M (g·mol ⁻¹)	T_m (°C)	T_b (°C)	d (g·cm ⁻³)	H Statement	P Statement
		Health hazard					H361, H373, H412	P242, P243, P260, P261, P264, P271, P273, P280, P281, P301+P310, P302+P352, P303+P361+P3 53, P304+P340, P308+P313, P312, P314, P321, P331, P332+P313, P362, P370+P378, P403+P233, P403+P235, P405, P501
Thionyl chloride		Toxic Harmful Corrosive	118.97	-105	79	1.6	H302, H314, H318, H330, H331, H332, H335	P260, P261, P264, P270, P271, P280, P284, P301+P312, P301+P330+P3 31, P303+P361+P3

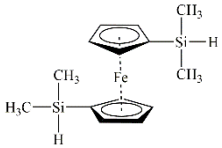
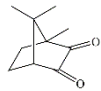
Name	Formula	GHS Keyword	M (g·mol ⁻¹)	T_m (°C)	T_b (°C)	d (g·cm ⁻³)	H Statement	P Statement
								53, P304+P312, P304+P340, P305+P351+P3 38, P310, P311, P312, P320, P321, P330, P363, P403+P233, P405, P501
Ethanol	CH ₃ CH ₂ OH	Flammable Harmful Health hazard	46.07	-114	78	0.8	H225, H319, H371	P210, P233, P240, P241, P242, P243, P260, P264, P270, P280, P303+P361+P3 53, P305+P351+P3 38, P309+P311, P337+P313, P370+P378, P403+P235, P405, P501
Aluminum chloride	AlCl ₃	Harmful Corrosive	133.34	194	180	2.4	H302, H314, H318, H341,	P201, P202, P260, P264, P270, P273,

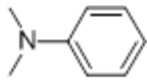
Name	Formula	GHS Keyword	M (g·mol ⁻¹)	T_m (°C)	T_b (°C)	d (g·cm ⁻³)	H Statement	P Statement
		Health hazard Environmental hazard					H361, H373, H400, H410	P280, P281, P301+P312, P301+P330+P3 31, P303+P361+P3 53, P304+P340, P305+P351+P3 38, P308+P313, P310, P314, P321, P330, P363, P391, P405, P501
Aluminum Bromide	AlBr ₃	Harmful Corrosive	266.69	94- 98	265	3.2	H302, H314	P260, P264, P270, P280, P301+P312, P301+P330+P3 31, P303+P361+P3 53, P304+P340, P305+P351+P3 38, P310, P321, P330, P363, P405, P501
2-Chloro-2-methylpropane	(CH ₃) ₃ CCl	Flammable	92.57	-25	51-52	0.8	H225	P210, P233, P240, P241,

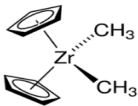
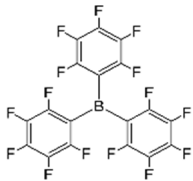
Name	Formula	GHS Keyword	M (g·mol ⁻¹)	T_m (°C)	T_b (°C)	d (g·cm ⁻³)	H Statement	P Statement
								P242, P243, P280, P303+P361+P3 53, P370+P378, P403+P235, P501
Trifluoromethanesulfonic acid		Harmful Corrosive	150.07	-40	162	1.7	H290, H302, H314, H335	P234, P260, P261, P264, P270, P271, P280, P301+P312, P301+P330+P3 31, P303+P361+P3 53, P304+P340, P305+P351+P3 38, P310, P312, P321, P330, P363, P390, P403+P233, P404, P405, P501
Perchloric acid	HClO ₄	Harmful Corrosive	100.46	-18	203	1.6	H271, H290, H302, H314, H373	P210, P220, P221, P234, P260, P264,

Name	Formula	GHS Keyword	M (g·mol ⁻¹)	T_m (°C)	T_b (°C)	d (g·cm ⁻³)	H Statement	P Statement
		Health hazard Oxidizing						P270, P280, P283, P301+P312, P301+P330+P331, P303+P361+P353, P304+P340, P305+P351+P338, P306+P360, P310, P314, P321, P330, P363, P370+P378, P371+P380+P375, P390, P404, P405, P501
Stearic acid		Harmful	284.48	67-72	361	0.8	H315, H319, H335, H412	P261, P264, P271, P273, P280, P302+P352, P304+P340, P305+P351+P338, P312, P321, P332+P313, P337+P313, P362,

Name	Formula	GHS Keyword	M (g·mol ⁻¹)	T_m (°C)	T_b (°C)	d (g·cm ⁻³)	H Statement	P Statement
								P403+P233, P405, P501
Aluminum nitrate	Al(NO ₃) ₃	Harmful Corrosive Health hazard Oxidizing Toxic	213.00	73	-	-	H271, H272, H301, H315, H318, H319, H361	P201, P202, P210, P220, P221, P264, P270, P280, P281, P283, P301+P310, P302+P352, P305+P351+P3 38, P306+P360, P308+P313, P310, P321, P330, P332+P313, P337+P313, P362, P370+P378, P371+P380+P3 75, P405, P501
Sulfuric acid	H ₂ SO ₄	Corrosive	178.14	2	290	1.9	H290, H314, H318	P234, P260, P264, P280, P301+P330+P3 31, P303+P361+P3

Name	Formula	GHS Keyword	M (g·mol ⁻¹)	T_m (°C)	T_b (°C)	d (g·cm ⁻³)	H Statement	P Statement
								53, P304+P340, P305+P351+P338, P310, P321, P363, P390, P404, P405, P501
Montmorillonite clay	Al ₂ O ₃ , SiO ₂ etc	Harmful Corrosive	-	-	-	2~3	H315, H318, H335	P261, P264, P271, P280, P302+P352, P304+P340, P305+P351+P338, P310, P312, P321, P332+P313, P362, P403+P233, P405, P501
1,1'-bis(dimethylsilyl)ferrocene		Flammable	302.34	-	294-295	1.0	H226	-
Camphorquinone		Harmful	166.22	197-203	234.44	1.0	H315, H319, H335	P261, P264, P271, P280, P302+P352,

Name	Formula	GHS Keyword	M (g·mol ⁻¹)	T_m (°C)	T_b (°C)	d (g·cm ⁻³)	H Statement	P Statement
								P304+P340, P305+P351+P3 38, P312, P321, P332+P313, P337+P313, P362, P403+P233, P405, P501
<i>N,N</i> -Dimethylaniline		Harmful Toxic Health hazard Environmental hazard	121.18	-36	213-226	1.0	H227, H302, H312, H319, H330, H336, H351, H370, H372, H401, H411	P201, P202, P210, P260, P261, P264, P270, P271, P273, P280, P281, P284, P301+P312, P302+P352, P304+P340, P305+P351+P3 38, P307+P311, P308+P313, P310, P312, P314, P320, P321, P322, P330, P337+P313, P363,

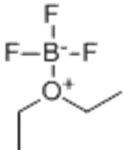
Name	Formula	GHS Keyword	M (g·mol ⁻¹)	T_m (°C)	T_b (°C)	d (g·cm ⁻³)	H Statement	P Statement
								P370+P378, P391, P403+P233, P403+P235, P405, P501
Bis(cyclopentadienyl)dimethyl zirconium		Harmful	251.48	170	170	-	H315, H319, H335	P261, P304+P340, P305+P351+P338, P405
Tris(pentafluorophenyl) borane		Harmful Toxic Environmental hazard	511.98	126-131	-	0.7	H301, H315, H319, H335, H400, H410	P261, P264, P270, P271, P273, P280, P301+P310, P302+P352, P304+P340, P305+P351+P338, P312, P321, P330, P332+P313, P337+P313, P362, P391, P403+P233, P405, P501

Name	Formula	GHS Keyword	M (g·mol ⁻¹)	T_m (°C)	T_b (°C)	d (g·cm ⁻³)	H Statement	P Statement
Hydrazine hydrate	NH ₂ NH ₂ ·H ₂ O	Flammable Harmful Corrosive Health hazard Toxic Environmental hazard	50.06	-51. 7	120.1	1.0	H226, H301, H311, H314, H317, H330, H331, H350, H401, H411	P201, P202, P210, P233, P240, P241, P242, P243, P260, P261, P264, P270, P271, P272, P273, P280, P281, P284, P301+P310, P301+P330+P3 31, P302+P352, P303+P361+P3 53, P304+P340, P305+P351+P3 38, P308+P313, P310, P311, P312, P320, P321, P322, P330, P333+P313, P361, P363, P370+P378, P391, P403+P233,

Name	Formula	GHS Keyword	M (g·mol ⁻¹)	T_m (°C)	T_b (°C)	d (g·cm ⁻³)	H Statement	P Statement
								P403+P235, P405, P501
Aluminum oxide	Al ₂ O ₃	Harmful Health hazard	101.96	2040	2980	4.0	H335, H370, H372	P260, P261, P264, P270, P271, P304+P340, P307+P311, P312, P314, P321, P403+P233, P405, P501
Methanesulfonic acid	CH ₃ SO ₃ H	Corrosive Harmful	96.11	19	167	1.5	H290, H302+H312, H302, H312, H314, H318 H335	P234, P260, P261, P264, P270, P271, P280, P301+P312, P301+P330+P3 31, P302+P352, P303+P361+P3 53, P304+P340, P305+P351+P3 38, P310, P312, P321, P322, P330, P363, P390,

Name	Formula	GHS Keyword	M (g·mol ⁻¹)	T_m (°C)	T_b (°C)	d (g·cm ⁻³)	H Statement	P Statement
								P403+P233, P404, P405, P501
Hydroxylamine hydrochloride	NH ₂ OH·HCl	Harmful Corrosive Health hazard Toxic Environmental hazard	69.49	155- 157	-	1.7	H290, H301, H302, H312, H315, H317, H319, H351, H373, H400	P201, P202, P234, P260, P261, P264, P270, P272, P273, P280, P281, P301+P310, P301+P312, P302+P352, P305+P351+P3 38, P308+P313, P312, P314, P321, P322, P330, P332+P313, P333+P313, P337+P313, P362, P363, P390, P391, P404, P405, P501

Name	Formula	GHS Keyword	M (g·mol ⁻¹)	T_m (°C)	T_b (°C)	d (g·cm ⁻³)	H Statement	P Statement
Trifluoroacetic acid	CF ₃ COOH	Harmful Corrosive	114.02	-15	72.4	1.5	H290, H302, H314, H318, H332, H412	P234, P260, P261, P264, P270, P271, P273, P280, P301+P312, P301+P330+P331, P303+P361+P353, P304+P312, P304+P340, P305+P351+P338, P310, P312, P321, P330, P363, P390, P404, P405, P501
1,2-ethanedithiol	HS-CH ₂ -CH ₂ -SH	Flammable Harmful Toxic	94.20	-41	144-146	1.1	H226, H301, H302, H310, H312, H319, H330	P210, P233, P240, P241, P242, P243, P260, P262, P264, P270, P271, P280, P284, P301+P310, P301+P312, P302+P350,

Name	Formula	GHS Keyword	M (g·mol ⁻¹)	T_m (°C)	T_b (°C)	d (g·cm ⁻³)	H Statement	P Statement
								P302+P352, P303+P361+P3 53, P304+P340, P305+P351+P3 38, P310, P312, P320, P321, P322, P330, P337+P313, P361, P363, P370+P378, P403+P233, P403+P235, P405, P501
Boron trifluoride diethyl etherate		Flammable Harmful Corrosive Health hazard Toxic	141.93	-58	126-129	1.2	H226, H302, H302, H310, H314, H318, H330, H331, H372	P210, P233, P240, P260, P264, P270, P280, P284, P303+P361+P3 53, P304+P340, P305+P351+P3 38, P309, P310, P320, P403+P235, P405, P501

9. List of GHS Hazard and Precautionary Statements

Hazard Statements (H-codes)

Physical hazards

H200: Unstable explosive
H201: Explosive; mass explosion hazard
H202: Explosive; severe projection hazard
H203: Explosive; fire, blast or projection hazard
H204: Fire or projection hazard
H205: May mass explode in fire
H220: Extremely flammable gas
H221: Flammable gas
H222: Extremely flammable aerosol
H223: Flammable aerosol
H224: Extremely flammable liquid and vapour
H225: Highly flammable liquid and vapour
H226: Flammable liquid and vapour
H227: Combustible liquid
H228: Flammable solid
H229: Pressurized container: may burst if heated
H230: May react explosively even in the absence of air
H231: May react explosively even in the absence of air at elevated pressure and/or temperature
H240: Heating may cause an explosion
H241: Heating may cause a fire or explosion
H242: Heating may cause a fire
H250: Catches fire spontaneously if exposed to air
H251: Self-heating; may catch fire
H252: Self-heating in large quantities; may catch fire
H260: In contact with water releases flammable gases which may ignite spontaneously
H261: In contact with water releases flammable gas
H270: May cause or intensify fire; oxidizer
H271: May cause fire or explosion; strong oxidizer
H272: May intensify fire; oxidizer
H280: Contains gas under pressure; may explode if heated
H281: Contains refrigerated gas; may cause cryogenic burns or injury
H290: May be corrosive to metals

Health hazards

H300: Fatal if swallowed
H301: Toxic if swallowed
H302: Harmful if swallowed
H303: May be harmful if swallowed
H304: May be fatal if swallowed and enters airways
H305: May be harmful if swallowed and enters airways
H310: Fatal in contact with skin
H311: Toxic in contact with skin
H312: Harmful in contact with skin
H313: May be harmful in contact with skin
H314: Causes severe skin burns and eye damage
H315: Causes skin irritation
H316: Causes mild skin irritation
H317: May cause an allergic skin reaction
H318: Causes serious eye damage
H319: Causes serious eye irritation
H320: Causes eye irritation
H330: Fatal if inhaled
H331: Toxic if inhaled

H332: Harmful if inhaled
H333: May be harmful if inhaled
H334: May cause allergy or asthma symptoms or breathing difficulties if inhaled
H335: May cause respiratory irritation
H336: May cause drowsiness or dizziness
H340: May cause genetic defects
H341: Suspected of causing genetic defects
H350: May cause cancer
H351: Suspected of causing cancer
H360: May damage fertility or the unborn child
H361: Suspected of damaging fertility or the unborn child
H361d: Suspected of damaging the unborn child
H361f: Suspected of damaging fertility
H362: May cause harm to breast-fed children
H370: Causes damage to organs
H371: May cause damage to organs
H372: Causes damage to organs through prolonged or repeated exposure
H373: May cause damage to organs through prolonged or repeated exposure
H300+H310: Fatal if swallowed or in contact with skin
H300+H330: Fatal if swallowed or if inhaled
H310+H330: Fatal in contact with skin or if inhaled
H300+H310+H330: Fatal if swallowed, in contact with skin or if inhaled
H301+H311: Toxic if swallowed or in contact with skin
H301+H331: Toxic if swallowed or if inhaled
H311+H331: Toxic in contact with skin or if inhaled
H301+H311+H331: Toxic if swallowed, in contact with skin or if inhaled
H302+H312: Harmful if swallowed or in contact with skin
H302+H332: Harmful if swallowed or if inhaled
H312+H332: Harmful in contact with skin or if inhaled
H302+H312+H332: Harmful if swallowed, in contact with skin or if inhaled

Environmental hazards

H400: Very toxic to aquatic life
H401: Toxic to aquatic life
H402: Harmful to aquatic life
H410: Very toxic to aquatic life with long-lasting effects
H411: Toxic to aquatic life with long-lasting effects
H412: Harmful to aquatic life with long-lasting effects
H413: May cause long-lasting harmful effects to aquatic life
H420: Harms public health and the environment by destroying ozone in the upper atmosphere

Precautionary Statements (P-codes)

General precautionary statements

P101: If medical advice is needed, have product container or label at hand
P102: Keep out of reach of children
P103: Read label before use

Prevention precautionary statements

P201: Obtain special instructions before use
P202: Do not handle until all safety precautions have been read and understood
P210: Keep away from heat, hot surfaces, sparks, open flames and other ignition sources. No smoking
P211: Do not spray on an open flame or other ignition source.
P220: Keep/Store away from clothing/.../combustible materials
P221: Take any precaution to avoid mixing with combustibles
P222: Do not allow contact with air
P223: Do not allow contact with water
P230: Keep wetted with ...
P231: Handle under inert gas

P232: Protect from moisture
 P233: Keep container tightly closed
 P234: Keep only in original container
 P235: Keep cool
 P240: Ground/bond container and receiving equipment
 P241: Use explosion-proof electrical/ventilating/lighting/.../equipment
 P242: Use only non-sparking tools
 P243: Take precautionary measures against static discharge
 P244: Keep valves and fittings free from oil and grease
 P250: Do not subject to grinding/shock/.../friction
 P251: Do not pierce or burn, even after use
 P260: Do not breathe dust/fumes/gas/mist/vapours/spray
 P261: Avoid breathing dust/fumes/gas/mist/vapours/spray
 P262: Do not get in eyes, on skin, or on clothing
 P263: Avoid contact during pregnancy/while nursing
 P264: Wash ... thoroughly after handling
 P270: Do not eat, drink or smoke when using this product
 P271: Use only outdoors or in a well-ventilated area
 P272: Contaminated work clothing should not be allowed out of the workplace
 P273: Avoid release to the environment
 P280: Wear protective gloves/protective clothing/eye protection/face protection
 P282: Wear cold insulating gloves/face shield/eye protection
 P283: Wear fire/flame resistant/retardant clothing
 P284: [In case of inadequate ventilation] wear respiratory protection
 P231+232: Handle under inert gas. Protect from moisture
 P235+410: Keep cool. Protect from sunlight

Response precautionary statements

P301: IF SWALLOWED:
 P302: IF ON SKIN:
 P303: IF ON SKIN (or hair):
 P304: IF INHALED:
 P305: IF IN EYES:
 P306: IF ON CLOTHING:
 P307: IF EXPOSED:
 P308: If EXPOSED or concerned:
 P309: IF EXPOSED or if you feel unwell:
 P310: Immediately call a POISON CENTER/doctor/...
 P311: Call a POISON CENTER/ doctor/...
 P312: Call a POISON CENTER/ doctor/.../if you feel unwell
 P313: Get medical advice/attention
 P314: Get medical advice/attention if you feel unwell
 P315: Get immediate medical advice/attention
 P320: Specific treatment is urgent (see ... on this label)
 P321: Specific treatment (see ... on this label)
 P330: Rinse mouth
 P331: Do NOT induce vomiting
 P332: If skin irritation occurs:
 P333: If skin irritation or a rash occurs:
 P334: Immerse in cool water/wrap in wet bandages
 P335: Brush off loose particles from skin
 P336: Thaw frosted parts with lukewarm water. Do not rub affected areas
 P337: If eye irritation persists:
 P338: Remove contact lenses if present and easy to do. Continue rinsing
 P340: Remove person to fresh air and keep comfortable for breathing
 P342: If experiencing respiratory symptoms:
 P351: Rinse cautiously with water for several minutes
 P352: Wash with plenty of water/...

P353: Rinse skin with water/shower
P360: Rinse immediately contaminated clothing and skin with plenty of water before removing clothes
P361: Take off immediately all contaminated clothing
P362: Take off contaminated clothing
P363: Wash contaminated clothing before reuse
P364: And wash it before reuse
P370: In case of fire:
P371: In case of major fire and large quantities:
P372: Explosion risk in case of fire
P373: DO NOT fight fire when fire reaches explosives
P374: Fight fire with normal precautions from a reasonable distance
P375: Fight fire remotely due to the risk of explosion
P376: Stop leak if safe to do so
P377: Leaking gas fire - do not extinguish unless leak can be stopped safely
P378: Use ... to extinguish
P380: Evacuate area
P381: Eliminate all ignition sources if safe to do so
P391: Collect spillage
P301+310: IF SWALLOWED: Immediately call a POISON CENTER/doctor/...
P301+312: IF SWALLOWED: Call a POISON CENTER/doctor/.../if you feel unwell.
P301+330+331: IF SWALLOWED: Rinse mouth. Do NOT induce vomiting
P302+334: IF ON SKIN: Immerse in cool water/wrap in wet bandages
P302+352: IF ON SKIN: Wash with plenty of water/...
P303+361+353: IF ON SKIN (or hair): Take off immediately all contaminated clothing. Rinse skin with water/shower
P304+312: IF INHALED: Call a POISON CENTER or doctor/physician if you feel unwell
P304+340: IF INHALED: Remove person to fresh air and keep comfortable for breathing.
P305+351+338: IF IN EYES: Rinse cautiously with water for several minutes. Remove contact lenses if present and easy to do –continue rinsing
P306+360: IF ON CLOTHING: Rinse immediately contaminated clothing and skin with plenty of water before removing clothes
P308+311: If exposed or concerned: Call a POISON CENTER/ doctor/...
P308+313: If exposed: Call a POISON CENTER or doctor/physician
P332+313: If skin irritation occurs: Get medical advice/attention
P333+313: If skin irritation or a rash occurs: Get medical advice/attention
P335+334: Brush off loose particles from skin. Immerse in cool water/wrap in wet bandages
P337+313: If eye irritation persists get medical advice/attention
P342+311: If experiencing respiratory symptoms: Call a POISON CENTER/doctor/...
P361+364: Take off immediately all contaminated clothing and wash it before reuse
P362+364: Take off contaminated clothing and wash it before reuse
P370+376: In case of fire: Stop leak if safe to do so
P370+378: In case of fire: Use ... to extinguish
P370+380: In case of fire: Evacuate area
P370+380+375: In case of fire: Evacuate area. Fight fire remotely due to the risk of explosion
P371+380+375: In case of major fire and large quantities: Evacuate area. Fight fire remotely due to the risk of explosion

Storage precautionary statements

P401: Store ...
P402: Store in a dry place
P403: Store in a well ventilated place
P404: Store in a closed container
P405: Store locked up
P406: Store in a corrosive resistant/... container with a resistant inner liner
P407: Maintain air gap between stacks/pallets
P410: Protect from sunlight. P411: Store at temperatures not exceeding ... °C/... °F
P412: Do not expose to temperatures exceeding 50°C/122°F
P413: Store bulk masses greater than ... kg/... lbs at temperatures not exceeding ... °C/... °F

P420: Store away from other materials

P422: Store contents under ...

P402+404: Store in a dry place. Store in a closed container

P403+233: Store in a well ventilated place. Keep container tightly closed

P403+235: Store in a well ventilated place. Keep cool

P410+403: Protect from sunlight. Store in a well-ventilated place

P410+412: Protect from sunlight. Do not expose to temperatures exceeding 50°C/122°F

P411+235: Store at temperatures not exceeding ... °C/... °F. Keep cool

Disposal precautionary statements

P501: Dispose of contents/container to ... [... in accordance with local/regional/national/international regulation (to be specified)].

GHS Pictograms



GHS01 Explosive



GHS04 Compressed Gas



GHS07 Harmful



GHS02 Flammable



GHS05 Corrosive



GHS08 Health Hazard



GHS03 Oxidizing



GHS06 Toxic



GHS09 Environmental Hazard

Résumé

Ce travail vise à synthétiser avec un rendement satisfaisant de nouvelles architectures de polymères à hautes performances, possédant une structure définie et une bonne fenêtre de transformation, sur la base de cétènes aliphatiques ou aromatiques disubstitués.

Les synthèses de diméthylcétène (DMK), méthyléthylcétène (MEK), diéthylcétène (DEK), éthylphénylcétène (EPK) et diphénylcétène (DPK) ont été étudiées. Puis l'homo- et la copolymérisation de ces monomères avec différents amorceurs ont été étudiées. L'influence de l'encombrement stérique présent sur les cétènes influence grandement leur réactivité. Ainsi, des mélanges DMK / DEK et DMK / DPK ont été copolymérisés avec succès pour donner des polycétones dont les propriétés thermiques présentent une plage de transformation satisfaisante ($T_f \sim 160^\circ\text{C}$ et $T_d^{5\%} \sim 260^\circ\text{C}$). Le DMK est le seul monomère conduisant à un homopolymère par voie cationique classique. Les tentatives de photopolymérisation cationique n'ont pas conduit à la polycétone attendue. L'utilisation de métallocènes conduit à la structure polyester. Des structures semi cristallines de très haute masse molaire et faible polydispersité ont été ainsi obtenues ($\overline{M}_n \sim 300\,000\text{ g}\cdot\text{mol}^{-1}$, $D_M < 2$, $T_g \sim 70^\circ\text{C}$, $T_f \sim 200^\circ\text{C}$, $T_d^{5\%} \sim 330^\circ\text{C}$).

Mots clés: cétènes, diméthylcétène, méthyléthylcétène, diéthylcétène, éthylphénylcétène, diphénylcétène, polymérisation cationique, polycétone, polyester, métallocène

Abstract

This study is aimed at synthesizing with a satisfying yield new architectures of high performance polymers, possessing a neat structure and good processing window, on the basis of disubstituted aliphatic or aromatic ketenes.

The synthesis of dimethylketene (DMK), methylethylketene (MEK), diethylketene (DEK), ethylphenylketene (EPK) and diphenylketene (DPK) were approached. Then homo and copolymerization of these monomers with different initiators were studied. The influence in steric hindrance of the monomers affected their reactivity. Thus copolymers based on DMK / DEK and DMK / DPK were successfully obtained and afforded polyketones having good thermal properties and processing window ($T_m \sim 160^\circ\text{C}$ and $T_d^{5\%} \sim 260^\circ\text{C}$).

Only DMK homopolymerized by classic cationic initiation. Photopolymerization did not lead to any polymer formation. Initiation with metallocenes polymerized DMK to a crystallized polyester in an insertion chain growth mechanism. Excellent properties ($\overline{M}_n \sim 300\,000\text{ g}\cdot\text{mol}^{-1}$, $T_g \sim 70^\circ\text{C}$, $T_m \sim 200^\circ\text{C}$, $T_d^{5\%} \sim 330^\circ\text{C}$) were obtained.

Keywords: ketenes, dimethylketene, methylethylketene, diethylketene, ethylphenylketene, diphenylketene, cationic polymerization, polyketone, polyester, metallocene

Equipe de Matériaux Macromoléculaires
UMR 6270 CNRS Polymères, Biopolymères, Surfaces (PBS)
INSA de Rouen Normandie
BP 08 – Avenue de l'Université
76800 Saint-Etienne-du-Rouvray